

Faculty of Graduate Studies,

University of Jordan.

PERFORMANCE COMPARISON OF PARALLEL TUBE AND SERPENTINE TYPE SOLAR COLLECTORS

BY

FAYSAL AHMAD ABU-YAHIA

٢
٢٩٠٢

SUPERVISOR

Prof. MOHAMMED AL-SAAD

Submitted in partial fulfillment of the requirements for the degree of master of
science in mechanical engineering.

Faculty of Graduate Studies,

University of Jordan.

عميد كلية الدراسات العليا

Amman , Jordan

December , 1992

The Examining Committee considers this thesis satisfactory and acceptable for the award of the Degree of Master of Science in Mechanical Engineering on December 19, 1992.

Prof. Mohammed Al-Saad
Mechanical Engineering Department
University of Jordan

Chairman of Committee



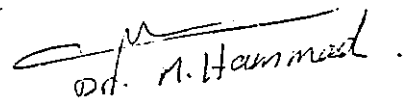
Dr. Ali Badran
Mechanical Engineering Department
University of Jordan

Member of Committee



Dr. Mahmoud Hammad
Mechanical Engineering Department
University of Jordan

Member of Committee



Contents

ACKNOWLEDGEMENTS	viii
List of Figures	ix
List of Tables	xxi
NOMENCLATURE	xxii
ABSTRACT	xxvii
1 INTRODUCTION AND LITERATURE REVIEW	1
1.1 Introduction	1
1.2 Types of Solar Collectors	2
1.3 Serpentine And Parallel Types Solar Collectors	4
1.4 Literature Survey	5
1.5 Objectives of The Present Work	7
1.6 Layout of The Thesis	8
2 MANUFACTURING AND SPECIFICATIONS OF SERPENTINE AND PARALLEL TYPES SOLAR COLLECTORS	9
2.1 Introduction	9
2.2 Collectors Specifications	10
2.2.1 Absorber Plate	10

2.2.2	Tube Material, Diameter And Spacing	10
2.2.3	Absorber Plate-Tube Configuration	11
2.2.4	Transparent Cover	11
2.2.5	Insulation Material	12
2.3	Manufacturing Process	13
3	EXPERIMENTAL ARRANGEMENTS AND TEST PROCEDURE	18
3.1	Introduction	18
3.2	Assumptions	18
3.3	Flat Plate Collector Performance	19
3.4	Experiment Set-Up	22
3.5	Measuring Instruments	23
3.5.1	Incident Solar Radiation Measurement	23
3.5.2	Temperature Measurement	23
3.5.3	Flow Rate Measurement:	24
3.5.4	Wind Velocity Measurement:	24
3.6	Experimental Test Conditions	24
3.7	Experimental Tests And Procedures	25
3.7.1	Forced Circulation Test With No Load Conditions	27
3.7.2	Forced Circulation Test With Load Conditions	28
3.7.3	Forced Circulation Test With Intermittent Load	28
3.7.4	Stagnation Test	29
3.7.5	No-Load Thermosyphon Test	30
3.7.6	Intermittent Load Thermosyphon Test	30

3.7.7	Time Constant Test	31
4	RESULTS AND DISCUSSION	39
4.1	Introduction	39
4.2	Performance Calculations And Results	39
4.2.1	Results of The Forced Circulation Test With No Load Condi- tions	40
4.2.2	Results of The Forced Circulation Test With Load Conditions	43
4.2.3	Results of The Forced Circulation Test With Intermittent Load	44
4.2.4	Stagnation Test Results	45
4.2.5	Results of The No-Load Thermosyphon Test	45
4.2.6	Results of The Intermittent Load Thermosyphon Test	51
4.2.7	Time Constant Test Results	51
4.3	Discussion of Results	128
4.3.1	Temperature Distribution of Water Inside Collectors And Stor- age Tanks	128
4.3.2	Useful Heat Gain	131
4.3.3	Instantaneous And Daily Efficiencies	133
4.3.4	Heat Removal Factors And Overall Heat Loss Coefficients . .	135
4.3.5	Time Constant	136
5	CONCLUSIONS AND RECOMENDATIONS	144
5.1	CONCLUSIONS	144
5.2	RECOMENDATIONS	146

References	148
APPENDIX (A) EXPERIMENTAL AVERAGED MEASURED DATA . . .	151
APPENDIX (B) THE COMPUTER PROGRAM	164
APPENDIX (C) CALCULATED PERFORMANCE PARAMETERS . . .	166

ACKNOWLEDGEMENTS

I am deeply indebted to Mr. Abdul Ruhman Manko for his generous grant which helped me secure the required materials for this research.

My deep thanks to Prof. Mohammad Al-Saad who guided me and helped me with his utmost efforts to accomplish this work in a proper way. I am grateful to Dr. Mahmoud Hammad and Dr. Ali Badran for their valuable comments in the discussion.

My thanks to the Staff working at the Industrial Engineering Workshop and at the Laboratories of Mechanical Engineering Departement at the University of Jordan, special thanks to Eng. Ahmad Al- Qaisia, Mr. Aref Shaheen and Mr. Sayer Abwi. Also, my thanks to the Staff working at the Faculty of Engineering and Technology Computer Centre.

My appreciation and thanks are extended, as well, to all those who were of good support and assistance for me throughout my preparing for this work.

List of Figures

Figure (1.1) Different liquid collector designs	3
Figure (2.1) Absorber plate, tubes configuration and thermocouple wires location for the parallel tubes flat plate solar collectors. All dimensions in mm.	15
Figure (2.2) Absorber plate, tubes configuration and thermocouple wires location for the parallel tubes flat plate solar collectors. All dimensions in mm.	16
Figure (2.3) Storage tanks: (a) Well mixed storage tank of 150 l. (b) Stratified storage tank of 50 l, showing the thermocou[les locations. All dimensions in mm.	17
Figure (3.1) Three photographs of the experiment set-up.	32
Figure (3.2) Closed loop set-up for no load tests based on ASHRAE Standard 93-77 (1977)	33
Figure (3.3) Closed loop set-up for no load tests and the stagnation test, where both collectors are connected to the same storage tank	34
Figure (3.4) Open-loop set-up for load tests based on ASHRAE Standard 93-77 (1977)	35

Figure (3.5) A loop set up for the forced circulation test with intermittent load conditions	36
Figure (3.6) Closed loop set-up for the no load thermosyphon test	37
Figure (3.7) A loop set-up for the intermittent load thermosyphon test. . .	38
Figure (4.1) Variation of inlet temperature, outlet temperature, and the ambient temperature with time for the serpentine and the parallel tubes flat plate solar collectors ($m = 0.02Kg/s$, $V_s = 150l$)	53
Figure (4.2) Variation of inlet temperature, outlet temperature, and the ambient temperature with time for the serpentine and the parallel tubes flat plate solar collectors ($m = 0.03Kg/s$, $V_s = 150l$)	54
Figure (4.3) Variation of inlet temperature, outlet temperature, and the ambient temperature with time for the serpentine and the parallel tubes flat plate solar collectors ($m = 0.05Kg/s$, $V_s = 150l$)	55
Figure (4.4) Variation of inlet temperature, outlet temperature, and the ambient temperature with time for the serpentine and the parallel tubes flat plate solar collectors ($m = 0.07Kg/s$, $V_s = 150l$)	56
Figure (4.5) Variation of inlet temperature, outlet temperature, and the ambient temperature with time for the serpentine tube flat plate solar collector ($m = 0.02Kg/s$, $V_s = 50l$)	57
Figure (4.6) Variation of inlet temperature, outlet temperature, and the ambient temperature with time for the parallel tube flat plate solar collector ($m = 0.02Kg/s$, $V_s = 50l$)	58

Figure (4.7) Variation of inlet temperature, outlet temperature, and the ambient temperature with time for the serpentine tube flat plate solar collector ($m = 0.03\text{Kg/s}$, $V_s = 50\text{l}$)	59
Figure (4.8) Variation of inlet temperature, outlet temperature, and the ambient temperature with time for the parallel tube flat plate solar collector ($m = 0.03\text{Kg/s}$, $V_s = 50\text{l}$)	60
Figure (4.9) Variation of inlet temperature, outlet temperature, and the ambient temperature with time for the serpentine tube flat plate solar collector ($m = 0.05\text{Kg/s}$, $V_s = 50\text{l}$)	61
Figure (4.10) Variation of inlet temperature, outlet temperature, and the ambient temperature with time for the parallel tube flat plate solar collector ($m = 0.05\text{Kg/s}$, $V_s = 50\text{l}$)	62
Figure (4.11) Variation of inlet temperature, outlet temperature, and the ambient temperature with time for the serpentine tube flat plate solar collector ($m = 0.07\text{Kg/s}$, $V_s = 50\text{l}$)	63
Figure (4.12) Variation of inlet temperature, outlet temperature, and the ambient temperature with time for the parallel tube flat plate solar collector ($m = 0.07\text{Kg/s}$, $V_s = 50\text{l}$)	64
Figure (4.13) Variation of inlet temperature, outlet temperature, and the ambient temperature with time for the serpentine and the parallel tubes flat plate solar collectors at two different mass flow rates($m_s = 0.015\text{Kg/s}$, $m_p = 0.105\text{Kg/s}$ and $V_s = 50\text{l}$)	65

Figure (4.14) Temperature distribution of water inside the serpentine tube flat plate solar collector and ambient temperature during the test day ($m = 0.02Kg/s$, $V_s = 150l$)	66
Figure (4.15) Temperature distribution of water inside the serpentine tube flat plate solar collector and ambient temperature during the test day ($m = 0.03Kg/s$, $V_s = 150l$)	67
Figure (4.16) Temperature distribution of water inside the serpentine tube flat plate solar collector and ambient temperature during the test day ($m = 0.05Kg/s$, $V_s = 150l$)	68
Figure (4.17) Temperature distribution of water inside the serpentine tube flat plate solar collector and ambient temperature during the test day ($m = 0.07Kg/s$, $V_s = 150l$)	69
Figure (4.18) Temperature distribution of water inside the serpentine tube flat plate solar collector at different times of the day ($m = 0.02Kg/s$, $V_s = 150l$)	70
Figure (4.19) Temperature distribution of water inside the serpentine tube flat plate solar collector at different times of the day ($m = 0.03Kg/s$, $V_s = 150l$)	71
Figure (4.20) Temperature distribution of water inside the serpentine tube flat plate solar collector at different times of the day ($m = 0.05Kg/s$, $V_s = 150l$)	72

Figure (4.21) Temperature distribution of water inside the serpentine tube flat plate solar collector at different times of the day ($m = 0.07Kg/s$, $V_s = 150l$)	73
Figure (4.22) Temperature distribution of water inside the serpentine tube flat plate solar collector at different times of the day ($m = 0.02Kg/s$, $V_s = 50l$)	74
Figure (4.23) Temperature distribution of water inside the serpentine tube flat plate solar collector at different times of the day ($m = 0.03Kg/s$, $V_s = 50l$)	75
Figure (4.24) Temperature distribution of water inside the serpentine tube flat plate solar collector at different times of the day ($m = 0.05Kg/s$, $V_s = 50l$)	76
Figure (4.25) Temperature distribution of water inside the serpentine tube flat plate solar collector at different times of the day ($m = 0.07Kg/s$, $V_s = 50l$)	77
Figure (4.26) Temperature distribution of water inside the serpentine tube flat plate solar collector at different times of the day ($m_s = 0.015Kg/s$, $V_s = 50l$)	78
Figure (4.27) Variation of incident energy and useful energy for the serpen- tine and the parallel tubes flat plate solar collectors ($m = 0.02Kg/s$, $V_s = 150l$)	79

Figure (4.28) Variation of incident energy and useful energy for the serpentine and the parallel tubes flat plate solar collectors ($m = 0.03Kg/s$, $V_s = 150l$)	80
Figure (4.29) Variation of incident energy and useful energy for the serpentine and the parallel tubes flat plate solar collectors ($m = 0.05Kg/s$, $V_s = 150l$)	81
Figure (4.30) Variation of incident energy and useful energy for the serpentine and the parallel tubes flat plate solar collectors ($m = 0.07Kg/s$, $V_s = 150l$)	82
Figure (4.31) Variation of incident energy and useful energy for the serpentine and the parallel tubes flat plate solar collectors ($m = 0.02Kg/s$, $V_s = 50l$)	83
Figure (4.32) Variation of incident energy and useful energy for the serpentine and the parallel tubes flat plate solar collectors ($m = 0.03Kg/s$, $V_s = 50l$)	84
Figure (4.33) Variation of incident energy and useful energy for the serpentine and the parallel tubes flat plate solar collectors ($m = 0.05Kg/s$, $V_s = 50l$)	85
Figure (4.34) Variation of incident energy and useful energy for the serpentine and the parallel tubes flat plate solar collectors ($m = 0.07Kg/s$, $V_s = 50l$)	86

Figure (4.35) Variation of incident energy and useful energy for the serpentine and the parallel tubes flat plate solar collectors at different mass flow rates ($m_s = 0.02Kg/s$, $m_p = 0.105Kg/s$ and $V_s = 150l$) . . . 87

Figure (4.36) Variation of instantaneous efficiency against $(T_i - T_a)/I$ for the serpentine and the parallel tubes flat plate solar collectors ($m = 0.02Kg/s$, $V_s = 150l$) 88

Figure (4.37) Variation of instantaneous efficiency against $(T_i - T_a)/I$ for the serpentine and the parallel tubes flat plate solar collectors ($m = 0.03Kg/s$, $V_s = 150l$) 89

Figure (4.38) Variation of instantaneous efficiency against $(T_i - T_a)/I$ for the serpentine and the parallel tubes flat plate solar collectors ($m = 0.05Kg/s$, $V_s = 150l$) 90

Figure (4.39) Variation of instantaneous efficiency against $(T_i - T_a)/I$ for the serpentine and the parallel tubes flat plate solar collectors ($m = 0.07Kg/s$, $V_s = 150l$) 91

Figure (4.40) Variation of instantaneous efficiency against $(T_i - T_a)/I$ for the serpentine and the parallel tubes flat plate solar collectors ($m = 0.02Kg/s$, $V_s = 50l$) 92

Figure (4.41) Variation of instantaneous efficiency against $(T_i - T_a)/I$ for the serpentine and the parallel tubes flat plate solar collectors ($m = 0.03Kg/s$, $V_s = 50l$) 93

Figure (4.42) Variation of instantaneous efficiency against $(T_i - T_a)/I$ for the serpentine and the parallel tubes flat plate solar collectors ($m = 0.05Kg/s$, $V_s = 50l$)	94
Figure (4.43) Variation of instantaneous efficiency against $(T_i - T_a)/I$ for the serpentine and the parallel tubes flat plate solar collectors ($m = 0.07Kg/s$, $V_s = 50l$)	95
Figure (4.44) Variation of instantaneous efficiency against $(T_i - T_a)/I$ for the serpentine and the parallel tubes flat plate solar collectors with two different mass flow rates. ($m_s = 0.015Kg/s$, $m_p = 0.105Kg/s$ and $V_s = 50l$)	96
Figure (4.45) Variation of inlet temperature, outlet temperature, and the ambient temperature with time for the serpentine and the parallel tubes flat plate solar collector ($m = 0.02Kg/s$)	97
Figure (4.46) Variation of inlet temperature, outlet temperature, and the ambient temperature with time for the serpentine and the parallel tubes flat plate solar collector ($m = 0.05Kg/s$)	98
Figure (4.47) Temperature distribution of water inside the serpentine tube flat plate solar collector and ambient temperature during the test day ($m = 0.02Kg/s$)	99
Figure (4.48) Temperature distribution of water inside the serpentine tube flat plate solar collector and ambient temperature during the test day ($m = 0.05Kg/s$)	100

Figure (4.49) Temperature distribution of water inside the serpentine tube flat plate solar collector at different times of the day ($m = 0.02Kg/s$)	101
Figure (4.50) Temperature distribution of water inside the serpentine tube flat plate solar collector at different times of the day ($m = 0.05Kg/s$)	102
Figure (4.51) Variation of incident energy and useful energy for the serpen- tine and the parallel tubes flat plate solar collectors ($m = 0.02Kg/s$)	103
Figure (4.52) Variation of incident energy and useful energy for the serpen- tine and the parallel tubes flat plate solar collectors ($m = 0.05Kg/s$)	104
Figure (4.53) Variation of useful water temperature and ambient temper- ature with time of day for the serpentine and the parallel tubes flat plate solar collectors under a load of 5 l/h ($m = 0.02Kg/s$)	105
Figure (4.54) Variation of useful water temperature and ambient temper- ature with time of day for the serpentine and the parallel tubes flat plate solar collectors under a load of 10 l/h ($m = 0.02Kg/s$)	106
Figure (4.55) Variation of useful water temperature and ambient temper- ature with time of day for the serpentine and the parallel tubes flat plate solar collectors under a load of 15 l/h ($m = 0.02Kg/s$)	107
Figure (4.56) Variation of useful water temperature and ambient temper- ature with time of day for the serpentine and the parallel tubes flat plate solar collectors under a load of 5 l/h ($m = 0.05Kg/s$)	108
Figure (4.57) Variation of useful water temperature and ambient temper- ature with time of day for the serpentine and the parallel tubes flat plate solar collectors under a load of 10 l/h ($m = 0.05Kg/s$)	109

Figure (4.58) Variation of useful water temperature and ambient temperature with time of day for the serpentine and the parallel tubes flat plate solar collectors under a load of 15 l/h ($m = 0.05Kg/s$)	110
Figure (4.59) Variation of incident energy and useful energy for the serpentine and the parallel tubes flat plate solar collectors under a load of 5 l/h, ($m = 0.02Kg/s$)	111
Figure (4.60) Variation of incident energy and useful energy for the serpentine and the parallel tubes flat plate solar collectors under a load of 10 l/h, ($m = 0.02Kg/s$)	112
Figure (4.61) Variation of incident energy and useful energy for the serpentine and the parallel tubes flat plate solar collectors under a load of 15 l/h, ($m = 0.02Kg/s$)	113
Figure (4.62) Variation of incident energy and useful energy for the serpentine and the parallel tubes flat plate solar collectors under a load of 5 l/h, ($m = 0.05Kg/s$)	114
Figure (4.63) Variation of incident energy and useful energy for the serpentine and the parallel tubes flat plate solar collectors under a load of 10 l/h, ($m = 0.05Kg/s$)	115
Figure (4.64) Variation of incident energy and useful energy for the serpentine and the parallel tubes flat plate solar collectors under a load of 15 l/h, ($m = 0.05Kg/s$)	116

- Figure (4.65) Variation of inlet temperature, outlet temperature, and the ambient temperature with time for the serpentine and the parallel tubes flat plate solar collectors, under no load thermosyphon circulation 117
- Figure (4.66) Temperature distribution of water inside the serpentine tube flat plate solar collector and ambient temperature during the day under no load thermosyphon circulation 118
- Figure (4.67) Temperature distribution of water inside the storage tank of the serpentine type solar collector under no load thermosyphon circulation 119
- Figure (4.68) Temperature distribution of water inside the storage tank of the parallel type solar collector under no load thermosyphon circulation 120
- Figure (4.69) Temperature distribution of water inside the serpentine tube flat plate solar collector at different times of the day under no load thermosyphon circulation 121
- Figure (4.70) Variation of incident energy and useful energy for the serpentine and the parallel tubes flat plate solar collectors under no load thermosyphon circulation 122
- Figure (4.71) Variation of instantaneous efficiency against $(T_i - T_a)/I$ for the serpentine and the parallel tubes flat plate solar collectors under no load thermosyphon circulation 123
- Figure (4.72) Variation of inlet, outlet, ambient and used hot water temperatures with time for the serpentine and the parallel tubes flat plate solar collectors (load= 5 l/h) 124

Figure (4.73) Variation of inlet,outlet, ambient and used hot water temperatures with time for the serpentine and the parallel tubes flat plate solar collectors (load= 10 l/h)	125
Figure (4.74) Variation of inlet,outlet, ambient and used hot water temperatures with time for the serpentine and the parallel tubes flat plate solar collectors (load= 15 l/h)	126
Figure (4.75) A time temperature plot for the serpentine and the parallel tubes flat plate solar collectors showing temperature drop on sudden interruption of the solar radiation on the collectors	127
Figure (4.76) Variation of mass flow rate with time of day for the serpentine and the parallel tubes flat plate solar collectors under no load thermosyphon circulation	138
Figure (4.77) Heat removal factor vs. mass flow rate for the serpentine and the parallel tubes flat plate solar collector ($V_s = 150l$)	139
Figure (4.78) Heat removal factor vs. mass flow rate for the serpentine and the parallel tubes flat plate solar collector ($V_s = 50l$)	140
Figure (4.79) Heat loss coefficient vs. mass flow rate for the serpentine and the parallel tubes flat plate solar collector ($V_s = 150l$)	141
Figure (4.80) Heat loss coefficient vs. mass flow rate for the serpentine and the parallel tubes flat plate solar collector ($V_s = 50l$)	142
Figure (4.81) Variation of the heat removal factor with time for the serpentine and the parallel tubes flat plate solar collectors under no load thermosyphon circulation	143

List of Tables

Table (2.1) Sizes and material used for absorber plate and tubes of both models	11
Table (4.1) Instantaneous efficiency expressions for the serpentine type . . .	41
Table (4.2) Instantaneous efficiency expressions for the parallel type	41
Table (4.3) Daily efficiency of the tested solar models	44
Table 4.4 : Given and calculated parameters for the serpentine type	46
Table 4.5 : Given and calculated parameters for the parallel type	49
Table 4.6 : Results and conditions of the time constant test	52
Table 4.7 : Reynolds numbers and water flow velocities inside the tube segments of the serpentine and the parallel tubes.	137

NOMENCLATURE

- A_a absorber plate area; (m^2).
- A_c gross area of the collector; (m^2).
- b bond width; (m).
- B collector capacitance rate; (dimensionless).
- C parameter defined in equation (3.10); (dimensionless).
- C_b bond conductance; ($W/m.C^\circ$).
- C_p water specific heat; ($KJ/Kg.C^\circ$).
- D_i inside tube diameter; (m).
- D_o outside tube diameter; (m).
- F collector fin efficiency; (dimensionless).
- F_1 parameter defined in equation (3.7); (dimensionless).
- F_2 parameter defined in equation (3.9); (dimensionless).
- F_r collector heat removal factor; (dimensionless).
- $F_{r,p}$ heat removal factor of the parallel type; (dimensionless).
- $F_{r,s}$ heat removal factor of the serpentine type; (dimensionless).
- F' collector efficiency factor; (dimensionless).
- $h_{f,i}$ heat transfer coefficient inside tubes; ($W/m^2.C^\circ$).
- I incident solar radiation on tilted surfaces; (Wh/m^2).

- SI incident solar radiation on tilted surfaces; (KJ).
- k thermal conductivity; ($W/m.C^{\circ}$).
- K_b bond thermal conductivity; ($W/m.C^{\circ}$).
- L length of the serpentine segments in the flow direction; (m).
- m parameter equal to $\sqrt{\frac{U_i}{k_b}}$; (dimensionless).
- m mass flow rate of water; (Kg/s).
- m_p mass flow rate of water in the parallel type; (Kg/s).
- m_s mass flow rate of water in the serpentine type; (Kg/s).
- n parameter defined by equation (3.12); (dimensionless).
- N number of segments in the serpentine collector; (dimensionless).
- Q_u useful heat gain; (KJ).
- Q_{up} useful heat gain of the parallel type; (KJ).
- Q_{us} useful heat gain of the serpentine type; (KJ).
- Q_{ut} total useful heat gain during all the time intervals of the test day; (KJ).
- R thermal resistance between the absorbing plate and water; ($m.C^{\circ}/W$).
- Re Reynold's number of the flowing water; (dimensionless).
- Re_p Reynold's number of the flowing water in the parallel type; (dimensionless).
- Re_s Reynold's number of the flowing water in the serpentine type; (dimensionless).
- t bond average thickness; (m).
- T_a ambient temperature; (C°).
- T_i inlet water temperature to the collector; (C°).

- T_{ip} inlet water temperature to the parallel type; (C°).
- T_{is} inlet water temperature to the serpentine type; (C°).
- T_o outlet water temperature from the collector; (C°).
- T_{op} outlet water temperature from the parallel type; (C°).
- T_{os} outlet water temperature from the serpentine type; (C°).
- T_{lp} temperature of water inside the parallel type's storage tank at a distance of 0.15 m from the bottem of the storage tank; (C°).
- T_{mp} temperature of water inside the parallel type's storage tank at a distance of 0.30 m from the bottem of the storage tank; (C°).
- T_{tp} temperature of water inside the parallel type's storage tank at a distance of 0.45 m from the bottem of the storage tank; (C°).
- T_{ls} temperature of water inside the serpentine type's storage tank at a distance of 0.15 m from the bottem of the storage tank; (C°).
- T_{ms} temperature of water inside the serpentine type's storage tank at a distance of 0.30 m from the bottem of the storage tank; (C°).
- T_{ts} temperature of water inside the serpentine type's storage tank at a distance of 0.45 m from the bottem of the storage tank; (C°).
- T_{up} useful hot water from the parallel type; (C°).
- T_{us} useful hot water from the serpentine type; (C°).
- $T_{o,i}$ outlet water temperature when the solar radiation is shut off; (C°).
- $T_{o,\tau}$ water outlet temperature at time (τc); C°
- U_l overall heat loss coefficient from the collector; ($W/m^2.C^\circ$)
- U_{lp} overall heat loss coefficient from the parallel type; ($W/m^2.C^\circ$)

U_{ls}	overall heat loss coefficient from the serpentine type; ($W/m^2.C^{\circ}$)
V_s	storage tank volume, (litre).
V_w	wind speed; (m/s)
V_{wp}	water velocity inside the risers of the parallel type; (m/s)
V_{ws}	water velocity inside the segments of the serpentine type; (m/s)
W	distance between the tubes; (m).

Greek Symbols

α	absorbance; (dimensionless).
β	collector tilt angle; (degree).
δ	absorber plate thickness; (m).
γ	azimuth angle; (degree)
γ'	parameter defined by equation (3.13); (dimensionless)
η_d	collector daily efficiency; (dimensionless).
η_i	collector instantaneous efficiency; (dimensionless).
η_{ip}	instantaneous efficiency of the parallel type; (dimensionless).
η_{is}	instantaneous efficiency of the serpentine type; (dimensionless).
θ	latitude angle; (degree).
τ	transmissivity; (dimensionless).
τ_c	time constant; (minute)
$(\tau_c)_p$	time constant of the parallel type; (minute).
$(\tau_c)_s$	time constant of the serpentine type; (minute).
τ_t	time in seconds of the time interval; (second).
$(\tau\alpha)_e$	effective transmittance-absorbance product; (dimensionless).

Subscripts

<i>a</i>	absorber, ambient.
<i>b</i>	bond
<i>c</i>	collector.
<i>e</i>	effective
<i>i</i>	inlet.
<i>l</i>	loss, lower.
<i>m</i>	mid.
<i>o</i>	outlet.
<i>p</i>	parallel
<i>s</i>	serpentine.
<i>t</i>	top, total.
<i>u</i>	useful.
<i>w</i>	water, wind.

Abbreviations :

<i>DHW</i>	Domestic Hot Water.
<i>GSP</i>	Galvanized Steel Pipe.
<i>I.D</i>	Inside Diameter.
<i>O.D</i>	Outside Diameter.

ABSTRACT

Preheating of domestic water is considered as the major application of solar energy in Jordan. This is because of the modest investment and immediate return.

In this study two flat plate solar collectors were manufactured and tested under the same experimental conditions. One of the serpentine type and the other of the parallel type .

The collectors used in this study were tested according to ASHRAE standard 93- 77 (1977). Moreover, the following tests were performed on both collectors: forced circulation test with intermittent load conditions, stagnation test , no load thermosyphon test, and thermosyphon test with intermittent load conditions.

Both collectors were tested outdoors, under Jordan's climatic conditions. The tests were performed in July, August, and September, 1991, where the working fluid was fresh water. The investigated flow rates were 0.02, 0.03, 0.05, 0.07 Kg/s. The selected test period ranges from 08:00 to 17:00.

This study shows that under forced circulation, the serpentine type has a superior performance parameters when compared to the parallel type, for all the investigated flow rates and time intervals. This superiority, becomes more evident during the time interval 09:30-15:00. After the time 15:00 the performance parameters of both models come nearer to each other. The reason for this performance degradation of

the serpentine type is due to the shading effect.

On the other hand, the serpentine type has an inferior performance when compared to the parallel type under thermosyphon circulation. This is due to the ability of the parallel type to circulate water naturally at higher flow rates.

This study comes to conclude that since most of the solar domestic hot water (DHW) systems used in Jordan are thermosyphon systems, then choosing the serpentine type as a solar collector is not a suitable choice. The parallel type still a convenient selection. On the other hand, the selection of the serpentine type for forced flow systems, where pumps are used, is more suitable than the parallel type. The application of such systems are industrial hot water requirements, space heating and building air conditioning, where the circulation of water to the collector will usually be kept high.

Chapter 1

INTRODUCTION AND LITERATURE REVIEW

1.1 Introduction

The most abundant continuing energy source available to the human race is solar energy. This solar energy is very attractive because it is nonpolluting, nondepletable, reliable, and free. On the other hand it is very dilute and it is not constant, and this dictates the use of large surface area collectors and systems to collect and concentrate the energy.

The flat plate collector is the simplest and most widely used means to convert the sun's radiation into useful heat. Such type of collectors can be designed for applications requiring energy delivery at moderate temperatures, up to perhaps $100C^{\circ}$ above ambient temperature [1]. They use both beam and diffuse solar radiation, do not require tracking of the sun, and they require little maintenance. They are mechanically simpler than concentrating collectors. The major applications of these units are in solar water heating and building heating, whereas potential uses include building air conditioning and industrial process heat.

In the mid 1970s, many new collector designs appeared on the commercial mar-

ket, and each one of these collectors has its own performance , characteristics, advantages and disadvantages. Serpentine flat plate solar collector is one of these designs.

1.2 Types of Solar Collectors

Solar collectors can be categorized into four basic classes [2]:

1. Flat plate collectors which collect but don't concentrate the sun's radiant energy. Figure (1.1) shows a number of different liquid flat plate solar collector designs of this type.
2. Vacuum tube collectors, where the space around the absorber surface is evacuated, so the convective heat losses are eliminated or minimized.
3. Medium performance focusing collectors which utilize a curved surface to focus the sun's rays on a heat exchanger, such as a collecting pipe or plate-pipe collector, such collectors are adopted for slightly higher temperature than that of the flat plate type.
4. Concentrating collectors which utilize large curved surfaces composed of multiple mirrors, such collectors can attain high temperature ranges for use in operating steam generators, turbines and the like.

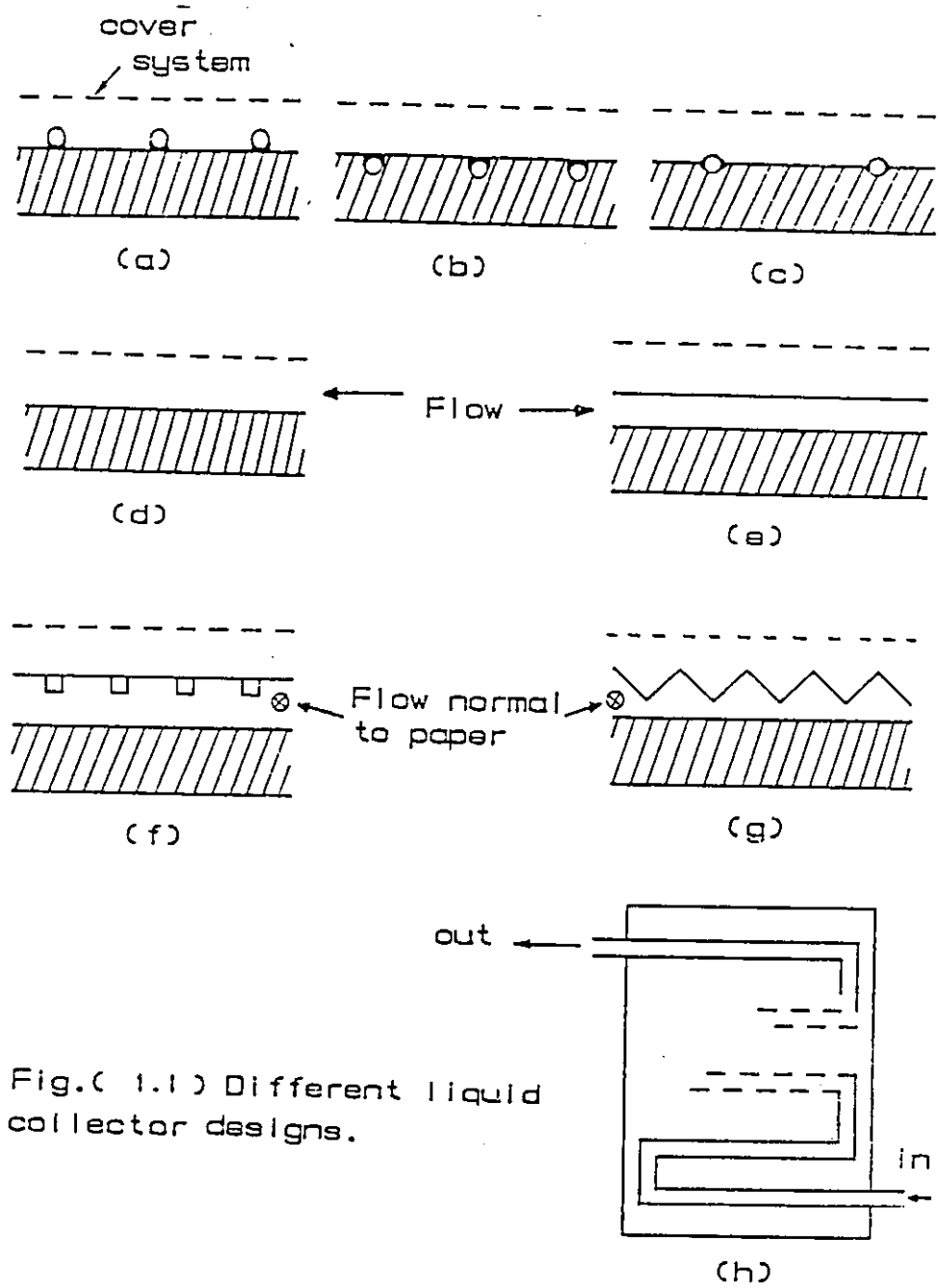


Fig.(1.1) Different liquid collector designs.

1.3 Serpentine And Parallel Types Solar Collectors

In the parallel type flat plate solar collector the flow occurs in parallel risers connected between inlet and outlet plenums. While in the serpentine type the tube is fixed to the absorber plate in a serpentine fashion, therefore, the flow passages can be constructed from a single integral length of tubing.

Manufacturing serpentine type is easier than manufacturing parallel type, since it consists of one tube and a plate to fit the tube on. This means saving of time and money, thus welding is no longer needed to join the pipes together as for the case of parallel type where risers must be joined with headers. So, welding failure can be eliminated, especially, in cold winter days where thermal and residual stresses occur. Also, the replacement of the serpentine tube for any defects is made easier than the parallel tubes, this allows the same plate to be used for many times.

In the serpentine type the flow is forced to travel in one passage. Thus any deposit formed on the internal surface of the tube will represent an obstruction to all the flow. The case in the parallel type is different, since there are at least seven risers where the flow can travel through. From this it is obvious that the life cycle of the serpentine type is lower than that of the parallel type.

The pressure drop in the serpentine type is higher than that of the parallel type, this is due to the accumulation of pressure drops in the bends and straight runs. Thus the driving force in the case of the serpentine type is less than that of the parallel type when natural circulation is used.

1.4 Literature Survey

Performance of parallel tubes flat plate solar collectors has received a lot of investigations, while the performance of the serpentine collectors has received a little attention. In this study the relative performance between the serpentine and the parallel types flat plate solar collectors is studied and analyzed experimentally under the same experimental conditions.

The first detailed study of the performance of the parallel type was introduced by Hottel and Woertz[3]. The study was based on energy balance measurements of an array of collectors on an experimental solar heated building. The performance calculations were based on mean plate temperature . A correlation for thermal losses was reported.

Moore et al. [4] made extensive comparisons of the performance of a flat plate liquid heating collector with results predicted by use of the Hottel and Woertz method. The operating conditions were similar to those of Hottel and Woertz and good agreement was reported. Several studies were investigated by many researchers thereafter, relating the parallel type performance[2,5-9]

The first real and valuable study on serpentine type was presented by Abdel-Kalik[10]. He obtained an analytical solution for heat removal factor (F_r) for a serpentine absorber plate of a single bend (two segments). He solved the problem numerically for larger values of segments and showed that this solution was within 5 percent of numerical solutions of the general case with any number of bends. He concluded that the dependence of the heat removal factor on the number of segments is slight.

Zhang and Lavan [12] analyzed the thermal performance of a serpentine absorber plate. They obtained analytical solutions for three and four segments. They showed that, what was concluded by Abdel-Kalik was in error for a certain range.

On the other hand, Akgün [11] presented two analytical solutions resulting from two separate assumptions which uncouple the governing matrix differential equation. He concluded that, the dependence of the heat removal factor on the number of segments is slight, which is the same conclusion reached by Abdel-Kalik.

Relative performance comparison studies between the serpentine and the parallel tubes flat plate solar collectors show different results [13-17]. Brode et al.[13] tested the parallel and the serpentine types under near identical conditions. They found experimentally that the thermal efficiency was higher for the parallel type than for the serpentine type, and that the difference between the two diminishes with increasing flow rate.

Chiou and Perera [14] reported an analysis and experimental study of a serpentine collector. Their results were compared to prior experiments with serpentine type [15] and parallel type [16]. The comparison showed higher performance of the parallel type during mid-day, but conversely, higher performance for the serpentine type during early morning.

Lund [17] presented a direct analytical comparison between the two types. He rendered the conduction and transport equations in nondimensional form. Thus he generalized the results for various flow duct designs. The resulting equations were solved over one panel of the absorber plate, between the flow ducts. The panel performance results are combined serially to produce the overall absorber

performance. This work was compared with a previous work of Lund [9] on the parallel type. The result indicates superior performance of the serpentine type.

From the previous presentaion, it is obvious that the question of relative thermal performance of the parallel and the serpentine types is yet open to question. So, a direct simultaneous experimental thermal performance comparison between both types is needed.

1.5 Objectives of The Present Work

Two solar collector arrangements representing the parallel and the serpentine types are constructed and tested under Jordan's climatic conditions. Both collectors have the same effective tubing length and same absorber plate area. All the construction parameters are made identical for both types. The thermal performance parameters of each type are studied and analyzed experimentaly. The following parameters are evaluated:

1. The heat removal factor.
2. The collector overall heat loss coefficient.
3. Instantaneous and daily effeciencies of both collectors.
4. Hourly and daily heat collected per unit area of the collector.
5. Temperature level of the circulating water in different components of the collectors.
6. Temperature distribution of the water inside the storage tanks under thermosyphon flow with no-load conditions.

1.6 Layout of The Thesis

The thesis is divided into five chapters of which this introduction and literature review are the first chapter. Chapter Two describes the manufacturing processes and specifications of the serpentine and the parallel types flat plate solar collectors. Chapter Three is devoted to describe the experimental apparatus, arrangements and the testing procedure . Chapter Four shows the results and their discussion. Finally, Chapter Five lists the general conclusions and recommendations reached by the present study.

Chapter 2

MANUFACTURING AND SPECIFICATIONS OF SERPENTINE AND PARALLEL TYPES SOLAR COLLECTORS

2.1 Introduction

Many types of solar water heaters are commercially available. They differ in design and performance and, of course, in price. They have to meet demands in operation, configuration and meteorological conditions.

Flat plate solar collector performance depends to a large extent, on the used materials and the absorber plate-tube configuration of the collector.

In this study two collectors of different tube configuration were built: The conventional type of parallel tubes collector and the serpentine type. Both collectors were built in the Workshops of Mechanical Engineering Departement at the University of Jordan.

414343

This chapter is devoted to describe the different components that were selected to form the body mass of both collectors, and to describe the manufacturing processes that are followed to build them.

2.2 Collectors Specifications

The following parameters were considered for the specifications of both collectors:

2.2.1 Absorber Plate

The radiation characteristics of the absorber plate are of great importance to the efficiency with which the light striking the collector can be collected as useful heat. So, the absorber plate should have maximum absorptivity.

Different materials can be used as absorber plates, such as copper, aluminum, steel and selective surfaces, where using of these metals is limited by cost and availability.

In the present work, black steel with an ordinary black paint is used as an absorber plate for both collectors, because it is the cheapest available metal that provides good bonding with the paint.

The plate efficiency increases as the plate thickness increase up to a value of 1 mm, after which there is no significant increase [2]. Based on these, black steel of 1 mm thickness was used.

2.2.2 Tube Material, Diameter And Spacing

The tube size should be selected in such a way to minimize the pressure drop in the collector. The pressure drop is directly proportional to the square of the flow rate and inversely proportional to the fifth power of tube diameter.

In the present work the selection of the tube diameter is governed by the purposes of comparison and the local availability of materials.

Table (2.1) summerizes the sizes and materials that are used for the absorber

plate and tubes of both collectors. Spacing between risers is chosen to be 100 mm for both collectors.

Table (2.1) Sizes and materials used for absorber plate and tubes of
both collectors

collector type	Absorber Plate		I-D (mm)		O-D (mm)		Tube
	Dimension	Material	Riser	Header	Riser	Header	material
Serpentine	1590 * 730 * 1	Black steel	17	—	21.5	—	GSP
Parallel	1590 * 730 * 1	Black steel	17	28.4	21.5	34	GSP

2.2.3 Absorber Plate-Tube Configuration

There are different configurations by which the tubes are fixed with the absorber plate. For the purposes of comparison of the present work, two configurations were considered. In the first one, a parallel tube configuration with risers and headers were welded to the absorber plate, where the length of the absorber plate was limited to 1590 mm due to the size limitation of the die used. In the second configuration the pipe is bonded to the absorber plate in a serpentine fashion where the length of the absorber plate is limited to 1590 mm. In both cases the tube configurations have the same effective tubing length of 11.13 m.

2.2.4 Transparent Cover

A material must have high transmissivity to be useful as a cover, and therefore the absorbtivity and reflectivity must be minimized.

Transparent cover can reduce convective and radiative losses. Glass or plastics can be used for these purposes, where they can be arranged in single, double or multiple layers. Glass has a higher transmittance factor than plastic, it does not suffer from corrosion or ultra-violet instability, also it has a considerable life if handled

carefully.

Ordinary window glass 4.0mm thick with 760 × 1730mm dimensions, of an average transmissivity of 0.87 was used.

The top heat transfer coefficient of the collector is dependent on the spacing between the transparent cover and the absorber plate. The top heat transfer coefficient is not substantially affected for spacing more than 25 mm [2]. So, a single glass cover with a spacing of 25 mm was used for both collectors.

2.2.5 Insulation Material

The overall efficiency of the solar water heating system depends to a large extent on the effective reduction of heat losses from the collector plate, connecting pipes and the storage tank. In selecting the insulating material, one must consider cost, durability, toxicity, fabrication, and free of an organic binder, because high collector temperatures, cause this material to deposit on the underside of the transparent cover, adversely affecting the collector transmissivity.

Of the ordinary insulating materials, only fiberglass or rock wool batts are satisfactory. It is recommended that, a minimum of 50 mm of good insulation material must be used at the bottom and the exposed sides of the collector [18].

So, a rock wool -locally available and inexpensive- of 70 mm thickness and 0.0346 $W/m.c^{\circ}$ thermal conductivity is used for insulating the collector. Also, the connecting pipes are insulated by a 30 mm thickness rock wool.

The storage tanks are insulated by using 60 mm thickness polyurethane foam whose thermal conductivity is 0.0245 $W/m.c^{\circ}$.

2.3 Manufacturing Process

The following procedure was followed to build the two collectors used for this study:

1. Two black steel sheets of dimensions $1000 \times 1590mm$ were used to prepare the absorber plates of both collectors. The grooving of each plate was done using a pneumatic die. The groove diameter was chosen to match the risers diameters for a mechanically forced fit. The width of the absorber plate and the tube spacing lead to seven grooves.
2. For the parallel type the risers were joined to the headers by oxy- acetylene welding. The tube arrangements were then welded to the absorber plate as shown in Figure (2.1).

for the serpentine type seven segments were welded to the absorber plate. The segments were then connected to each other as shown in Figure (2.2). Then both absorber plates-tube arrangements were painted with ordinary black paint.
3. Four storage tanks were manufactured. Two of them are mixed, each has a capacity of 150 litre as shown in Figure (2.3.a). The other two tanks are of stratified type with 50 litre capacity as shown in Figure (2.3.b).
4. Fifteen thermocouple wires were used to study the collectors' thermal performance as shown in Figures (2.1-2.3). These thermocouple wires were installed as follows:

- (a) Two thermocouple wires were installed at the inlet and outlet of each model, in order to measure the inlet and outlet temperatures, respectively.
 - (b) Three thermocouple wires were installed at an equal distances at the center of the serpentine tube as shown in Figure (2.2). The thermocouple wires were used to study the temperature distribution of the hot water.
 - (c) Three thermocouple wires were installed at an equal distances inside each of the 50 litre capacity storage tanks, as shown in Figure (2.3.b). These thermocouple wires were used to determine the temperature distribution inside the storage tanks.
 - (d) One thermocouple wire was installed at the outlet of each the 50 litre storage tanks to measure the temperature of the used hot water.
5. The absorber plates and the tube arrangements were fixed inside their collector boxes. Then, the glass covers were placed on the collector boxes.

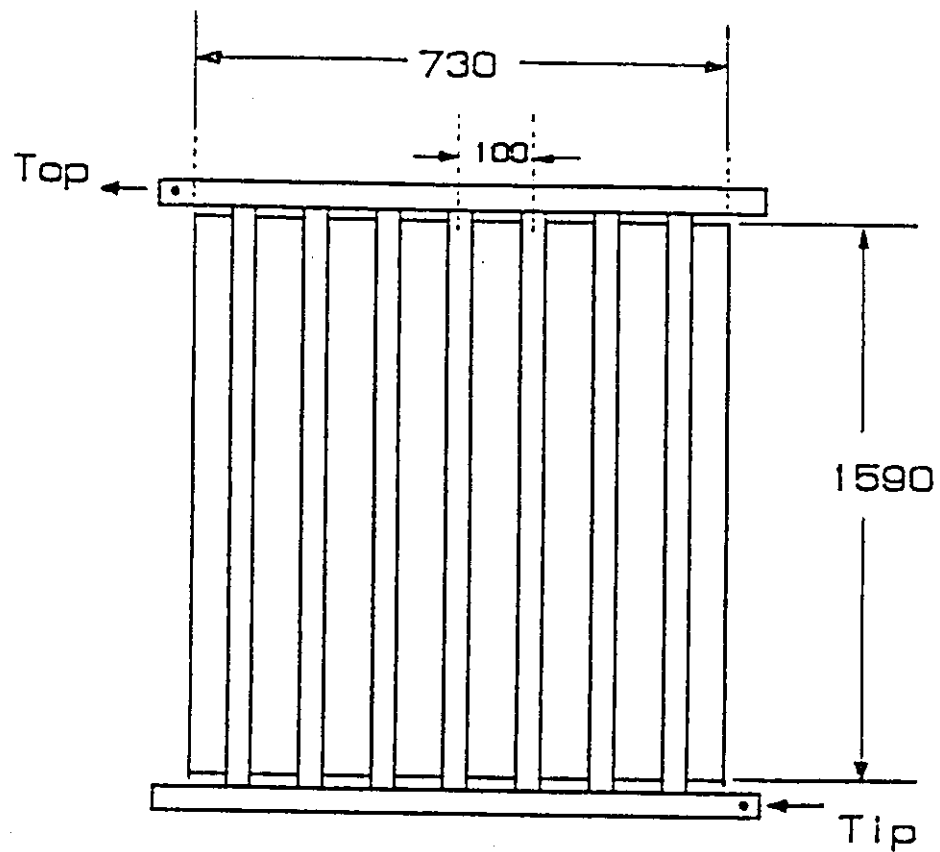


Fig.(2.1) Absorber plate-tubes configuration and thermocouple wires location for the parallel tubes flat plate solar collector. All dimensions in mm.

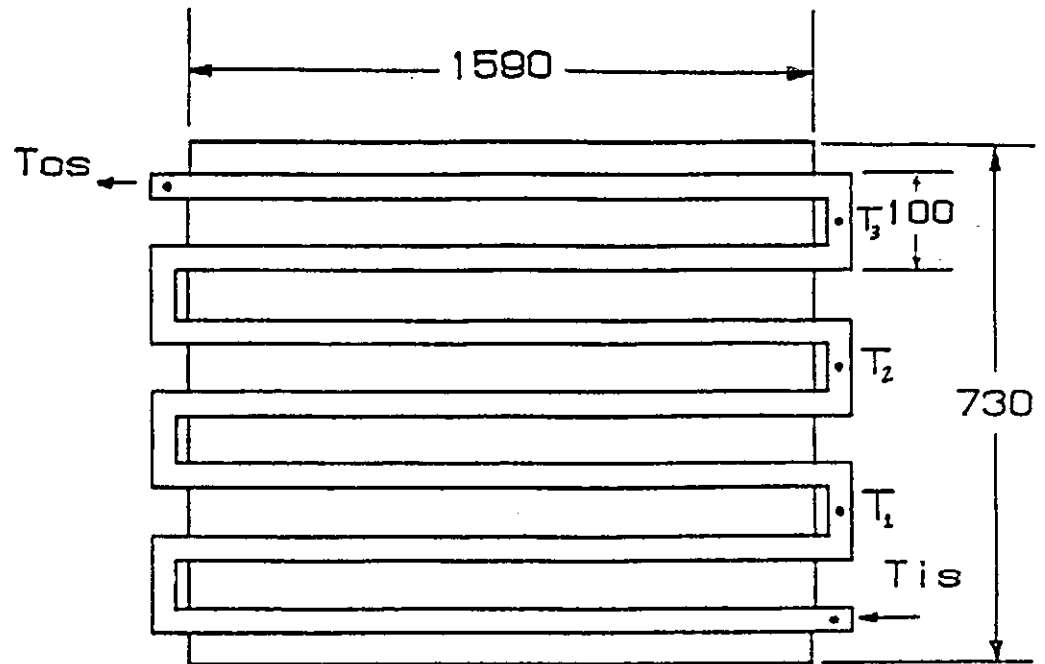


Fig.(2.2) Absorber plate – tubes configuration and thermocouple wires location for the serpentine type flat plate solar collector. All dimensions in mm.

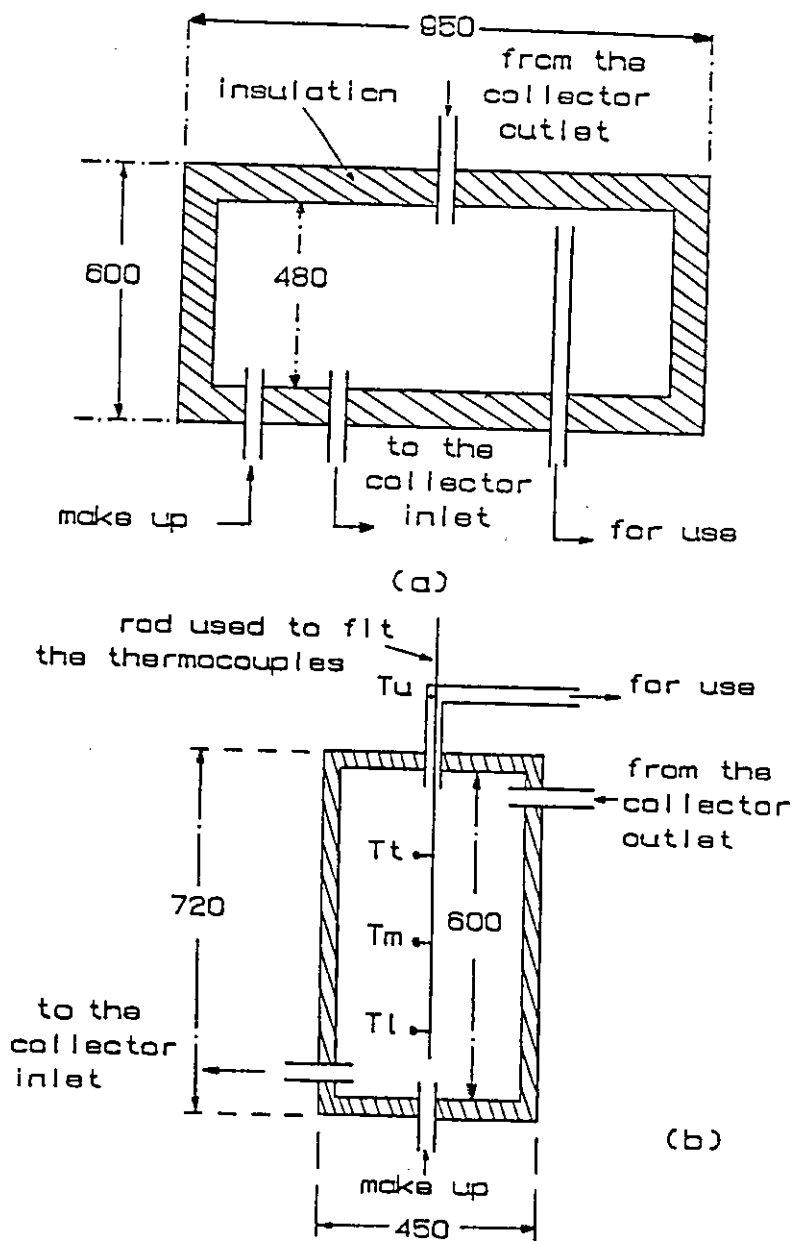


Fig.(2.3) Storage tanks:(a) Well mixed storage tank of 150 L.(b) Stratified storage tank of 50 L.showing the thermocouples locations.All dimensions in mm.

Chapter 3

EXPERIMENTAL ARRANGEMENTS AND TEST PROCEDURE

3.1 Introduction

The collectors of this experimental study were tested outdoors under Jordan's climatic conditions where the flowing fluid is fresh water .

A brief analysis of the flat plate collector performance is outlined in section (3.3). While sections (3.4) to (3.6) are devoted to describe the experiment set-up, the measuring instruments and the experimental test conditions, respectively.

The last section is introduced to describe the experimental tests and procedures. Seven tests are encountered: Forced circulation test with no load conditions, forced circulation test with load conditions, forced circulation test with intermittent load conditions, stagnation test, No- load thermosyphon test, intermittent-load thermosyphon test, and the time constant test.

3.2 Assumptions

The following assumptions are made:

1. Flow is steady.
2. Dust and dirt effects are negligible.
3. One dimensional heat flow through glass cover and back insulation.
4. Properties of working fluid are independent of temperature at the range of temperatures encountered.

3.3 Flat Plate Collector Performance

The performance of a solar collector is influenced by a large number of operational and design parameters. The useful energy gain of the collector can be readily evaluated upon knowledge of its three governing parameters, which are: the heat removal factor F_r , the heat loss coefficient U_l , and the effective transmittance-absorptance product of the cover system $(\tau\alpha)_e$. In terms of these parameters, the instantaneous useful energy gain of the collector per unit time Q_u is given by [1]:

$$Q_u = A_c F_r [I(\tau\alpha)_e - U_l(T_i - T_a)] \quad (3.1)$$

where A_c is the collector area, I is the incident solar flux on the collector, T_i is the inlet fluid temperature, T_a is the ambient air temperature, and the quantity $I(\tau\alpha)_e$ is the absorbed solar energy per unit area of the collector.

The value of $(\tau\alpha)_e$ is nearly equal to 1.02 times the product of τ and α (1), thus:

$$(\tau\alpha)_e \approx 1.02\tau\alpha \quad (3.2)$$

The heat removal factor for the parallel type is given by (1):

$$F_{rp} = \frac{\dot{m}C_p}{A_c U_l} [1 - \exp(-A_c U_l F' / \dot{m}C_p)] \quad (3.3)$$

F' is the collector efficiency factor and is given by [1]:

$$F' = \frac{1/U_i}{W \left[\frac{1}{U_i(D_o + (W - D_o)F)} + \frac{1}{C_b} + \frac{1}{\pi D_i h_{f,i}} \right]} \quad (3.4)$$

F is the collector fin efficiency expressed as:

$$F = \frac{\tanh[m(W - D_o)/2]}{m(W - D_o)/2} \quad (3.5)$$

Where,

\dot{m} is the mass flow rate to the parallel type.

C_p is the specific heat of the flowing fluid (which is equal to $4.186 \text{ KJ/Kg.C}^\circ$ for water at 20C°).

W is the distance between the tubes.

D_o is the outside tube diameter.

C_b is the bond conductance which is equal to $\frac{K_b b}{t}$ where K_b is the bond thermal conductivity, t is the bond average thickness, and b is the bond width.

D_i is the inside tube diameter.

$h_{f,i}$ is the heat transfer coefficient inside tubes.

m is a parameter equal to $\sqrt{\frac{U_i}{k\delta}}$, where k is the thermal conductivity of the absorber plate and δ is the absorber plate thickness.

The heat removal factor for the serpentine type is given by (12):

$$F_{r,s}/F_1 = B[1 - \exp[(F_2 - 1)/B]] \quad (3.6)$$

where,

$$F_1 = \frac{NK'L}{F_2 A_c U_i C} \quad (3.7)$$

$$(3.8) \quad B = \frac{mC_p F_1 A_c U_l}{I}$$

$$(3.9) \quad F_2 = \frac{[K'R(1+\gamma)^2 - 1 - \gamma' - K'R]}{I}$$

$$(3.10) \quad C = [K'R(1+\gamma) - 1]^2 - (K'R)^2$$

$$(3.11) \quad K' = \frac{(W - D) \sin hn}{k \delta n}$$

$$(3.12) \quad n^2 = (W - D)^2 \left(\frac{k \delta}{U_l}\right)$$

$$(3.13) \quad \gamma' = -2 \cosh n - \left(\frac{K'}{DU_l}\right)$$

$$(3.14) \quad R = \frac{C_b}{I} + \frac{\pi D_i h_{f,i}}{I}$$

where: B is the collector capacitance rate, N is the number of tube segments of the

serpentine type, L is the length of the tube segments of the serpentine type, and R

is the thermal resistance between the plate and the flowing fluid.

The useful heat gain is also given by (1):

$$(3.15) \quad Q_u = mC_p(T_o - T_i) \cdot \tau_i$$

where, T_o is the collector outlet fluid temperature and τ_i is time in seconds of the

test interval.

The instantaneous efficiency (η_i) can be expressed as:

$$(3.16) \quad \eta_i = \frac{Q_u}{A_c I} * 100\%$$

Also, it can be obtained from equation (3.1) as:

$$(3.17) \quad \eta_i = [F_2(\tau \alpha)_e - F_1 U_l \frac{I}{(T_i - T_a)}] * 100\%$$

Also, we can write:

$$(3.18) \quad \eta_i = \frac{A_c I}{mC_p(T_o - T_i)} * 100\%$$

If the three governing parameters were all constants then, the plot of η_i versus $(T_i - T_a)/I$ would be a straight line with intercept $F_r(\tau\alpha)_e$ and slope $-F_r U_l$.

The daily efficiency of the solar collector is the ratio of the useful energy gain obtained during the test day to the total radiation incident on the collector area during the complete day, thus,

$$\eta_d = \frac{Q_{ut}}{A_c I} * 100\% \quad (3.19)$$

3.4 Experiment Set-Up

The experiment set up consists of the, solar panels, constant head feed tank, storage tanks, circulation pumps, and the piping network.

1. Solar Panels:

Two solar panels are used, one of the serpentine type and the other of the parallel type. The panels are oriented to face south. They are mounted on a metal frame with tilt angle of 22° .

2. Constant Head Feed Tank:

One constant head tank of 1000 litre capacity is used as a feed tank for both collectors. It is made of galvanized steel of 1.25 mm thick. A constant head is maintained by a float, and the outlet flow is controlled by a gate valve. The tank is placed over a metal frame 1.5 m high.

3. Circulating Pumps:

A single-phase centrifugal pump of 0.5 hp was used to circulate the water through the solar panels of each model. By-pass valves are used to control the flow rate at any required value.

4. Piping Network:

Galvanized steel pipes (GSP), of 17 mm diameter are used in all connections except the connections between the outlet of each panel and the inlet of the storage tanks where a 28.4 mm diameter galvanized steel pipes were used. All pipes are insulated by 30 mm thick rock wool, to minimize heat losses.

3.5 Measuring Instruments

In this section a brief description of the used instruments will be introduced:

3.5.1 Incident Solar Radiation Measurement

Incident solar radiation is measured by a Kipp and Zonen pyranometer (type CM5). It was installed on the plane of the tested solar panels (22° tilt angle). A solar integrator (type CC11) is employed to record the incident solar radiation in Wh/m^2 . The incident solar radiation was measured at regular intervals of time of 30 minutes.

3.5.2 Temperature Measurement

The temperature at different locations in the test was measured by means of Copper Constantan thermocouples. Fifteen thermocouple wires are used to measure the water temperatures in this experiment, nine of which are used for the serpentine

model and the remaining six for the parallel model. The thermocouple wires were connected to two Multi-Point Digital Thermometers (Microprocessor Thermometer 6200).

3.5.3 Flow Rate Measurement:

Water flow rates are measured by means of two rotameters. One rotameter is placed at the inlet of each solar panel. The flow rate that can be measured by this device ranges from 0.01 to 0.1 Kg/s .

3.5.4 Wind Velocity Measurement:

Wind velocity is measured by means of a digital anemometer (type Edra 5). The velocity ranges that can be measured by this device ranges from 0.3 to 30 m/s .

Readings of wind velocity are recorded every 30 minutes over three selected locations around the solar panels. These readings were used to estimate the average wind velocities. These average velocities were used to estimate the daily wind velocity (V_w).

3.6 Experimental Test Conditions

Jordan lies between latitude 29° and 33° north and is bisected by the 36° meridian. The average dry bulb temperature ranges from $-5C^\circ$ in winter to $35C^\circ$ in summer. The sun hours duration averages 6 hours during winter months and 12.5 hours in summer. The average daily solar radiation is about $5 KWh/m^2$, and the sun-shine duration of about 3000 hours per year [2]. The recommended values for collector tilt are $\theta + 10$ for winter conditions and $\theta - 10$ for summer conditions where

θ is latitude angle [18].

The collectors of this study were mounted on the roof of the Mechanical Engineering Department, University of Jordan, Amman (Latitude = 32° , Longitude= 36° and height=980m), Jordan.

The relative performance comparison of the two collectors were studied under the following experimental test conditions:

1. Same effective tubing length, diameter and material.
2. Same absorber plate area, thickness and material.
3. Same transparent cover glass material and thickness ($\delta = 4.0mm$).
4. Same insulation material and thickness.
5. Same collector tilt angle ($\beta = 22^{\circ}$).
6. Same surface azimuth angle ($\gamma = 0$).
7. Same working fluid flow ((fresh water)).
8. Same coating material (ordinary black paint).

3.7 Experimental Tests And Procedures

Collectors can be tested either outdoors or indoors. In the present work the two collectors were tested outdoors.

The ASHRAE 93-77 standard procedure [19] was followed to test both collectors when they are operated as closed loop and open loop circulated flows.

The tests were performed on clear days during the months of July, August and September, 1991. In each experimental day, the glass covers of both collectors were cleaned before beginning the test, then the pyranometer was properly installed on the collectors plane. For the forced circulation tests, water was fed for each model at the same temperature at the beginning of each experiment by means of two identical circulated pumps. The required circulated flow rate was adjusted to a selected value with the help of the rotameter and the by pass valves of the pumps. All experiments were started at 08 : 00. At such time both collectors brought to the same identical experimental conditions. The experimental measurements were recorded every 30 minutes from 08:00 until 17 : 00. The recorded measurements are:

1. Inlet (T_{i_s}) and outlet (T_{o_s}) water temperatures for the serpentine collector.
2. Inlet (T_{i_p}) and outlet (T_{o_p}) water temperatures for the parallel collector.
3. Temperature distribution of the water flow inside the serpentine collector at certain distances, T_1 , T_2 , and T_3 .
4. Ambient temperature (T_a).
5. Temperature of the consumed water from the serpentine model (T_{u_s}).
6. Temperature of the consumed water from the parallel model (T_{u_p}).
7. Temperature distribution of the water inside the serpentine type storage tank T_{t_s} , T_{m_s} , T_{l_s} , and inside the parallel type storage tank T_{t_p} , T_{m_p} , and T_{l_p} .
8. Solar incident radiation on the collectors plane (I).

9. Water mass flow rate (\dot{m}).

10. Wind speed (V_w).

In this study, the word 'load' refers to the proposed amount of the used domestic hot water.

Figure (3.1) shows three photographs for the experiment set-up. The following tests were executed simultaneously for both collectors:

3.7.1 Forced Circulation Test With No Load Conditions

This test is performed based on two different storage tank volumes, which are 150 litre and 50 litre.

For the 150 litre storage tank, four tests were performed on August 5th, 4th, 3rd and July 25th, 1991 with flow rates of 0.02, 0.03, 0.05, and 0.07 Kg/s, respectively. The layout of this test is shown in Figure(3.2), while the averaged measured data are shown in Tables (A.1 – A.4) of Appendix A. The averaged data reported in these tests were obtained by adding the temperatures measured at the beginning and end of each time interval and dividing the result by 2.

For the 50 litre common storage tank another four tests were performed on September 3rd, 2nd, 4th and August 27th, 1991 with flow rates of 0.02, 0.03, 0.05 and 0.07 Kg/s, respectively. The averaged measured data of these tests are shown in Tables (A.5 – A.8) of Appendix A. For this test a common storage tank is used for both collectors in order to provide both collectors with the same inlet water temperature during all the experimental day. Layout of this test is shown in Figure(3.3).

Also, both collectors were tested on September 9th, 1991, with two different mass

flow rates, where the flow rates in tube segments are equal, the selected flow rates are 0.015 Kg/s for the serpentine type and 0.15 Kg/s for the parallel type. The averaged measured data for this test are shown in Table(A.9) in Appendix A.

The objectives of above tests are to evaluate the instantaneous efficiency and the other performance parameters for each model at different mass flow rates under no load conditions.

3.7.2 Forced Circulation Test With Load Conditions

In this test no storage tanks are needed. A constant head tank is used to supply a fresh water continuously at constant temperature to feed both collectors. The water level in the head tank is kept constant by connecting it with municipality line (tap) during the day of the test. The outlet hot water from each collector is used as a hot water load as shown in Figure (3.4). The layout shown in Figure (3.4) does not allow any mixing between the fresh feed water and the consumed hot water.

This test is performed on September 12th and 14th, 1991, with flow rates of 0.02 and 0.05 Kg/s , respectively. The averaged measured data are shown in Tables (A.10-A.11) of Appendix A.

The objectives of this test are to evaluate the daily efficiency for each model at different flow rates for various load conditions.

3.7.3 Forced Circulation Test With Intermittent Load

This test is based on consuming a certain amount of water (5, 10, and 15 l/h) at the end of each hour during the experimental day. A 50 litre storage tank was used for each model. A head tank is used to supply water for the storage tanks of

both collectors, so the temperature of the make up water for both collectors is the same. As in the forced circulation test with load conditions, the water level in the head tank is kept constant by connecting it with municipality line (tap) during the test day. The layout of the test is shown in Figure (3.5).

Two mass flow rates of 0.03 and 0.07, Kg/s are selected for this test. For the 0.03 Kg/s mass flow rate the test was performed on August 19th, 20th, and 21st, 1991, with intermittent loads of 5, 10, and 15 l/h , respectively. While for the 0.07 Kg/s flow rate the test was performed on August 24th, 25th, and 26th, 1991, with loads of 5, 10, and 15 l/h , respectively.

During this test the temperature of the consumed water from the serpentine model (T_{us}) as well as the parallel model (T_{up}) were measured and recorded. The averaged measured data of this test are shown in Tables (A.12-A.17) of Appendix A.

The objectives of this test is to examine the degree of response of each model for hot water demands, under different load conditions and various flow rates.

3.7.4 Stagnation Test

The stagnation conditions implies that the heat loss from the absorber plate is equal to the absorbed solar irradiance. This condition occurs when the useful heat removed from the collector will equal to zero.(i.e stagnation conditions are attained when the temperature rise across the solar panel reaches zero.). So,

$$F_r A_c [I(\tau\alpha)_e - U_l(T_i - T_a)] = 0$$

which yields:

$$U_l = \frac{I(\tau\alpha)_e}{T_i - T_a} \quad (3.20)$$

Experimentally, it is difficult to reach the stagnation conditions, especially, during hot summer days. In this test several experimental tests were performed until the stagnation conditions are attained on September 10th, 1991, where the flow rate was 0.02 Kg/s with a common storage tank of 50 litre for both collectors.

The averaged measured data of this test are presented in Table (A.18). The objectives of this test are to evaluate the overall heat loss coefficients for the serpentine and the parallel types. The stagnation test arrangement, which is used for this test is the same as that used for the forced circulation test with no load conditions with a common 50 litre capacity storage tank.

3.7.5 No-Load Thermosyphon Test

In this test a 50 litre capacity storage tank is used for each model as shown in Figure (3.6).

The objectives of this test are to evaluate the instantaneous efficiency and the other performance parameters for each model under no load natural flow conditions.

This test was performed on September 18th, 1991. The averaged measured data of this test are presented in Table (A.19) of Appendix A.

3.7.6 Intermittent Load Thermosyphon Test

This test is performed on September 19th, 21st, and 22nd, 1991, with intermittent loads of 5, 10, and 15 l/h, respectively. During this test the temperature of the consumed water from both collectors are measured. The averaged measured data

of this test are shown in Tables (A.20 -A.22) in Appendix A. Figure (3.7) shows a layout of the test arrangement.

The objectives of this test are to examine the degree of response of each model for hot water demands at different loads under natural flow conditions.

3.7.7 Time Constant Test

Time constant is a measure of the rapidity of a collector's response to transient solar conditions [20]. It is defined as the time required for a fluid leaving a collector to attain change through 0.632 of the total change from its initial to its ultimate steady value after a step change in incident radiation or inlet fluid temperature [1].

The outlined ASHRAE standard test procedure [19] were followed for estimating the time constants of both collectors. The systems were operated on September 11th, 1991. The test was performed with an inlet water temperature of 28.4C^o for both collectors., at 13.00 the solar radiation is abruptly shut off by shading the tested collectors, then the outlet temperature of each collector is recorded every minute until the equality of equation (3.21) is attained.

$$\frac{T_{o,rc} - T_i}{T_{o,i} - T_i} = 0.368 \quad (3.21)$$

where, $T_{o,rc}$ is the water outlet temperature at time rc where rc is the time constant. $T_{o,i}$ is the outlet temperature when solar radiation is interrupted. T_i is the inlet water temperature during the test.

The measurements of this test are shown in Table (A.23) in Appendix A. The layout of the time constant test is shown in Figure (3.4) which is the same arrangement of the forced circulation test with load conditions.

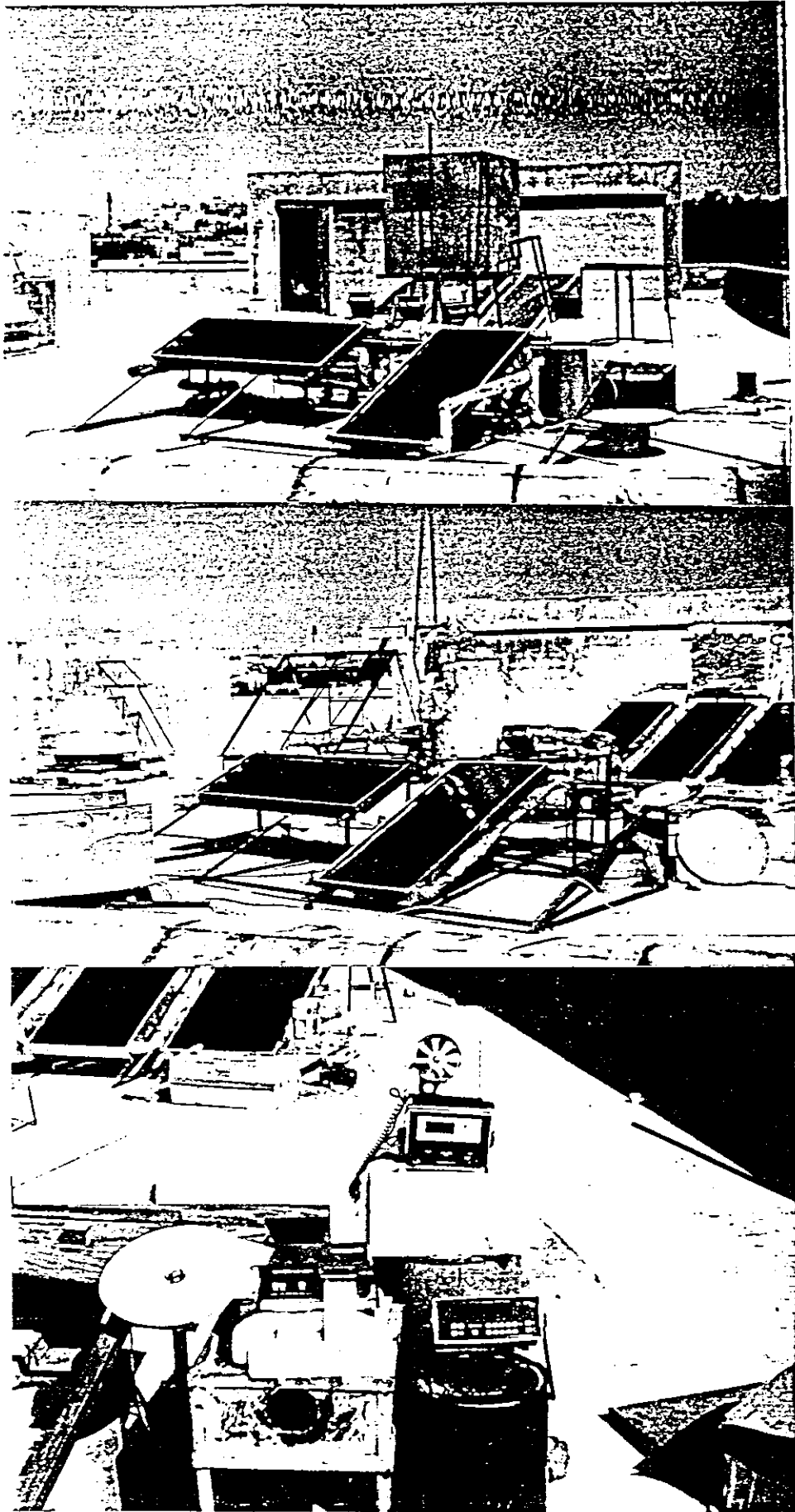


Fig.(3.1) Three photographs of the experiment set-up.

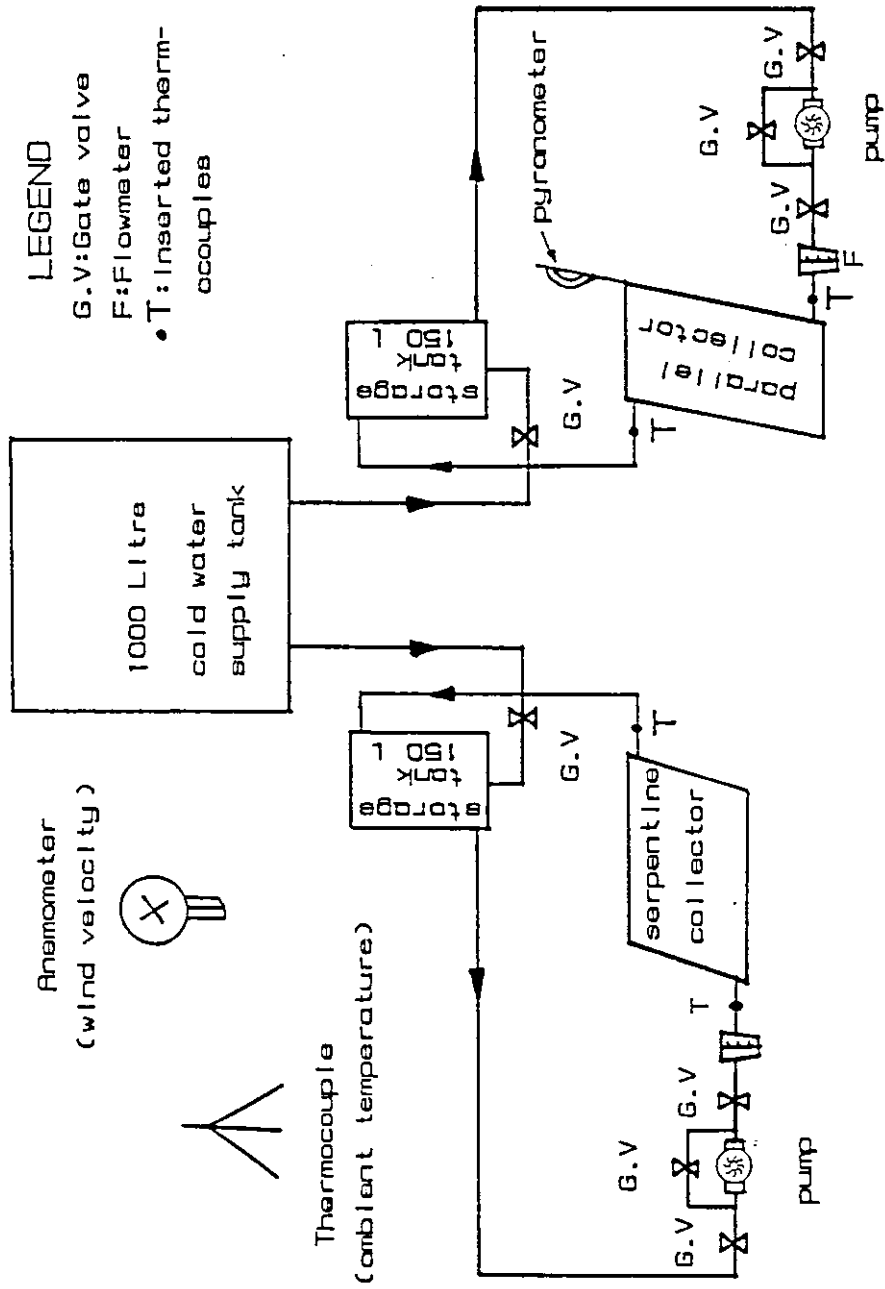
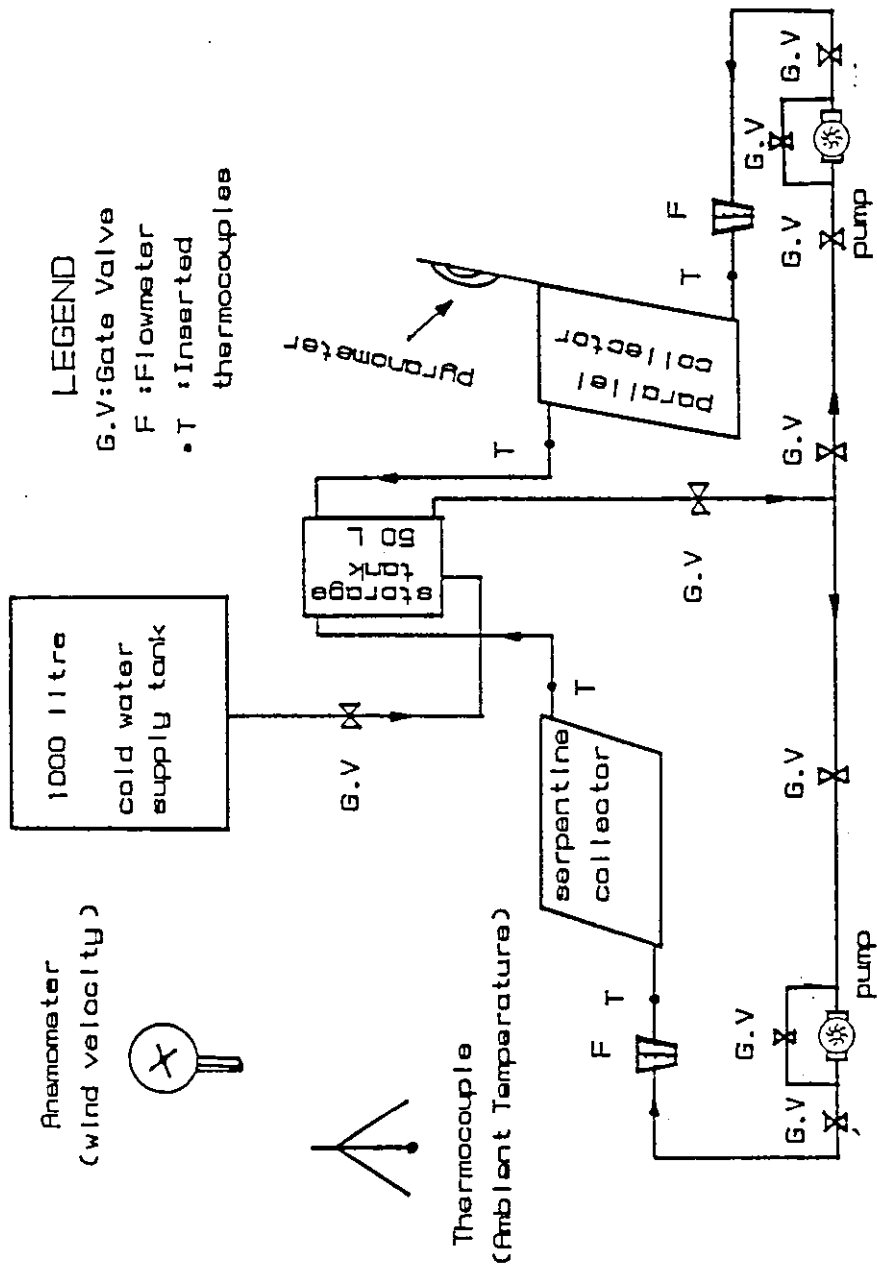


Fig. (3.2) Closed loop set-up for No-Load tests based on ASHRAE Standard 93-77 (1977).

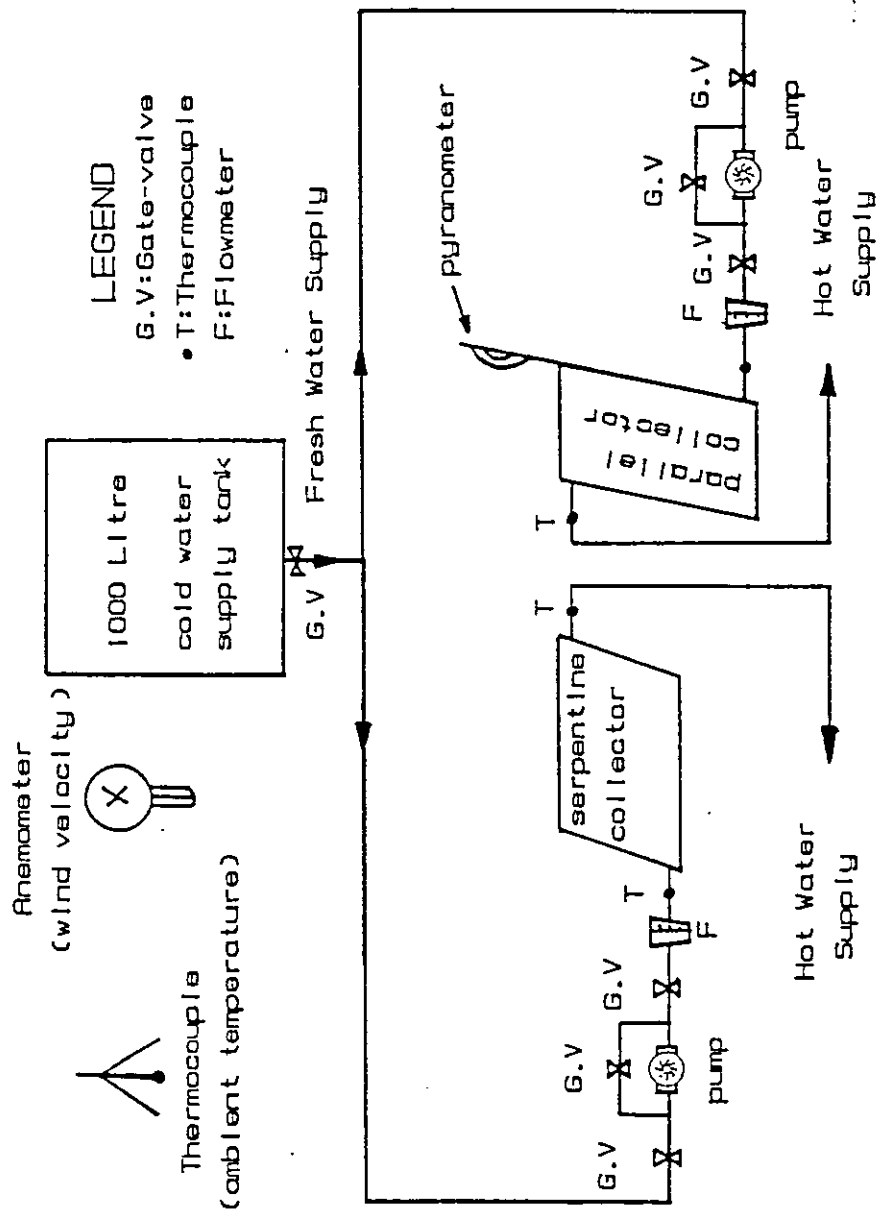


LEGEND
 G.V.: Gate Valve
 F : Flowmeter
 T : Inserted thermocouples

Anemometer
 (wind velocity)

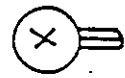
Thermocouple
 (Ambient Temperature)

Fig.(3.3) Closed loop set-up for No-Load tests and the stagnation test, where both collectors are connected to the same storage tank.



LEGEND
 G.V: Gate-valve
 • T: Thermocouple
 F: Flowmeter

Anemometer
 (wind velocity)



Thermocouple
 (ambient temperature)



Fig. (3.4) Open-loop set-up for load tests based on ASHRAE Standard 93-77 (1977).

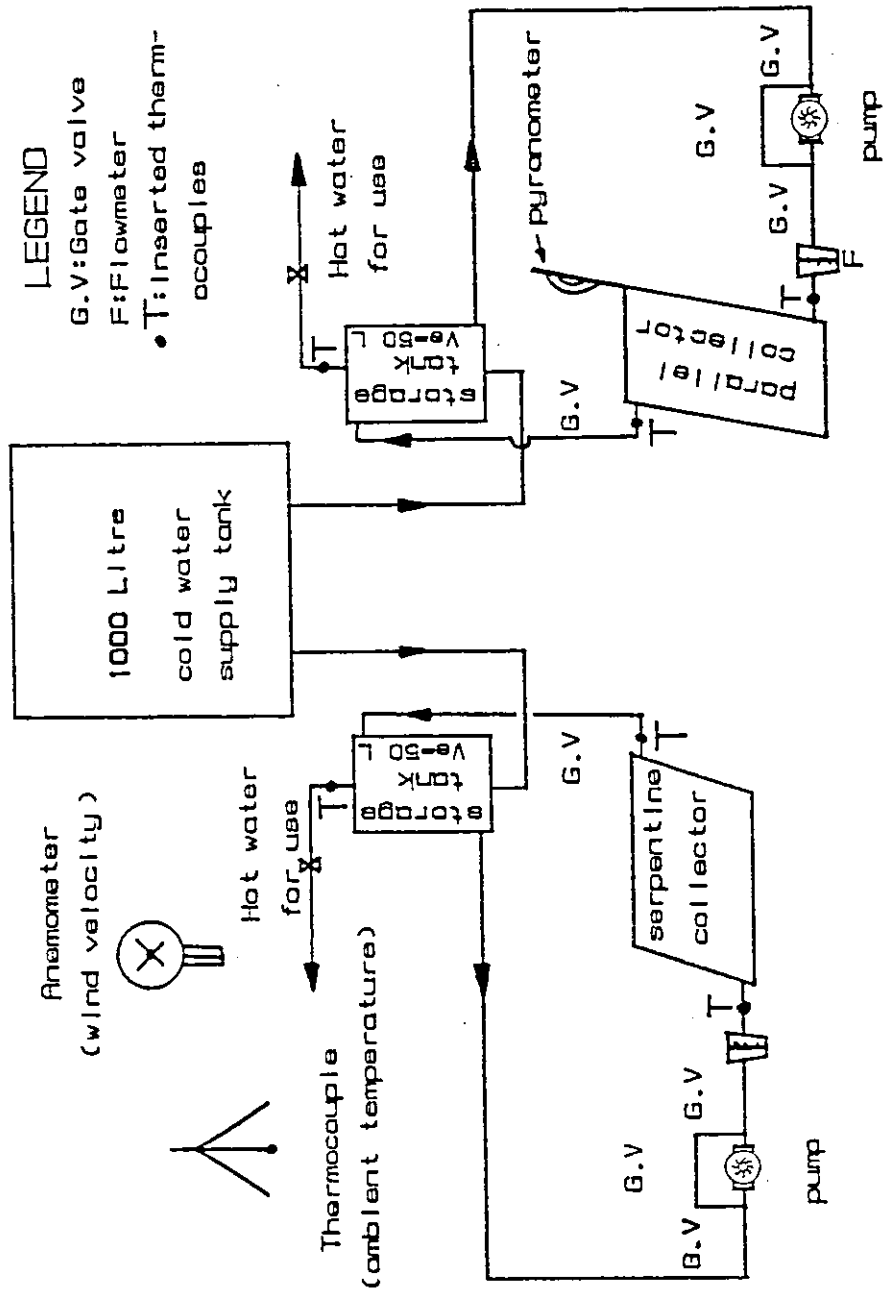


Fig.(3.5) A loop set up for the forced circulation test with intermittent load conditions.

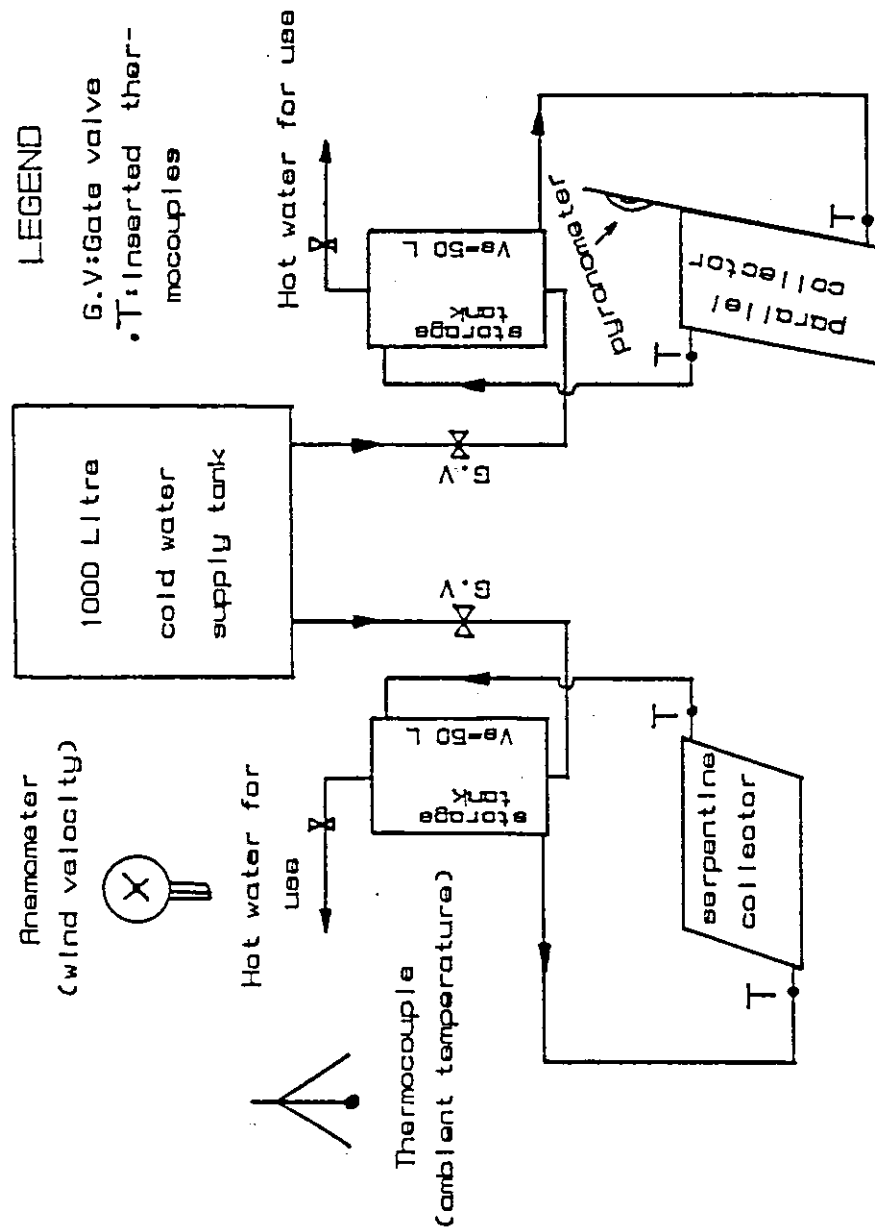


Fig.(3.7) A loop set-up for the intermittent load. thermosyphon test.

Chapter 4

RESULTS AND DISCUSSION

4.1 Introduction

The performance comparison between the serpentine and the parallel types is carried out by performing seven tests, as outlined in chapter three.

This chapter is divided into three sections of which this introduction . Section (4.2) deals with performance calculations and results. A sample calculation, showing the estimating procedure of each parameter for each test is outlined.

In the last section the results of this study are discussed and analyzed.

4.2 Performance Calculations And Results

Most of the calculations of this study were performed by using a Fortran Computer Program as presented in Appendix (B). For all tests, all measured temperatures during a given interval were averaged by using the values at the beginning and end of each time period. The calculations are based on the performance equations introduced in section (3.3) of the previous chapter. The results of these calculations are tabulated in Appendix (C). All calculations are based on the absorber plate area. Plots and Figures of this study are prepared by using the Computer Ener Graphics

Package.

In the following sub-sections, the results of all tests are introduced with a sample calculation for each test.

4.2.1 Results of The Forced Circulation Test With No Load Conditions

As outlined earlier in section (3.7.1), this test was performed by using three different arrangements as related to the storage tank used: The first arrangement when a storage tank of 150 *litre* capacity is used for each model, the water flow rates used are 0.02, 0.03, 0.05, and 0.07 *Kg/s*. The second considered arrangement is when both collectors have a common storage tank of 50 *litre* capacity, and water flow rates of 0.02, 0.03, 0.05, and 0.07 *Kg/s*. The third arrangement is when the flow rates in the tube segments of both collectors are equal, this lead to a flow rate of 0.015 *Kg/s* for the serpentine model and 0.105 *Kg/s* for the parallel model.

All averaged measured temperatures of this test, as presented in Tables (A.1-A.9) are plotted as a function of time as shown in Figures (4.1-4.17). On the other hand, Figures (4.18-4.26) show the temperature distribution of the water inside the serpentine collector at selected times of the day.

Using the averaged measured temperatures of Table (A.1-A.9) the useful energy gain is calculated using equation (3.15). The variation of the useful energy gain, as well as the incident solar radiation with time of day are shown in Figures (4.27-4.35) for both collectors at different flow rates.

The instantaneous efficiency is calculated using equation (3.18). This equation is applied assuming constant ambient temperature and radiation during each time

interval (30 minutes). The variations of the instantaneous efficiency with $(T_i - T_a)/I$ for both collectors at different flow rates are shown in Figures (4.36-4.44). The available Linear Least Squares fitting in the Ener Graphics Package was used to express these variations linearly. According to equation (3.17) the intercept with the Y - axis represents $F_r(\tau\alpha)_e$ and the slope of the equation represents $-F_r U_l$.

Tables (4.1) and (4.2) list the obtained instantaneous efficiency expressions for storage tank capacities of 50 and 150 litre for both the serpentine and the parallel types, respectively. Each expression of these instantaneous efficiencies represents a separate day, where the wind velocity is different from day to day.

Table (4.1) Instantaneous efficiency expressions for the serpentine type

\dot{m} Kg/s	Serpentine	
	$V_s = 50 l$	$V_s = 150 l$
0.02	$\eta_i = 0.5720 - 2.208(T_{i,s} - T_a)/I$	$\eta_i = 0.6912 - 4.002(T_{i,s} - T_a)/I$
0.03	$\eta_i = 0.6088 - 2.396(T_{i,s} - T_a)/I$	$\eta_i = 0.6972 - 3.197(T_{i,s} - T_a)/I$
0.05	$\eta_i = 0.6537 - 1.975(T_{i,s} - T_a)/I$	$\eta_i = 0.7171 - 3.176(T_{i,s} - T_a)/I$
0.07	$\eta_i = 0.7076 - 2.694(T_{i,s} - T_a)/I$	$\eta_i = 0.7207 - 3.613(T_{i,s} - T_a)/I$

Table (4.2) Instantaneous efficiency expressions for the parallel type

\dot{m} Kg/s	parallel	
	$V_s = 50 L$	$V_s = 150 L$
0.02	$\eta_i = 0.5460 - 2.153(T_{i,p} - T_a)/I$	$\eta_i = 0.6252 - 3.845(T_{i,p} - T_a)/I$
0.03	$\eta_i = 0.5600 - 2.272(T_{i,p} - T_a)/I$	$\eta_i = 0.6518 - 3.386(T_{i,p} - T_a)/I$
0.05	$\eta_i = 0.5812 - 1.862(T_{i,p} - T_a)/I$	$\eta_i = 0.6675 - 3.565(T_{i,p} - T_a)/I$
0.07	$\eta_i = 0.6069 - 2.342(T_{i,p} - T_a)/I$	$\eta_i = 0.6817 - 3.877(T_{i,p} - T_a)/I$

To illustrate the calculation procedure for determining the instantaneous efficiency needed to obtain the expressions of Tables (4.1) and (4.2), the averaged measured data for the time interval 11 : 00 - 11 : 30 is considered. Referring to Table (A.1) the mass flow rate is 0.02 Kg/s and $V_s = 150 l$ the averaged measured data for this time interval are:

$$T_{i,s} = 34.0C^\circ \quad T_{o,s} = 38.2C^\circ \quad T_a = 23.3C^\circ \quad \text{and} \quad I = 487.8Wh/m^2$$

The useful energy gain is calculated using equation (3.15) as follows:

$$\begin{aligned} Q_{us} &= \dot{m}C_p(T_{os} - T_{is}) \cdot \tau_t \\ &= 0.02 * 4.186(38.2 - 34.0) * 1800 \\ &= 632.9KJ \end{aligned}$$

The incident solar energy (I) in KJ/m^2 is calculated as follows:

$$\begin{aligned} I &= 487.8 * 1800 \\ &= 878.0KJ/m^2 \end{aligned}$$

The instantaneous efficiency of the collector during this interval is evaluated using equation (3.16):

$$\eta_i = \frac{Q_{us}}{IA_a} * 100\%$$

Where, A_a is the absorber plate area which is equal to:

$$\begin{aligned} A_a &= 0.73 * 1.59 \\ &= 1.161m^2 \\ \eta_i &= \frac{632.9}{878.0 * 1.161} * 100\% \\ &= 62.1\% \end{aligned}$$

The term $(T_{i_s} - T_a)/I$ for the same time interval is obtained as follows:

$$\frac{T_{i_s} - T_a}{I} = \frac{34.0 - 23.3}{487.8}$$

$$= 0.02194m^2.C^{\circ}/Wh$$

The values of the above parameters for all time intervals are obtained following similar procedure. The results of these calculations for all tests are shown in Tables (C.1-C.9).

4.2.2 Results of The Forced Circulation Test With Load Conditions

The variation of all the averaged measured temperatures for this test with time of day as expressed in Tables (A.10-A.11) are plotted in Figures (4.45-4.48). The temperature distribution of water inside the serpentine collector are shown in Figures (4.49-4.50) at selected times in the day.

The useful energy gain for each test interval (30 minutes) is calculated using equation (3.15). The results of such calculations are shown in Tables (C.10-C.11) in Appendix (C). The useful energy gain as well as the incident solar radiation are plotted versus time of day for each model as shown in Figures (4.51-4.52).

The daily efficiency is calculated using equation (3.19) for flow rates of 0.02 and 0.05 Kg/s. Table (4.3) presents the daily efficiencies for both collectors at two different flow rates.

Table (4.3) Daily efficiency of the tested solar collectors

Model	\dot{m}	$\eta_d\%$
Serpentine	0.02	46.4
	0.05	58.8
Parallel	0.02	41.1
	0.05	49.5

To illustrate the calculation procedure of the daily efficiency, the useful energy gains for the serpentine type are considered. Referring to Table (C.10) the daily useful energy gain is 6670.8 KJ and the total radiation incident on the collector area during the complete day is 14373.2 KJ, so, using equation (3.19) the daily efficiency is:

$$\eta_d = \frac{6670.8}{14373.2} * 100\%$$

$$= 46.4\%$$

4.2.3 Results of The Forced Circulation Test With Intermittent Load

The averaged measured temperatures of the consumed water of Tables (A.12-A.17) are plotted versus time of day for the different loads and flow rates, and they are presented in Figures (4.53-4.58).

The useful heat gain is calculated based on equation (3.15). The results of these calculation are shown in Tables (C.12-C.17). Figures(4.59- 4.64) show the variation of the useful heat gain for both collectors as well as the incident solar radiation with time of day.

4.2.4 Stagnation Test Results

In this test the overall heat loss coefficients for both collectors were determined as follows:

As presented in Table (A.18) the stagnation conditions are attained during the time interval 14.00 – 14 : 30 for the serpentine and the parallel types. The averaged measured data during this interval are as follows:

$$T_{i_s} = 95.0C^{\circ} \quad T_{o_s} = 95.1C^{\circ} \quad T_{i_p} = 92.9C^{\circ} \quad T_{o_p} = 93.0C^{\circ}$$

$$T_a = 28.7C^{\circ} \quad \text{and} \quad I = 397.0Wh/m^2$$

The overall heat loss coefficient can be calculated by using equation (3.20) which yields:

$$U_{i_s} = \frac{397.0 * 0.81}{95.0 - 28.7}$$

$$= 4.85W/m^2C^{\circ}$$

similarly for the parallel type:

$$U_{i_p} = \frac{397.0 * 0.81}{92.4 - 28.7}$$

$$= 5.01W/m^2C^{\circ}$$

4.2.5 Results of The No-Load Thermosyphon Test

The averaged measured data for this test are presented in Table (A.19). Figures (4.65-4.68) show the variation of the averaged measured temperatures with time of day. Also, Figure (4.69) presents the temperature distribution of the water inside the serpentine collector at selected times in the day.

For the serpentine type, the heat removal factor $F_{r,s}$ is calculated by using equation (3.6) which requires the determination of, F_1 , F_2 , and B . The values of F_1 , and F_2 can be easily calculated from equation (3.7) and (3.9), respectively. Table (4.4) presents the calculated parameters needed to estimate $F_{r,s}$. Equations (3.7-3.14) were used for this purpose. Other parameters of the collector such as $(\tau\alpha)_e$, W , D_o , ...etc are also listed in this table.

Table 4.4 : Given and calculated parameters for the serpentine type

Given parameter	Value	Calculated parameter	Value
$(\tau\alpha)_e$	0.81	R	$0.0624m.C^\circ/W$
W	$0.1m$	n	0.7924
D_o	$0.0215m$	K'	$0.5473W/m.C^\circ$
D_i	$0.017m$	γ	-2.852
k	$47.6W/m.C^\circ$	C	1.1293
C_b	0	F_2	0.517
$h_{f,i}$	$300W/m^2.C^\circ$	F_1	1.8534
δ	$0.001m$	U_{ts}	$4.85W/m^2.C^\circ$

The collector capacitance rate, B , can't be evaluated without knowing the flow rate, \dot{m} , which is usually unknown. Trail and Error method can be followed for determining the heat removal factor, such procedure can be summerized as follows:

1. An initial guess of $F_{r,s}$ enables the estimation of \dot{m} , by using the relation:

$$\dot{m}C_p(T_{os} - T_{is}) = A_c F_{r,s} [I(\tau\alpha)_e - (T_{is} - T_a)] \quad (4.1)$$

Then,

$$\dot{m} = \frac{A_c F_{r,s} [I(\tau\alpha)_e - (T_{is} - T_a)]}{C_p (T_{os} - T_{is})} \quad (4.2)$$

2. The collector capacitance rate B , is evaluated by the use of equation (3.8).

This value of B , is substituted in equation (3.6) to find a new value of $F_{r,s}$.

3. The new $F_{r,s}$ is used as a second guess which can be used in equation (4.2) to evaluate m , and the procedure is repeated to new value of $F_{r,s}$.
4. The last two values of $F_{r,s}$ are compared until the difference in this value is smaller than a predetermined value of 10^{-3} .

The above procedure can be illustrated by considering the time interval 10 : 00 – 10 : 30. From Table (A.19) the averaged measured data are:

$$T_{i,s} = 32.8C^{\circ} \quad T_{o,s} = 46.0C^{\circ} \quad T_a = 25.2C^{\circ} \quad I = 407.5Wh/m^2$$

Substituting the given data into equation (4.2) yeilds:

$$\dot{m} = \frac{1.1607 \times F_{r,s} [0.81 \times 407.5 - 4.85(32.8 - 25.2)]}{4186(46.0 - 32.8)} \quad (4.3)$$

First Iteration:

let $F_{r,s} = 0.790$ and substitute in equation (4.3) yeilds:

$$\dot{m} = 4.86586 * 10^{-3} Kg/s$$

Put this value into equation (3.8), then:

$$B = 1.95222$$

And from equation (3.6):

$$F_{r,s} = 0.7931$$

So,

$$|F_{r,s}(old) - F_{r,s}(new)| = 3.1 * 10^{-3} > 10^{-3}$$

Second Iteration:

Take $F_{r,s} = 0.7931$

Then $\dot{m} = 4.88495 \times 10^{-3} \text{ Kg/s}$

So, $B = 1.95988$

Which yields:

$$F_{r,s} = 0.7934$$

$$|F_{r,s}(\text{old}) - F_{r,s}(\text{new})| = 2.458 \times 10^{-4} < 10^{-3}$$

So,

$$F_{r,s} = 0.7934$$

$$\dot{m} = 4.89 \times 10^{-3} \text{ Kg/s}$$

The useful heat gain is calculated using equation (3.15) as follows:

$$\begin{aligned} Q_{u,s} &= 0.00489 \times 4.186(46.0 - 32.8) \times 1800 \\ &= 486.4 \text{ KJ} \end{aligned}$$

And the instantaneous efficiency is evaluated using equation (3.16) as follows:

$$\eta_i = \frac{486.4}{733.5 \times 1.161} = 57.1\%$$

For the parallel type the heat removal factor is calculated using equation (3.3) which requires the determination of F , F' , and \dot{m} . The values of F and F' can be easily calculated from equations (3.5) and (3.4), respectively. Table (4.5) presents the given and the calculated parameters for the parallel type based on equations (3.4-3.5).

Table 4.5 : Given and calculated parameters for the parallel type

Given parameter	Value	Calculated parameter	Value
$(\tau\alpha)_e$	0.81	U_{lp}	$5.01W/m^2C^o$
W	0.1m	m	10.2592
D_o	0.0215m	F	0.9492
D_i	0.017m	F'	0.9322
k	47.6W/m.C ^o		
C_b	0		
$h_{f,i}$	300W/m ² C ^o		
δ	0.001m		

The unknown parameter in equation (3.3) is the flow rate. Trail and error method can be used for determining the heat removal factor which can be summerized as follows:

1. An initial guess of F_{rp} enables the estimation of m , by using the relation:

$$\dot{m}C_p(T_{op} - T_{ip}) = A_c F_{rp} [I(\tau\alpha)_e - U_{lp}(T_{ip} - T_a)] \quad (4.4)$$

2. The calculated flow rate \dot{m} is substituted in equation (3.3) to calculate a new value for F_{rp} .
3. The new F_{rp} is used as a second guess and entered in equation (4.4) to evaluate m .
4. The last two values of F_{rp} are compared until the difference in this value is smaller than a predetermined value of 10^{-3} .

The above procedure is illustrated by considering the time interval 10 : 00 – 10 :

30. From Table(A.19) the averaged measured data are:

$$T_{ip} = 33.5C^o \quad T_{op} = 45.6C^o \quad T_a = 25.2C^o \quad \text{and} \quad I = 407.5Wh/m^2$$

Using equation (4.4) and substituting the given parameters yields:

$$\dot{m} = \frac{1.1607 \times F_{rp} [0.81 \times 407.5 - 5.01(33.5 - 25.2)]}{4186(45.6 - 33.5)} \quad (4.5)$$

Also, from equation (3.3) F_{rp} is given by:

$$F_{rp} = 719.8492 \dot{m} \left[1 - \exp\left(\frac{-1.295 \times 10^{-3}}{\dot{m}}\right) \right] \quad (4.6)$$

First Iteration:

let $F_{rp} = 0.825$ and substitute in equation (4.5) yields:

$$\dot{m} = 5.45409 \times 10^{-3} \text{ Kg/s}$$

Then from equation (4.6):

$$F_{rp} = 0.8298$$

$$|F_{rp}(\text{old}) - F_{rp}(\text{new})| = 4.8 \times 10^{-3} > 10^{-3}$$

Second Iteration:

Take $F_{rp} = 0.8298$ Then $\dot{m} = 5.48583 \times 10^{-3} \text{ Kg/s}$ and, $F_{rp} = 0.8303$

$$|F_{rp}(\text{old}) - F_{rp}(\text{new})| = 5.0 \times 10^{-4} < 10^{-3}$$

So, $F_{rp} = 0.8303$ and $\dot{m} = 5.49 \times 10^{-3} \text{ Kg/s}$

The useful energy gain is calculated using equation (3.15) as follows:

$$Q_{up} = 0.00549 \times 4.186(45.6 - 33.5) \times 1800$$

$$= 500.5 \text{ KJ}$$

And the instantaneous efficiency is calculated using equation (3.16) as follows:

$$\begin{aligned}\eta_i &= \frac{500.5}{733.5 \times 1.161} \times 100\% \\ &= 58.8\%\end{aligned}$$

Table (C.18) shows the calculated performance parameters for this test. The useful heat gain as well as the incident solar radiation are plotted versus time of day for each model are shown in Figure (4.70). Figure (4.71) shows the variation of the instantaneous efficiency with $(T_i - T_a)/I$ for for both collectors.

4.2.6 Results of The Intermittent Load Thermosyphon Test

The averaged measured data for this test are shown in Tables (A.20)-(A.22). Based on these measurements, the variation of the inlet, outlet and the used hot water temperatures with time of day are shown in Figures (4.72 -4.74) for both collectors.

4.2.7 Time Constant Test Results

Based on Table (A.23), the outlet temperature for each model is plotted with time of day as shown in Figure (4.75). Using this figure and equation (3.21) the time constant is calculated for each model as follows:

From Table (A.23), the average ambient temperature, T_a is $28.5C^\circ$, the average inlet water temperature, $T_{i,s}$, during the day test is $28.4C^\circ$, and the average outlet water temperature, $T_{o,i}$, when solar radiation is suddenly interrupted is $32.9C^\circ$.

From equation (3.20) the average outlet water temperature, $T_{o,\tau c}$ at the time constant, τc , is :

$$T_{o,\tau c} = 0.368(T_{o,i} - T_i) + T_i$$

So,

$$T_{0,\tau c} = 0.368(32.9 - 28.4) + 28.4$$

$$= 30.056C^{\circ}$$

Referring to Table (A.23) or Figure(4.75), this value of, $T_{o,\tau c}$, corresponds to time constant of 3.83 minute. Table (4.6) summerizes the results of the time constant test for both collectors.

Table 4.6 : Results and conditions of the time constant test

collector	$T_i C^{\circ}$	$T_a C^{\circ}$	$T_{o,i} C^{\circ}$	$T_{o,\tau c} C^{\circ}$	$\tau c \text{ min.}$
Serpentine	28.4	28.5	37.5	31.75	3.83
Parallel	28.4	28.5	37.1	31.60	4.88

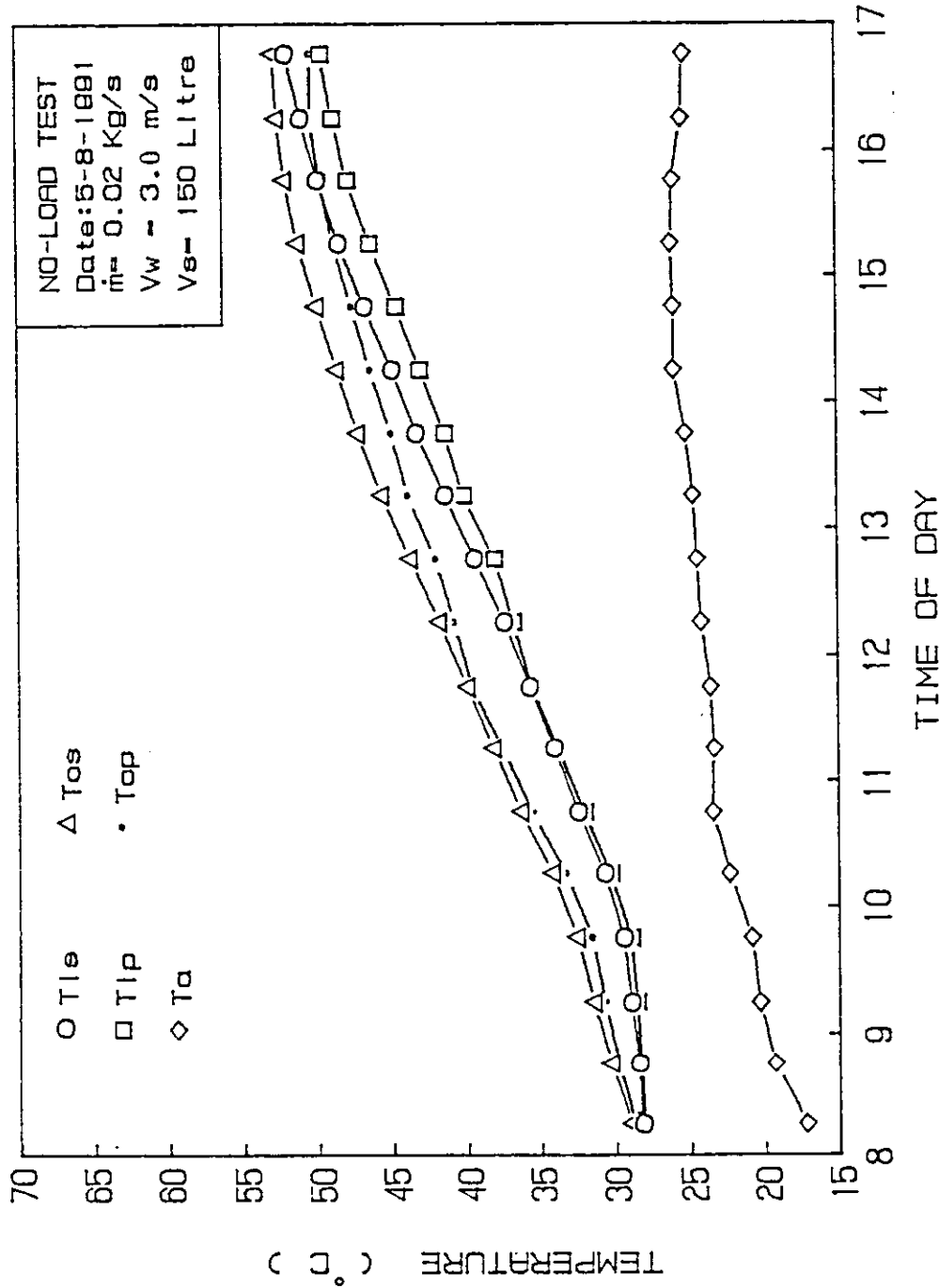


Fig.(4.1) Variation of Inlet temperature, outlet temperature, and the ambient temperature with time for the serpentine and the parallel tubes flat plate solar collectors.

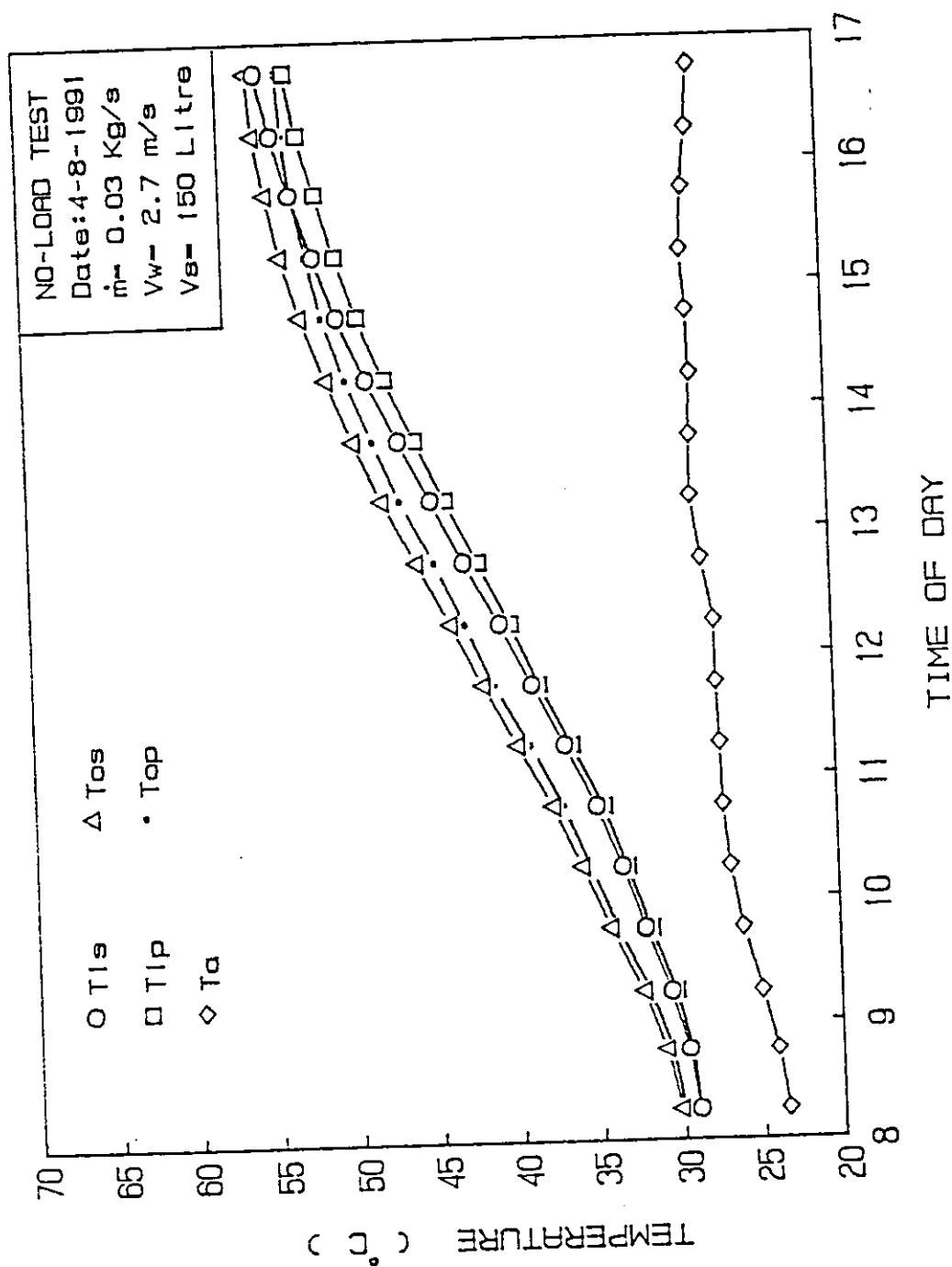


Fig. (4.2) Variation of Inlet temperature, outlet temperature, and the ambient temperature with time for the serpentine and the parallel tubes flat plate solar collectors.

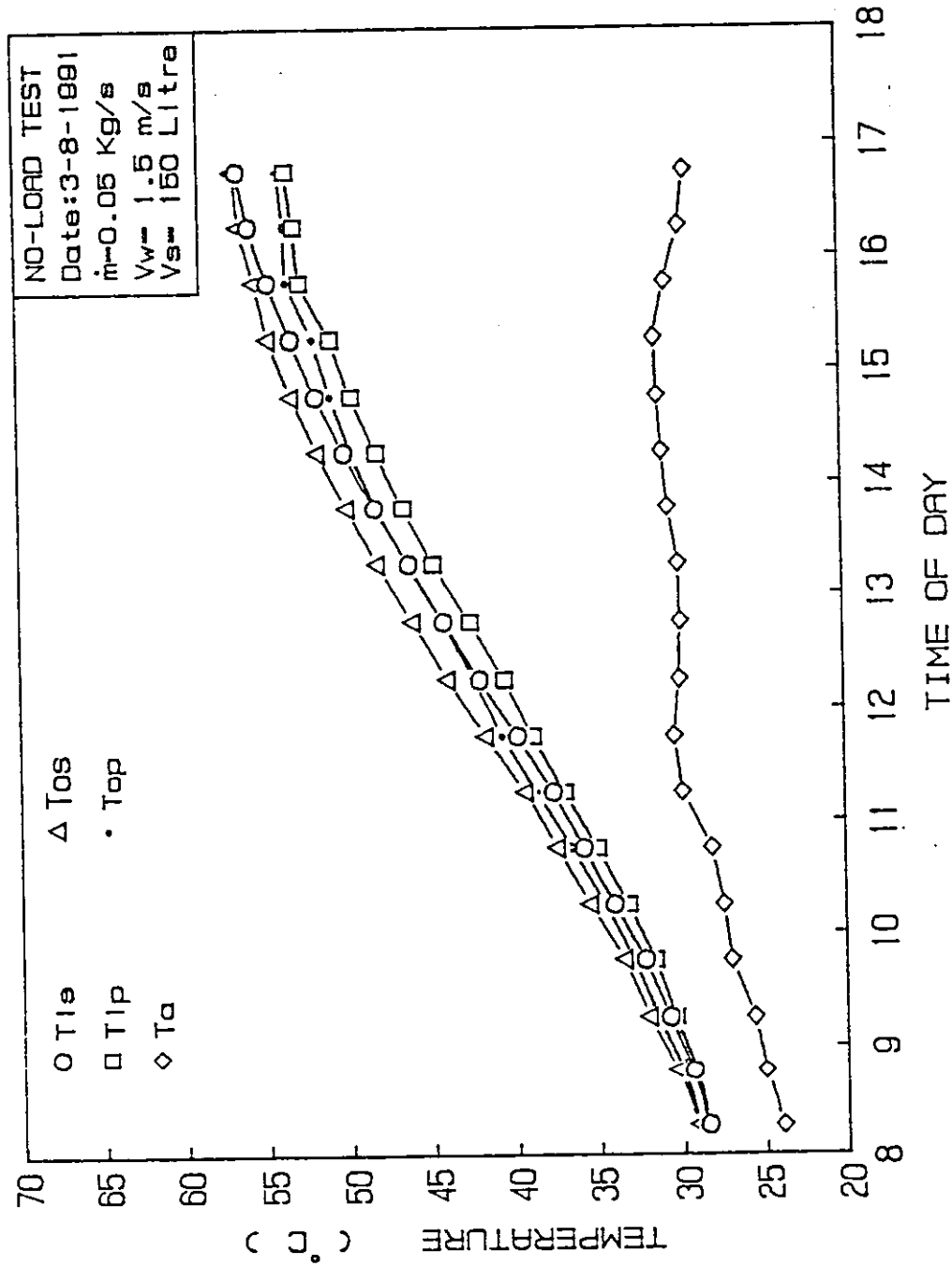


Fig. (4.3) Variation of Inlet temperature, outlet temperature, and the ambient temperature with time for the serpentine and the parallel tubes flat plate solar collectors.

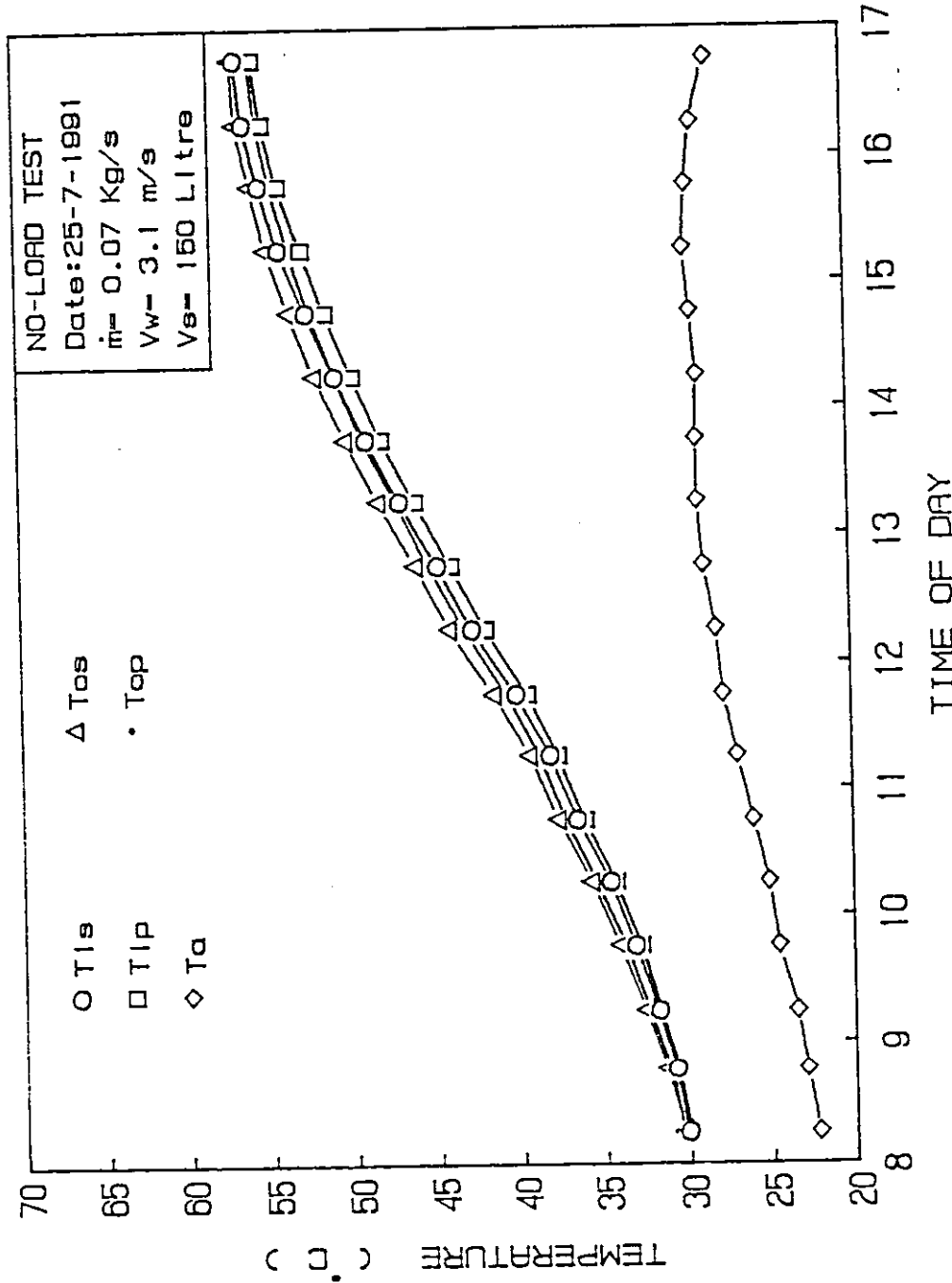


Fig.(4.4) Variation of Inlet temperature, outlet temperature, and the ambient temperature with time for the serpentine and the parallel tubes flat plate solar collectors.

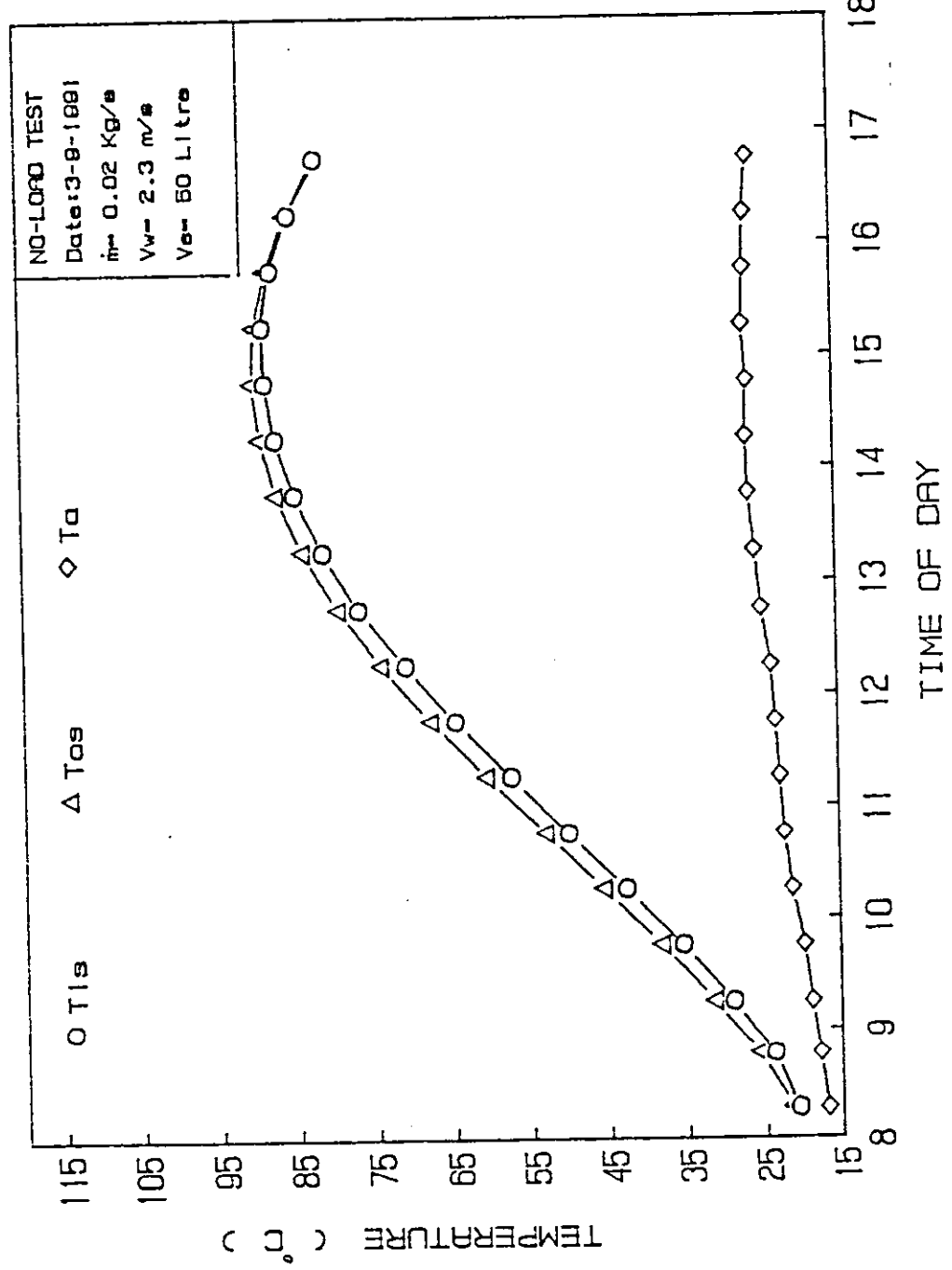


Fig.(4.5) Variation of Inlet temperature, outlet temperature and ambient temperature with time for the serpentine tube flat plate solar collector.

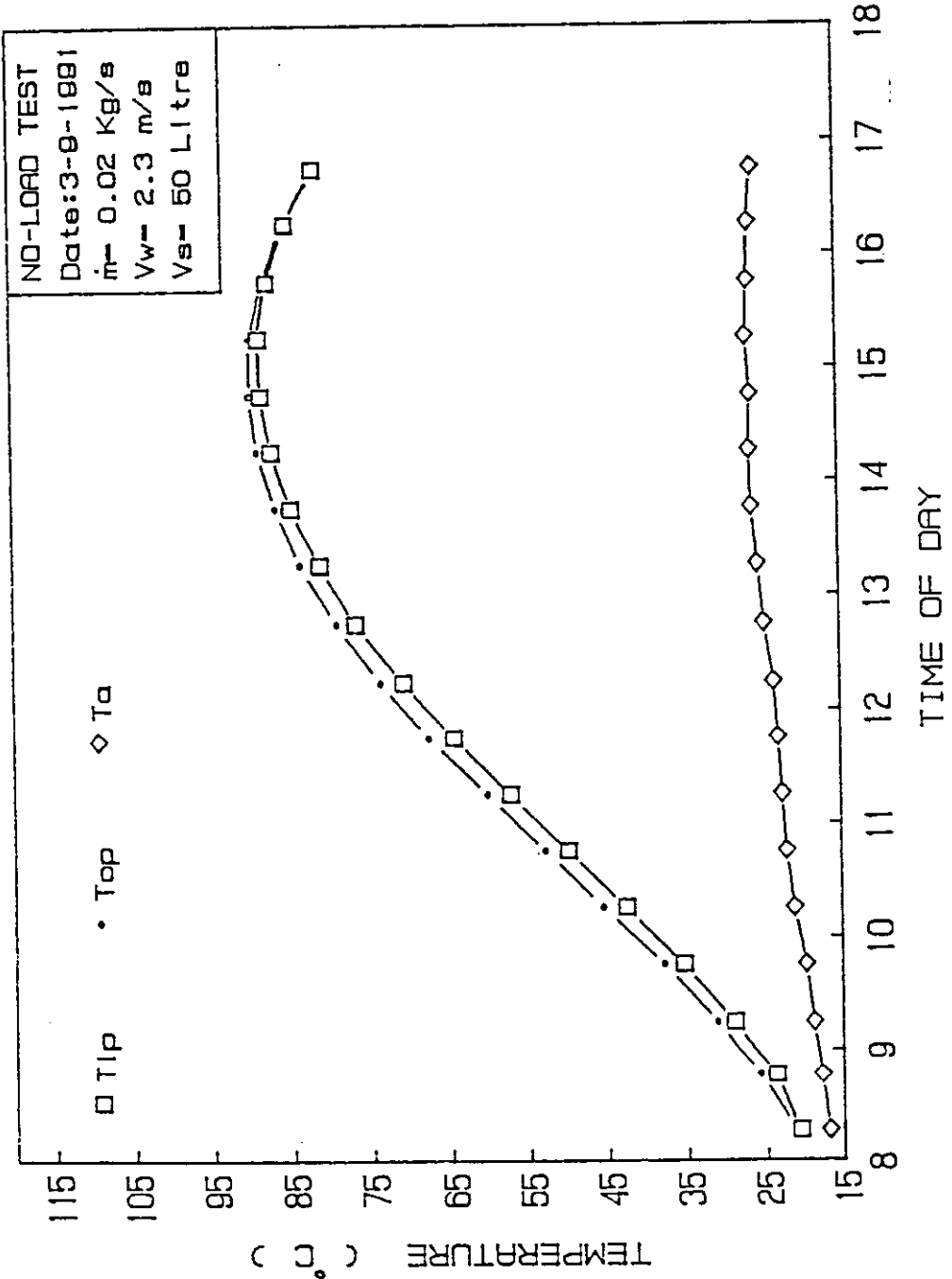


Fig.(4.6) Variation of Inlet temperature, outlet temperature and ambient temperature with time for the parallel tube flat plate solar collector.

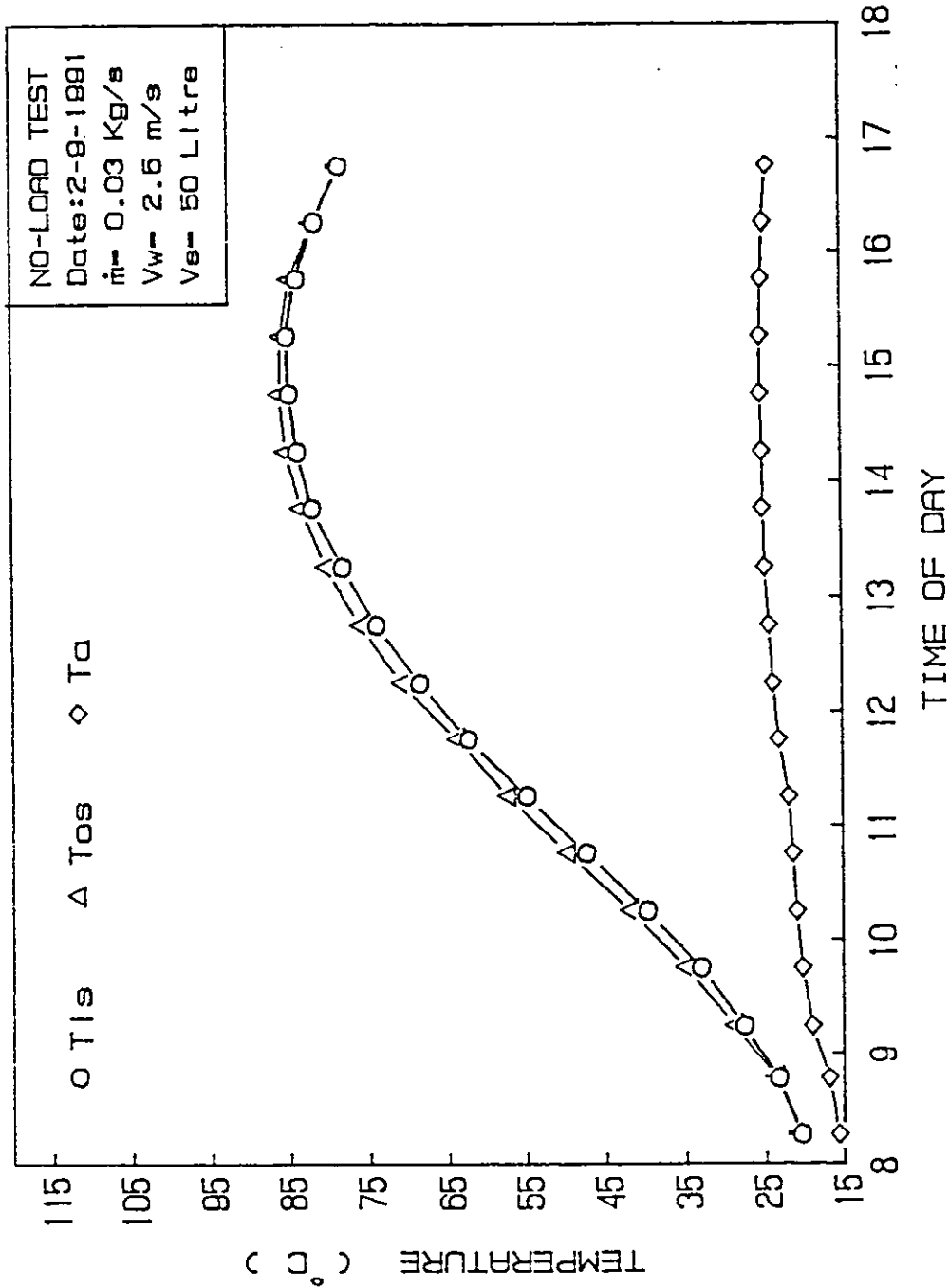


Fig.(4.7) Variation of Inlet temperature, outlet temperature and ambient temperature with time for the serpentine tube flat plate solar collector.

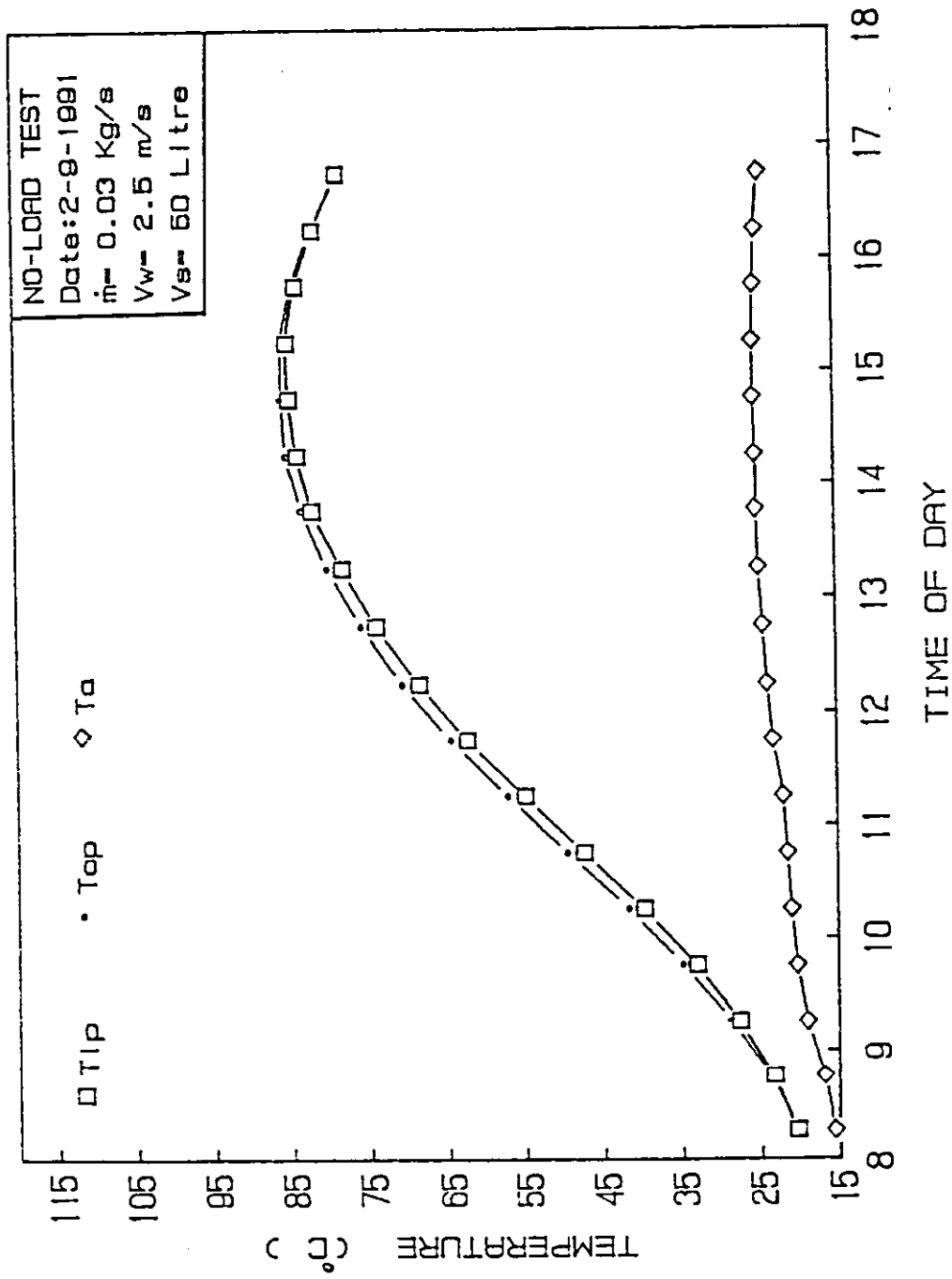


Fig. (4.8) Variation of Inlet temperature, outlet temperature and ambient temperature with time for the parallel tube flat plate solar collector.

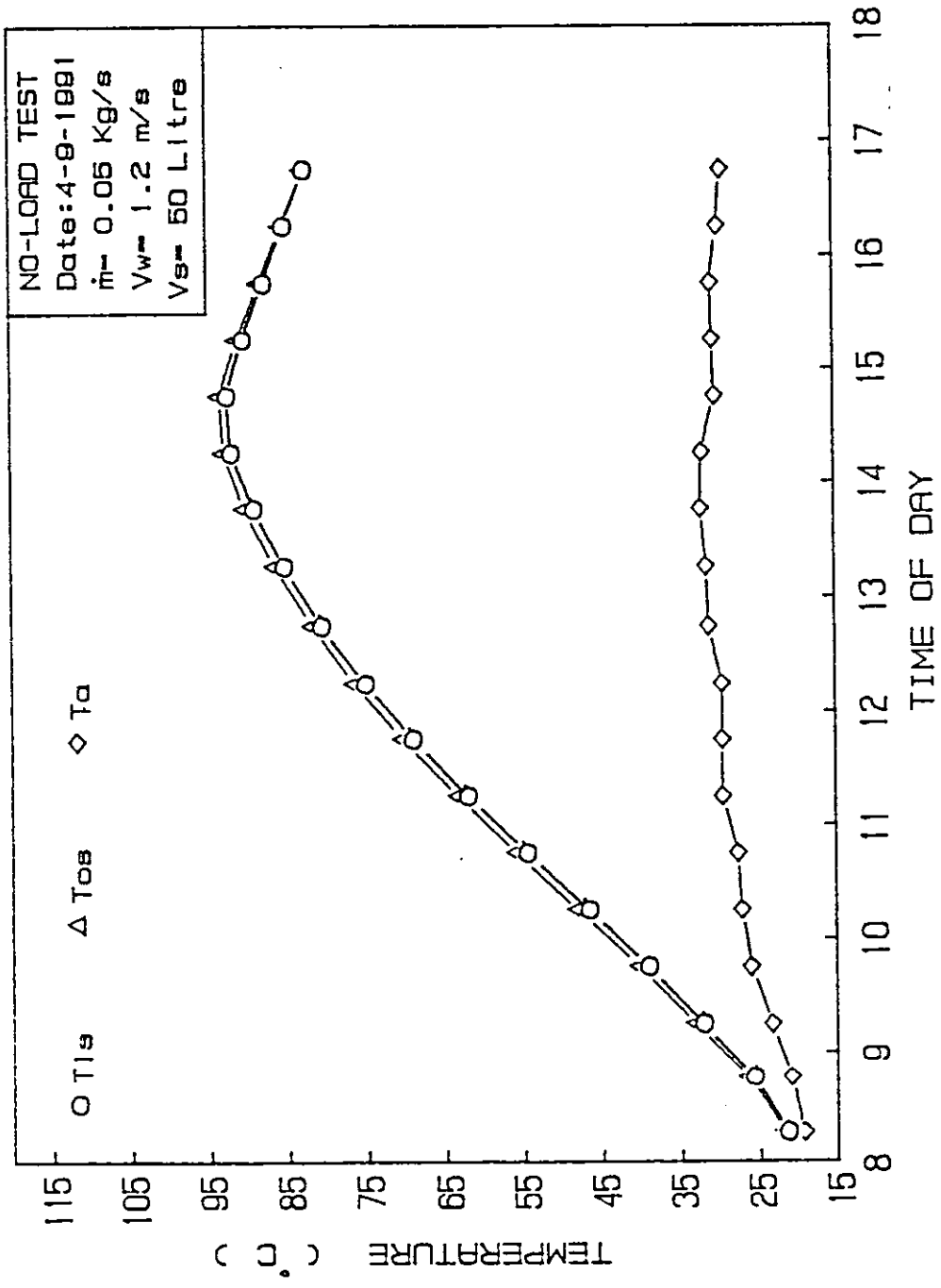


Fig.(4.9) Variation of inlet temperature, outlet temperature and ambient temperature with time for the serpentine tube flat plate solar collector.

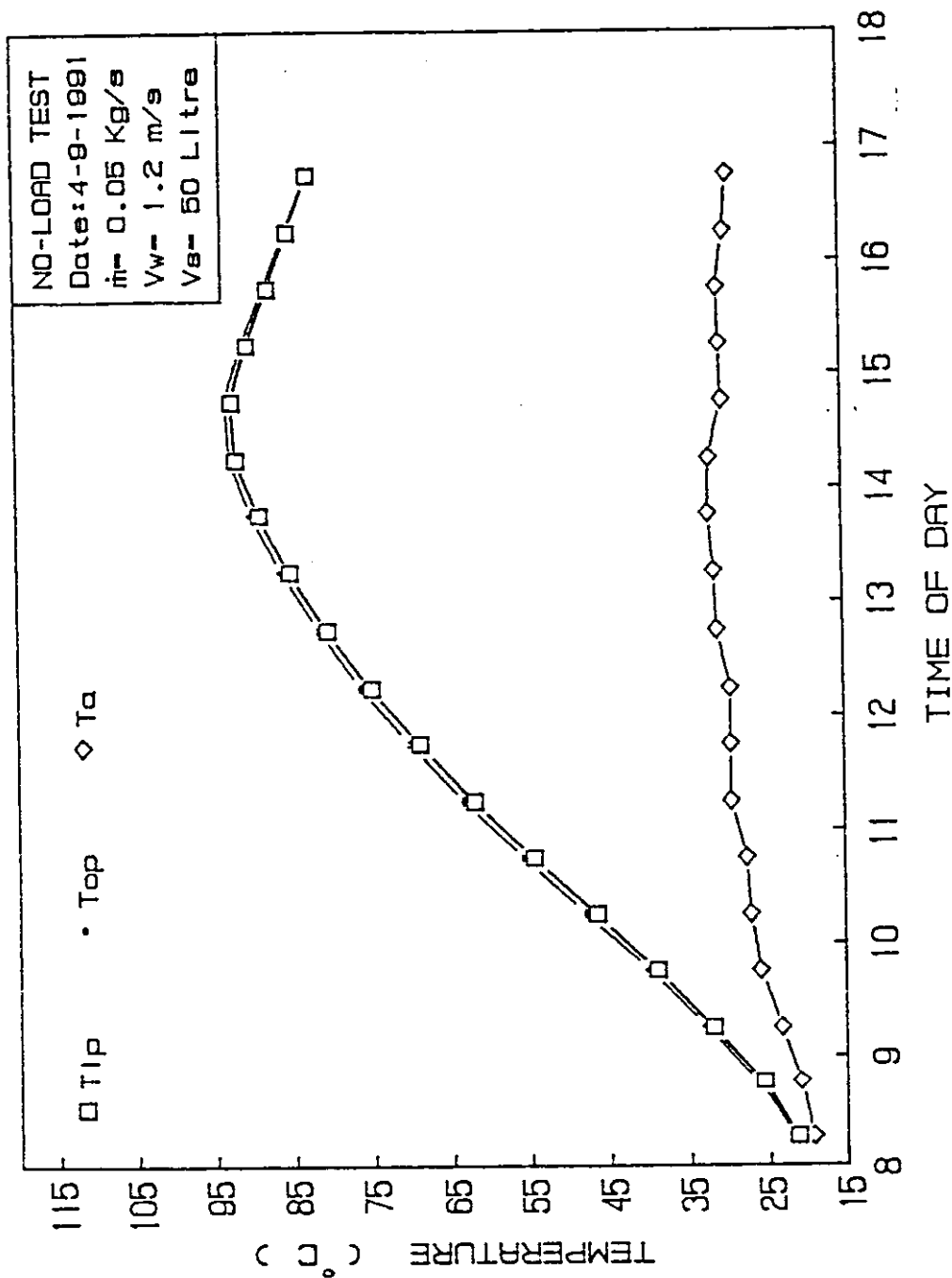


Fig.(4.10) Variation of inlet temperature, outlet temperature and ambient temperature with time for the parallel tube flat plate solar collector.

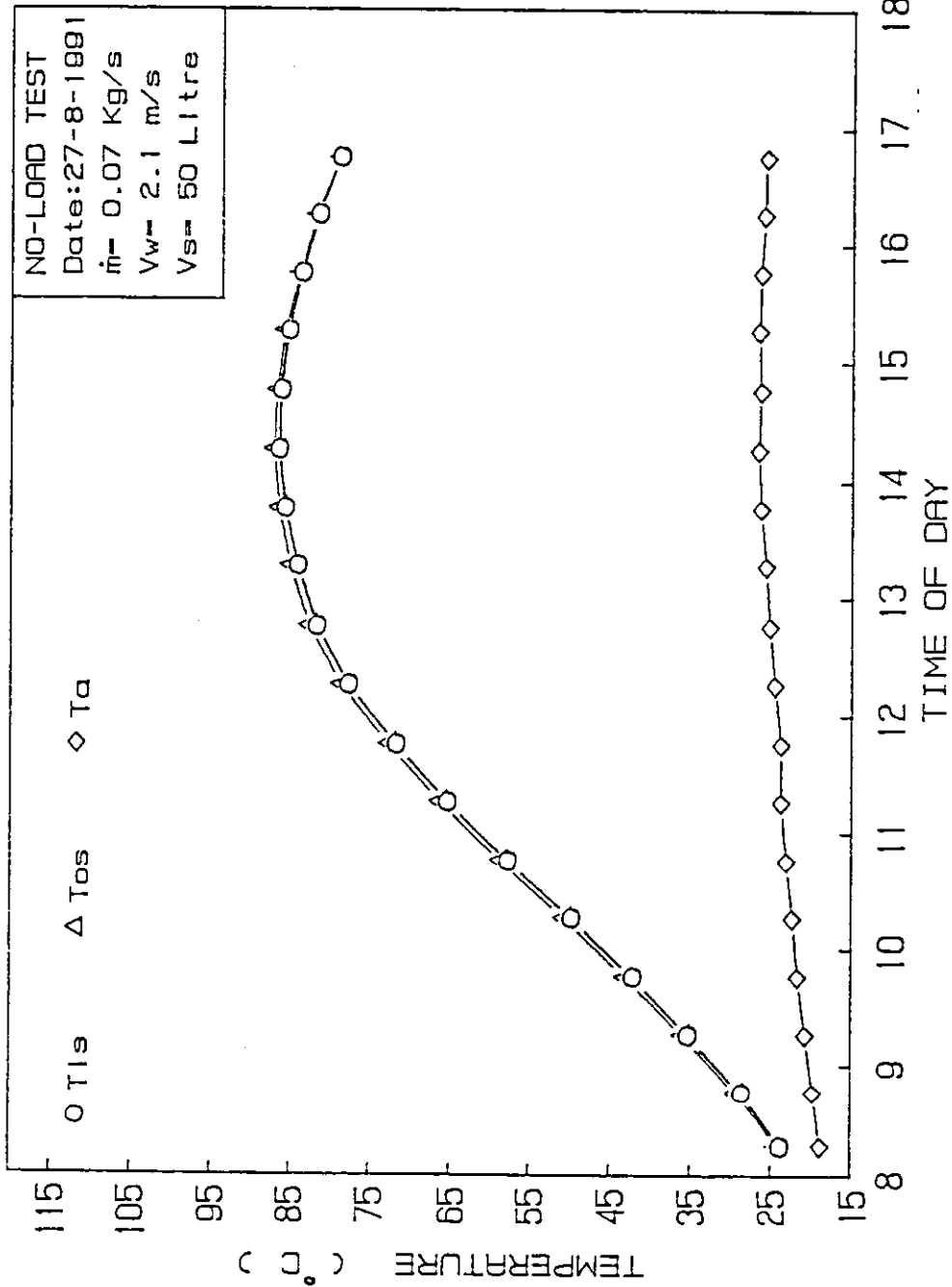


Fig.(4.11) Variation of Inlet temperature, outlet temperature and ambient temperature with time for the serpentine tube flat plate solar collector.

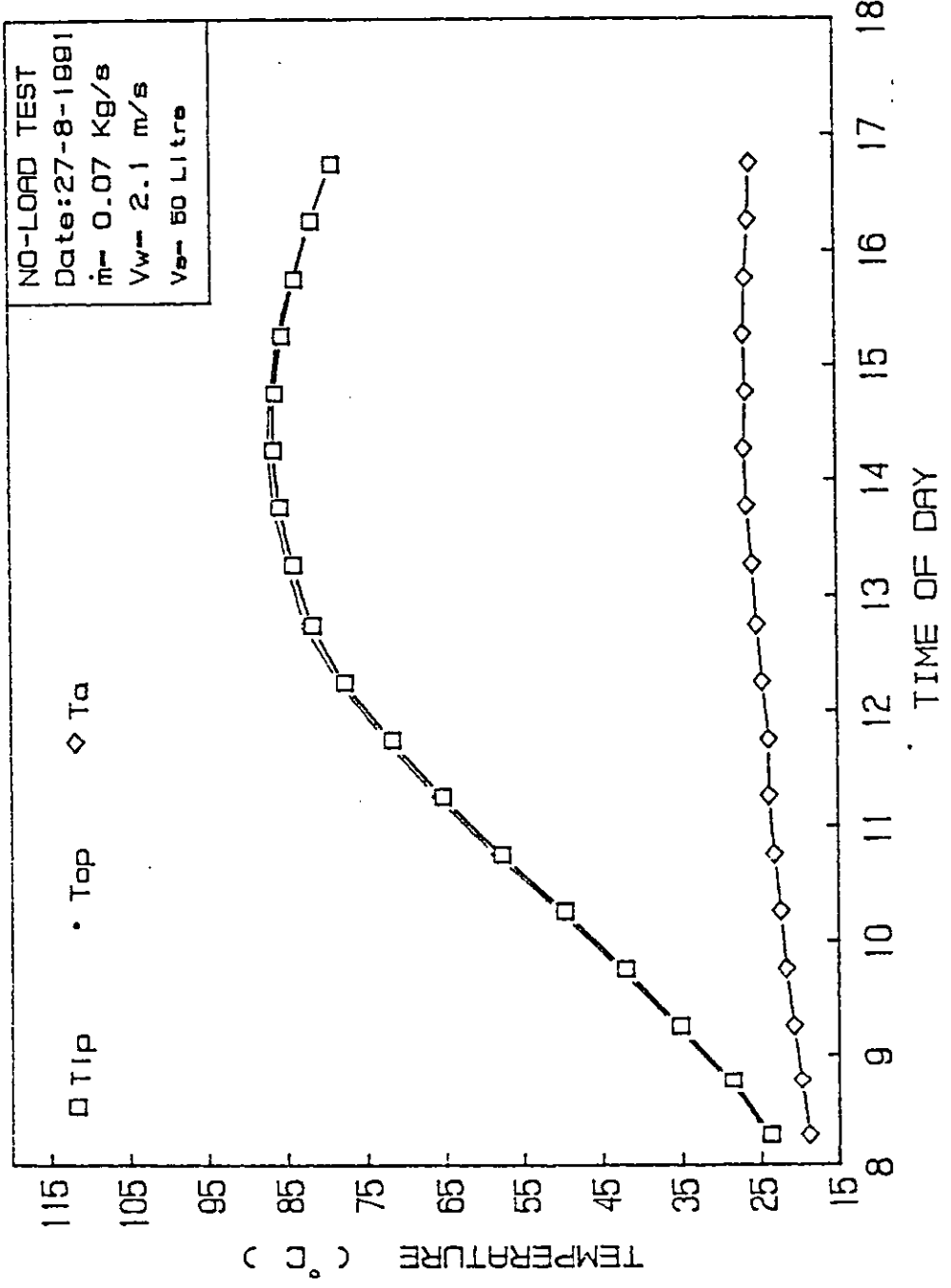


Fig.(4.12) Variation of inlet temperature, outlet temperature and ambient temperature with time for the parallel tube flat plate solar collector.

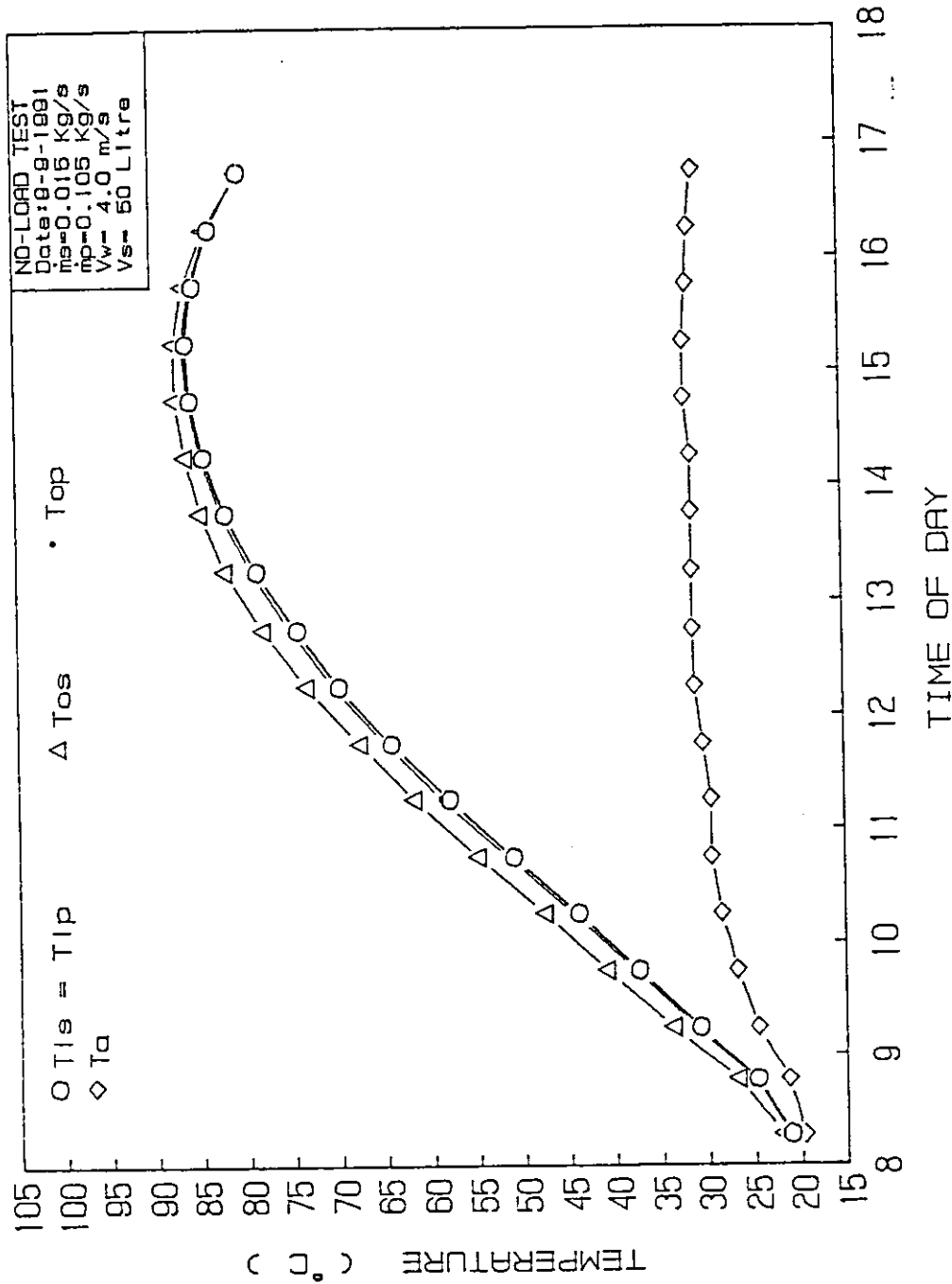


Fig.(4.13) Variation of Inlet temperature, outlet temperature, and ambient temperature with time for the serpentine and the parallel tubes flat plate solar collectors at two different mass flow rates.

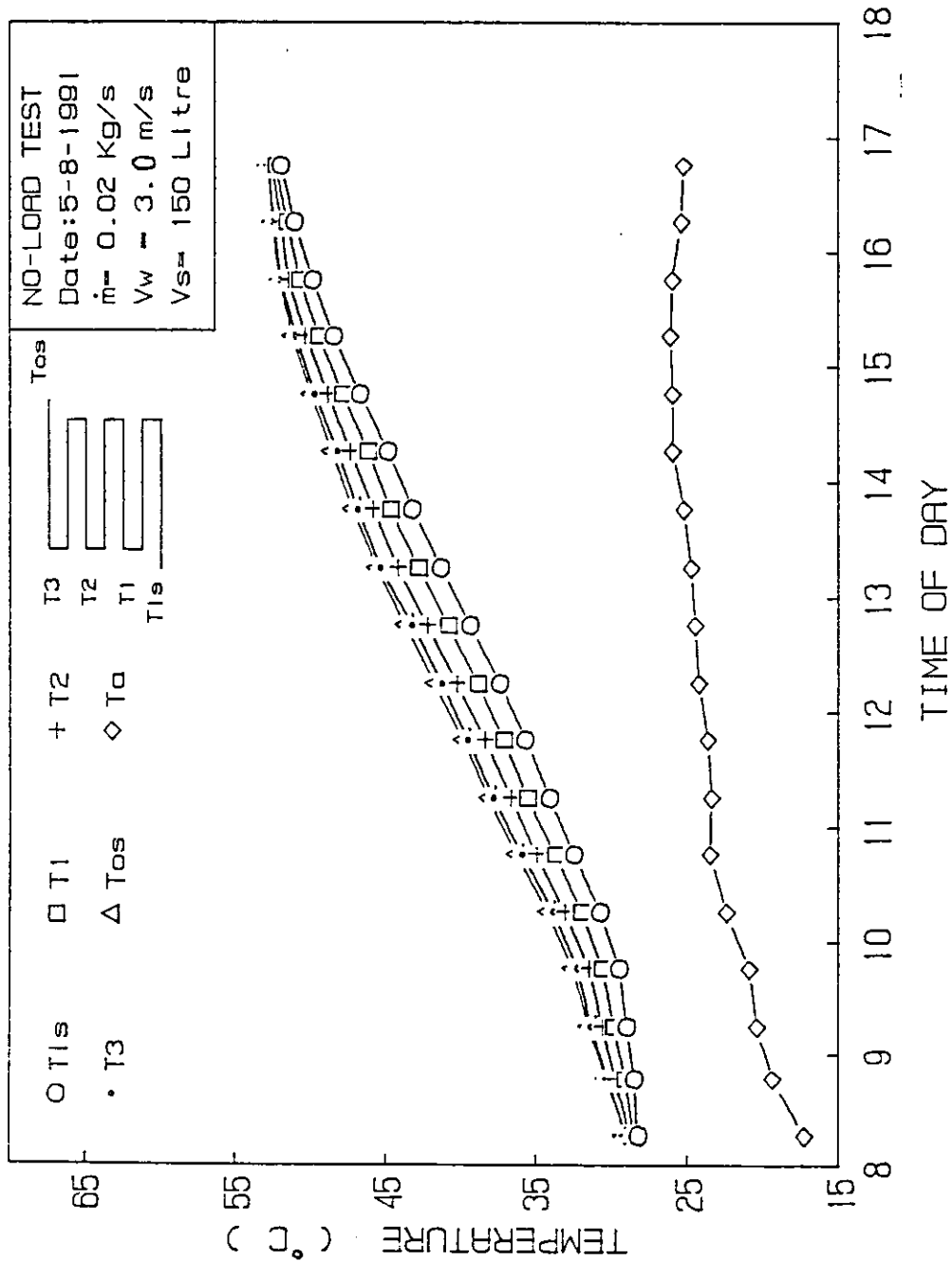


Fig. (4.14) Temperature distribution of the water inside the serpentine tube flat plate solar collector and ambient temperature during the day test.

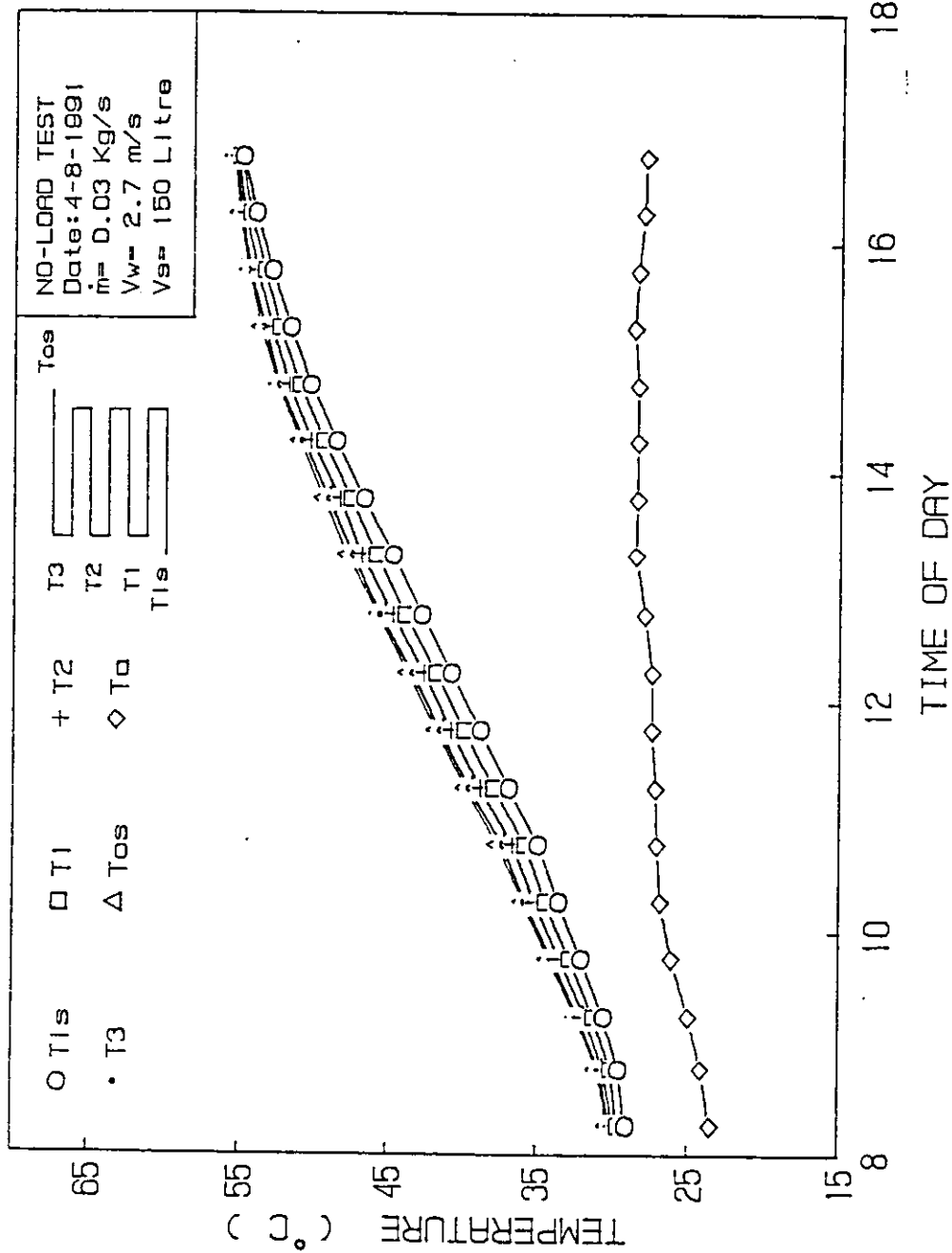


Fig.(4.15) Temperature distribution of the water inside the serpentine tube flat plate solar collector and ambient temperature during the day test.

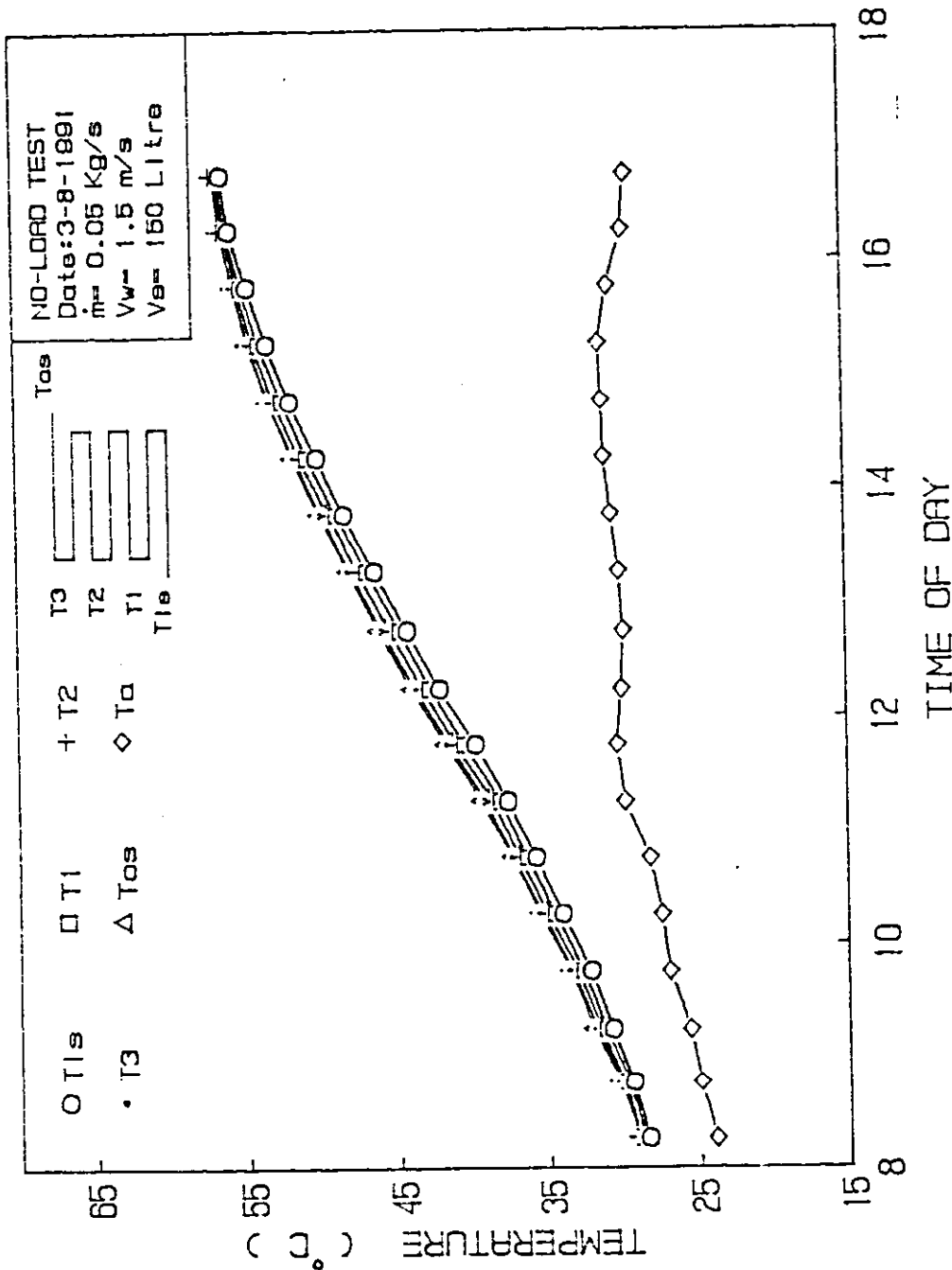


Fig.(4.16) Temperature distribution of the water inside the serpentine tube flat plate solar collector and ambient temperature during the day test.

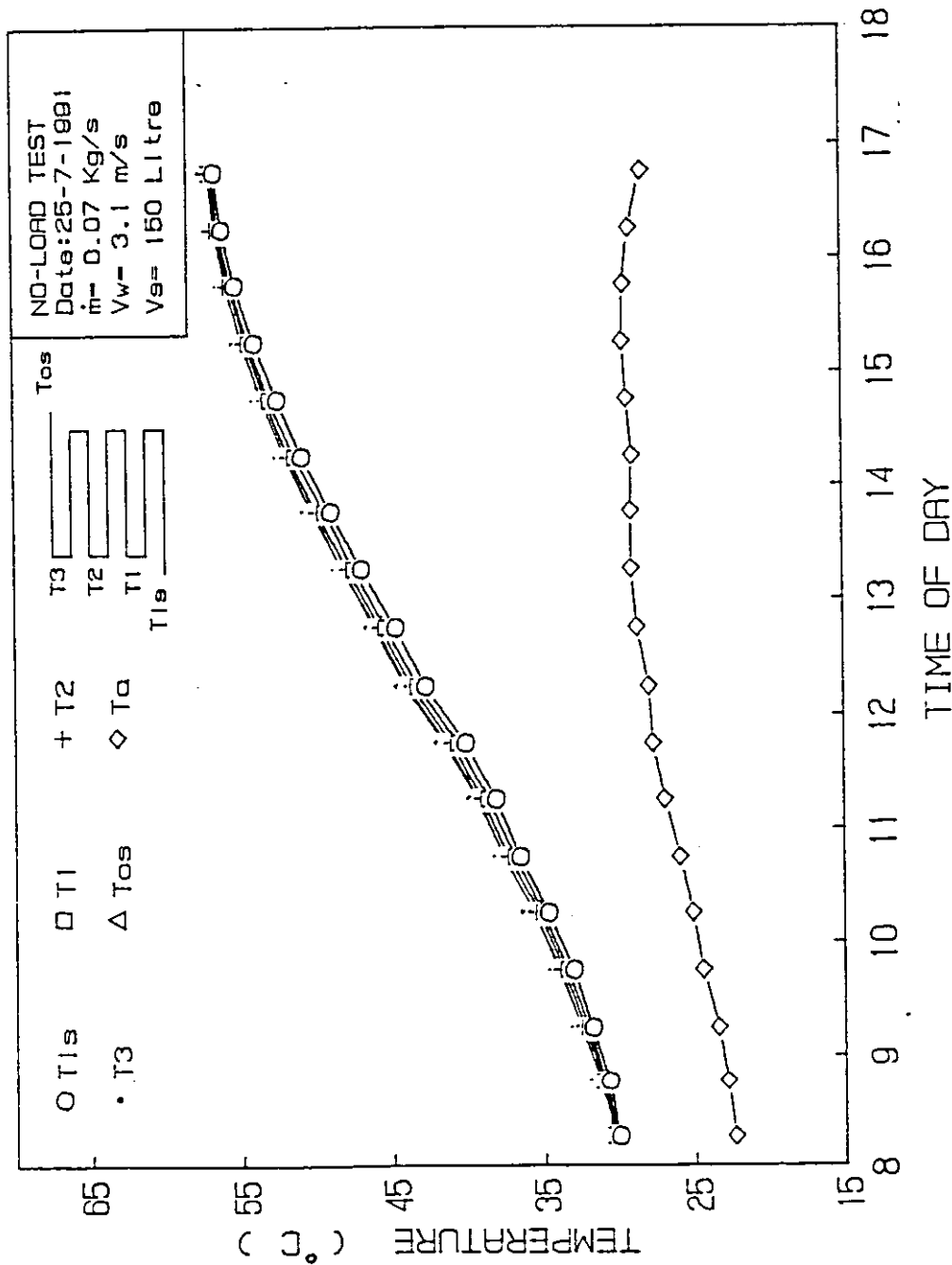


Fig. (4.17) Temperature distribution of the water inside the serpentine tube flat plate solar collector and ambient temperature during the day test.

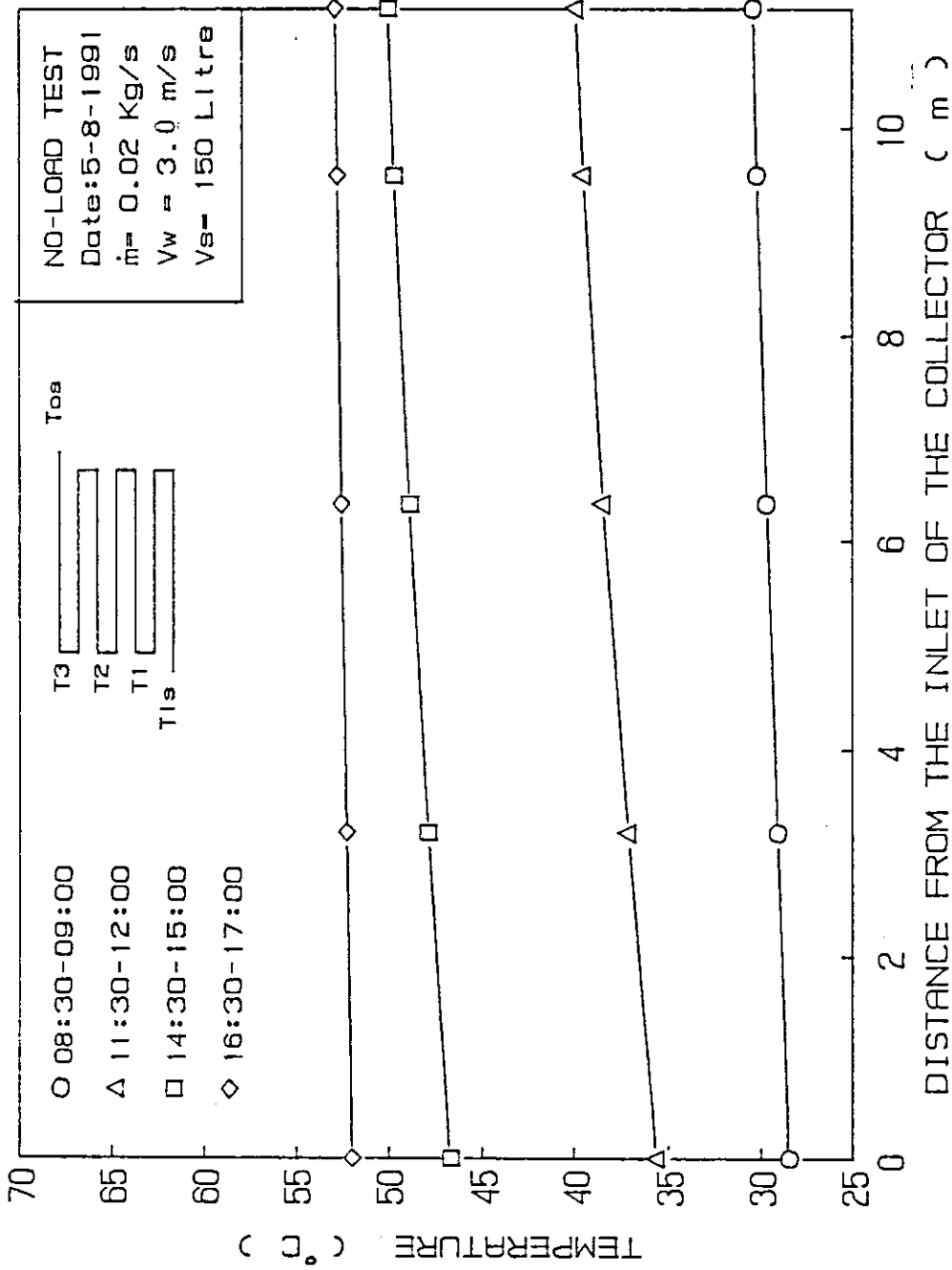


Fig.(4.18) Temperature distribution of the water inside the serpentine tube flat plate solar collector at different times of the day.

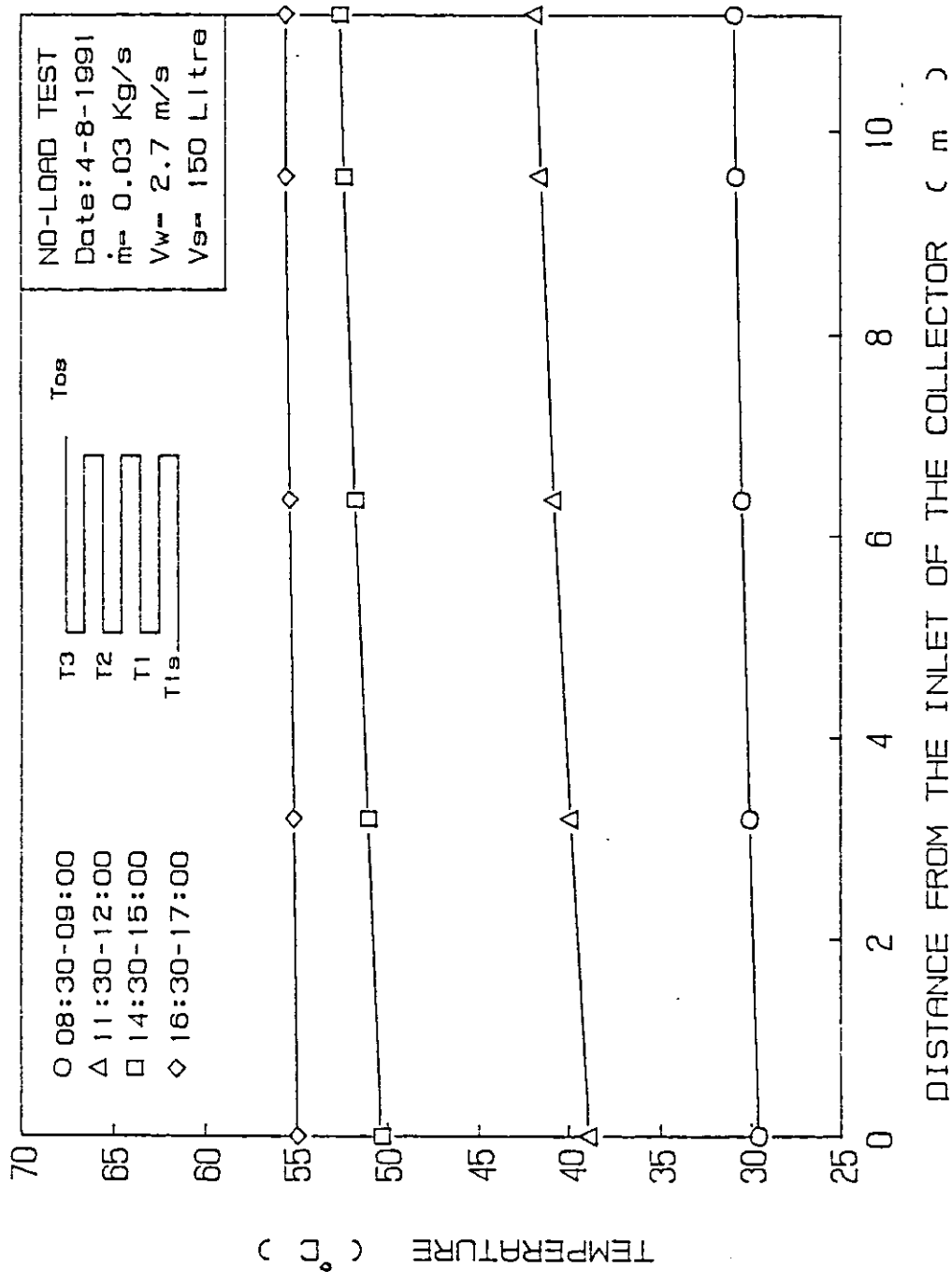


Fig.(4.19) Temperature distribution of the water inside the serpentine tube flat plate solar collector at different times of the day.

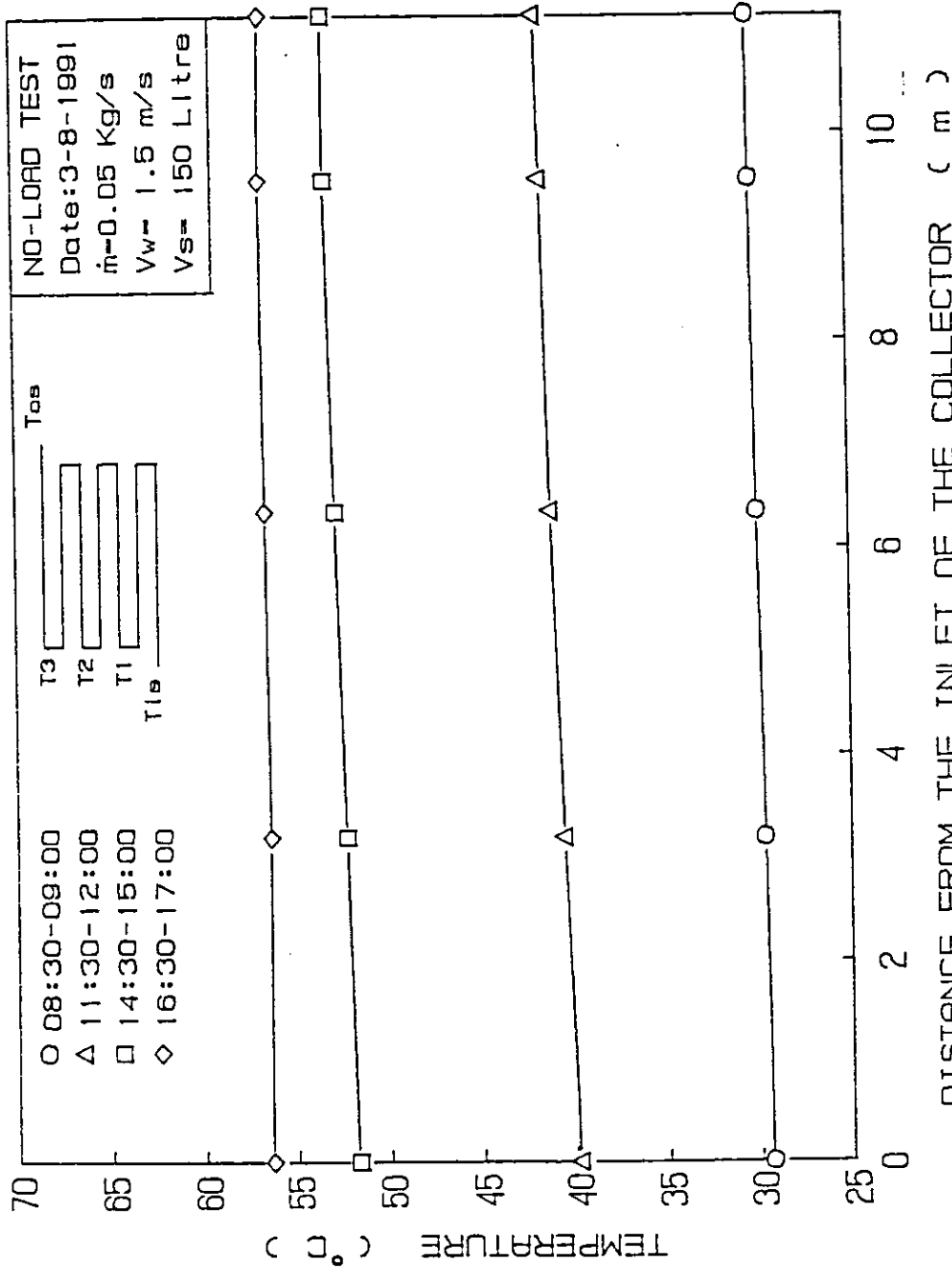


Fig.(4.20) Temperature distribution of the water inside the serpentine tube flat plate solar collector at different times of the day.

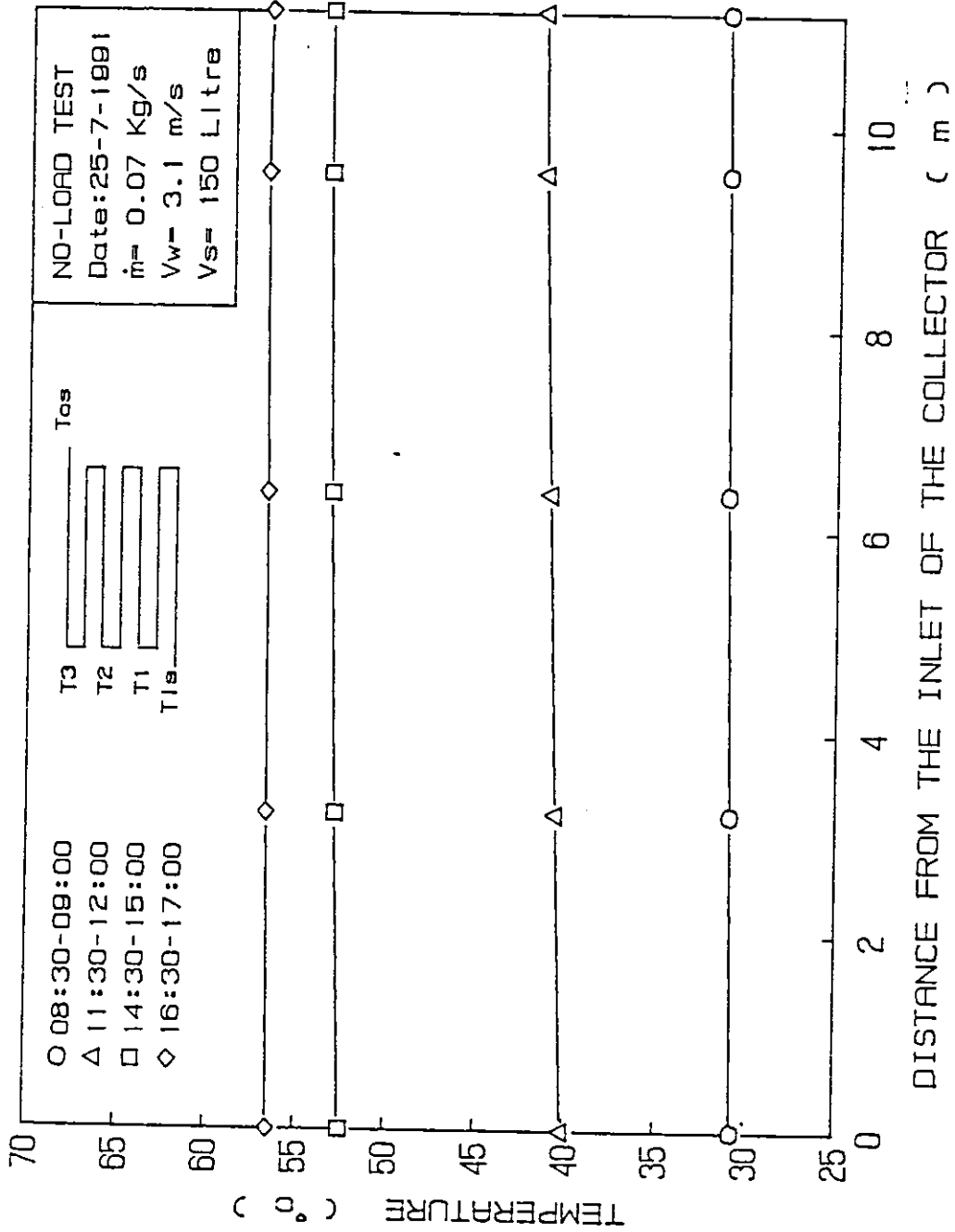


Fig. (4.21) Temperature distribution of the water inside the serpentine tube flat plate solar collector at different times of the day.

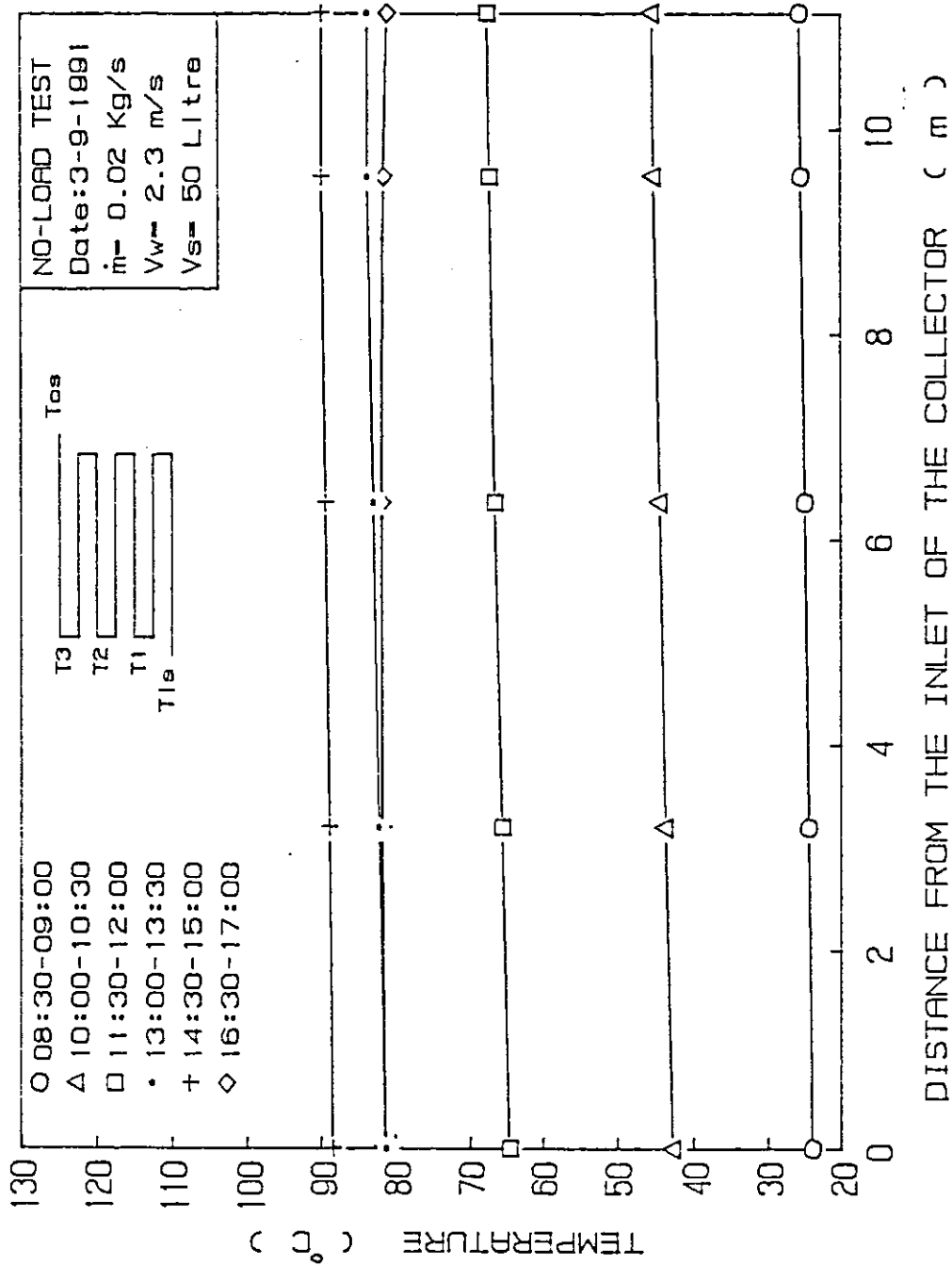


Fig.(4.22) Temperature distribution of the water inside the serpentine tube flat plate solar collector at different times of the day.

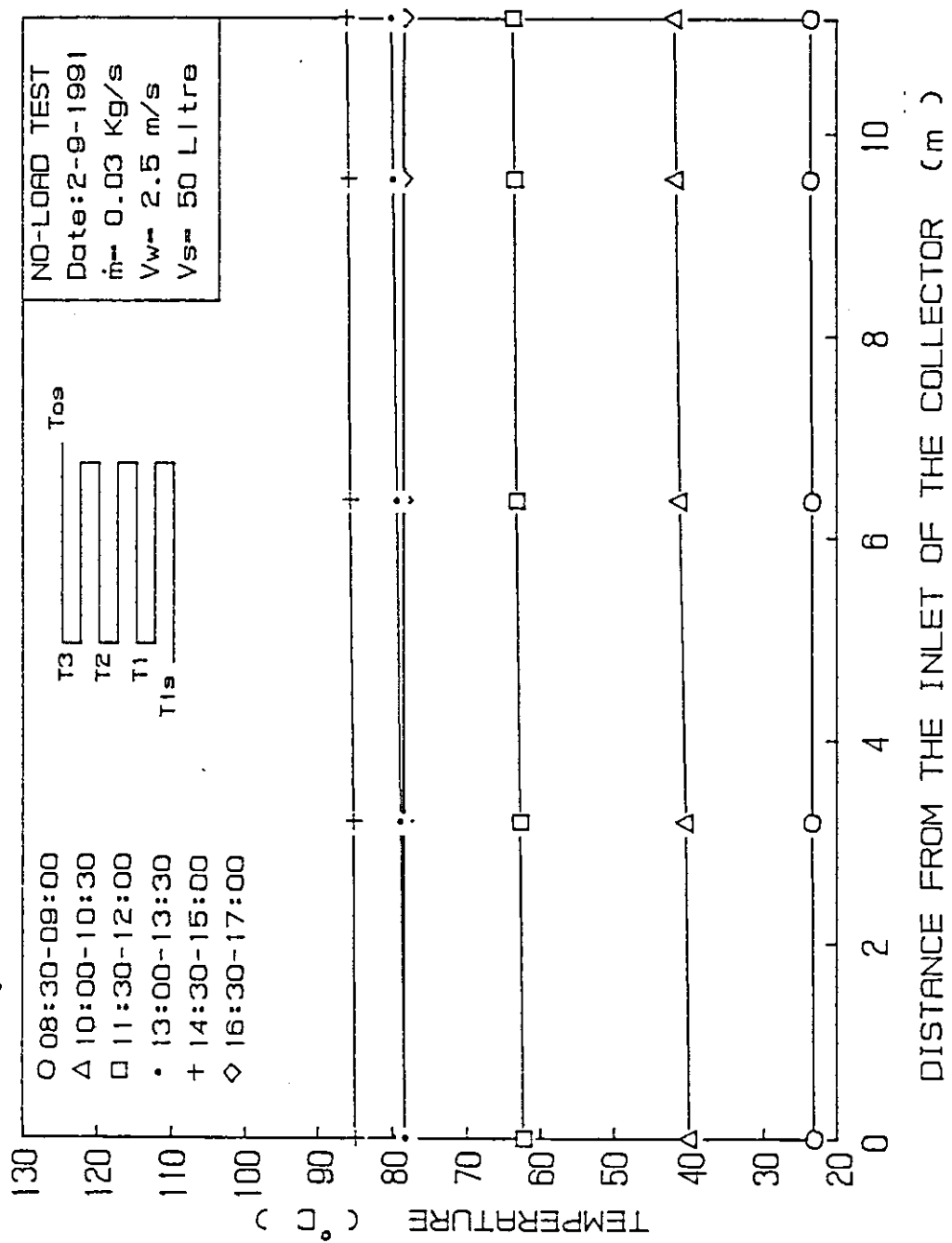


Fig.(4.23) Temperature distribution of the water inside the serpentine tube flat plate solar collector at different times of the day.

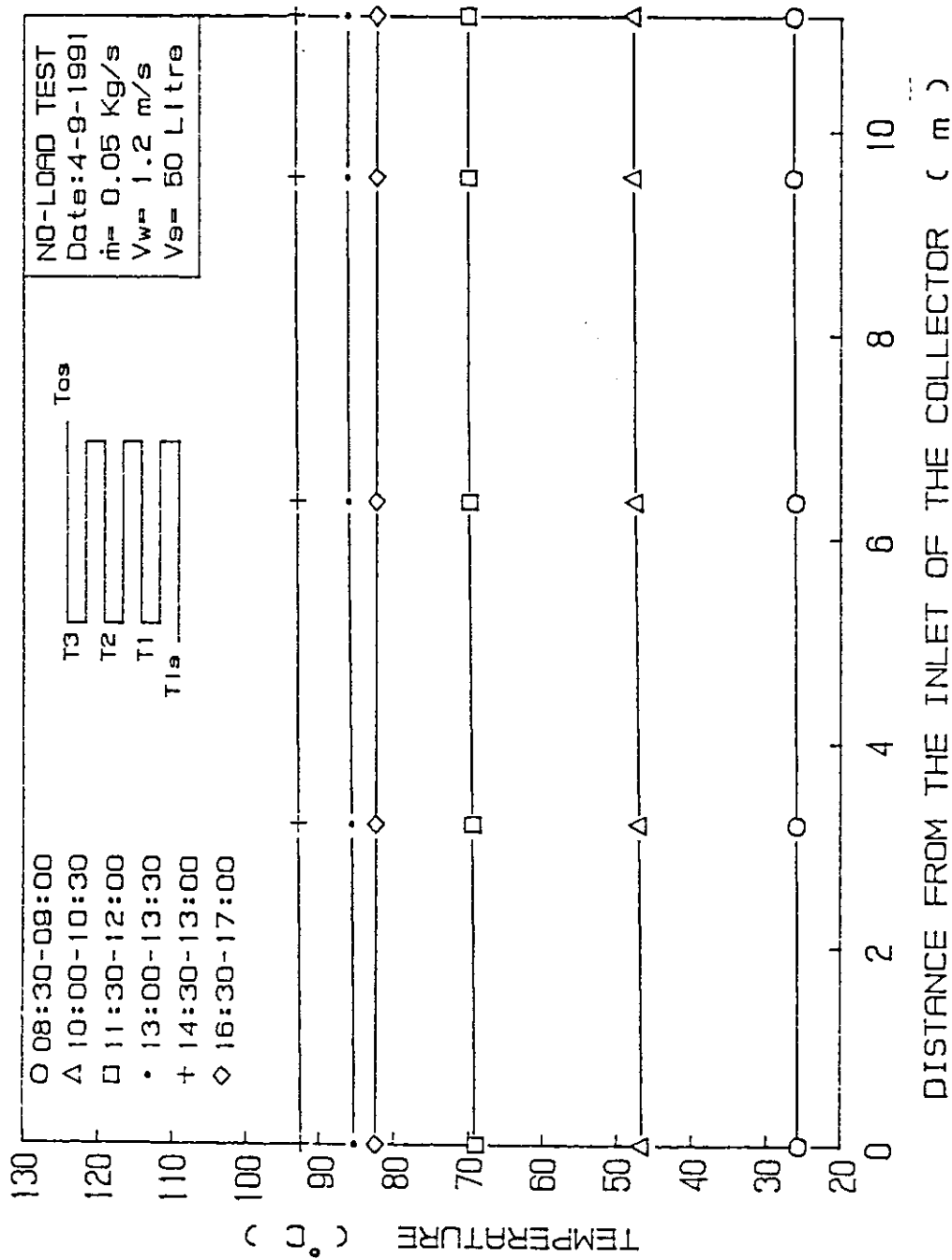


Fig. (4.24) Temperature distribution of the water inside the serpentine tube flat plate solar collector at different times of the day.

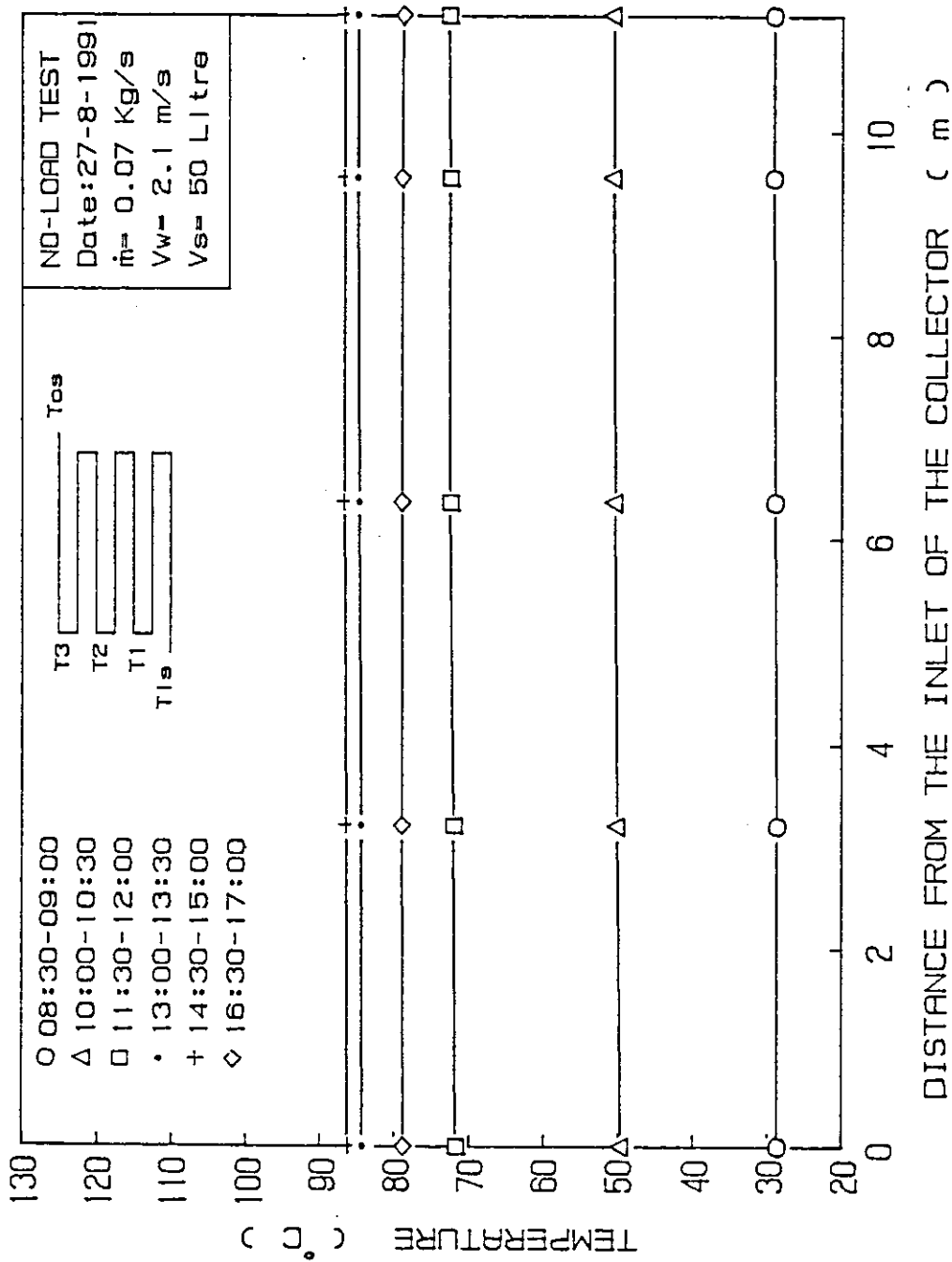


Fig.(4.25) Temperature distribution of the water inside the serpentine tube flat plate solar collector at different times of the day.

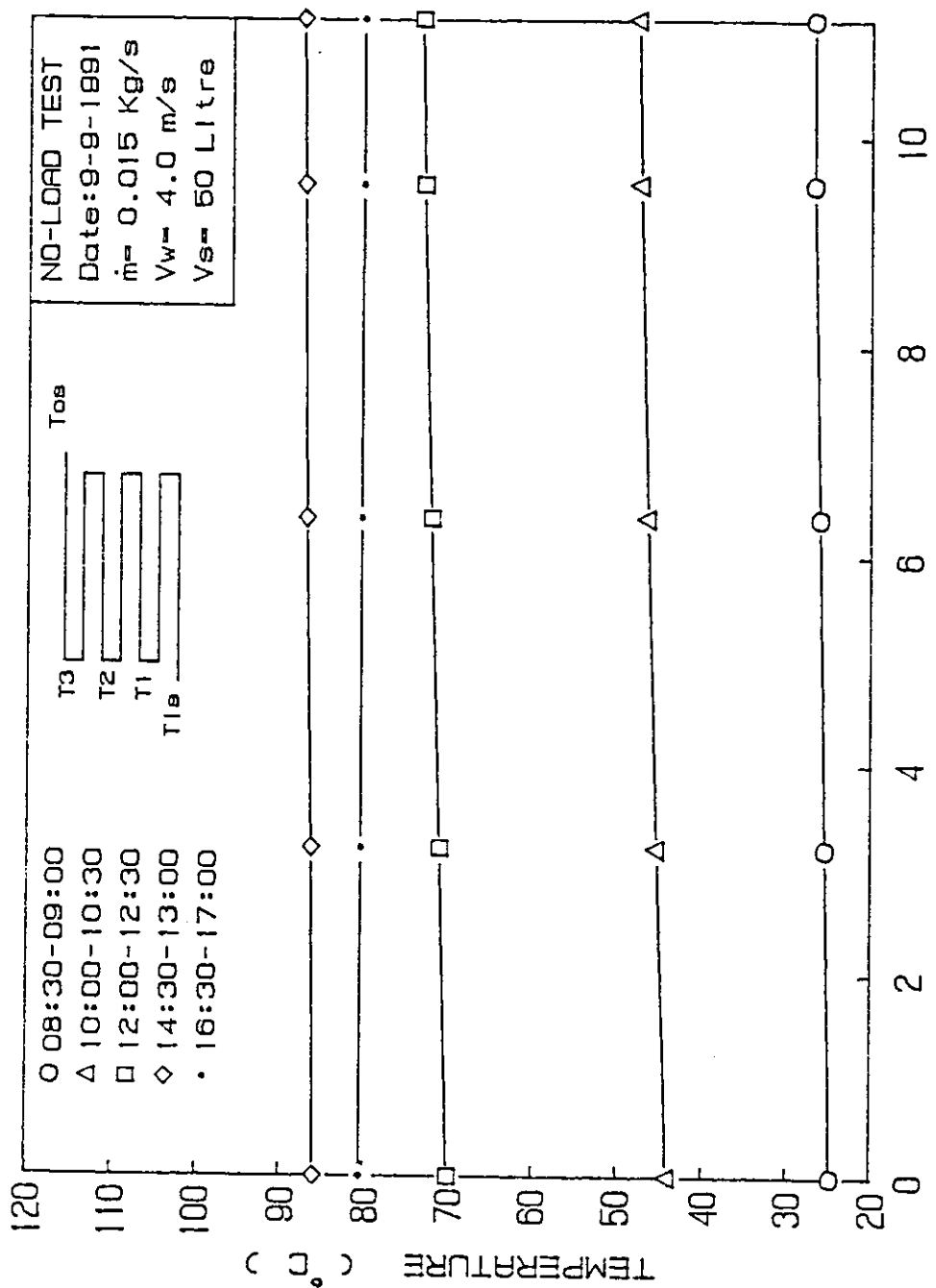


Fig.(4.26) Temperature distribution of the water inside the serpentine tube flat plate solar collector at different times of the day.

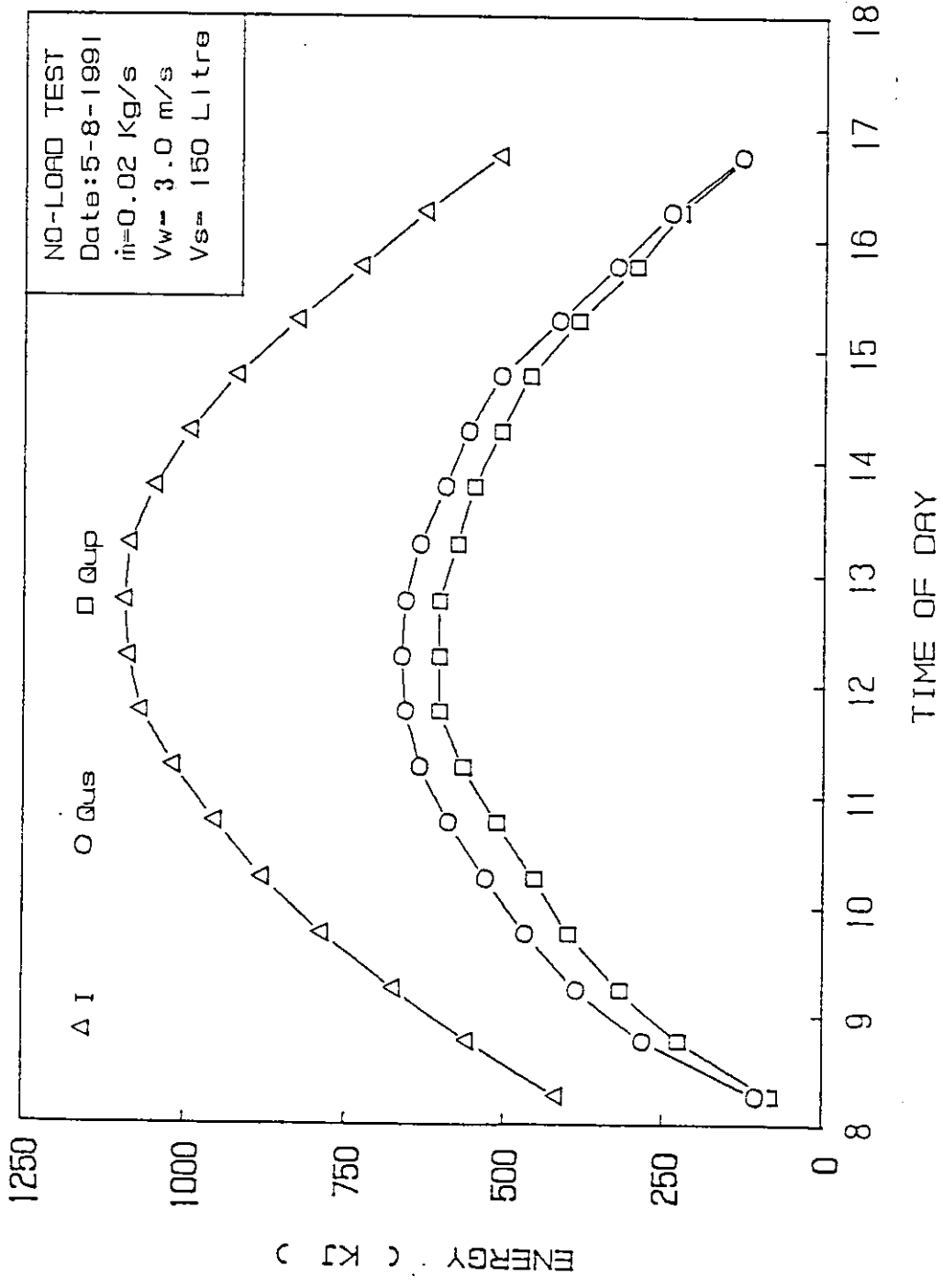


Fig.(4.27) Variation of incident energy and useful energy with time for the serpentine and the parallel tubes flat plate solar collectors.

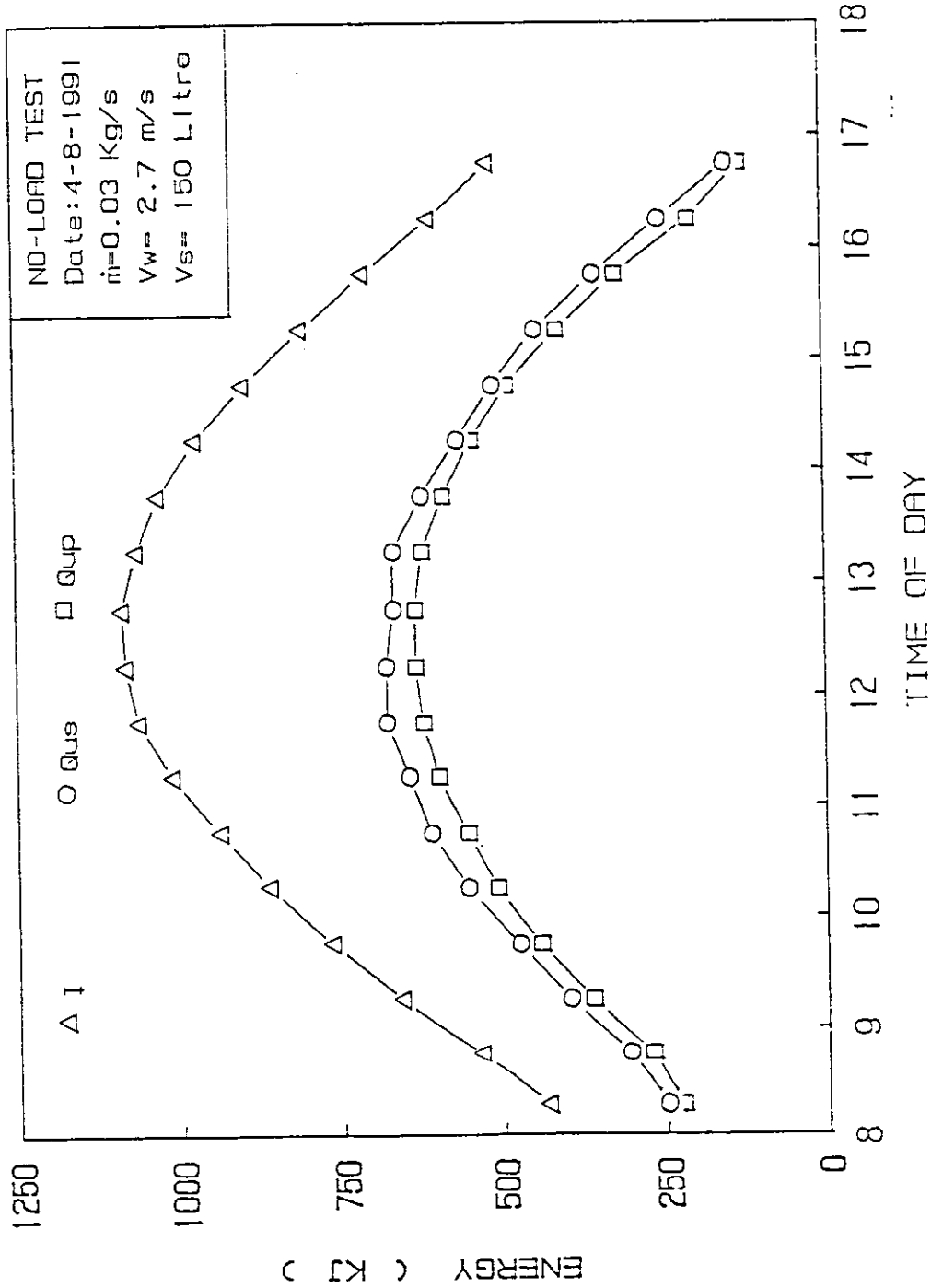


Fig.(4.28) Variation of Incident energy and useful energy with time for the serpentine and the parallel tubes flat plate solar collectors.

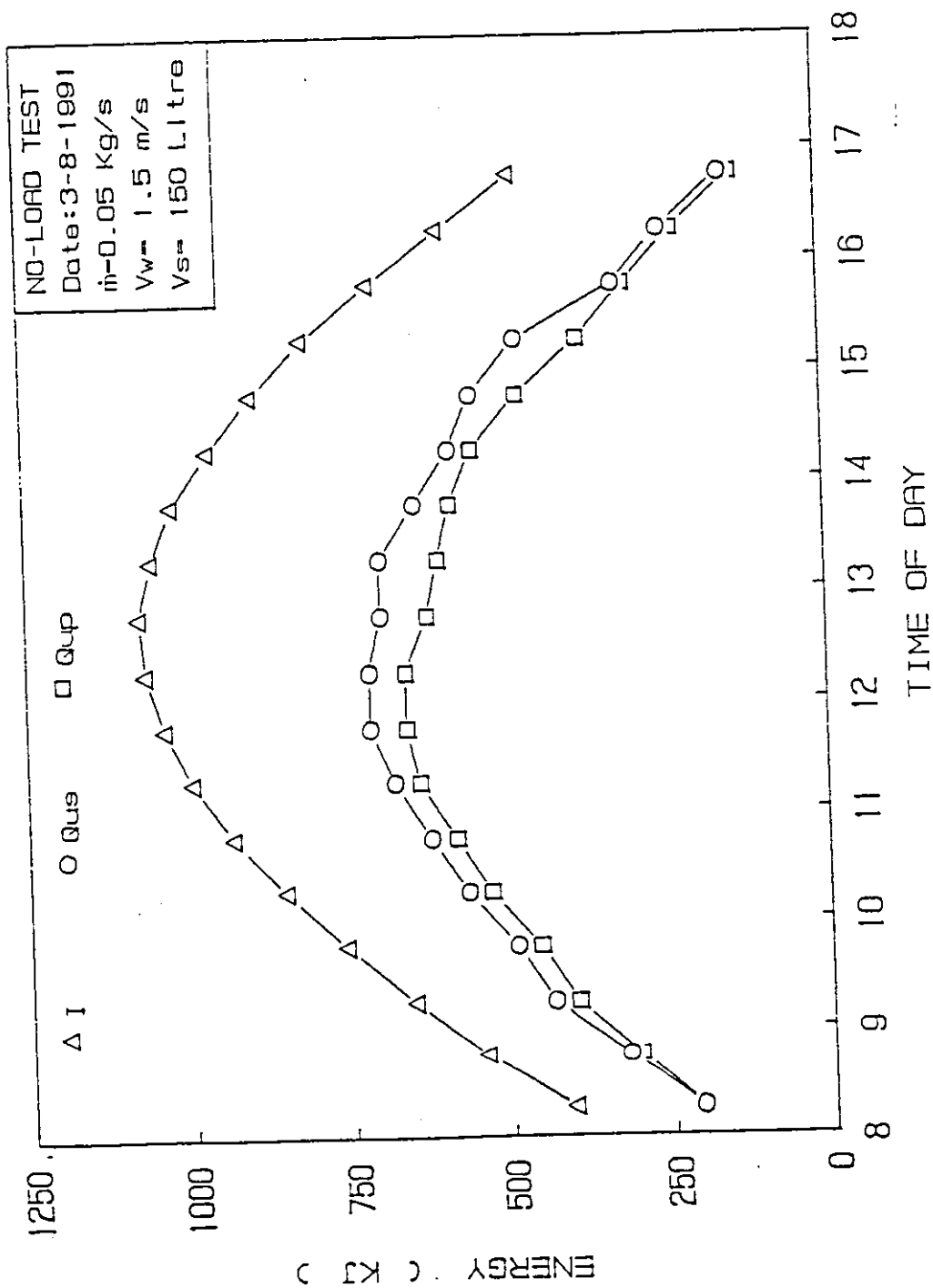


Fig.(4.29) Variation of incident energy and useful energy with time for the serpentine and the parallel tubes flat plate solar collectors.

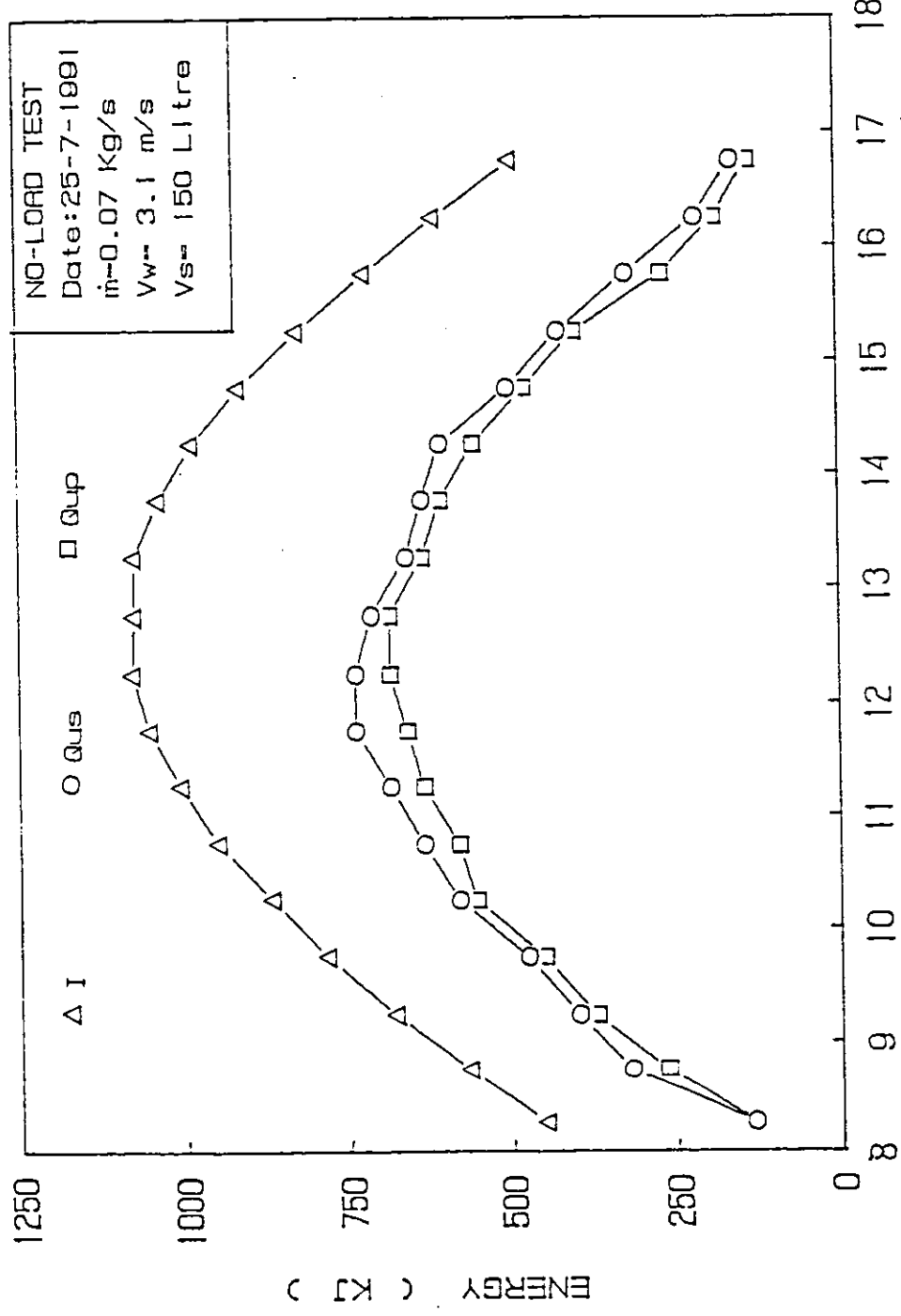


Fig.(4.30) Variation of Incident energy and useful energy with time for the serpentine and the parallel tubes flat plate solar collectors.

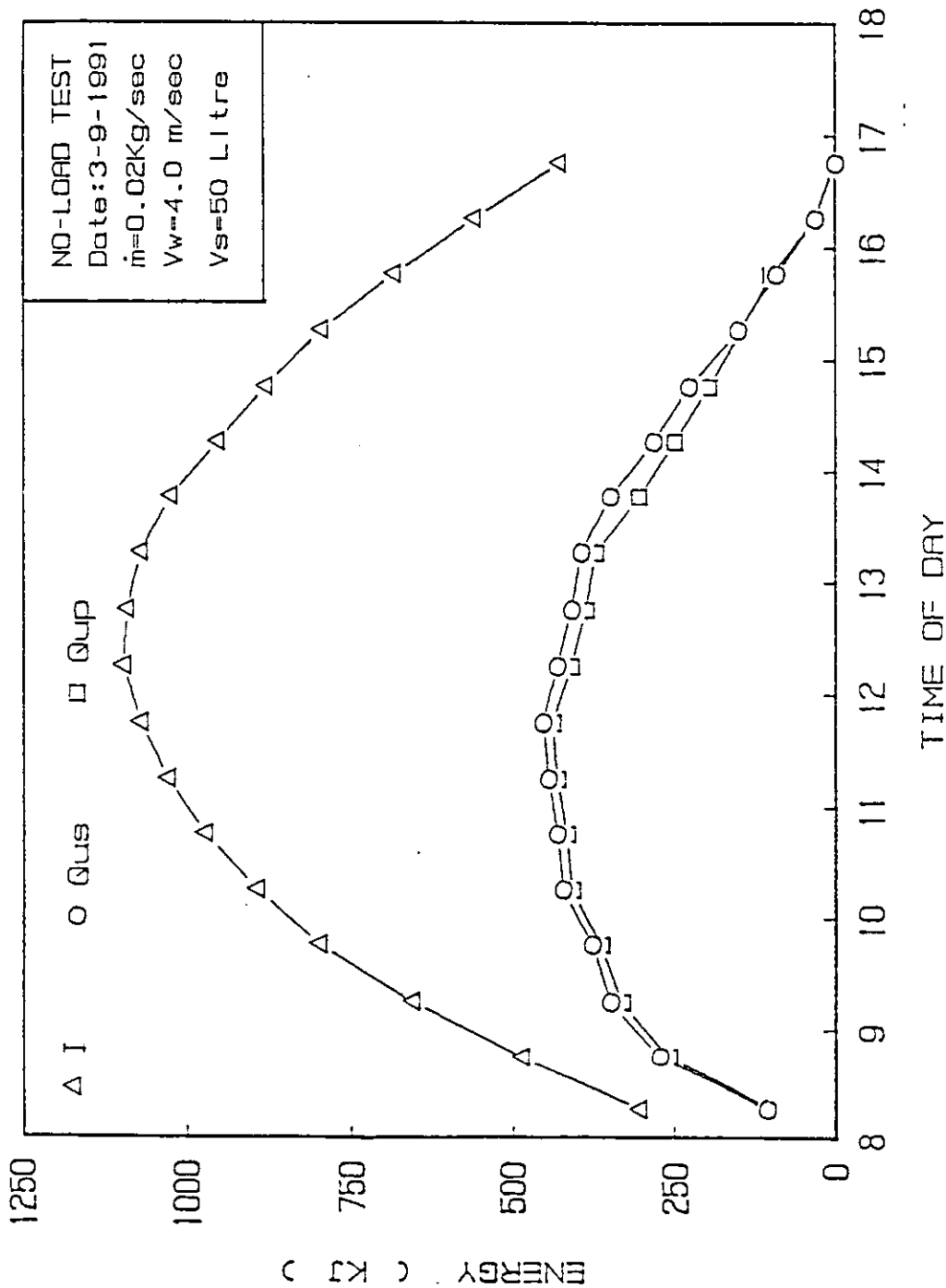


Fig. (4.3) Variation of incident energy and useful energy with time for the serpentine and the parallel tubes flat plate solar collectors.

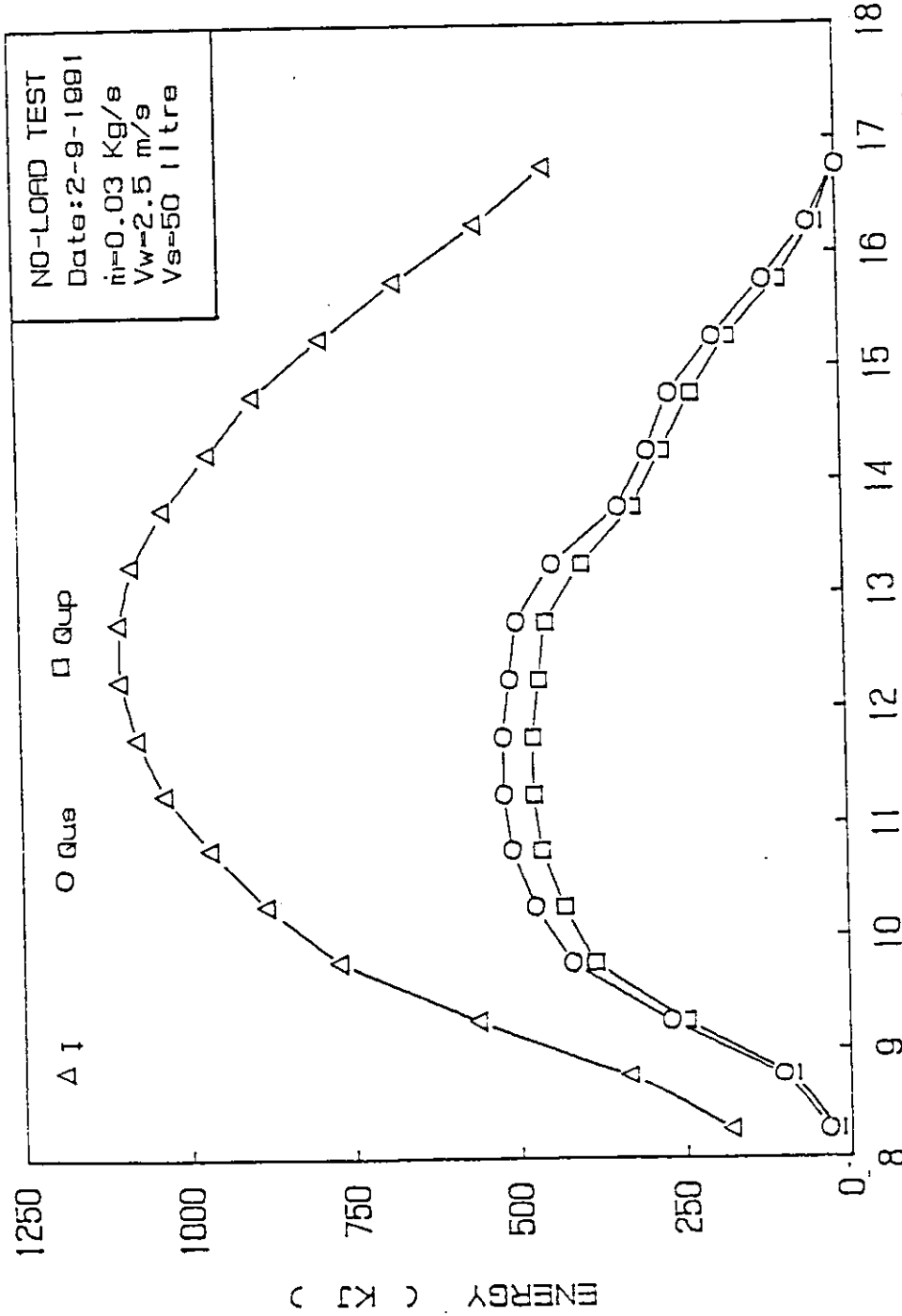


Fig.(4.32) Variation of Incident energy and useful energy with time for the serpentine and the parallel tubes flat plate solar collectors.

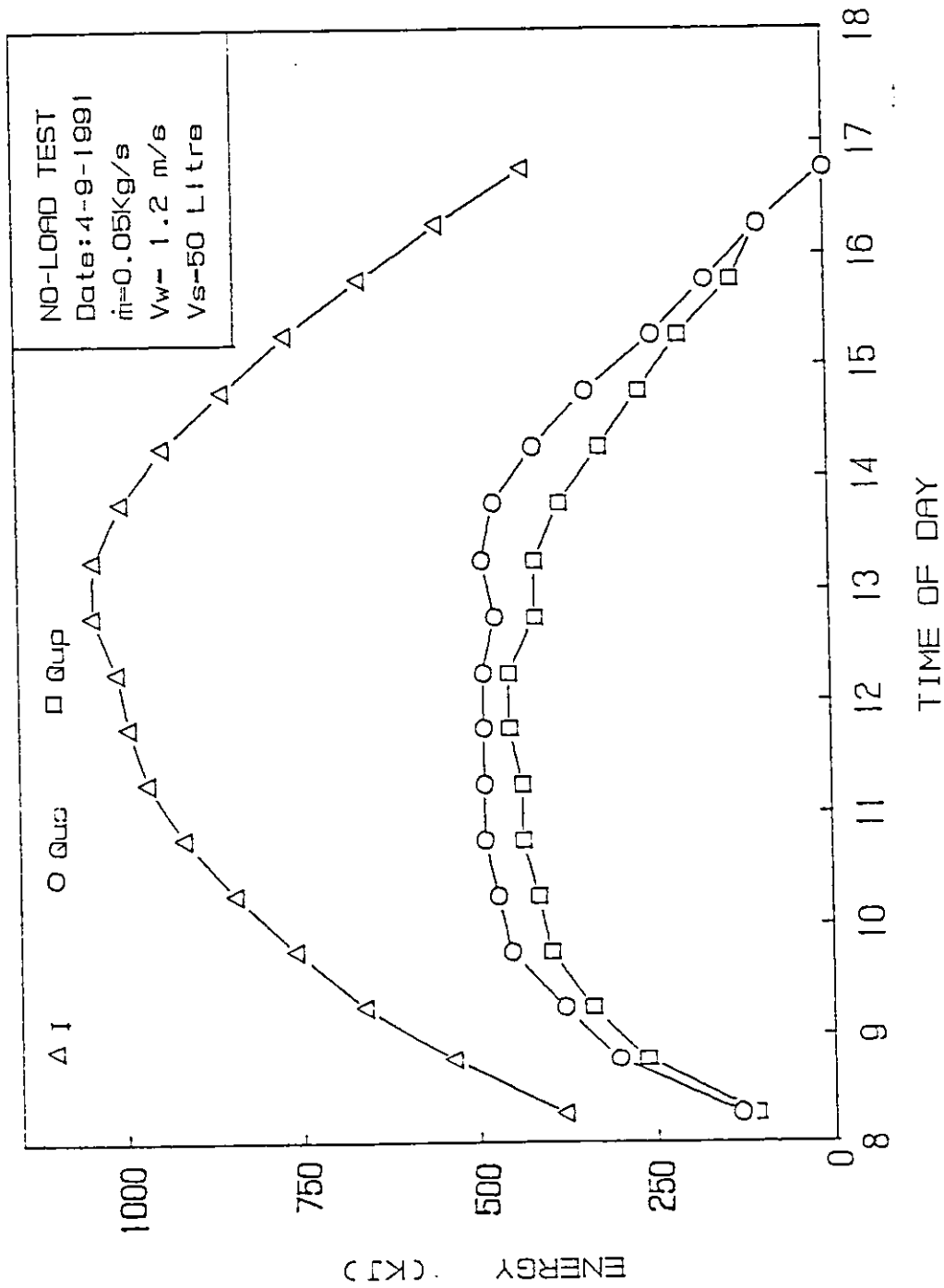


Fig.(4.33) Variation of incident energy and useful energy with time for the serpentine and the parallel tubes flat plate solar collectors.

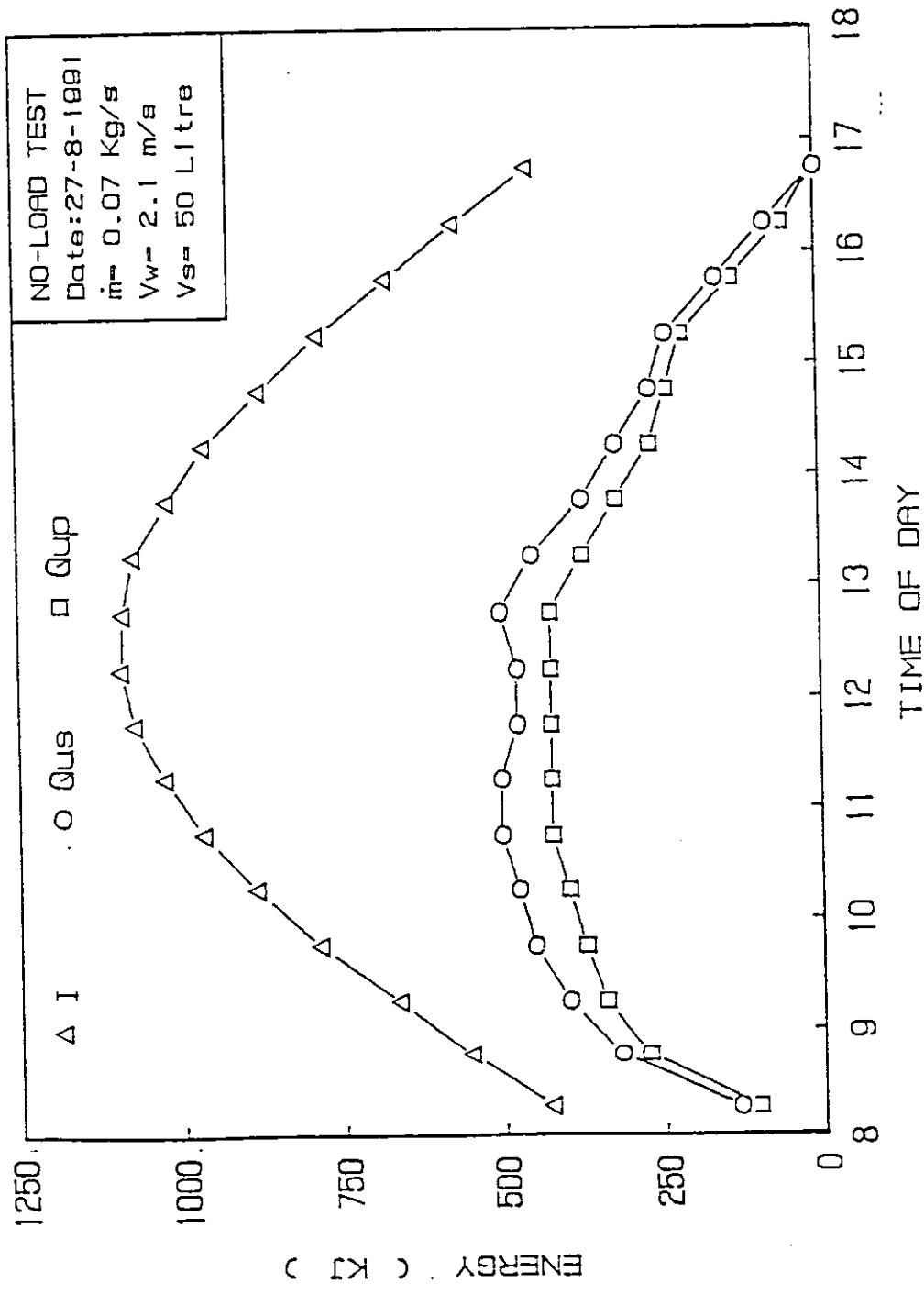


Fig.(4.34) Variation of Incident energy and useful energy with time for the serpentine and the parallel tubes flat plate solar collectors.

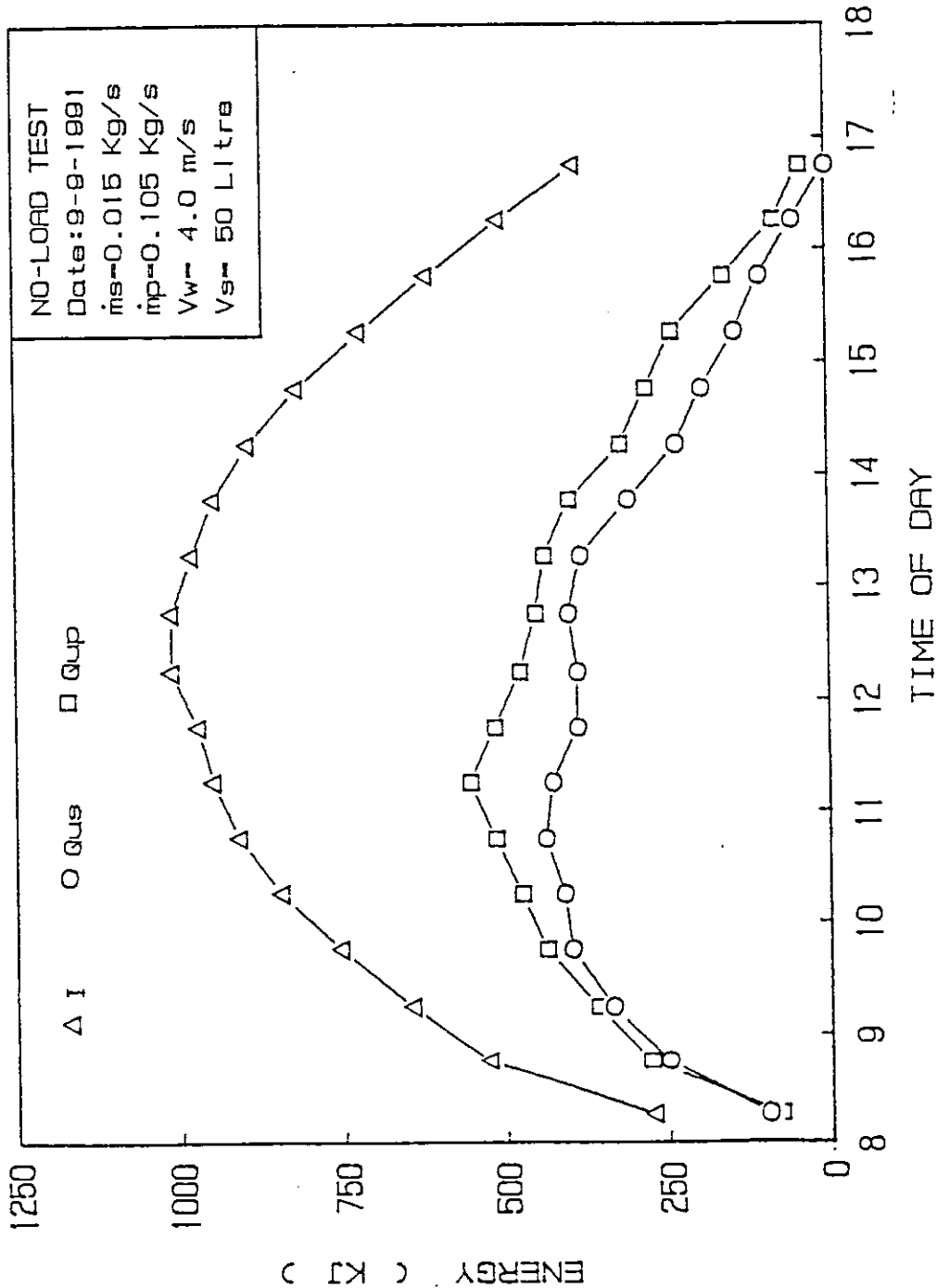


Fig. (4.35) Variation of incident energy and useful energy with time for the serpentine and the parallel tubes flat plate solar collectors at different mass flow rates.

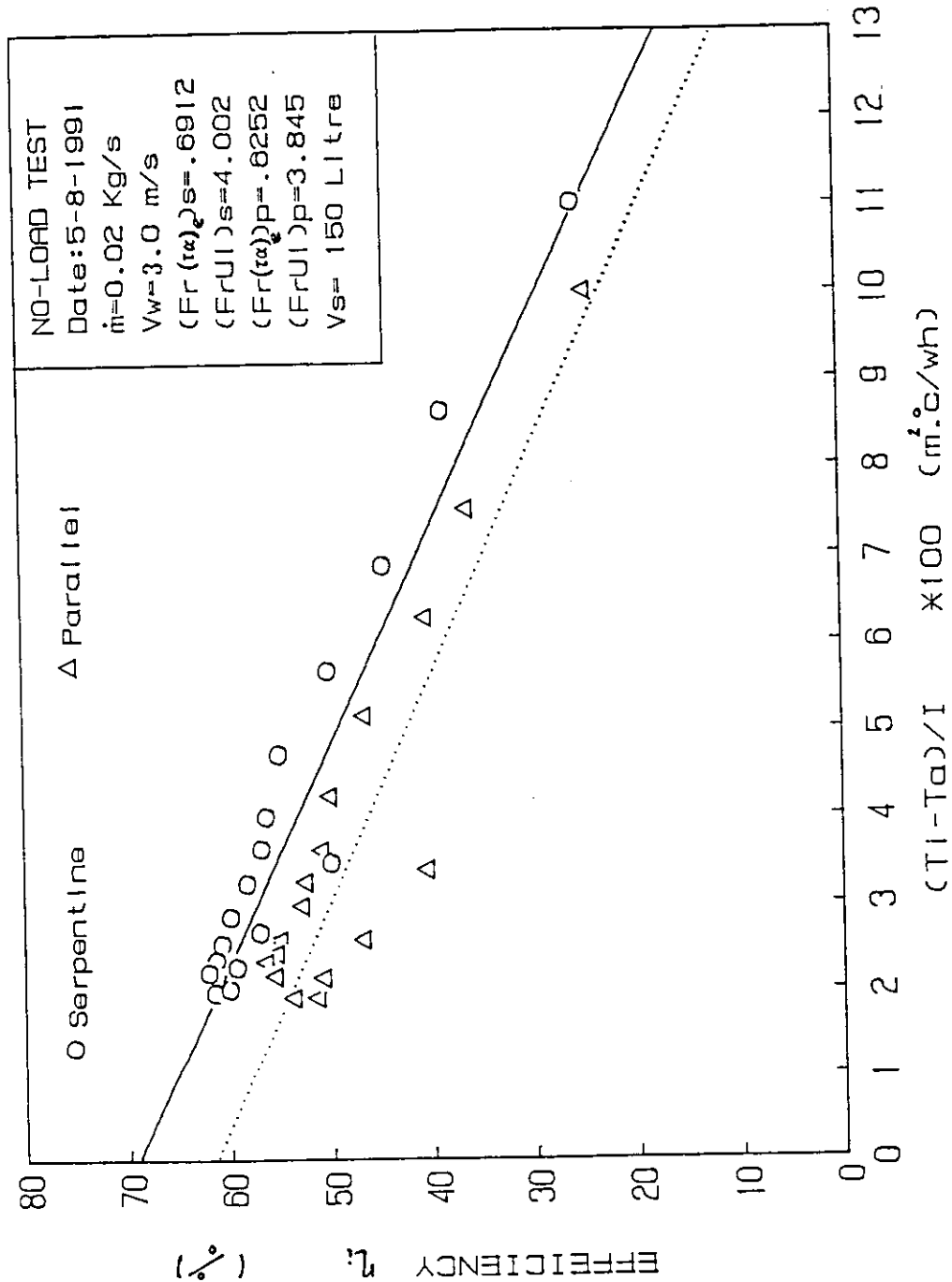


Fig.(4.38) Variation of instantaneous efficiency against $[(T_i - T_a)/I]$ for the serpentine and the parallel tubes flat plate solar collectors.

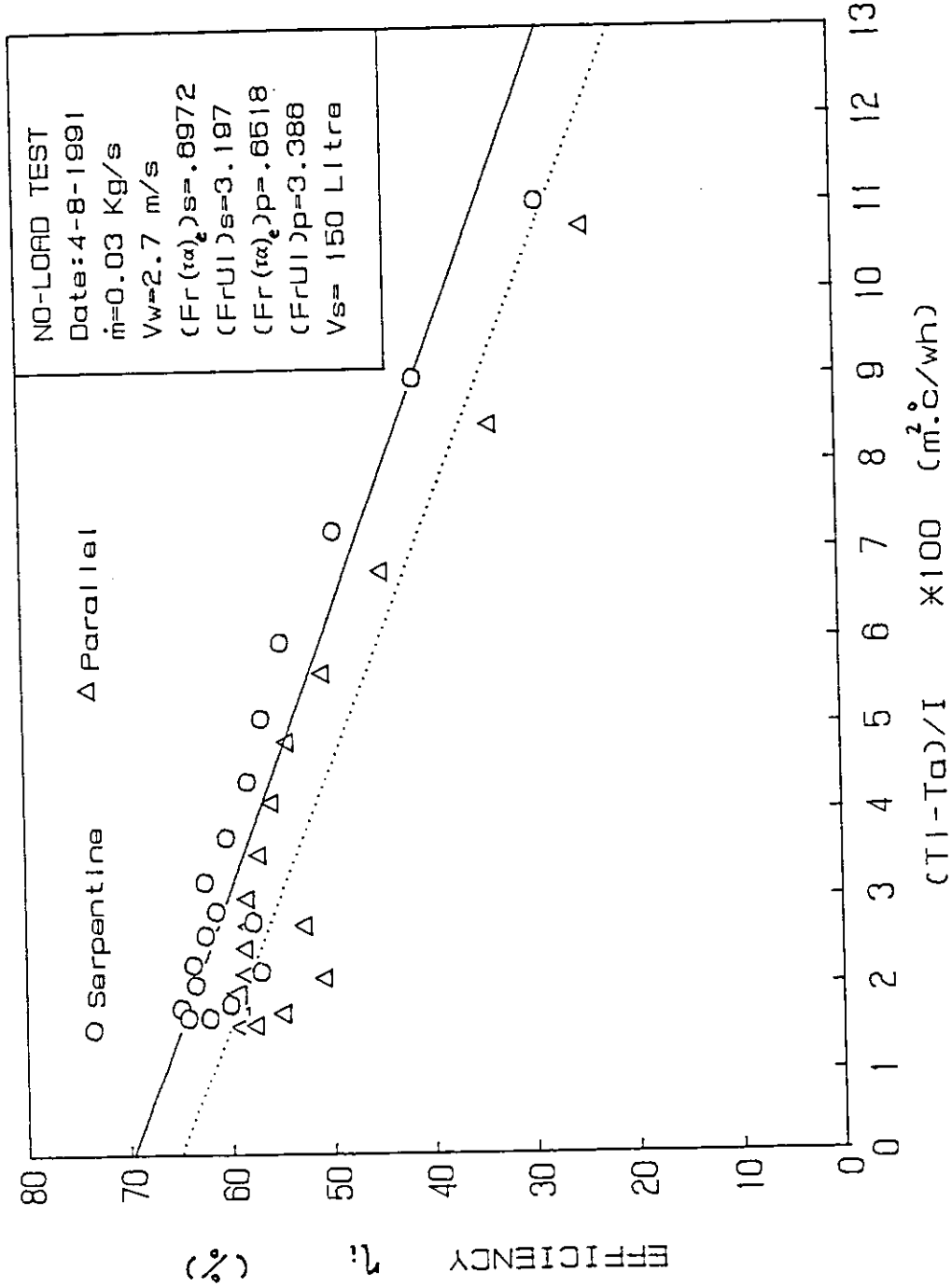


Fig.(4.37) Variation of instantaneous efficiency against $[(T_i - T_a)/I]$ for the serpentine and the parallel tubes flat plate solar collectors.

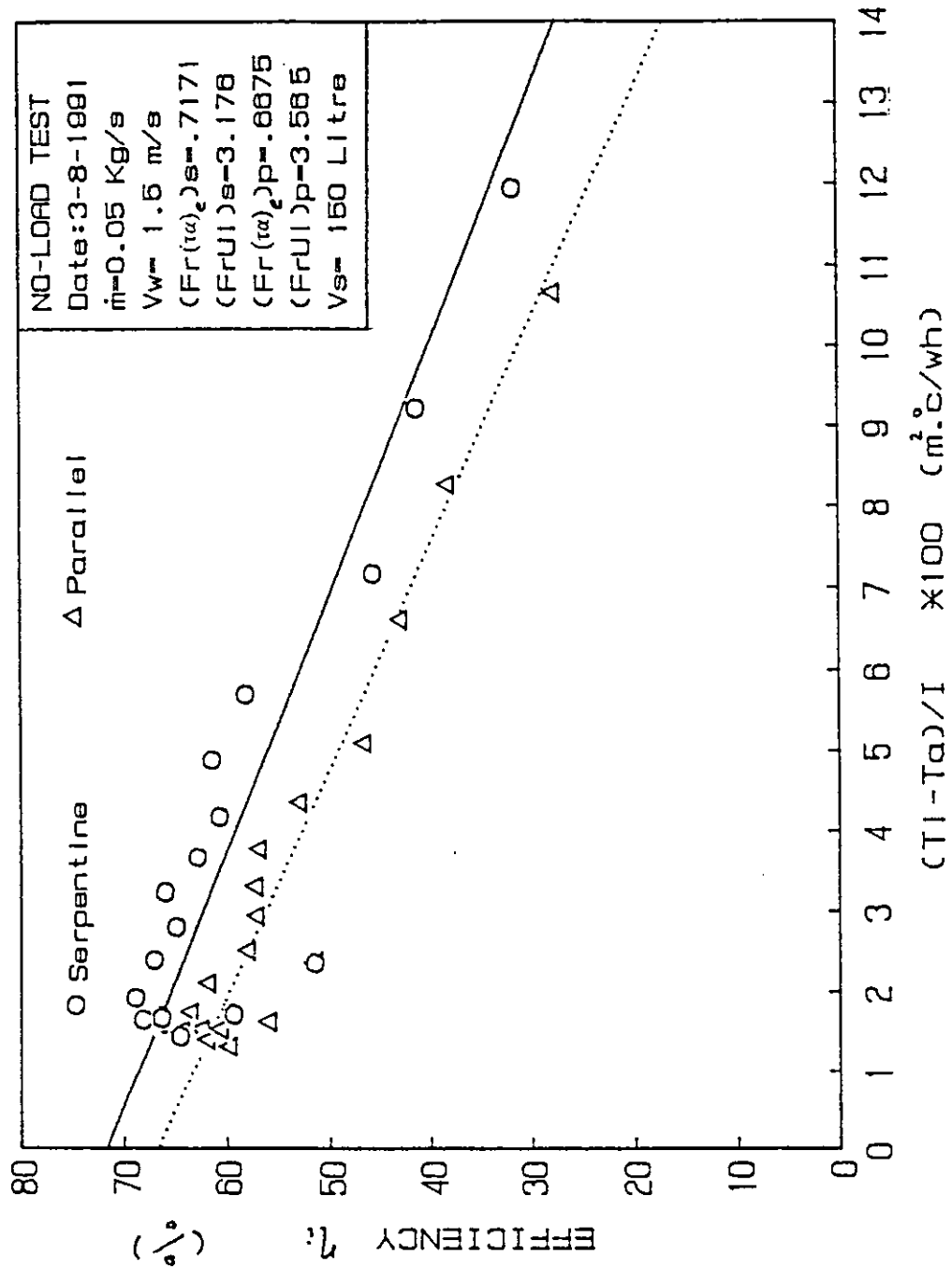


Fig.(4.38) Variation of Instantaneous efficiency against [(Ti-Ta)/I] for the serpentine and the parallel tubes flat plate solar collectors.

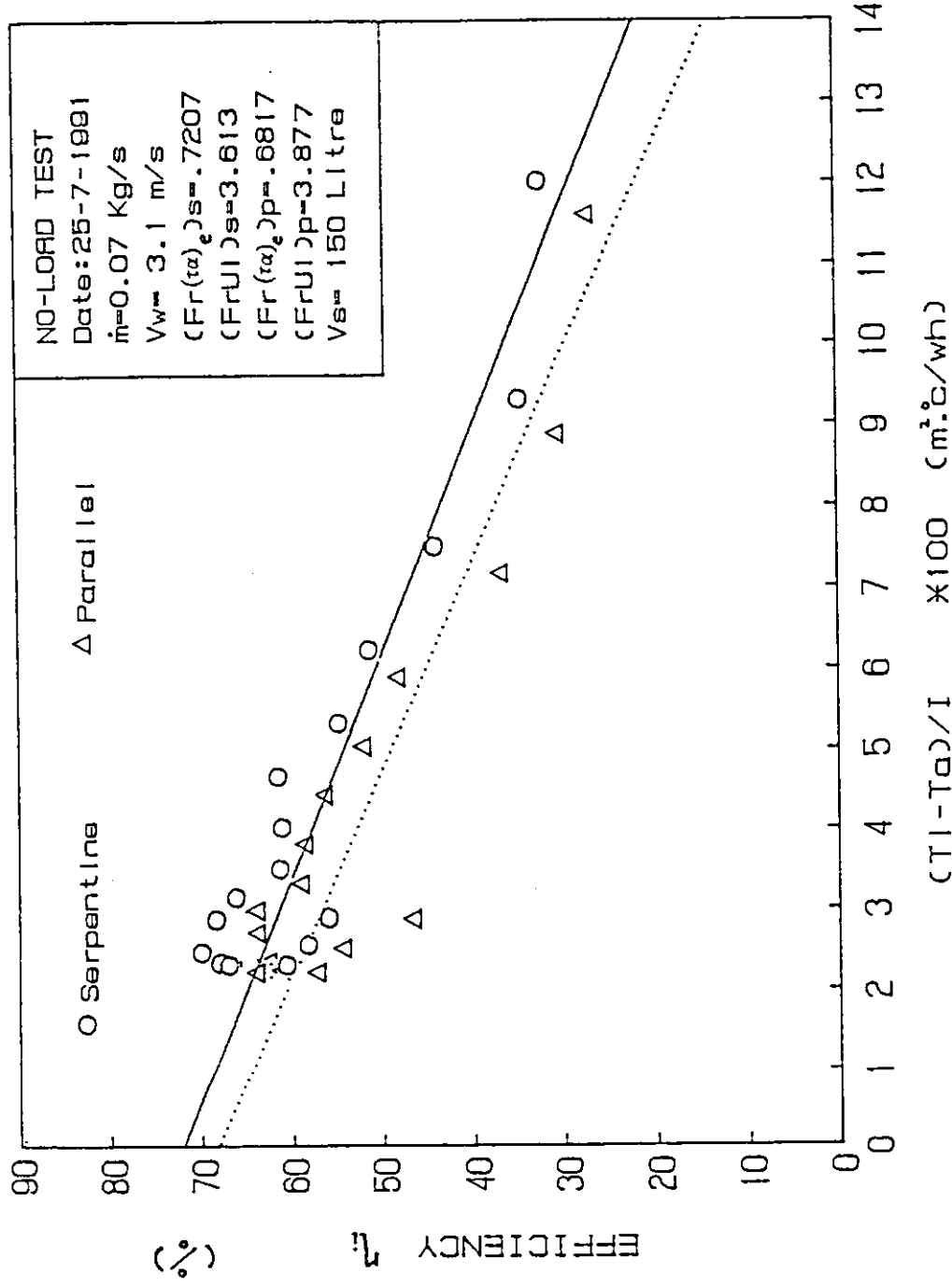


Fig.(4.39) Variation of instantaneous efficiency against $[(T_i - T_a)/I]$ for the serpentine and the parallel tubes flat plate solar collectors.

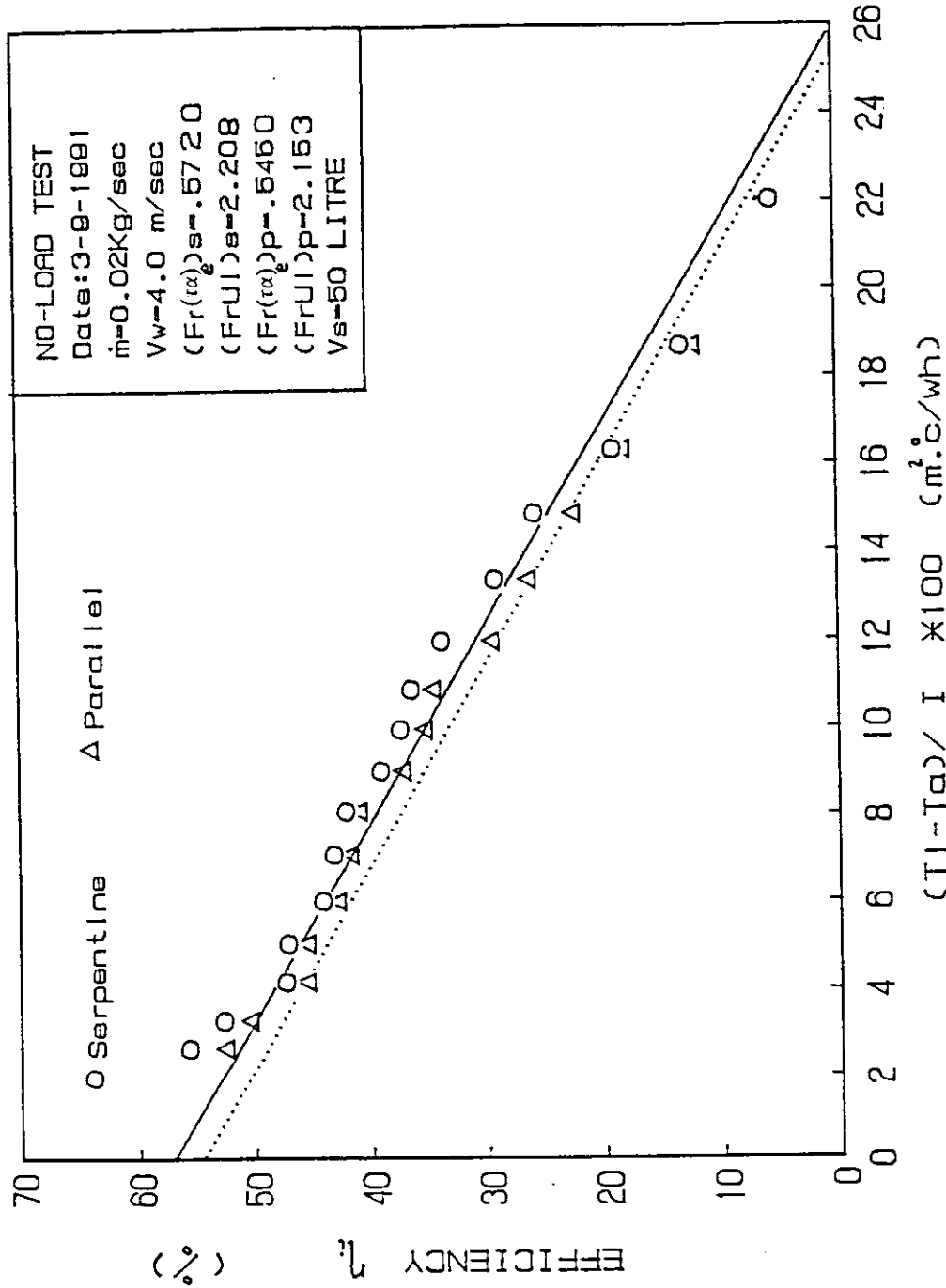


Fig.(4.40) Variation of instantaneous efficiency against $[(T_i - T_a) / I]$ for the serpentine and the parallel tubes flat plate solar collectors.

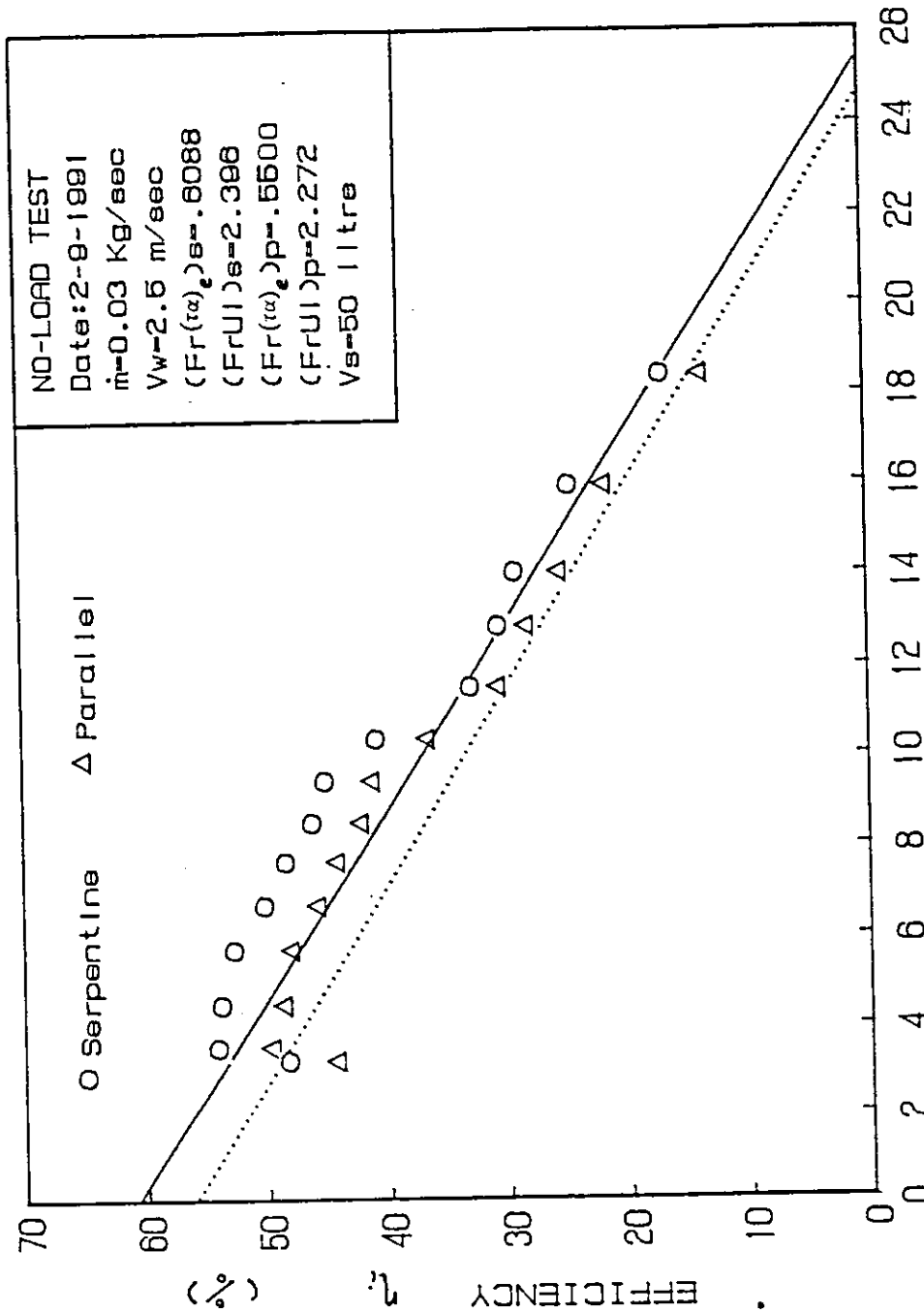


Fig.(4.41) Variation of Instantaneous efficiency against $[(T_I - T_a)/I]$ for the serpentine and the parallel tubes flat plate solar collectors.

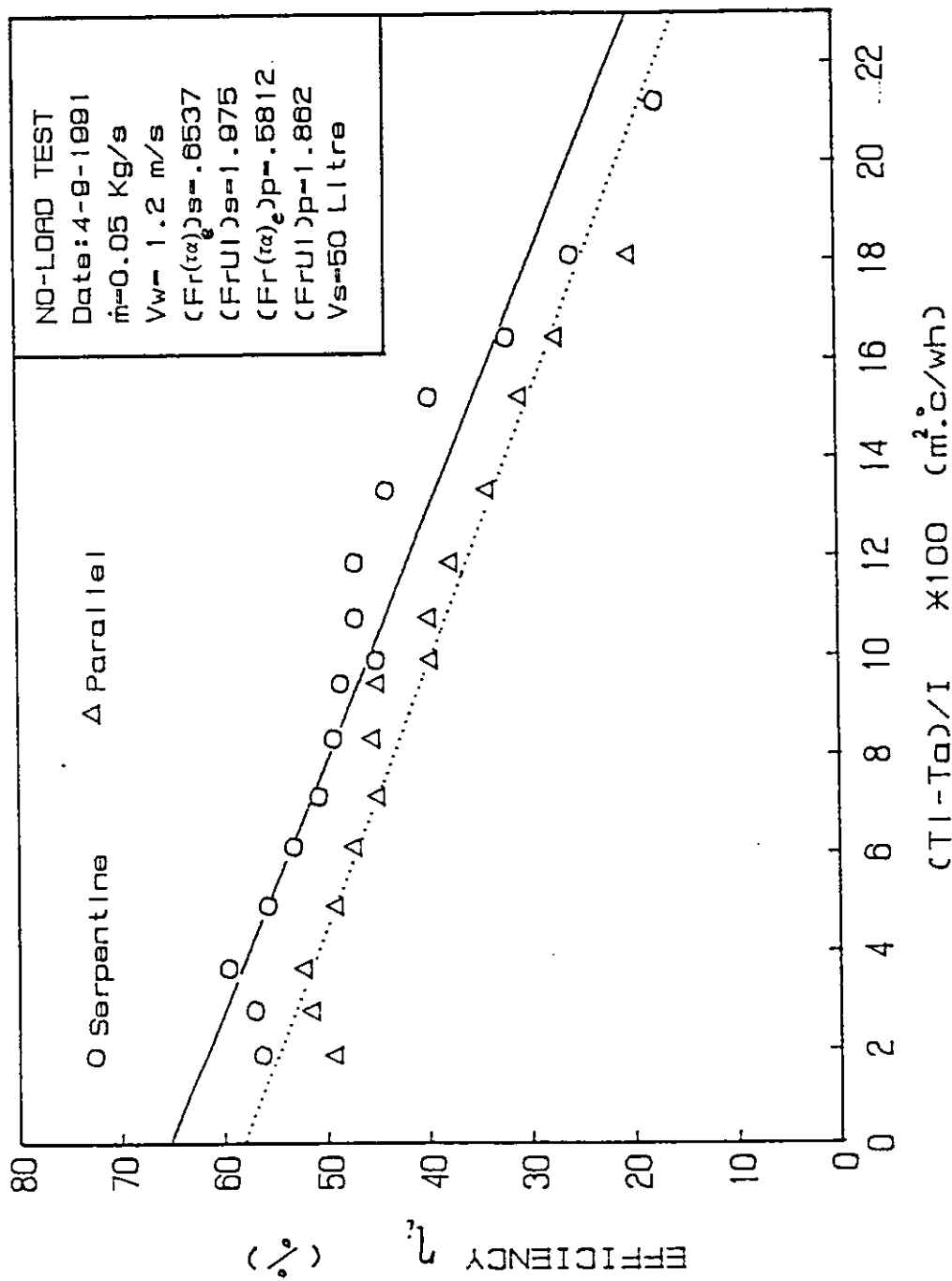


Fig.(4.42) Variation of Instantaneous efficiency against $[(T_i - T_a)/I]$ for the serpentine and the parallel tubes flat plate solar collectors.

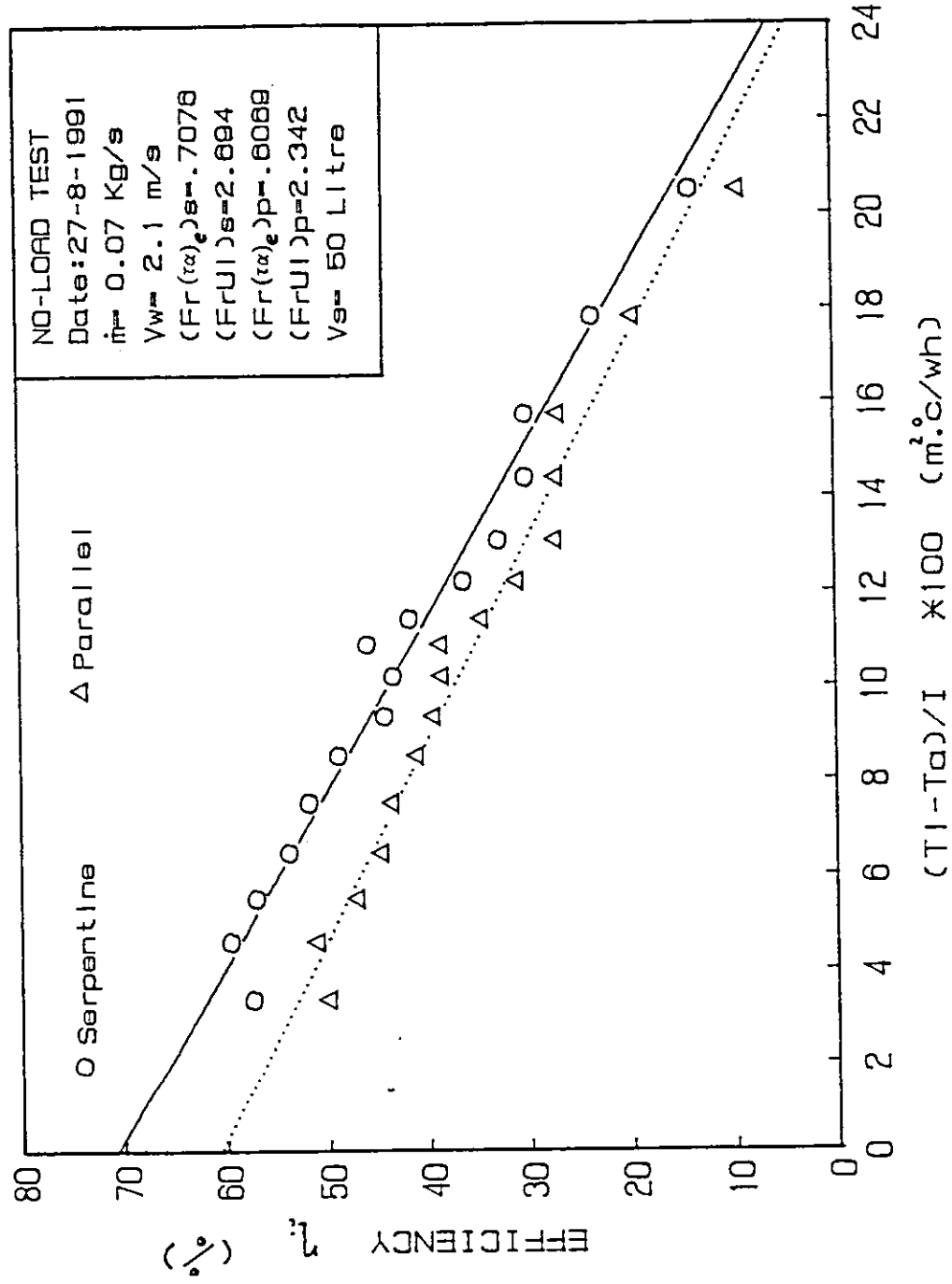


Fig.(4.43) Variation of Instantaneous efficiency against $[(T_i - T_a)/I] \times 100$ (m².c/wh) for the serpentine and the parallel tubes flat plate solar collectors.

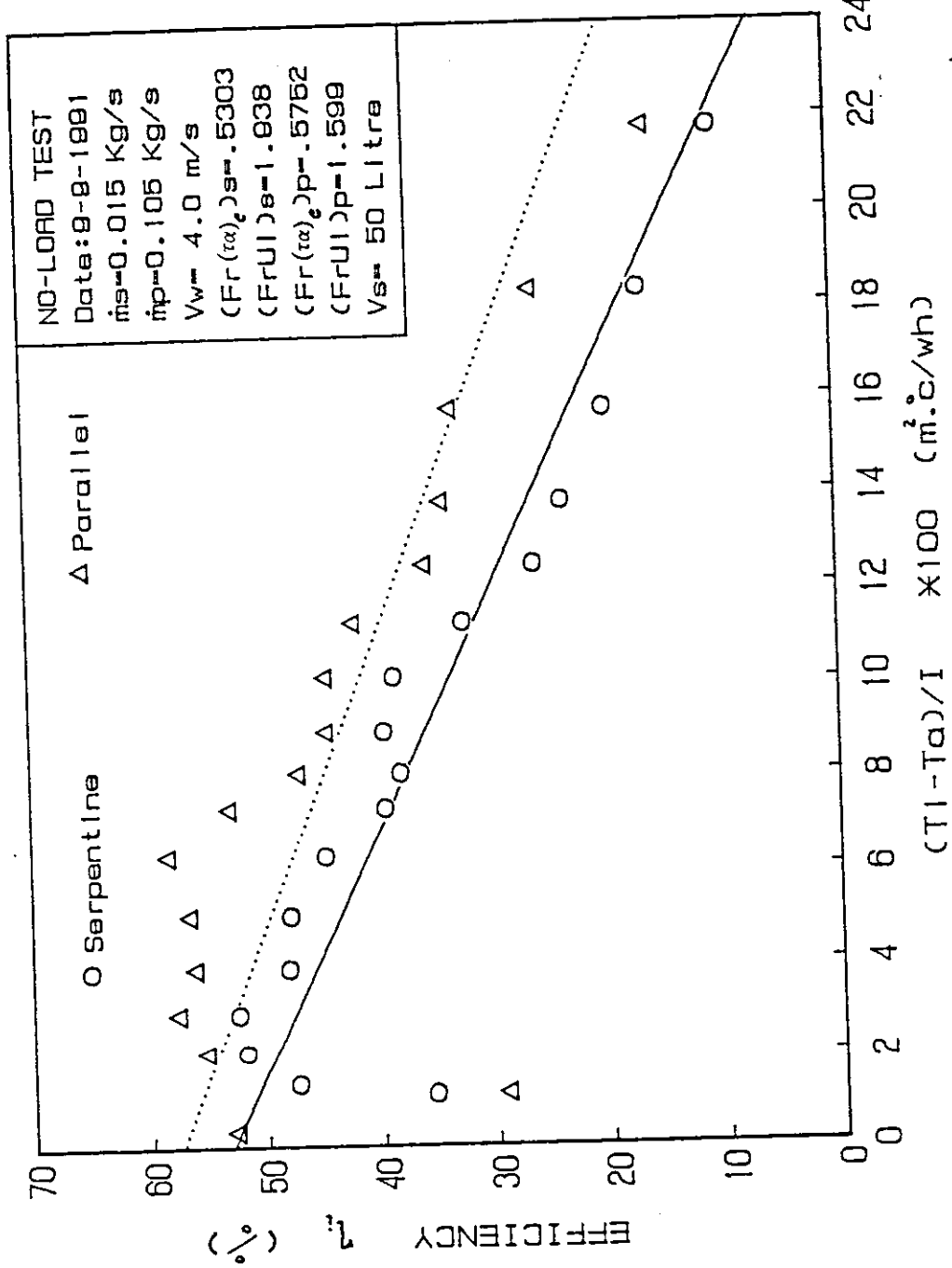


FIG.(4.44) Variation of instantaneous efficiency against $[(T_1 - T_a)/I] \times 100 \text{ (m.c/wh)}$ for the serpentine and the parallel tubes flat plate solar collectors with two different mass flow rates.

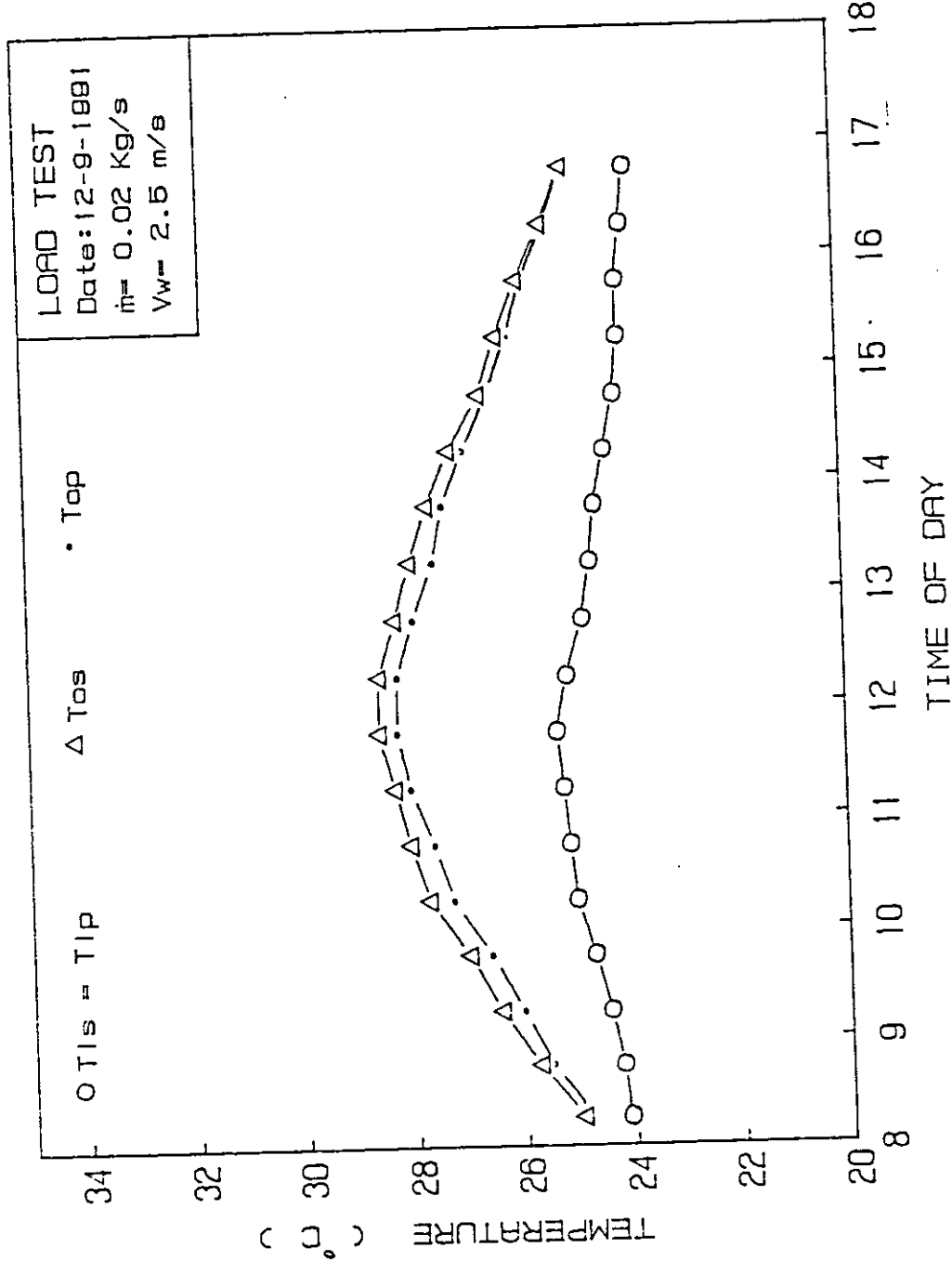


Fig.(4.45) Variation of inlet temperature, outlet temperature, and ambient temperature with time for the serpentine and the parallel tubes flat plate solar collectors.

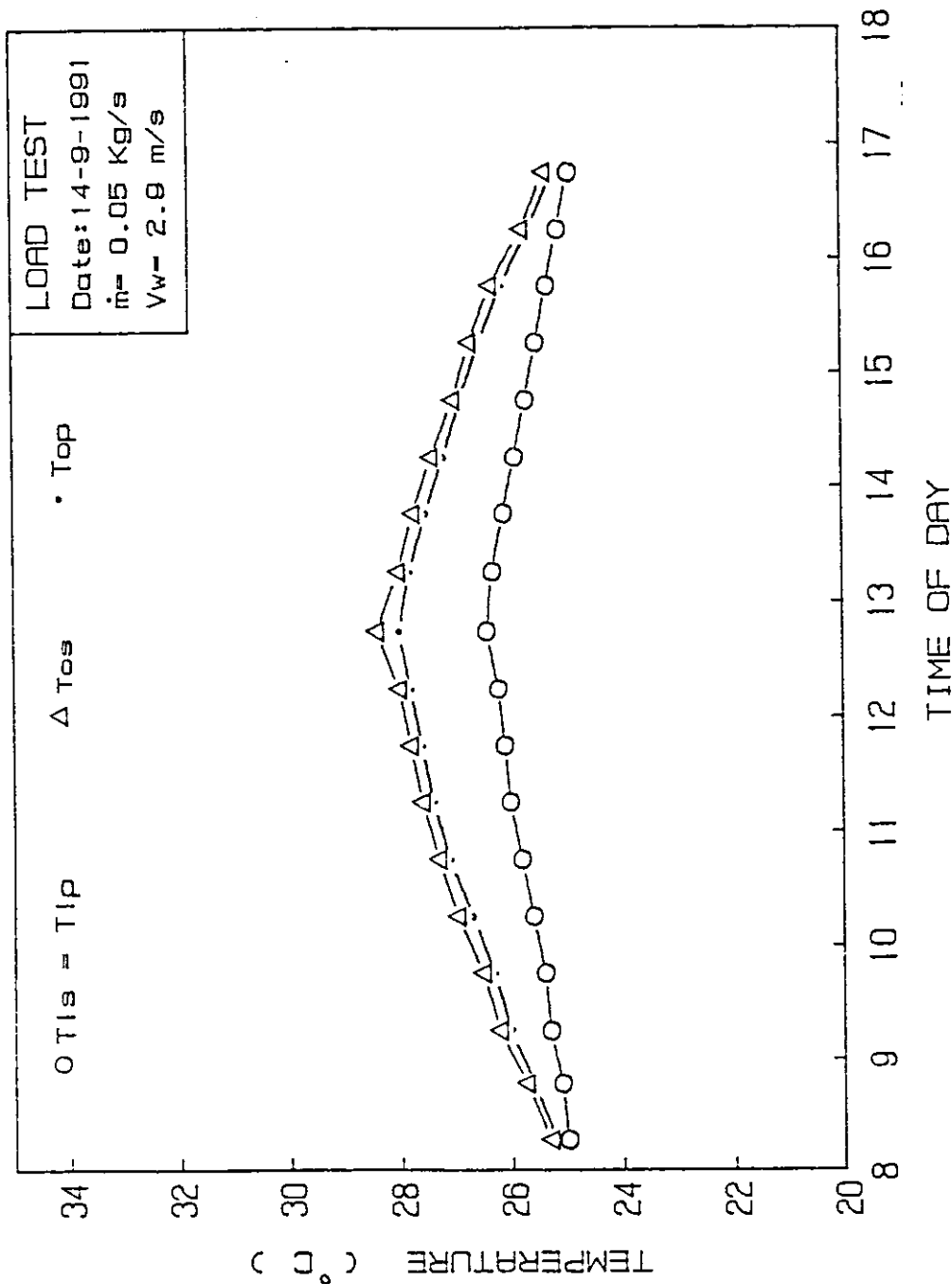
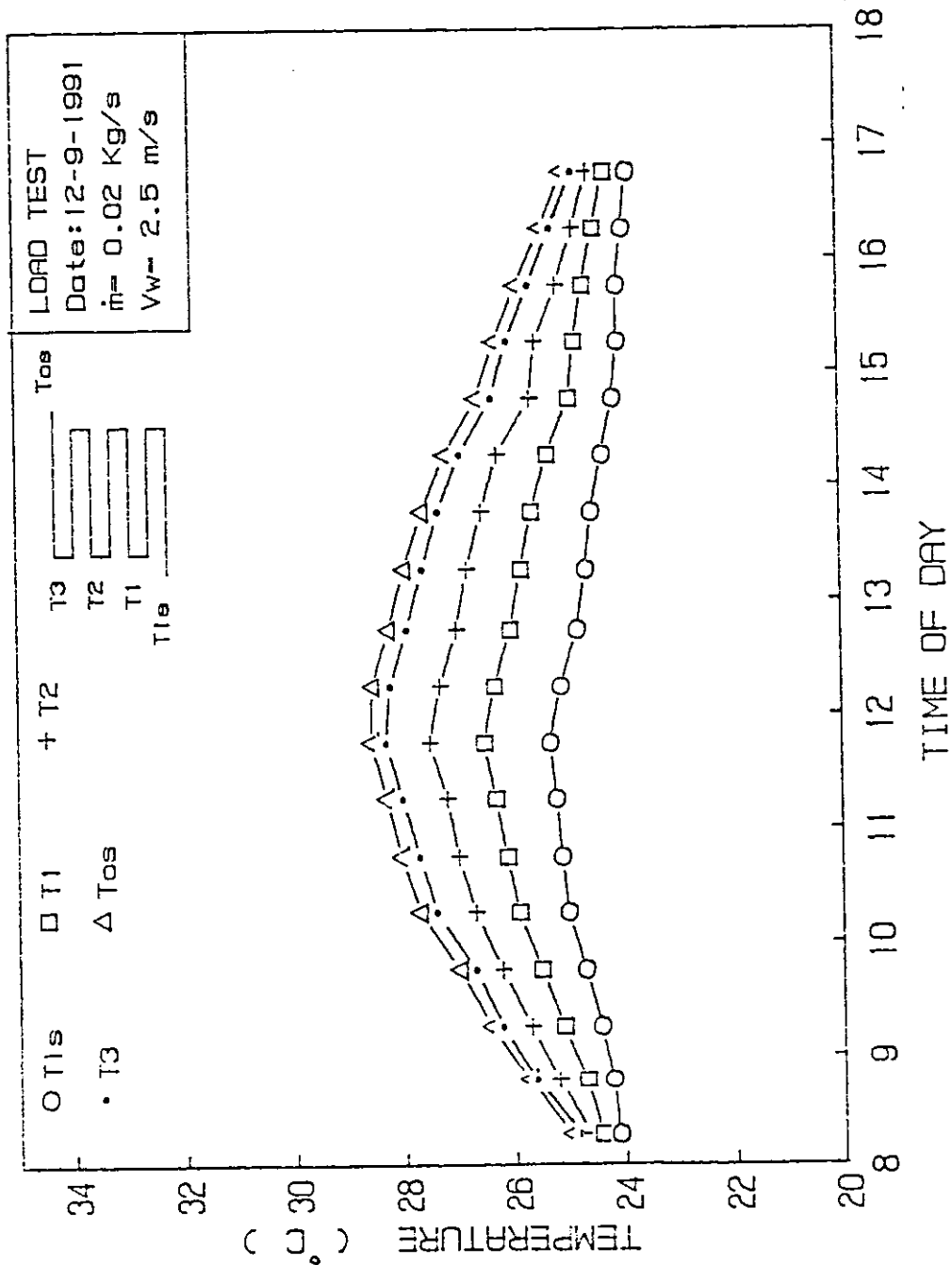


Fig.(4.46) Variation of Inlet temperature, outlet temperature, and ambient temperature with time for the serpentine and the parallel tubes flat plate solar collectors.



LOAD TEST
 Date: 12-9-1991
 $\dot{m} = 0.02 \text{ Kg/s}$
 $V_w = 2.5 \text{ m/s}$

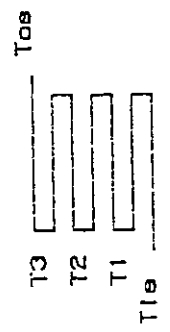


Fig. (4.47) Temperature distribution of the water inside the serpentine tube flat plate solar collector and ambient temperature during the day test.

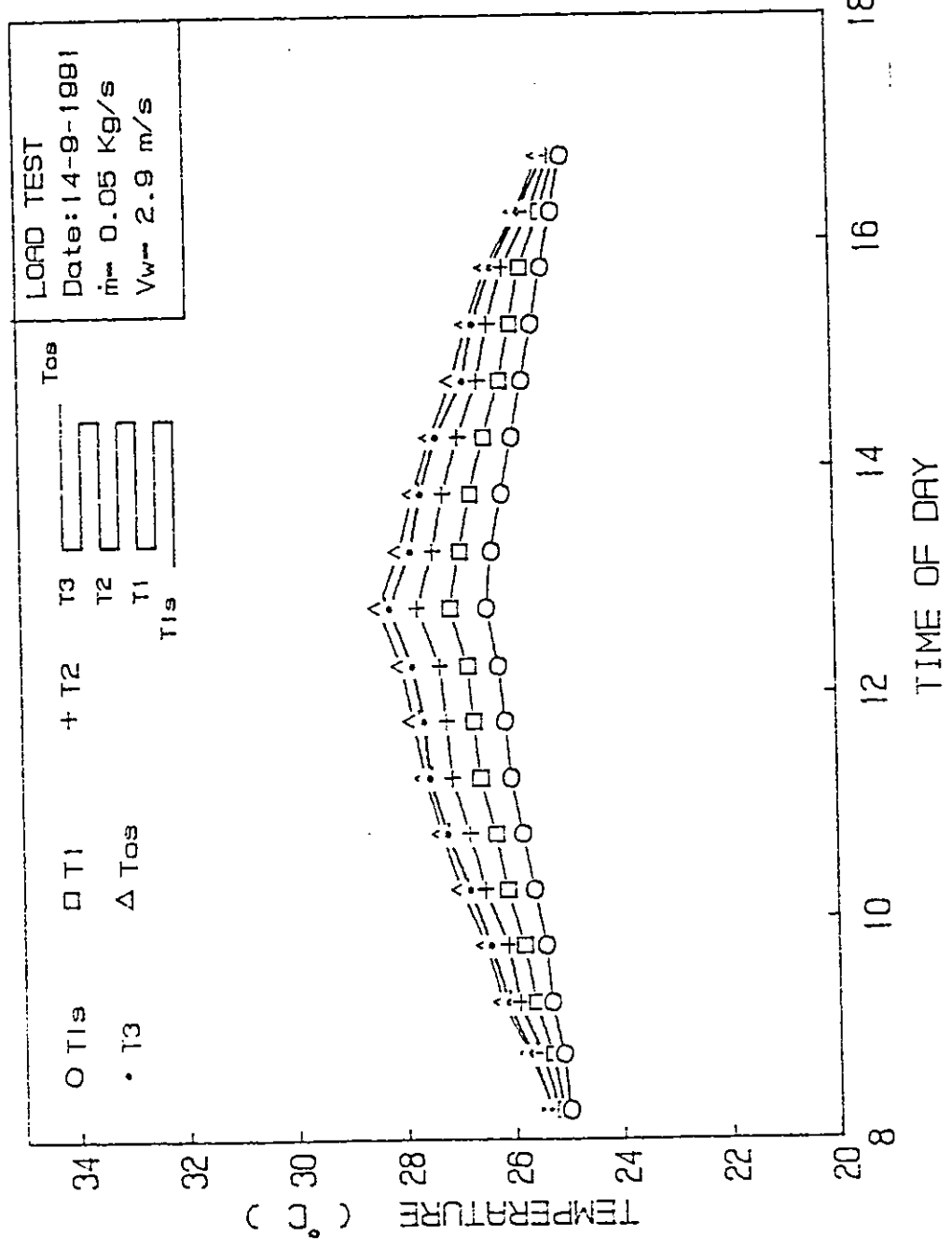
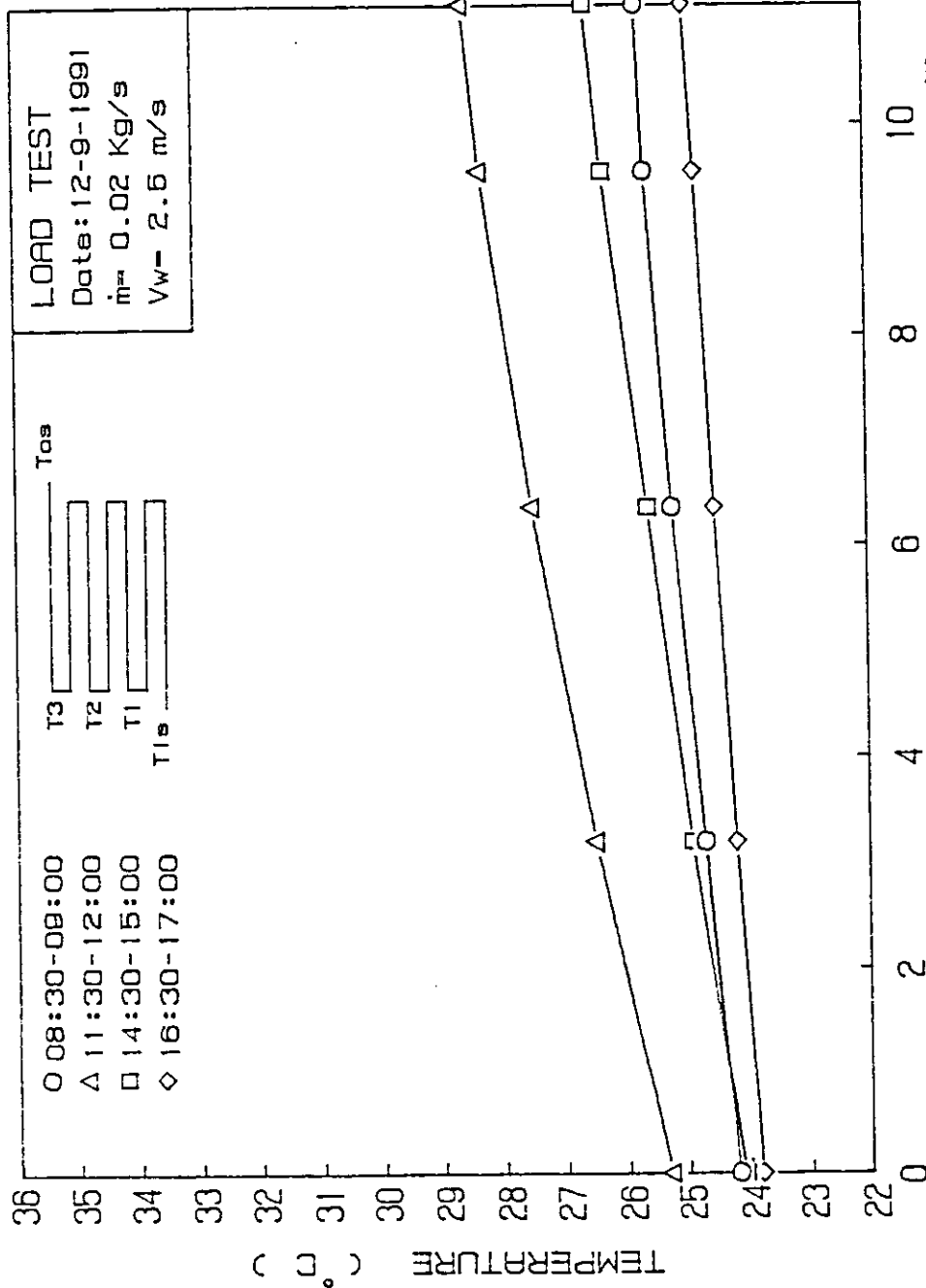


Fig.(4.48) Temperature distribution of the water inside the serpentine tube flat plate solar collector and ambient temperature during the day test.



DISTANCE FROM THE INLET OF THE COLLECTOR (m)

Fig.(4.49) Temperature distribution of the water inside the serpentine tube flat plate solar collector at different times of the day.

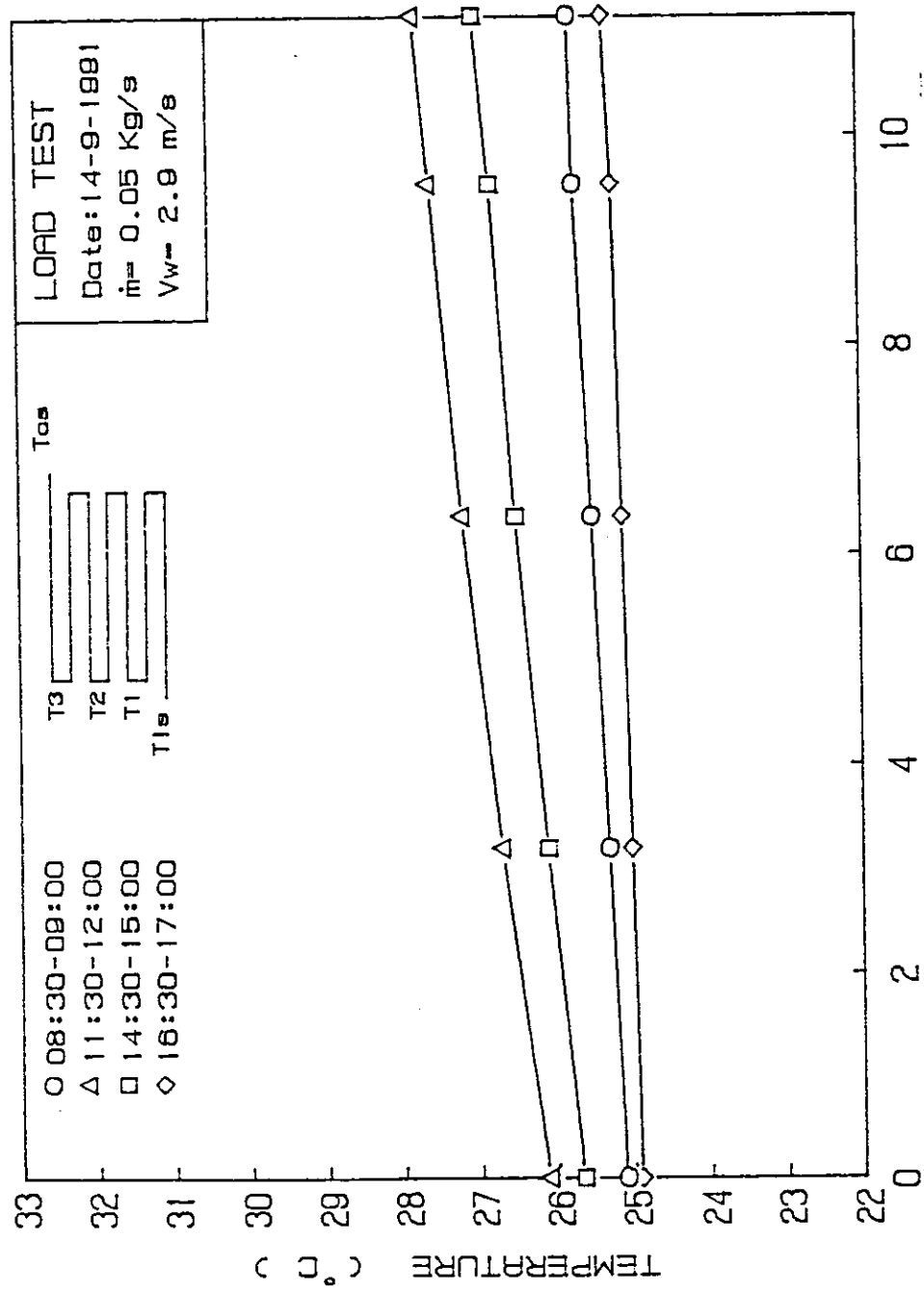


Fig.(4.50) Temperature distribution of the water inside the serpentine tube flat plate solar collector at different times of the day.

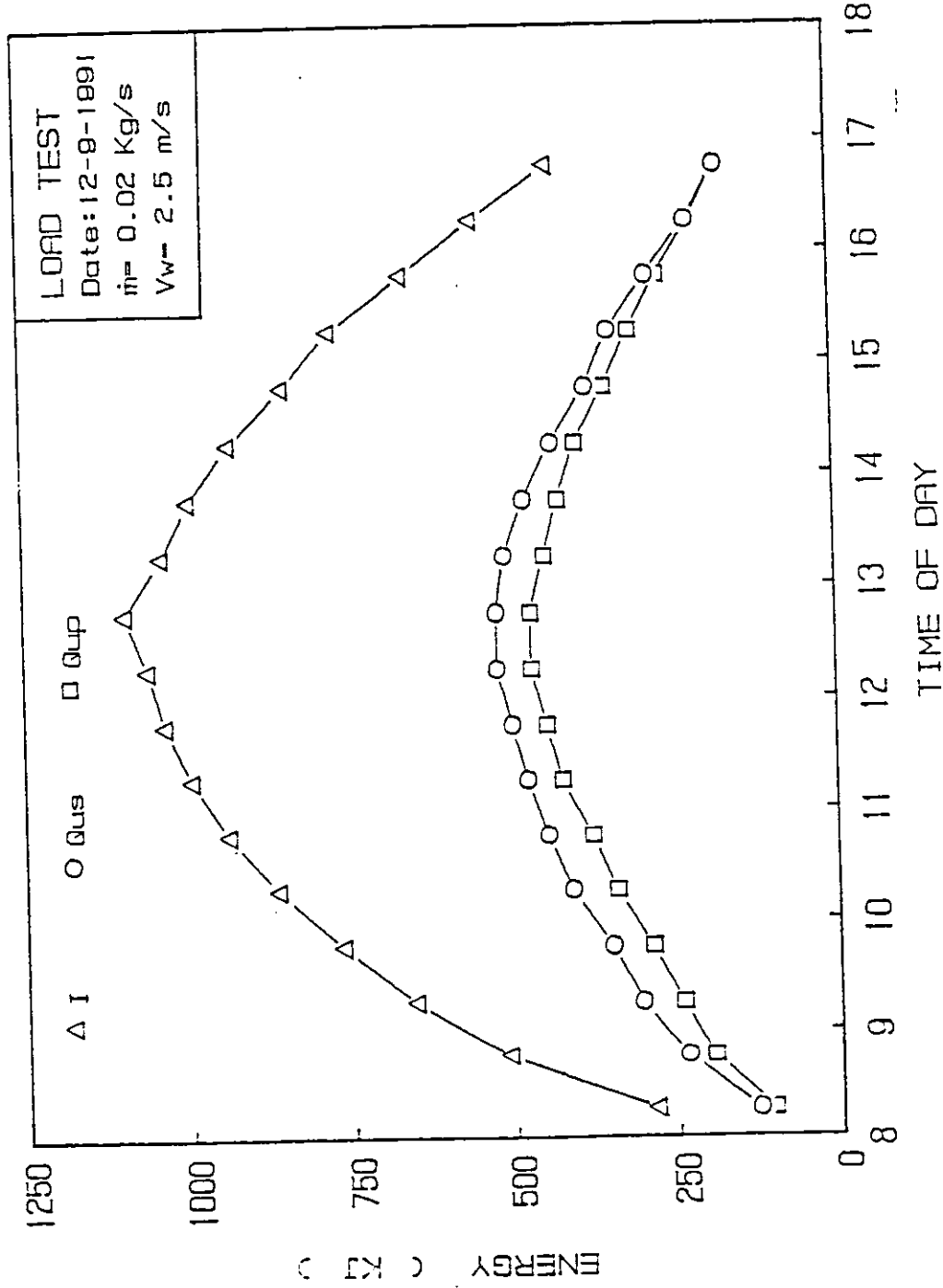


Fig.(4.51) Variation of incident energy and useful energy with time for the serpentine and the parallel tubes flat plate solar collectors.

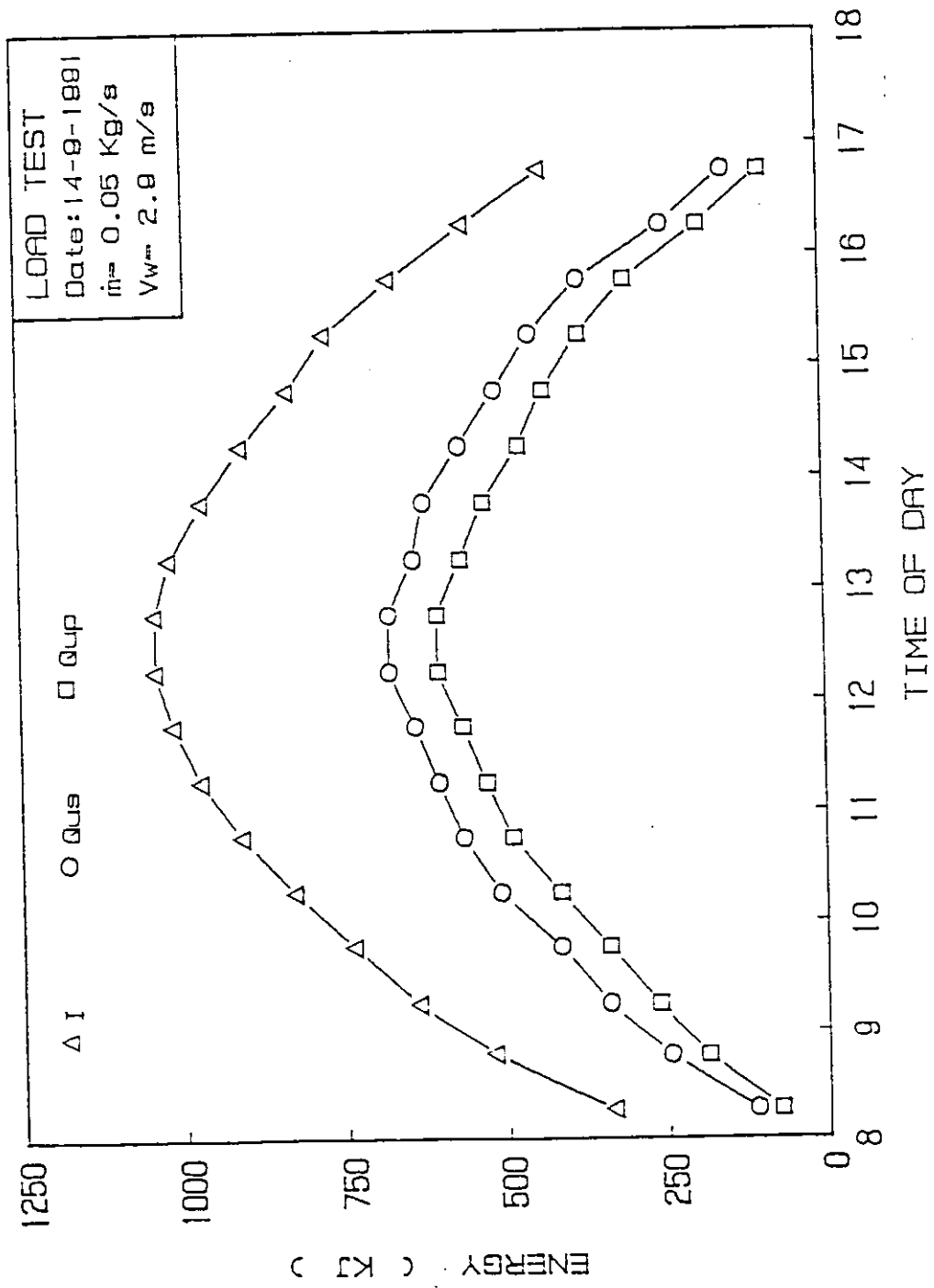


Fig. (4.52) Variation of Incident energy and useful energy with time for the serpentine and the parallel tubes flat plate solar collectors.

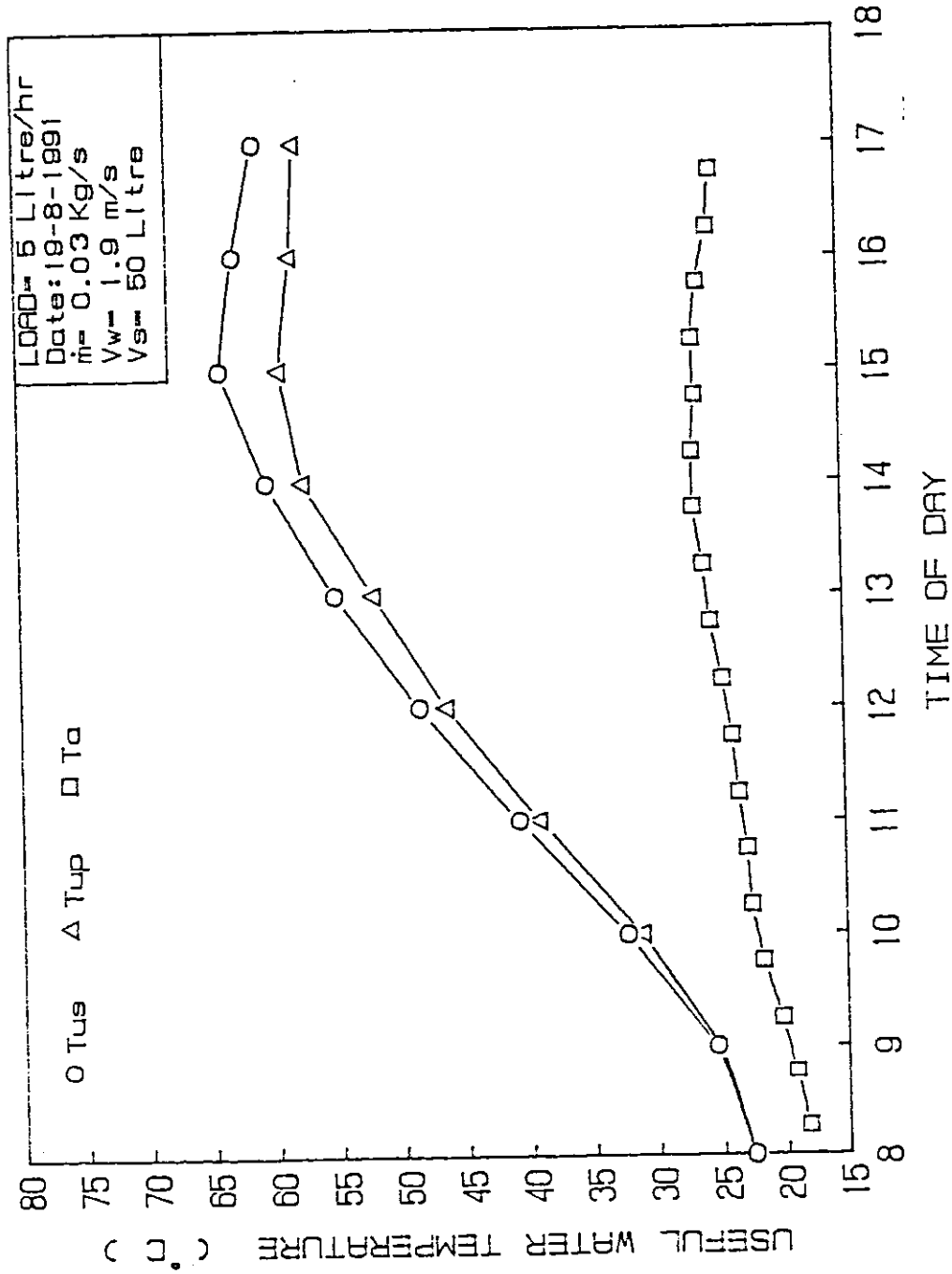


Fig.(4.53) Variation of useful water temperature and ambient temperature with time of day for the serpentine and parallel tubes flat plate solar collectors under a load of 5 Litre/hr.

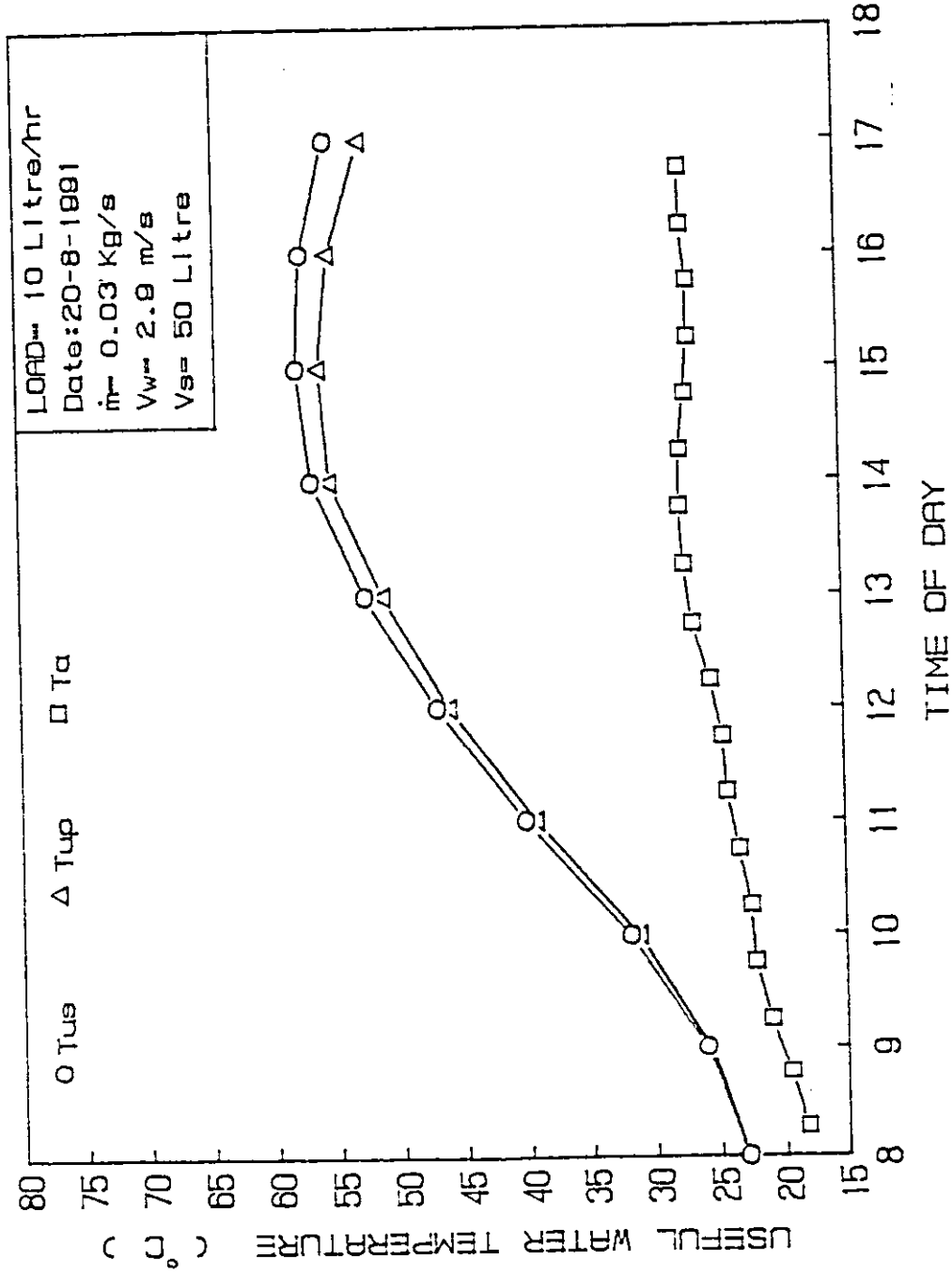


Fig.(4.54) Variation of useful water temperature and ambient temperature with time for the serpentine and the parallel tubes flat plate solar collectors under a load of 10 Litre/hr.

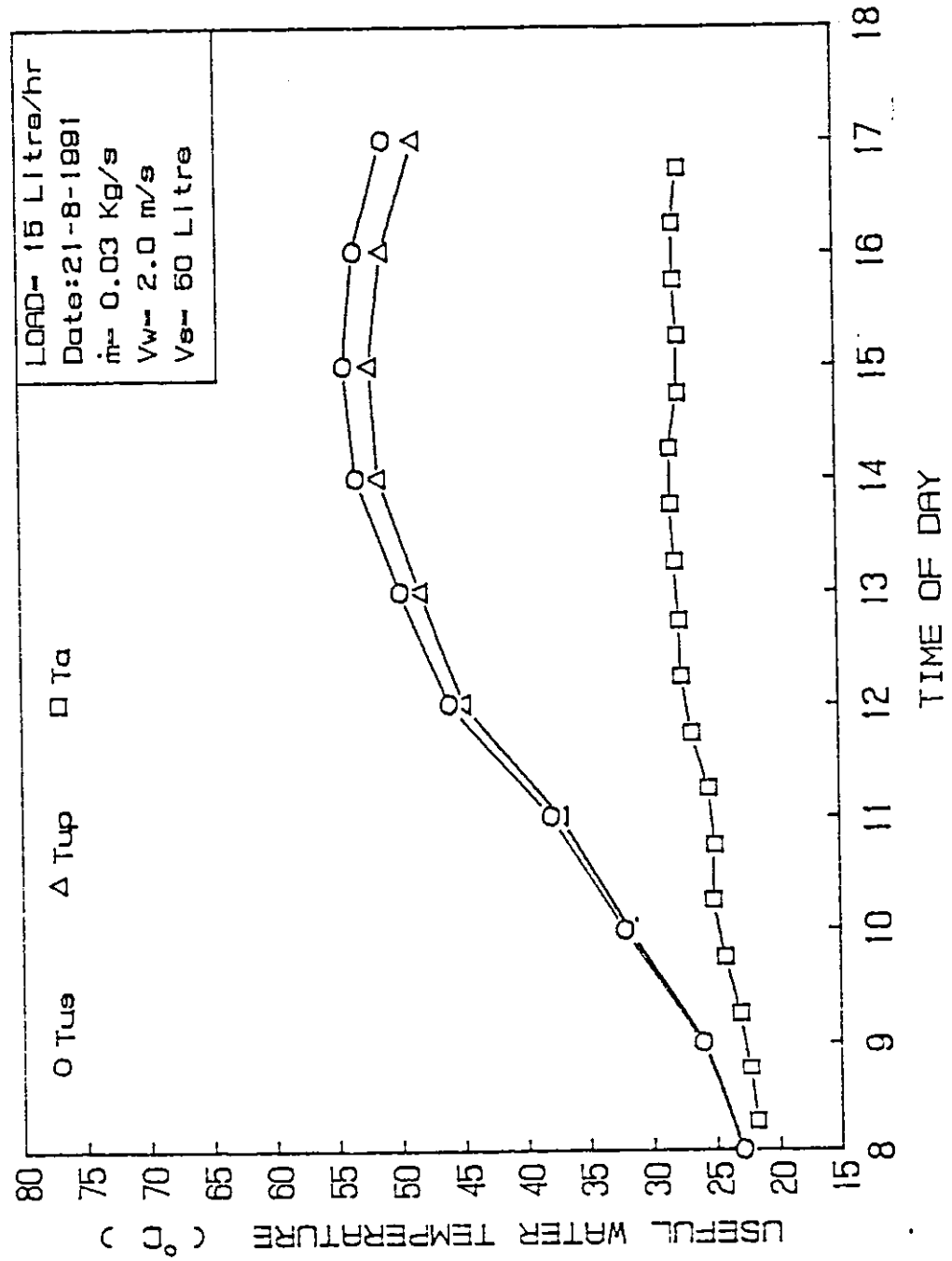


Fig. (4.55) Variation of useful water temperature and ambient temperature with time for the serpentine and the parallel tubes flat plate solar collectors under a load of 15 Litre/hr.

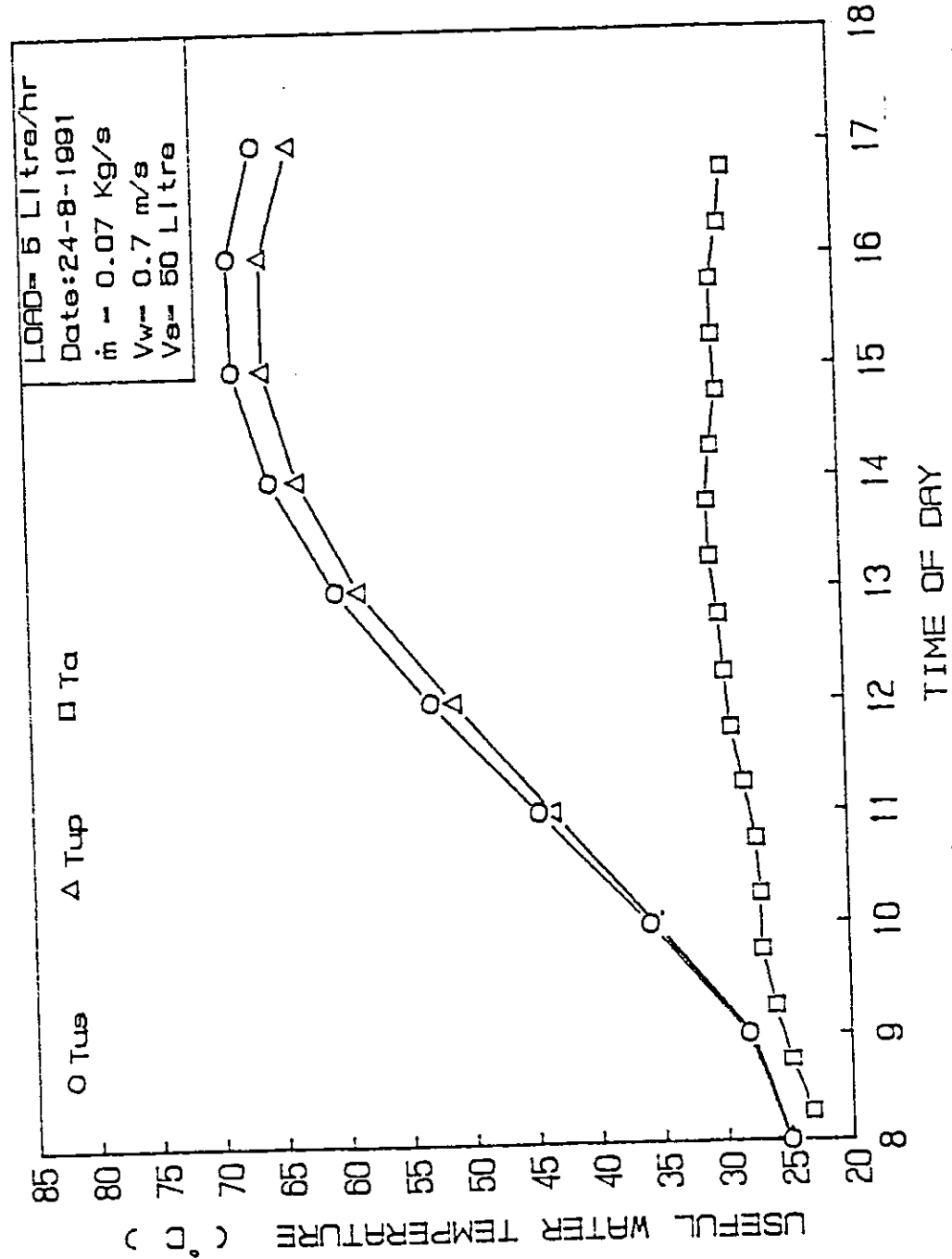


Fig. (4.56) Variation of useful water temperature and ambient temperature with time for the serpentine and the parallel tubes flat plate solar collectors under a load of 5 Litre/hr.

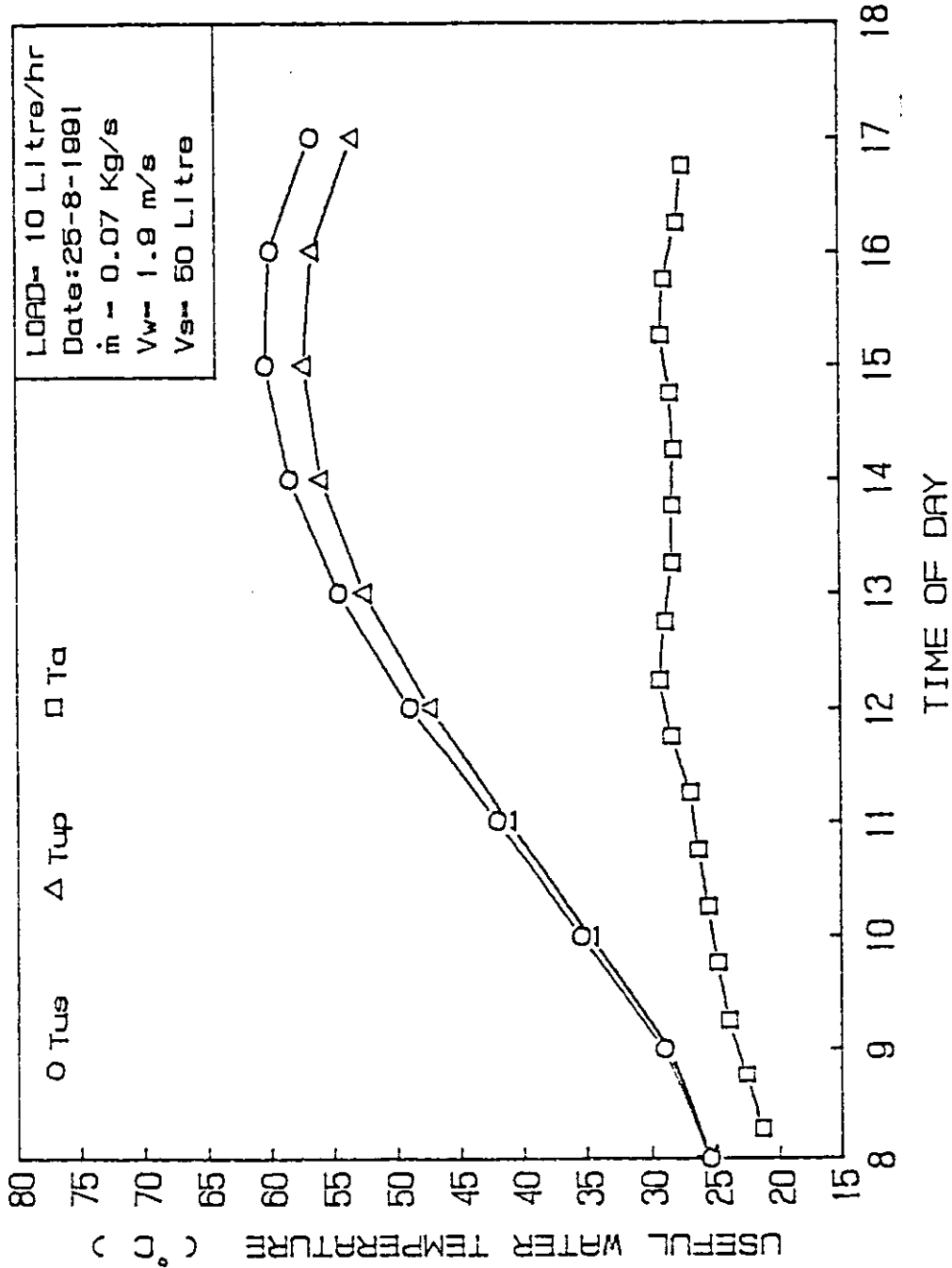


Fig. (4.57) Variation of useful water temperature and ambient temperature with time for the serpentine and the parallel tubes flat plate solar collectors under a load of 10 Litre/hr.

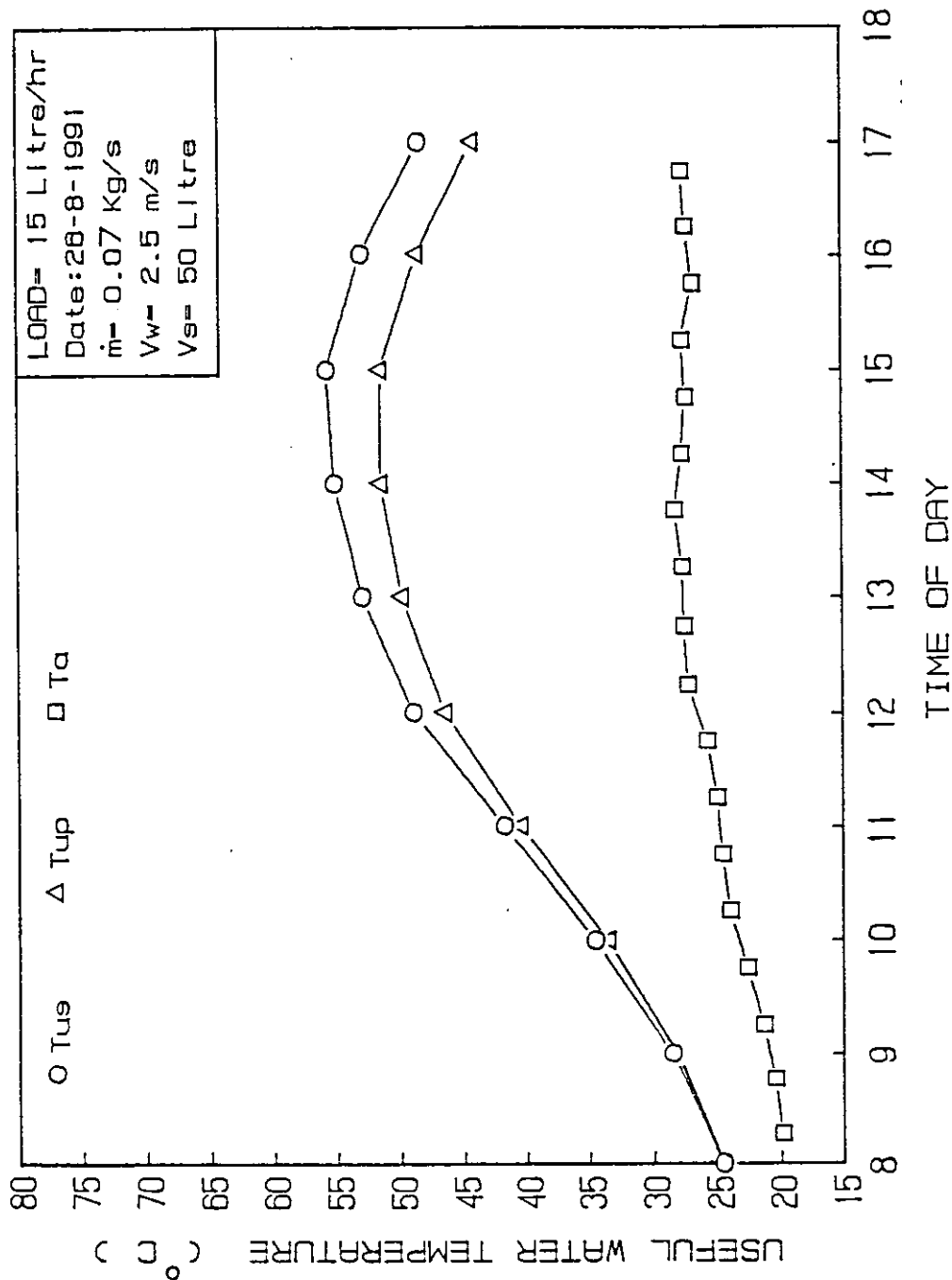


Fig.(4.58) Variation of useful water temperature and ambient temperature with time for the serpentine and the parallel tubes flat plate solar collectors under a load of 15 Litre/hr.

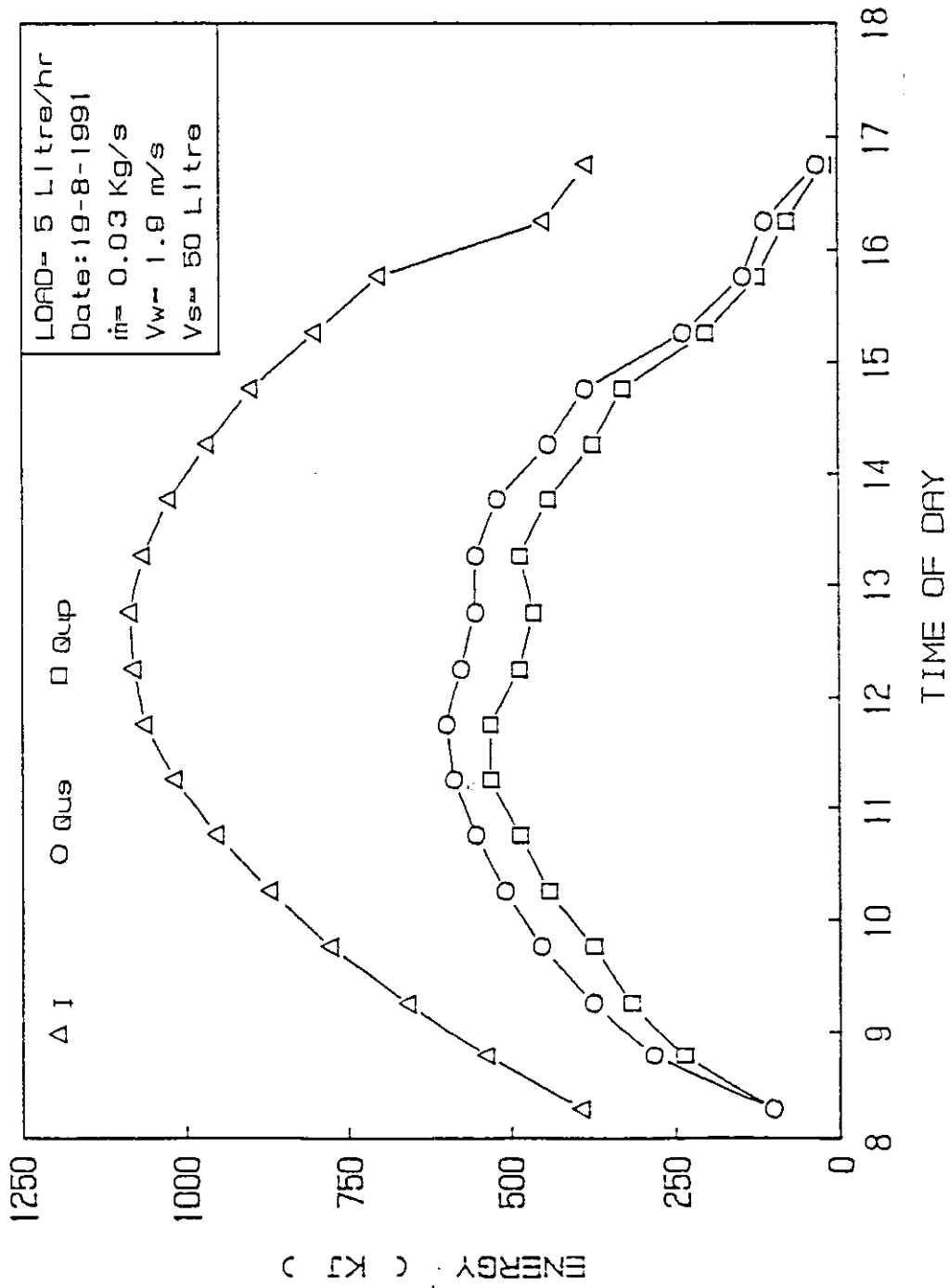


Fig.(4.69) Variation of Incident energy and useful energy with time for the serpentine and the parallel tubes flat plate solar collectors under a load of 5 Litre/hr.

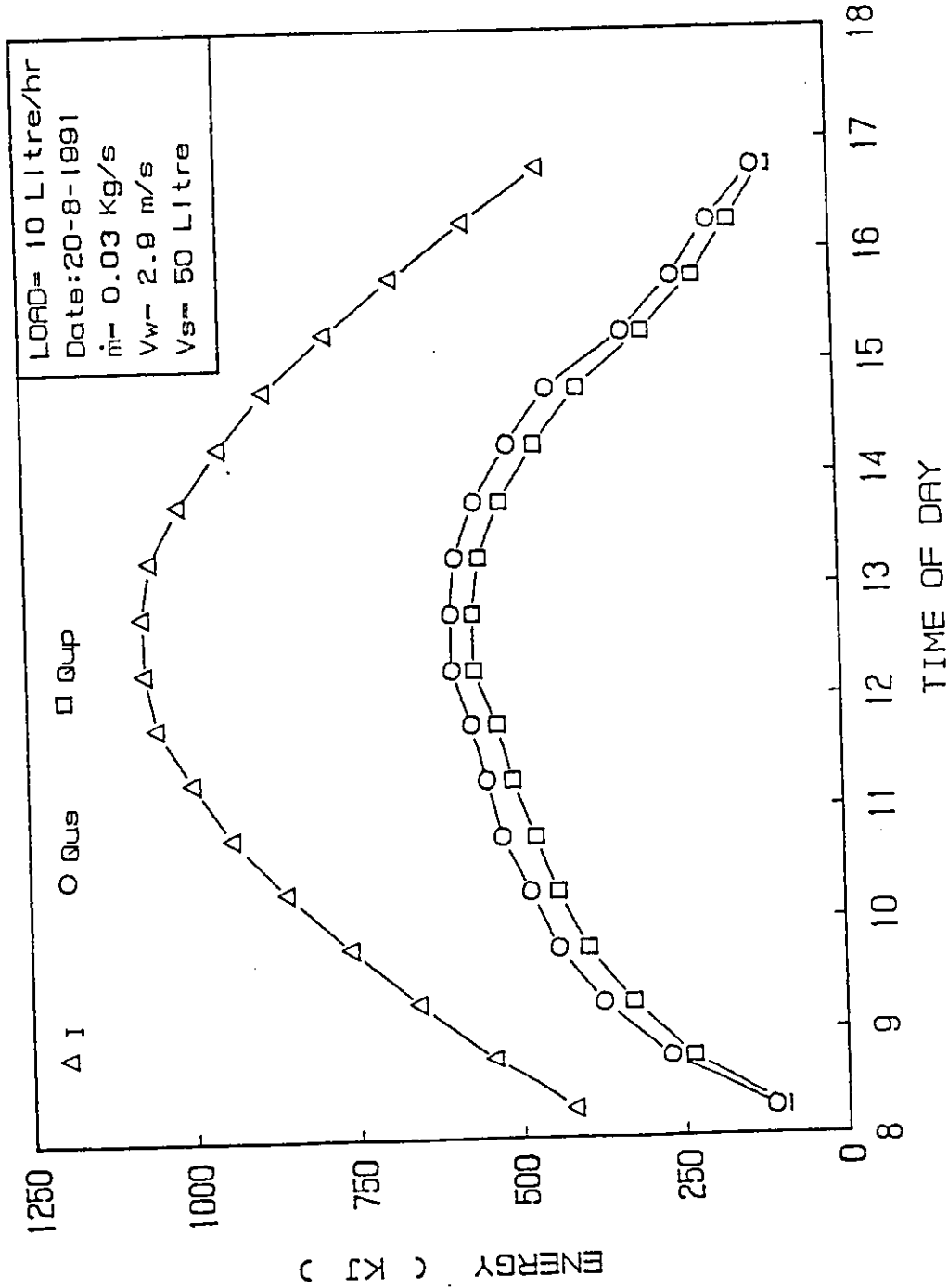


Fig. (4.60) Variation of incident energy and useful energy with time for the serpentine and the parallel tubes flat plate solar collectors under a load of 10 Litre/hr.

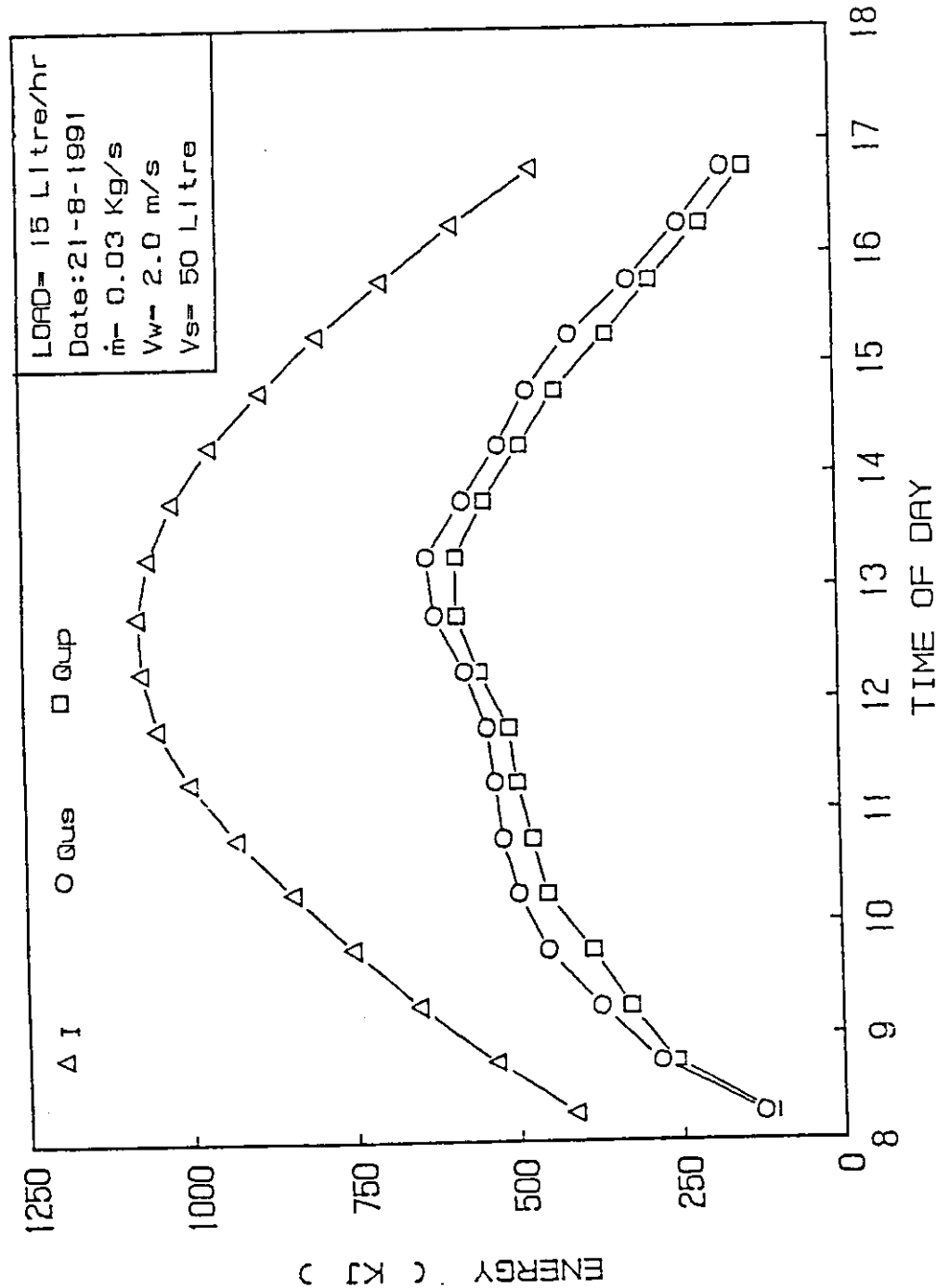


Fig.(4.61) Variation of incident energy and useful energy with time for the serpentine and the parallel tubes flat plate solar collectors under a load of 15 Litre/hr.

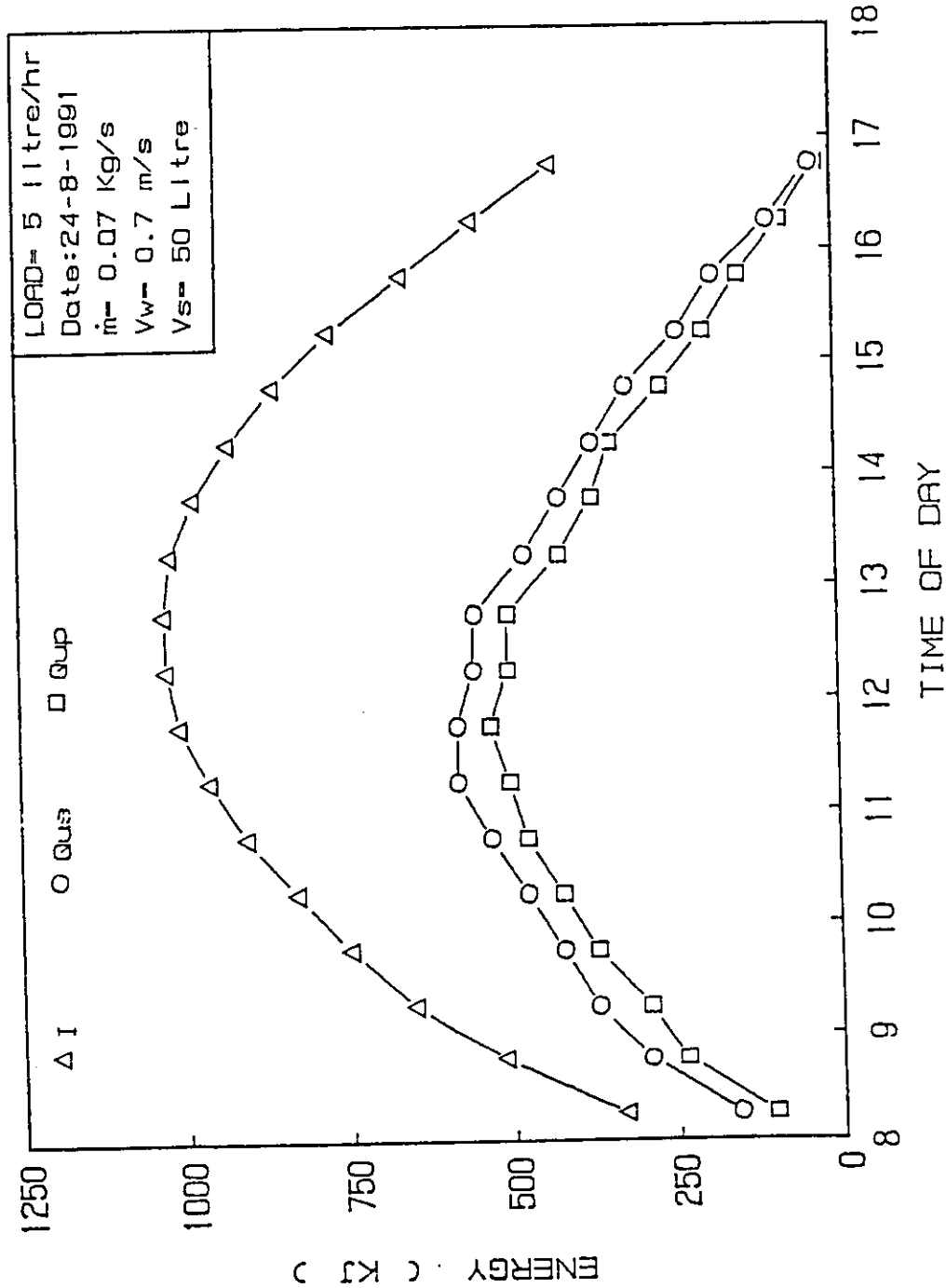


Fig.(4.62) Variation of incident energy and useful energy with time for the serpentine and the parallel tubes flat plate solar collectors under a load of 5 Litre/hr.

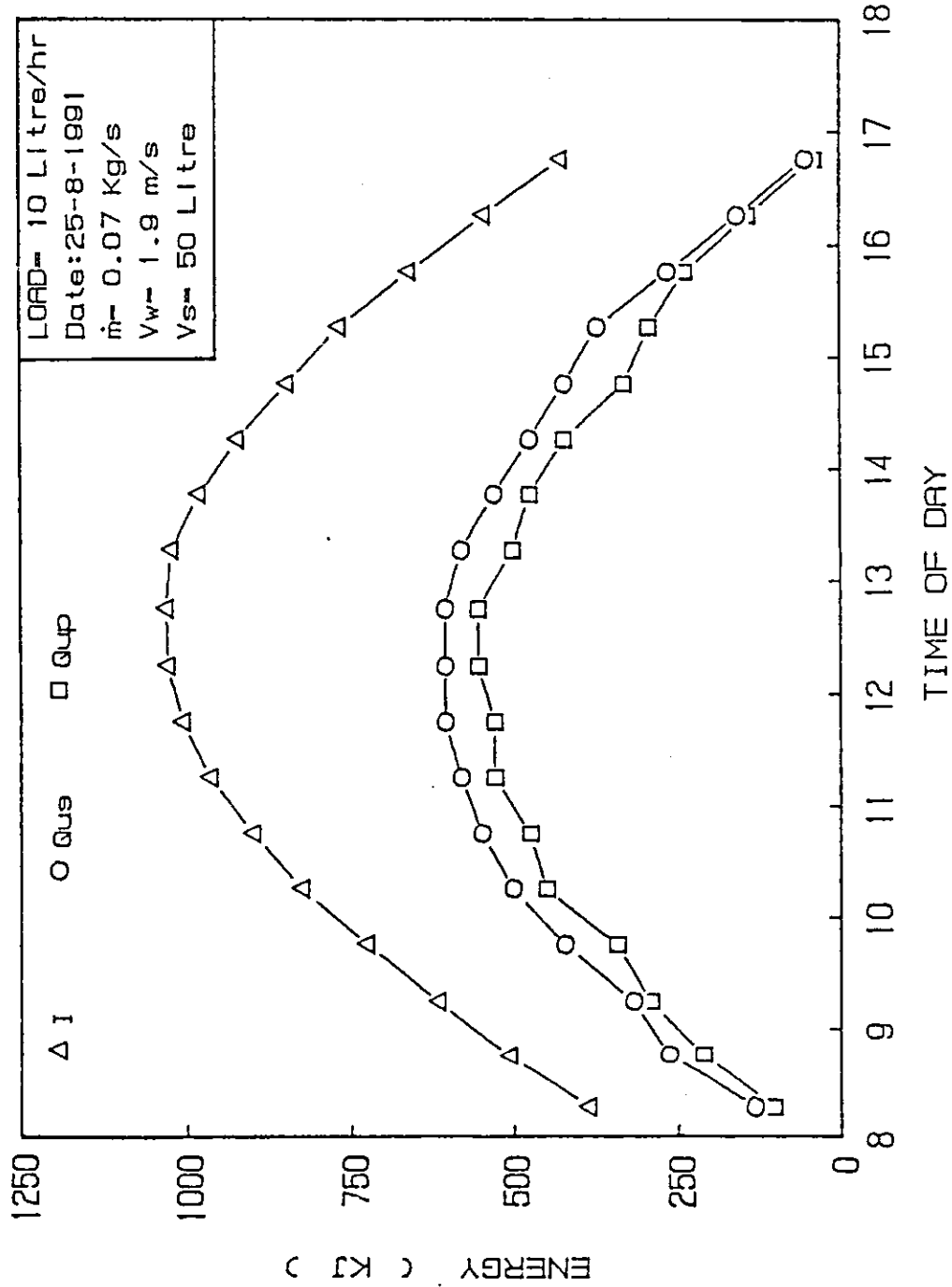


Fig.(4.63) Variation of incident energy and useful energy with time for the serpentine and the parallel tubes flat plate solar collectors under a load of 10 Litre/hr.

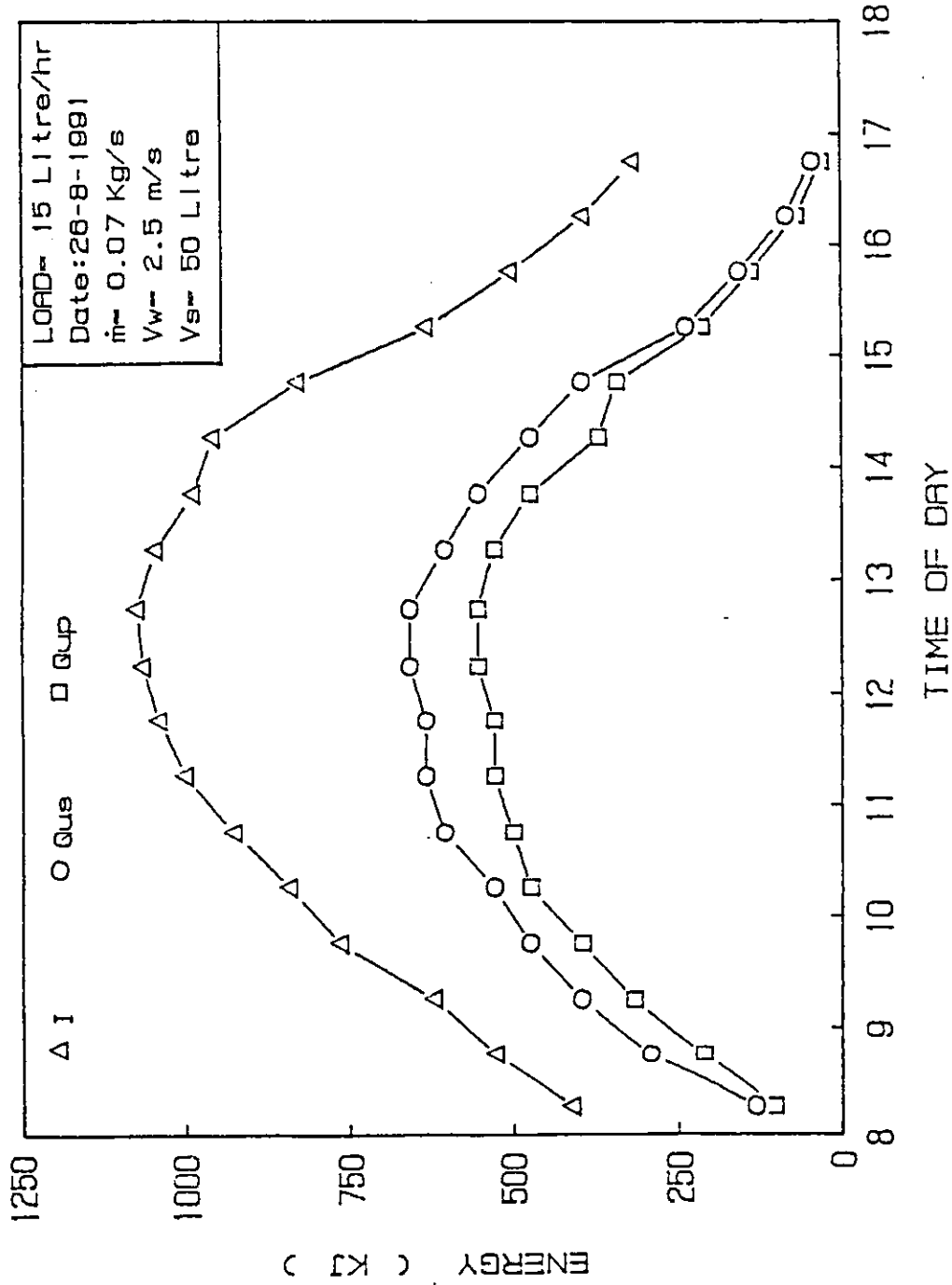


Fig.(4.64) Variation of incident energy and useful energy with time for the serpentine and the parallel tubes flat plate solar collectors under a load of 15 Litre/hr

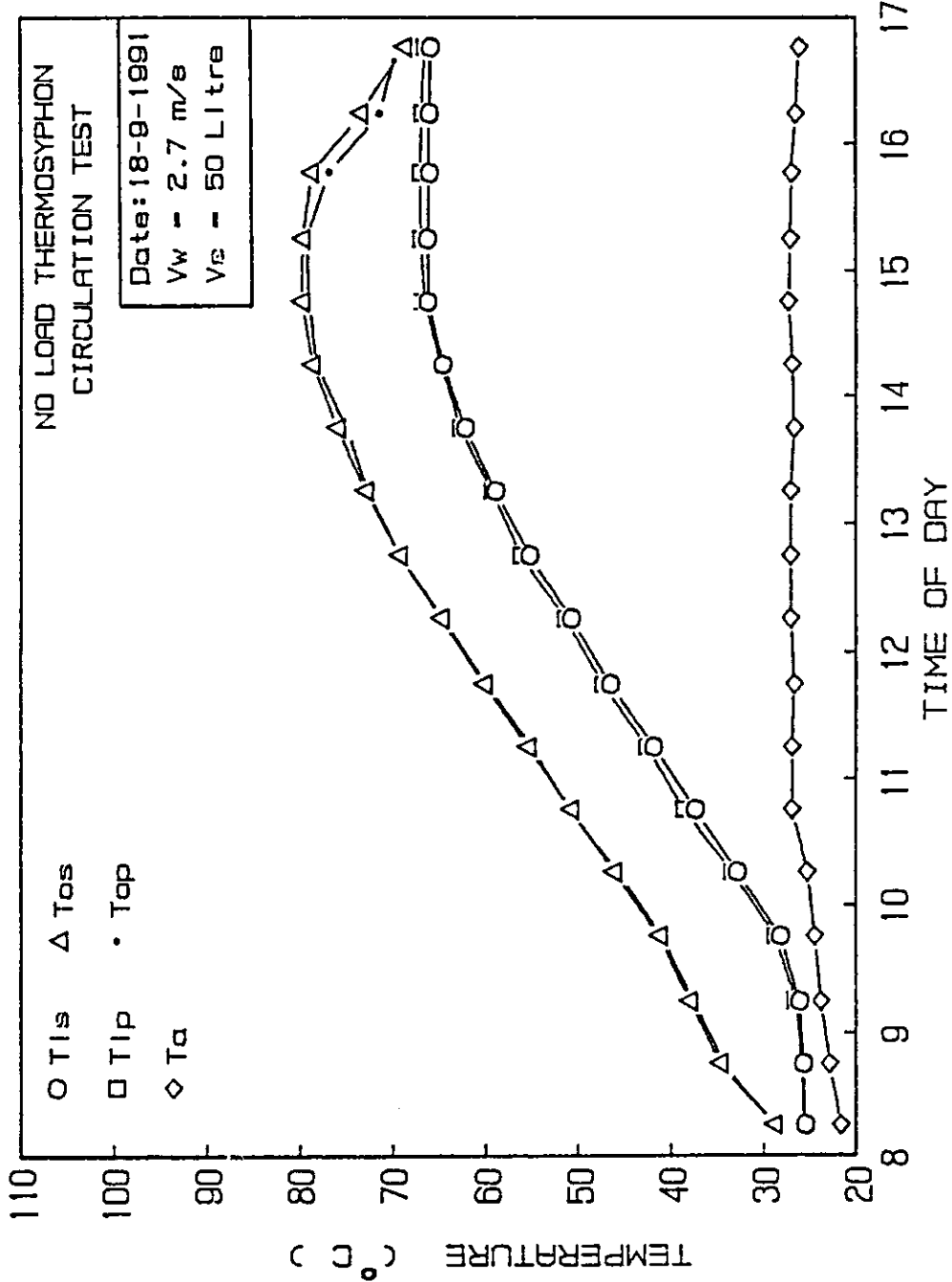


Fig.(4.65) Variation of Inlet temperature, outlet temperature, and the ambient temperature with time for the serpentine and the parallel tubes flat plate solar collectors under no load thermosyphon circulation.

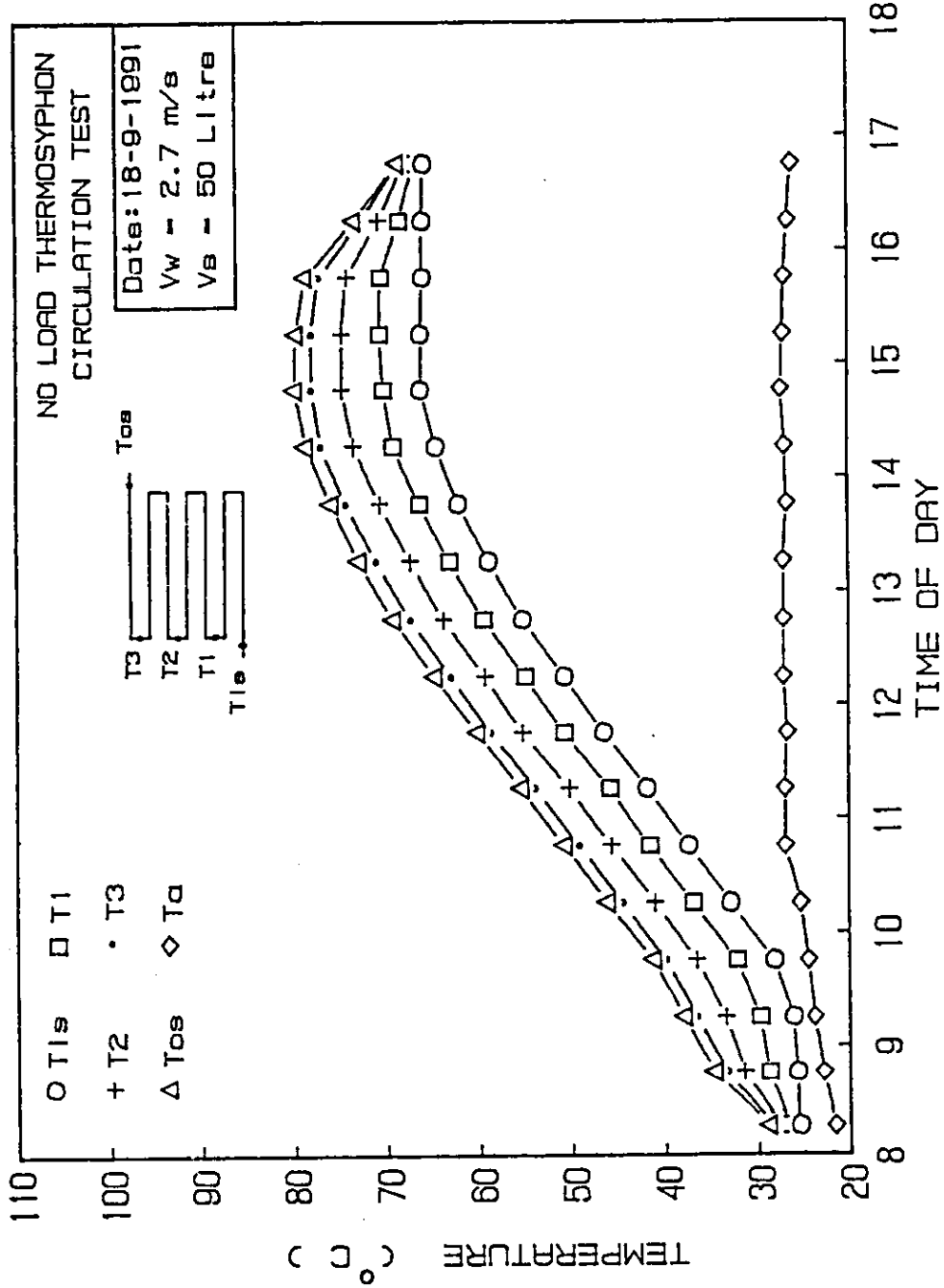


Fig.(4.66) Temperature distribution of water inside the serpentine tube flat plate solar collector and ambient temperature during the day of test under no load thermosyphon circulation.

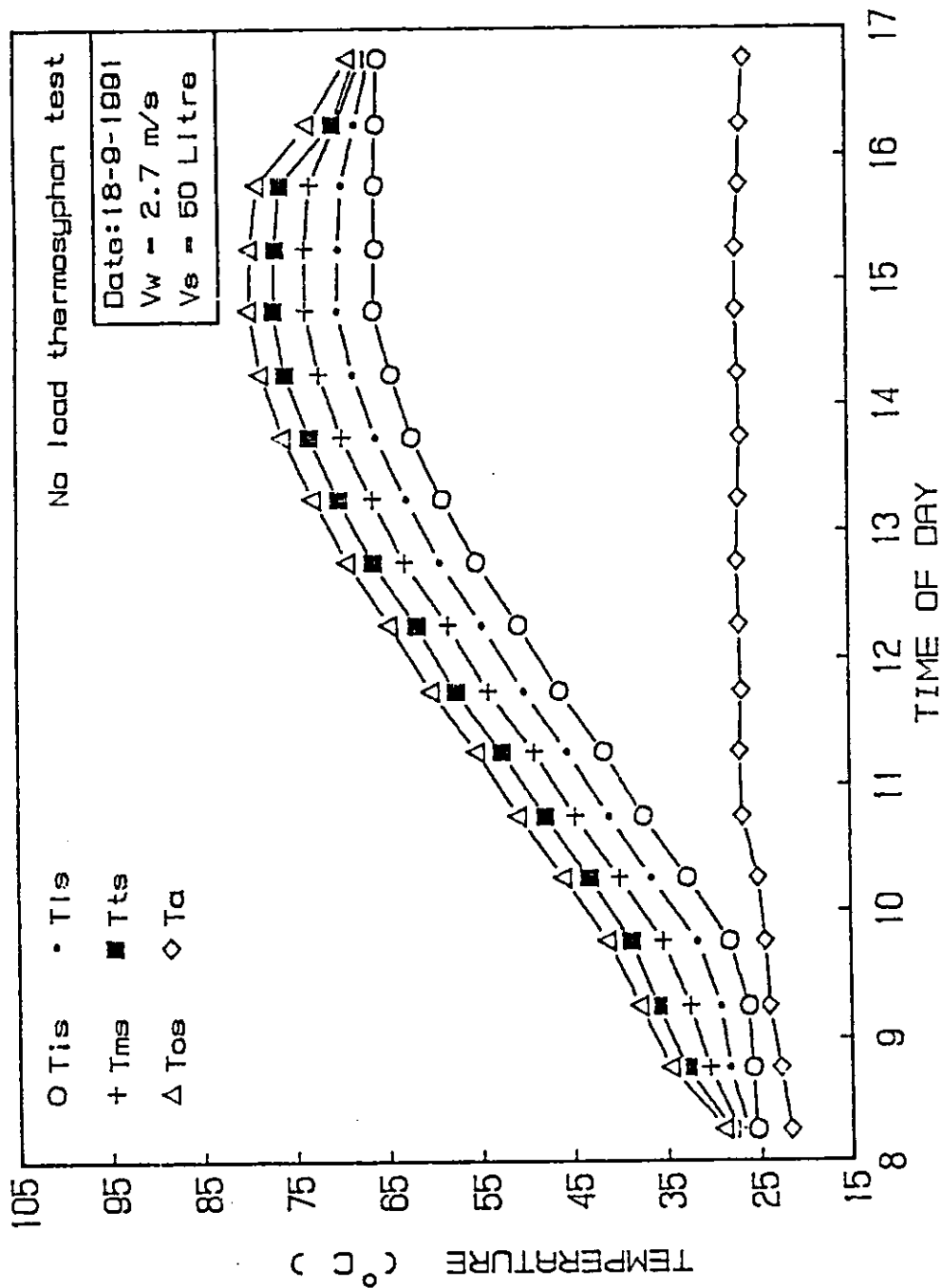


Fig.(4.87) Temperature distribution of water inside the storage tank of the serpentine type solar collector under no load thermosyphon circulation.

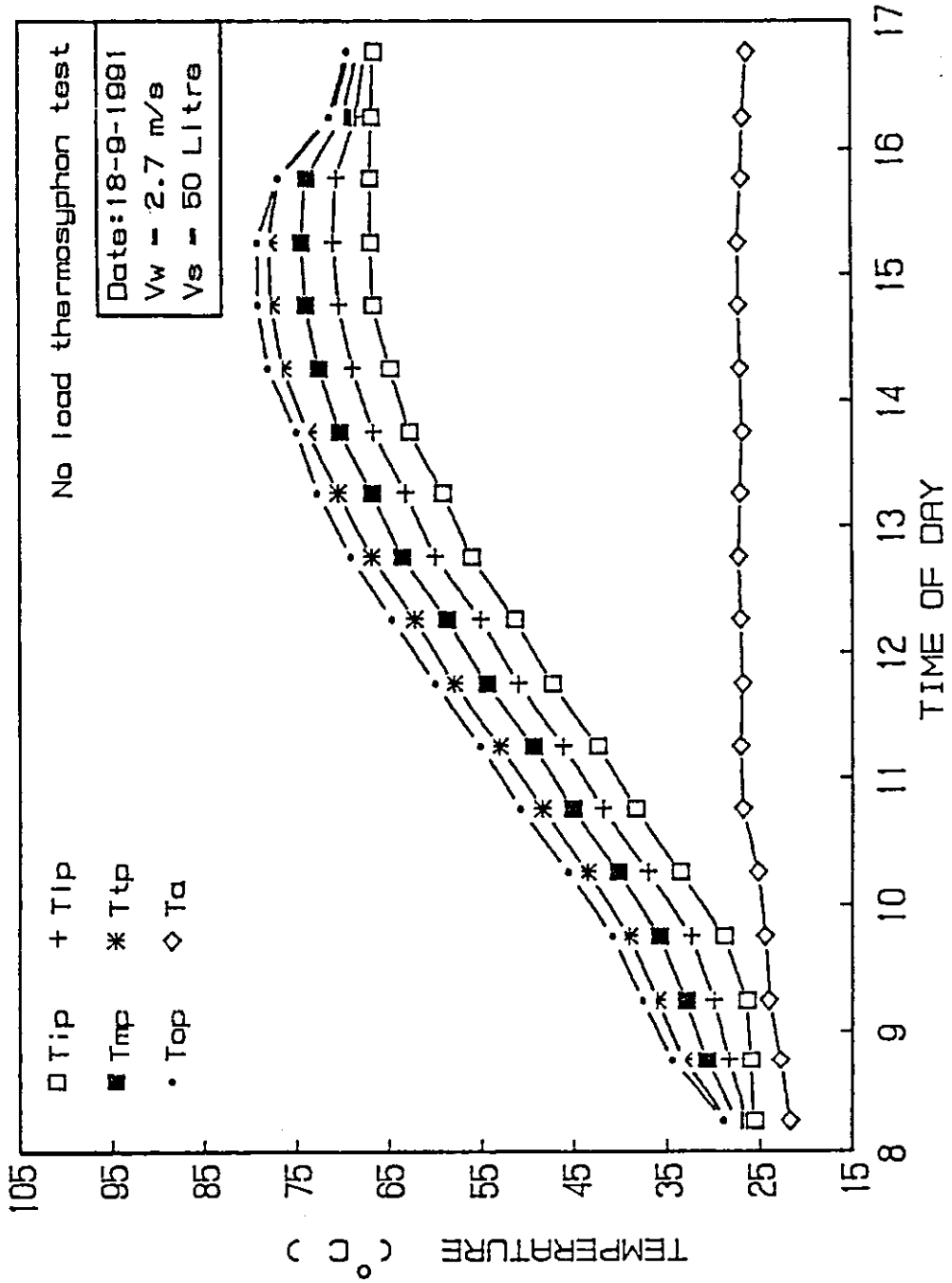


Fig.(4.88) Temperature distribution of water inside the storage tank of the parallel type solar collector under no load thermosyphon circulation.

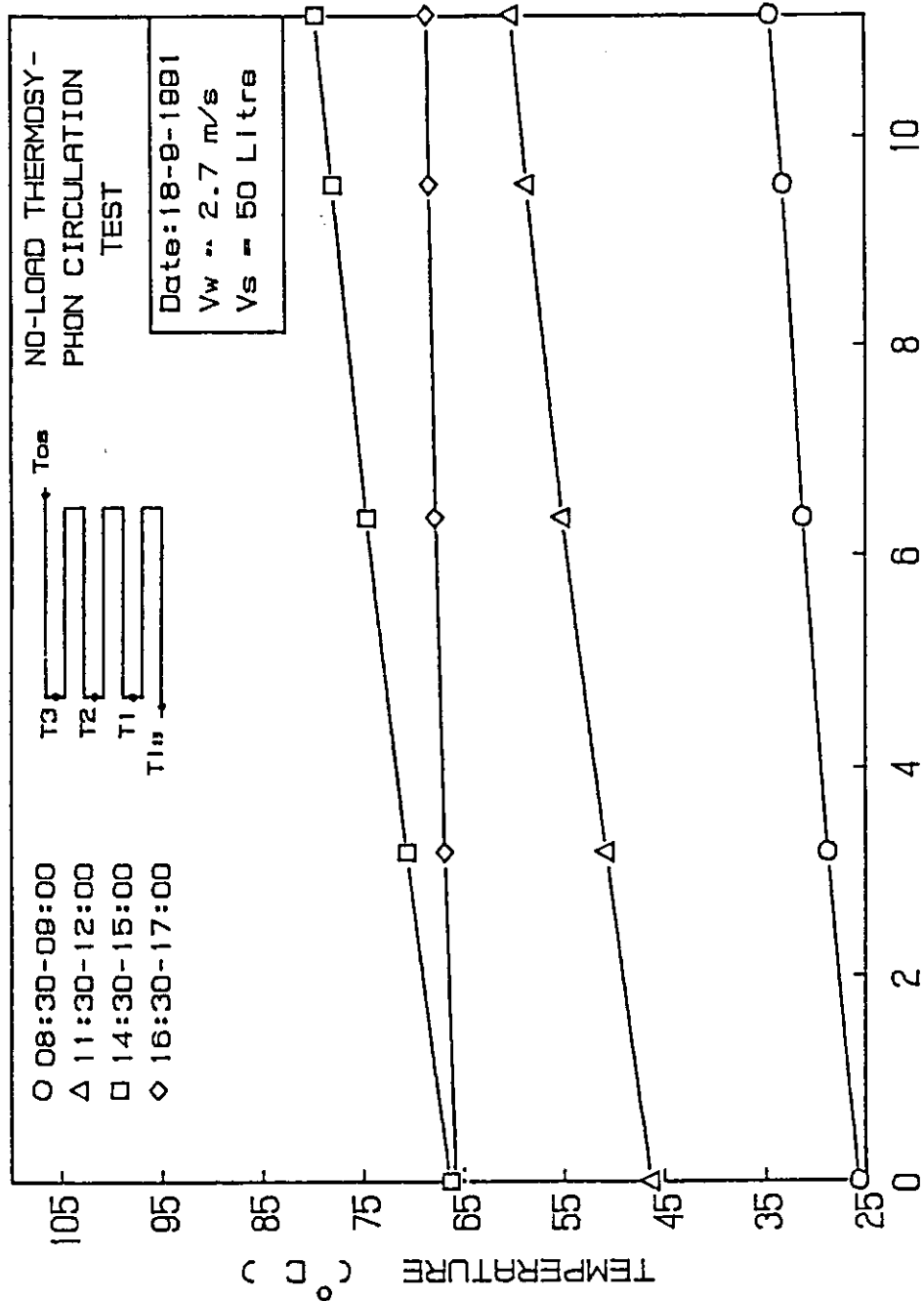


Fig.(4.69) Temperature distribution of the water inside the serpentine tube flat plate solar collector at different times of the day under no load thermosyphon circulation.

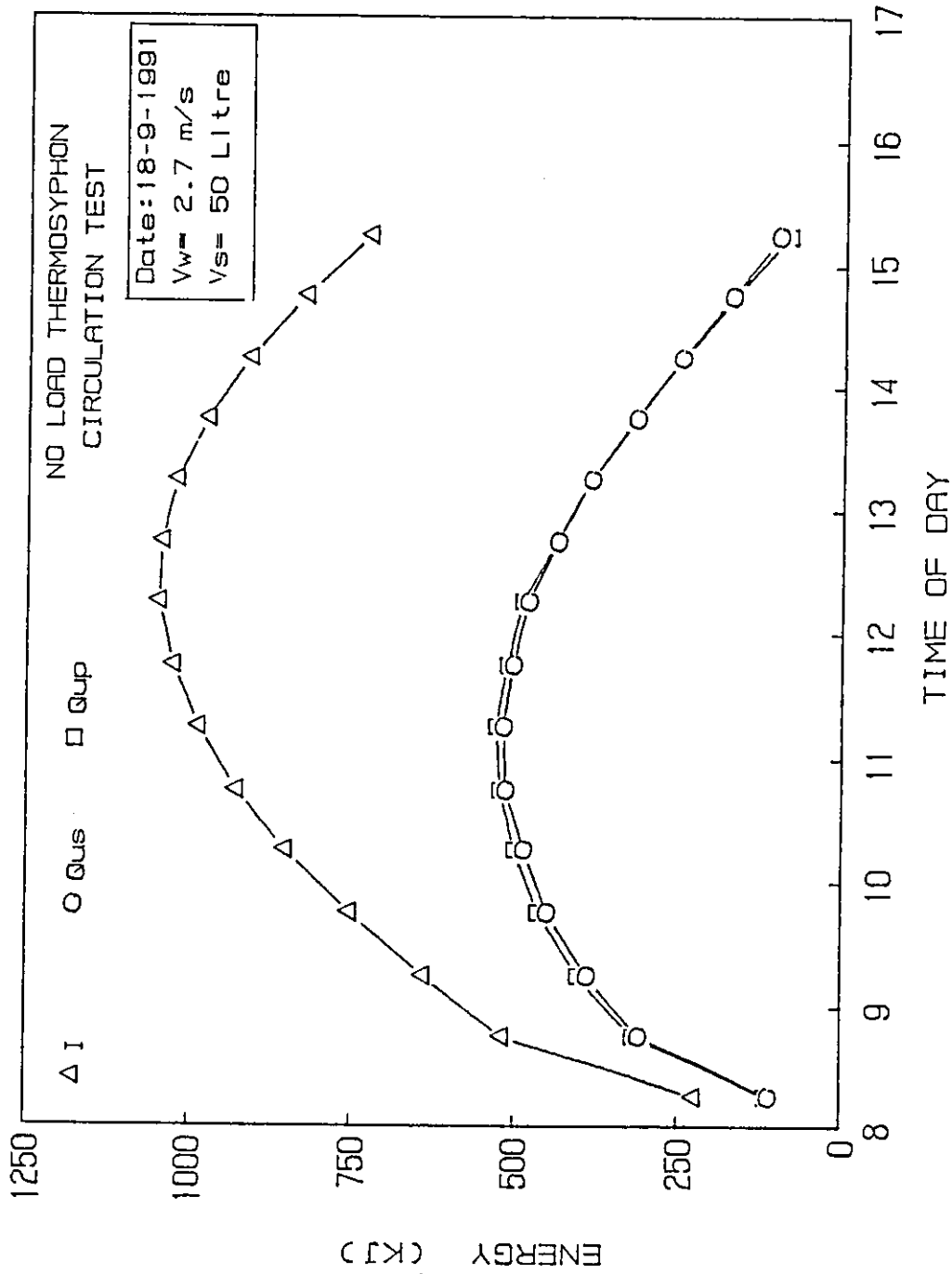


Fig.(4.70) Variation of incident energy and useful energy with time for the serpentine and the parallel tubes flat plate solar collectors no load thermosyphon circulation.

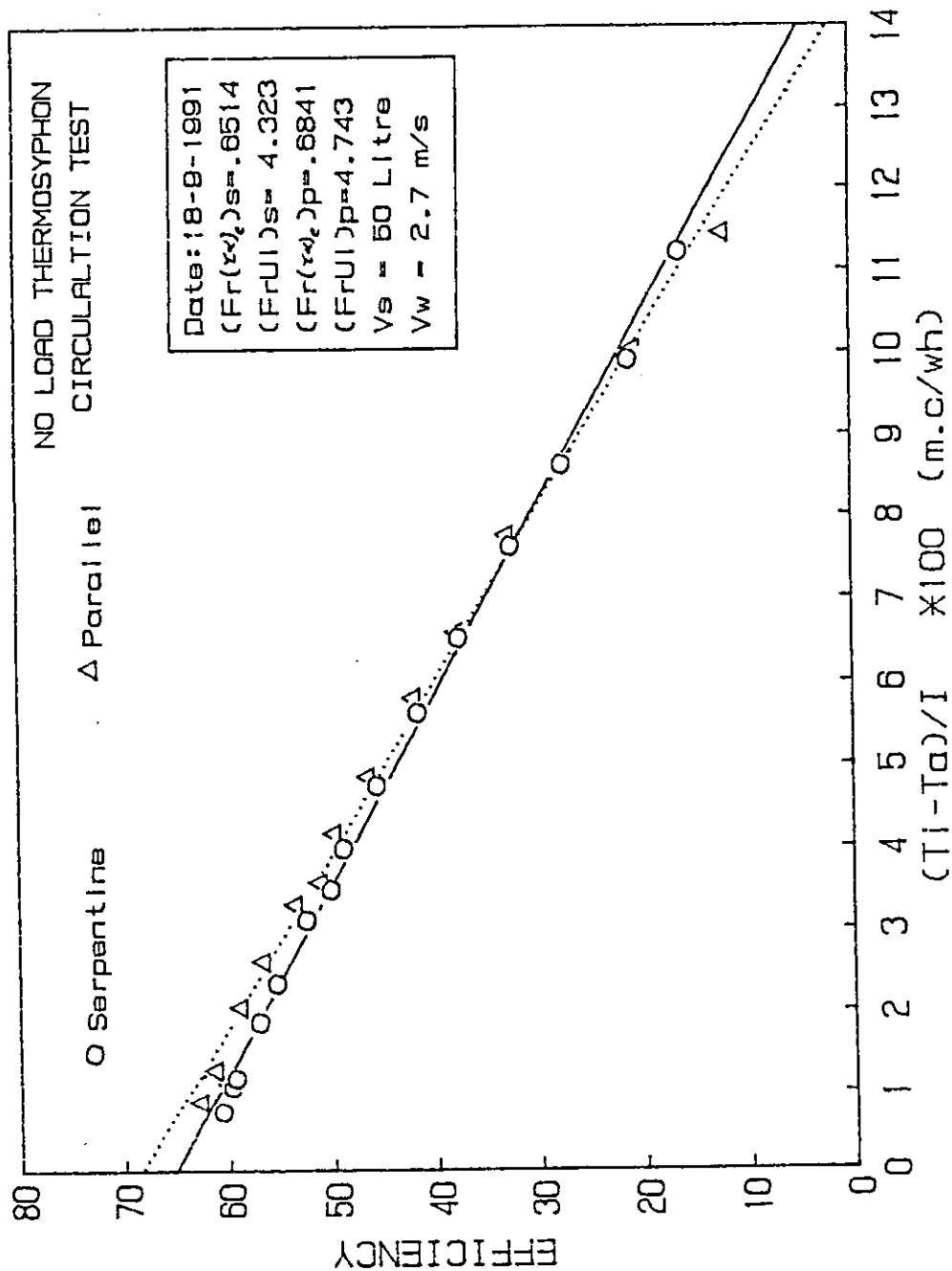


Fig.(4.71) Variation of instantaneous efficiency against $\{(T_i - T_a)/I\}$ for the serpentine and the parallel tubes for late plate solar collectors under no load thermosyphon circulation.

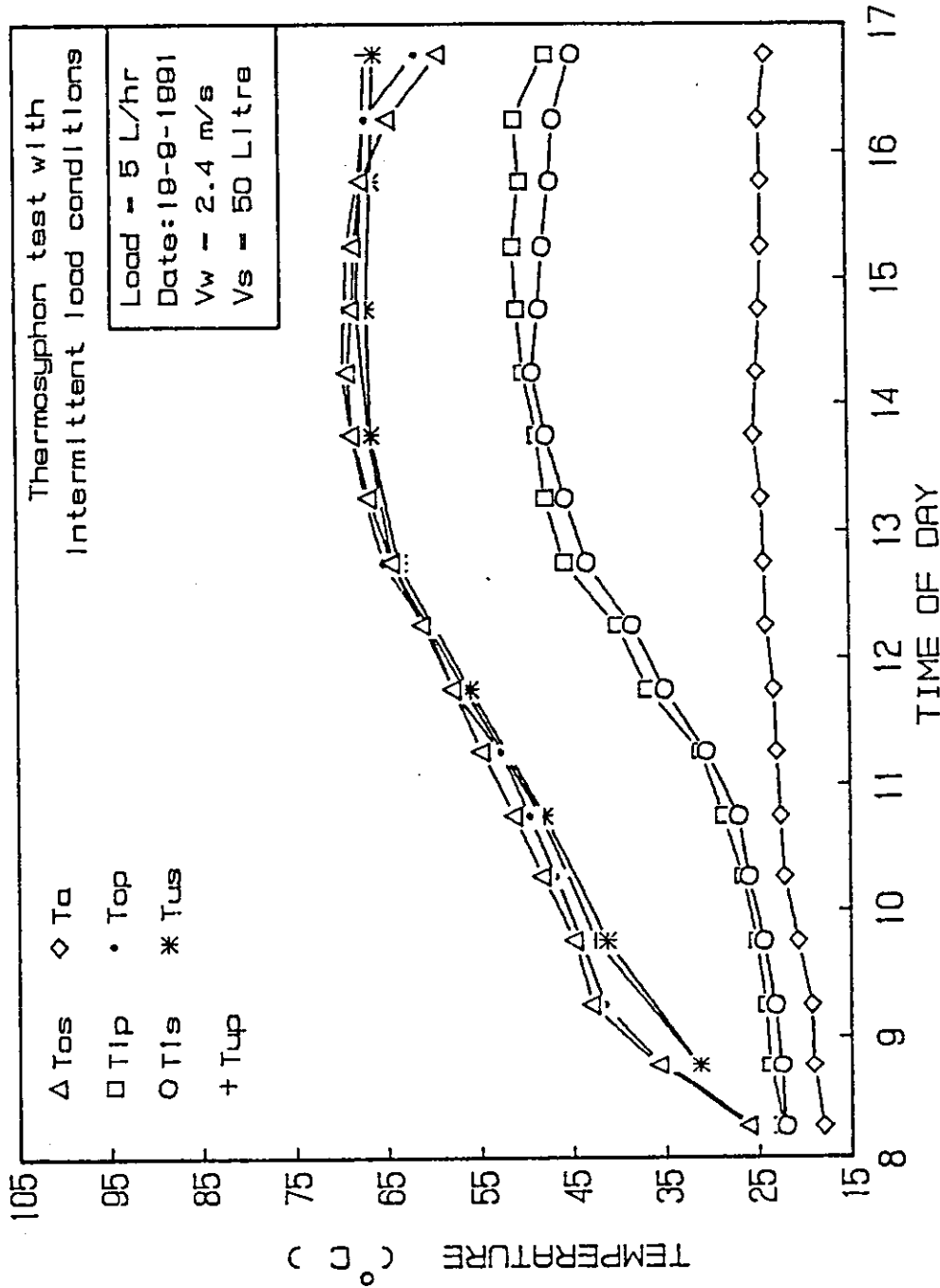


Fig.(4.72) Variation of inlet, outlet, ambient and used hot water temperatures with time for the serpentine and the parallel tubes flat plate solar collectors under an intermittent load of 5 L/hr.

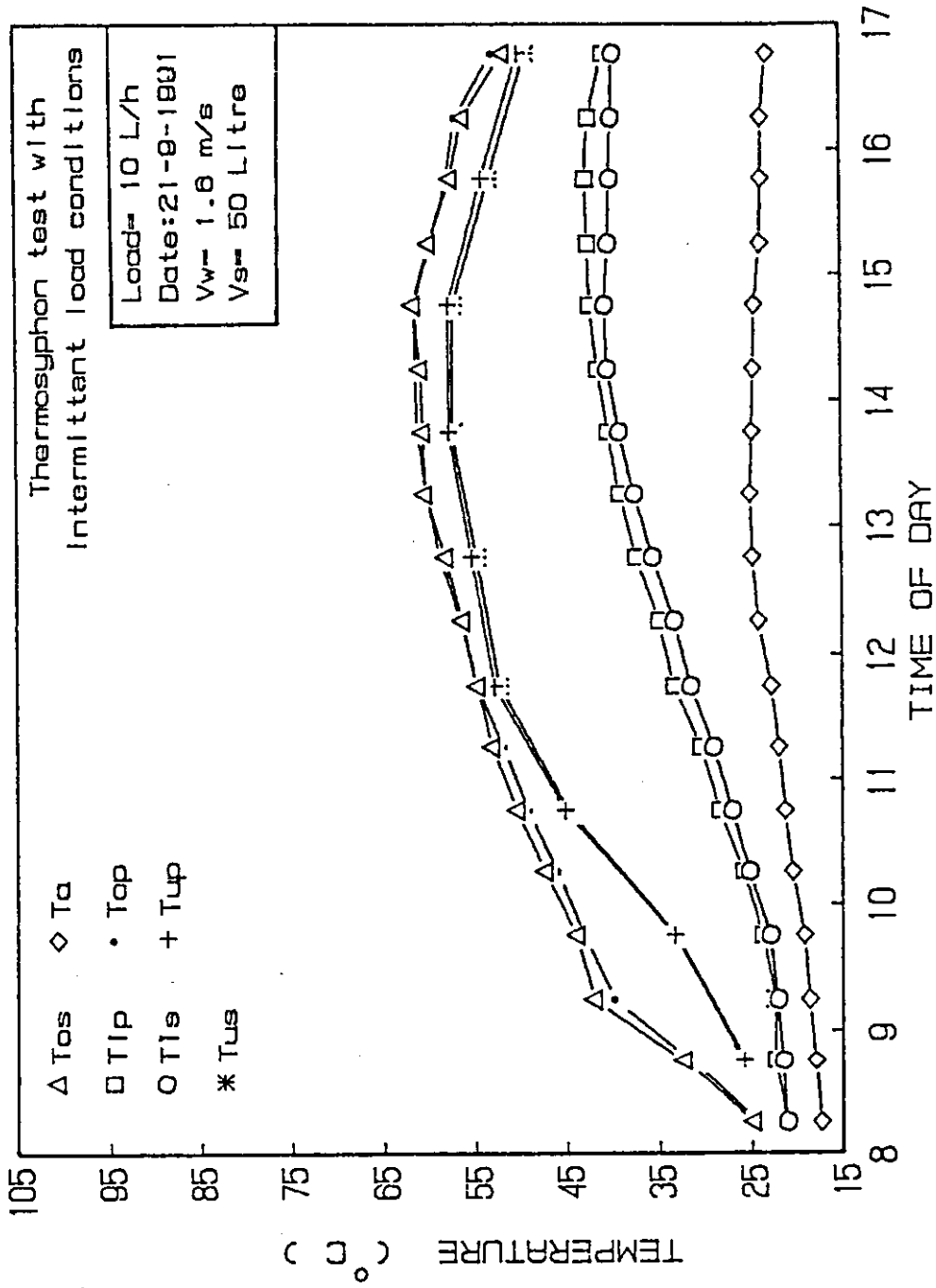


Fig.(4.73) Variation of Inlet, outlet, ambient and used hot water temperatures with time for the serpentine and the p-parallel tubes flat plate solar collectors.

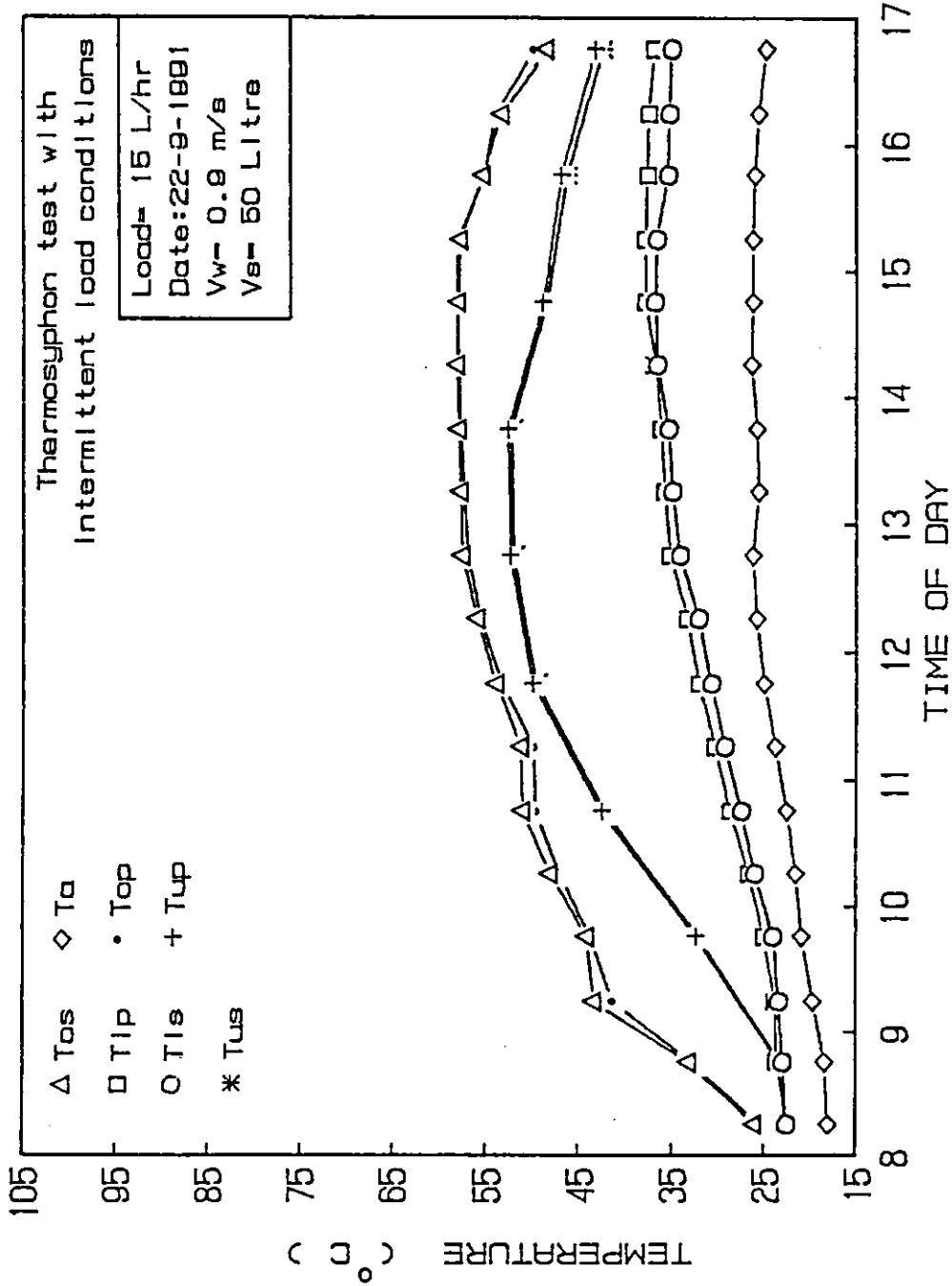


Fig. (4.74) Variation of Inlet, outlet, ambient and used hot water temperatures with time for the serpentine and the parallel tubes flat plate solar collectors.

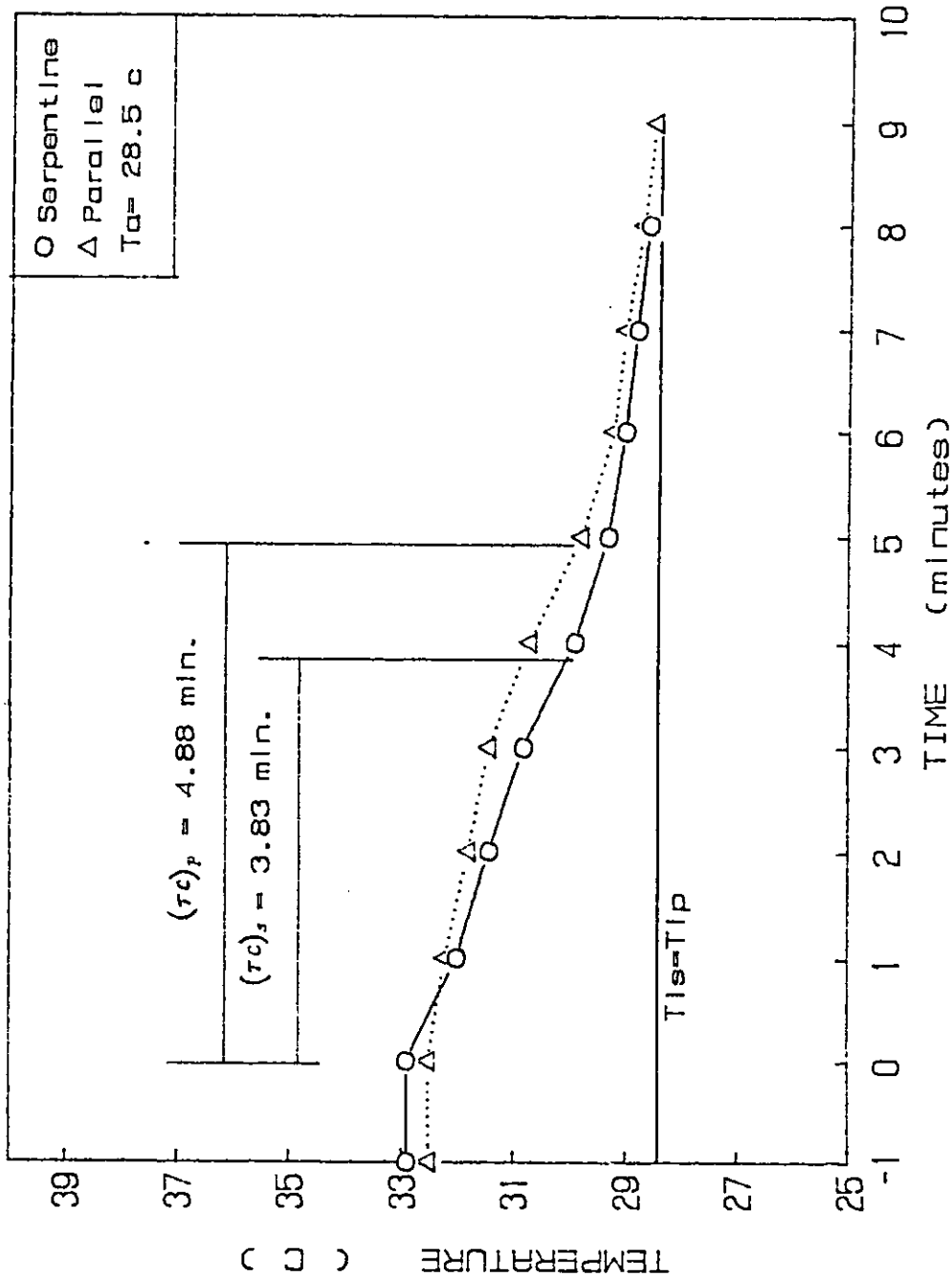


Fig.(4.75) A time- temperature plot for the serpentine and the parallel tubes flat plate solar collectors showing temperature drop on sudden interruption of the solar radiation on the collectors.

4.3 Discussion of Results

The performance of both collectors are studied at variable flow rates, while all other design parameters are kept fixed. The reasons why the performance is studied over a wide range of flow rates are:

1. If the collector is performing a function such as heating hot water in a single pass, the flow rate must be limited because a certain hot water temperature must be attained.
2. If the collector is used to collect heat for space heating, high temperatures are not necessary and circulation of water to the collector will usually be kept high so that the collector surface stays near the lowest possible temperature, that of the bulk of the stored fluid.

The discussion of the performance parameters is outlined in the following subsections:

4.3.1 Temperature Distribution of Water Inside Collectors And Storage Tanks

The averaged measured temperatures for all tests are presented in Tables (A.1-A.23). The variation of these temperatures with time of day, and the temperature distribution of water inside the serpentine collector are presented for all tests: Figures(4.1-4.26) show these variations for the forced circulation test with no load conditions, Figures(4.45-4.50) for the forced circulation test with load conditions, Figures(4.53-4.58) for the forced circulation test with intermittent loads of 5, 10, and

15 l/h, Figures(4.65-69) for the no load thermosyphon test, and Figures(4.72-4.74) for the thermosyphon test with intermittent loads of 5, 10, 15 l/h.

These figures show that the temperature difference across the serpentine collector is higher than that across the parallel collector for all the investigated forced circulation tests. When a two large separated storage tanks (150 l), were used the difference between the outlet temperatures of both collectors is increased as the time is increased. This difference attains its maximum value at the time interval 15:30-16:30. For this case, the difference between the outlet temperatures of both collectors ranges from 0.1 to 2.5 C° for all the investigated flow rates.

When a small common storage tank (50 l) was used, the difference between the outlet temperatures of both collectors is increased gradually from the early morning till it reaches a maximum value at the mid of the day. Then the difference drops gradually till it diminishes at the end of the test day . The maximum outlet temperature was attained during the time interval 14:00-15:00 for both collectors. For the time interval 16:00-17:00 both collectors have nearly, the same outlet temperatures. For this case, the difference between the outlet temperatures of both collectors ranges from 0.1 to 0.3 C° for all the investigated flow rates.

The forced circulation test with intermittent loads of 5, 10, 15 l/h , was performed to measure the useful hot water temperature every hour. Results of this test, show that the useful hot water temperature of the serpentine type is higher than that of the parallel type for all loads and flow rates investigated. It is noticed that, under low flow rates (0.02 Kg/s), the difference between the useful hot water temperatures of both collectors is decreased as the load is increased. On the contrary, under high

flow rates (0.07 Kg/s), this difference is increased as the load is increased. For a flow rate of 0.03 Kg/s , the maximum useful hot water temperature of the serpentine type is higher than that of the parallel type by about 7.0%, 4.1%, and 3.8% under loads of 5, 10, and 15 l/h , respectively. While, for a flow rate of 0.07 Kg/s it is higher by about 3.6%, 5.1%, and 7.6% under the previously mentioned loads.

According to the temperature distribution of water inside the serpentine collector it is found that the contribution of the first two segments is about 35% of the temperature difference across the collector. The last segment contributes by about 10%. The other contributions come from the rest four segments. When the temperature distribution of water inside the serpentine collector is plotted versus the distance from the inlet of the collector, it is noticed that the slope of the curve is increased as the time interval comes near to the mid of the day as shown in Figures (4.18-4.26).

When both collectors were operating under a thermosyphon flow with no load conditions, it is found that the temperature difference across the serpentine collector is higher than that across the parallel collector, because a higher density difference is needed for the flow movement to overcome the frictional losses.

The useful hot water temperature obtained from both collectors under thermosyphon flow with intermittent loads of 5, 10, and 15 l/h , reveals that, although the parallel type has higher temperature than the serpentine type, but the difference between these temperatures are decreased as the load increased.

The temperature distribution inside the storage tanks is studied only under no load thermosyphon circulation, because under forced flow rates the stratification

inside storage tanks is not significant. Figures (4.68-4.69) show the temperature distribution inside the storage tanks of both collectors for all the investigated time intervals. The maximum temperature distribution is attained at the time interval 13:00-13:30 for both collectors. After this time interval the differences between these distributions were decreased till a minimum value at the end of the day of test.

4.3.2 Useful Heat Gain

The useful heat gain, for each type was calculated using equation (3.15). The variations of the useful heat gain with time of day are plotted in: Figures (4.27-4.35) for the forced circulation test with no load conditions, Figures (4.51-4.52) for the forced circulation test with load conditions, Figures (4.59-4.64) for the forced circulation test with intermittent loads of 5, 10, and 15 l/h, and Figure(4.70) for the no load thermosyphon test.

Forced circulation tests, show that the useful heat gain of the serpentine type is higher than that of the parallel type for all time intervals and flow rates investigated. The useful heat gain of both collectors, increases gradually from the beginning of the test, till it attains a maximum value at the mid of the day, thereafter, it drops gradually. This is due to the decreasing rate of the incident solar flux during the afternoon hours.

The difference between the useful heat gain of both collectors increases gradually from the beginning of the day of test, till it reaches a maximum value at the time interval 12:00-13:30, then the difference drops gradually till it diminishes at the end of the test day, due to shading effect. Shading effect has greater effect on the serpentine type than on the parallel type, because all the flow in the serpentine

collector is forced to pass the shaded zone. The case in the parallel type is different, since only one seventh of the flow is forced to pass this zone.

When a 150 litre capacity storage tank was used for each model, the maximum heat gain was attained at the time interval 12:00-12:30 for both model. For this time interval the useful heat gain of the serpentine type is greater by about 8.4% than that of the parallel type.

When both collectors were operated under forced circulation with load conditions, the inlet water was provided for each model near the ambient temperature to minimize the heat losses from the collectors. For this test, and under low flow rates (0.02 Kg/s) the maximum heat gain of the serpentine type is greater by about 10% than that of the parallel type. For this flow rate and the time interval 16:30-17:00 both collectors have the same useful heat gain. The reason for this performance deceleration relating the serpentine type is due to shading effect. As the flow rate is increased (0.05 Kg/s) the shading effect on the serpentine type is decreased. This in turn, reflected on a superior performance of the serpentine type over the parallel type for all the investigated time intervals. For this flow rate, the maximum useful heat gain of the serpentine type is higher by about 11.1% than that of the parallel type .

When the flow rates in the tube segments of both collectors are equal (i.e $\dot{m}_s = 0.015 \text{ Kg/s}$ and $\dot{m}_p = 0.105 \text{ Kg/s}$) the serpentine type has an inferior performance when compared to the parallel type. For the time interval 11:00 -11:30 the useful heat gain of the parallel type is greater by about 30% than that of the serpentine type. This is due to that the flow rate in the serpentine type is only, one seventh of

that in the parallel type.

When both collectors were operated under forced circulation with intermittent loads of 5, 10, and 15 l/h , the serpentine type has a superior performance over the parallel type for all loads and flow rates investigated. For low flow rates (0.03 Kg/s) as the load is increased the difference between the useful heat gain of both collectors is decreased. For high flow rates (0.07 Kg/s) as the load is increased, this difference increased.

No load thermosyphon test shows that the parallel type has superior performance over the serpentine type under natural circulation. The maximum heat gain for both collectors was attained during the time interval 11:00-11:30 . For this time interval, the useful heat gain of the parallel type is greater by about 2.1% than that of the serpentine type. The superior performance of the parallel type is due to the ability of the parallel type to circulate water naturally at higher flow rates. Serpentine type circulate water at lower flow rates because of the frictional losses, where the driving force is the density difference between the hot and the cold water. Figure (4.76) shows the variation of mass flow rate with time of day for both collectors.

4.3.3 Instantaneous And Daily Efficiencies

The instantaneous efficiency, η_i , for each type was calculated using equation (3.16). The variations of the instantaneous efficiency with $(T_i - T_a)/I$ for both collectors are presented in Figures (4. 36-4.44) for the forced circulation test with no load conditions, and Figures (4.71) for the no load thermosyphon test.

Under forced flow circulation, the instantaneous efficiency of the serpentine type is higher than that of the parallel type for all the time intervals and flow rates

investigated. As the flow rate is increased the difference between the instantaneous efficiencies of both collectors increased. At the last two hours of the test day, the decreasing rate of the instantaneous efficiency of the serpentine type is higher than that of the parallel type. This is due to the shading effect.

When the flow rates in the tube segments of both collectors are equal ($\dot{m}_s = 0.015 \text{ Kg/s}$ and $\dot{m}_p = 0.105 \text{ Kg/s}$), the instantaneous efficiency of the parallel type is higher than that of the serpentine type for all the investigated time intervals.

No load thermosyphon test show that the instantaneous efficiency of the parallel type is higher than that of the serpentine type by about (1-2) % for all the investigated time intervals. This is because the parallel type circulates water at higher flow rates.

For load test, the daily efficiency of each model at each flow rate was evaluated from equation (3.19) using the corresponding averaged measured data. The daily efficiency was based on the summation of the incident solar energy and the useful heat gain for all time intervals during the test day.

The daily efficiency values are shown in Table (4.3) for each model at each water flow rate. Since the test conditions of both collectors are identical, this table shows that the increase of the daily efficiency is due to the increase in the water flow rate. As the water flow rate is increased from 0.02 to 0.05 Kg/s , the improvement in the daily efficiency of the serpentine type is 12.4%, while it is 8.4% for the parallel type. For the investigated flow rates the serpentine type has the highest daily efficiency. The daily efficiencies of the serpentine type are 46.1% and 58.8% , while for the parallel type they are 41.1% and 49.5% , when the flow rates are 0.02 Kg/s , and

0.05 Kg/s, respectively. The daily efficiency of the conventional solar collector is 45% [2].

4.3.4 Heat Removal Factors And Overall Heat Loss Coefficients

Based on Figures (4.36-4.44), Tables (4.1-4.2) presents the instantaneous efficiency expressions for the forced circulation test with no load conditions. These expressions show that the heat removal factor of the serpentine type, $F_{r,s}$, is higher than that of the parallel type, $F_{r,p}$, for all the investigated flow rates. The variation of these heat removal factors with mass flow rate are presented in Figures (4.77-4.78). These figures show that the heat removal factor, F_r , is more sensitive to flow rate variations when small storage tank is used. When a 150 litre capacity storage tank was used for each model, as the flow rate is increased from 0.02 to 0.07 Kg/s, the improvement in the heat removal factor of the serpentine type is only 4.3%, while it is 9.0% for the parallel type. On the other hand, when a common 50 liter capacity storage tank was used for both collectors, the improvements are 23% and 11% for the serpentine and the parallel types, respectively.

When the flow rates in the tube segments of both collectors are equal, the heat removal factor of the serpentine type is less only by about 6% than that of the parallel type. This is because the flow rate in the serpentine collector is one seventh of that in the parallel collector.

Heat removal factors for the no load thermosyphon test were evaluated using equations (3.3) and (3.6) for the parallel and the serpentine types, respectively. Table (B.19) presents the values of these heat removal factors. Results show that

the heat removal factor of the parallel type is higher than that of the serpentine type by about (2 – 4)% for all the investigated time intervals.

Figures (4.79-4.80) shows the variations of the overall heat loss coefficients of both collectors with the mass flow rate. These figures show that the dependence of the overall heat loss coefficient on the flow rate is poor. Results show that the overall heat loss coefficient depends mainly on the wind velocity. Stagnation test shows that the overall heat loss coefficient of the serpentine type is less than that of the parallel type by 3.3%.

4.3.5 Time Constant

The time constant for each model is evaluated according to equation (3.21). Table (A.23) presents the results of this test. The variation of the outlet temperatures of both collectors with time, after the sudden interruption of the solar radiation on the collectors is shown in Figure (4.75).

Results show that the time constant of the serpentine type is 3.83 minute, and 4.88 minute for the parallel type. These results are consistent with what stated by Duffie and Beckman [1], that the time constant of the metallic collectors is less than 5 minutes. The reason for this time constant variation between both collectors is that water temperature rise in the serpentine collector is higher than that in the parallel collector.

In general, the superior performance of the serpentine type over the parallel type under forced circulation can be understood by knowing that the most important single consideration in heat transfer to a flowing fluid is the character of the flow

regime, which is defined as either laminar or turbulent. Reynolds numbers below 2300 mean that the flow is laminar. Over 10000 the flow is turbulent [18].

If the flow regime is fully developed laminar flow ($Re \leq 1000$), as the case in the parallel type, the heat transfer coefficient is constant. In this case, the slipping layers do not mix and the fluid acts much like a solid, transferring heat by conduction.

For the case of the serpentine type, all the Reynolds numbers of the investigated flow rates are in the transition zone. For this case, better heat transfer coefficients were attained. The sharp turns (bends) cause the slipping layers of the flow to mix. This mixing improve the heat transfer coefficient. Table (4.7) presents the Reynolds numbers and water flow velocities inside the tube segments of both collectors.

Table 4.7 : Reynolds numbers and water flow velocities inside the tube segments of the serpentine and the parallel tubes.

\dot{m} Kg/s	Re_s	Re_p	V_{ws} m/s	V_{wp} m/s
0.02	2287	327	0.0884	0.0126
0.03	3430	490	0.1326	0.0189
0.05	5717	817	0.2209	0.0316
0.07	8004	1143	0.3093	0.0442

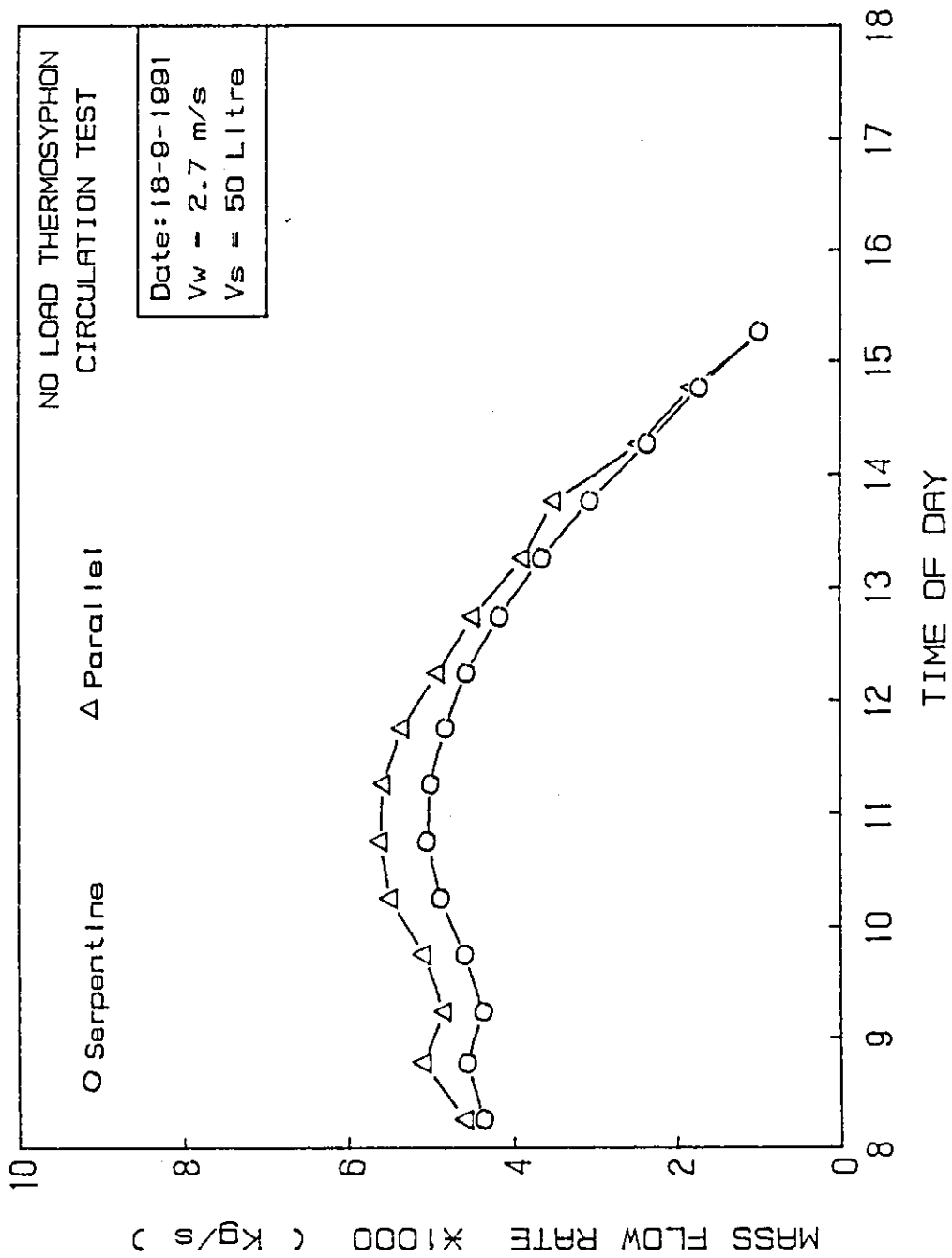


Fig.(4.76) Variation of mass flow rate with time of day for the serpentine and the parallel tubes flat plate solar collectors under no load thermosyphon circulation.

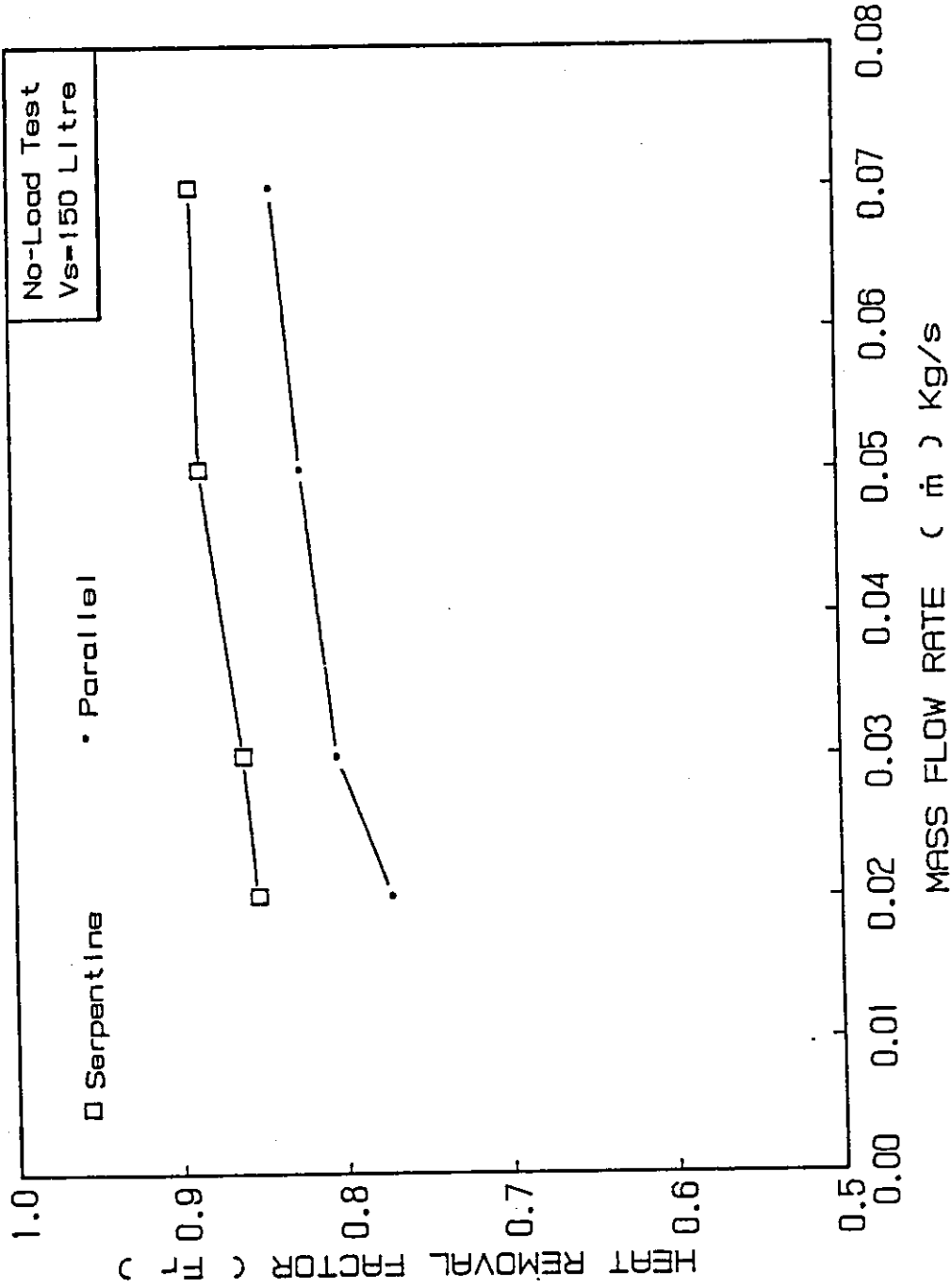


Fig.(4.77) Heat removal factor vs. mass flow rate for the serpentine and the parallel tubes flat plate solar collectors.

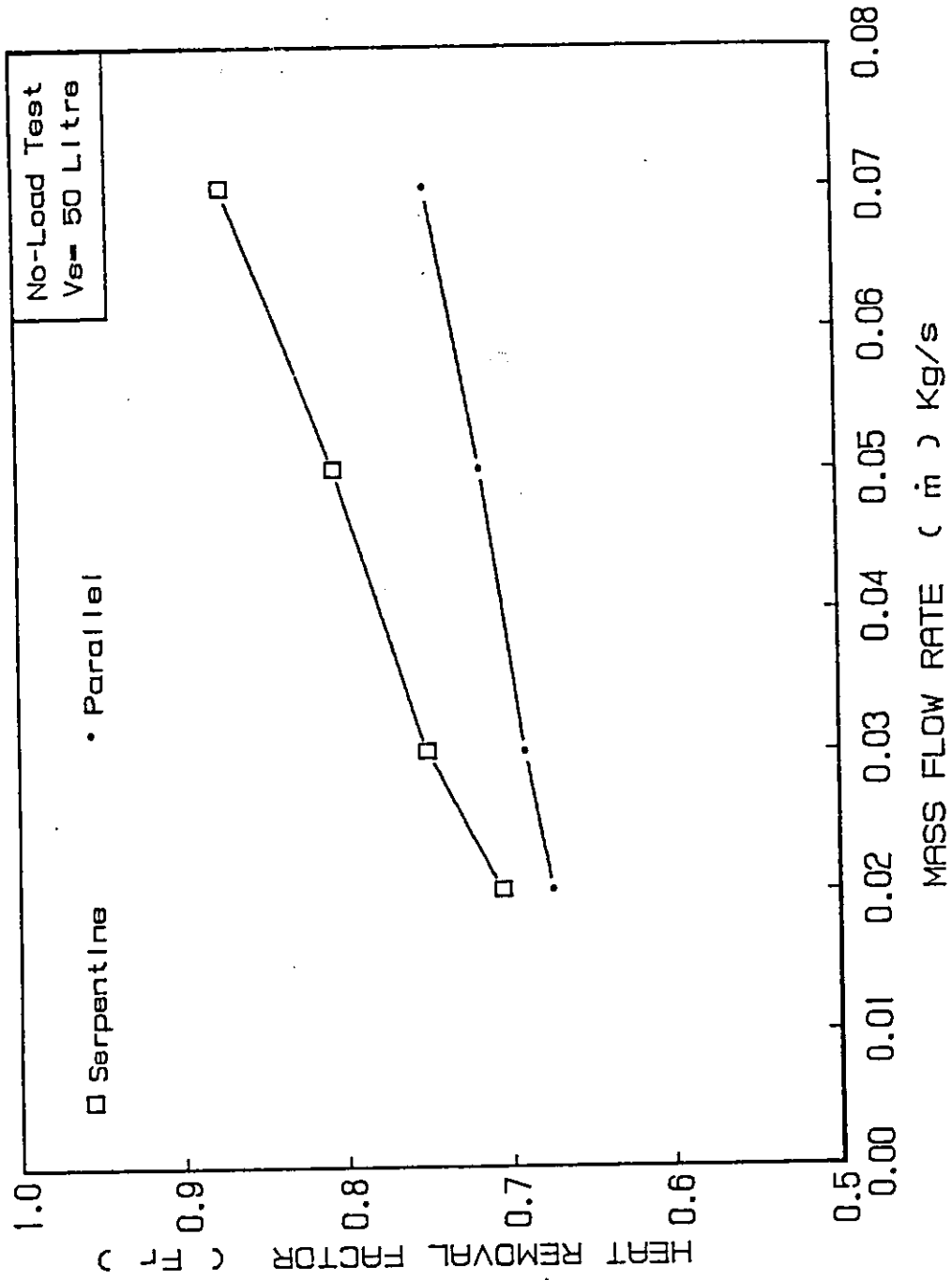


Fig.(4.78) Heat removal factor vs. mass flow rate for the serpentine and the parallel tubes flat plate solar collectors.

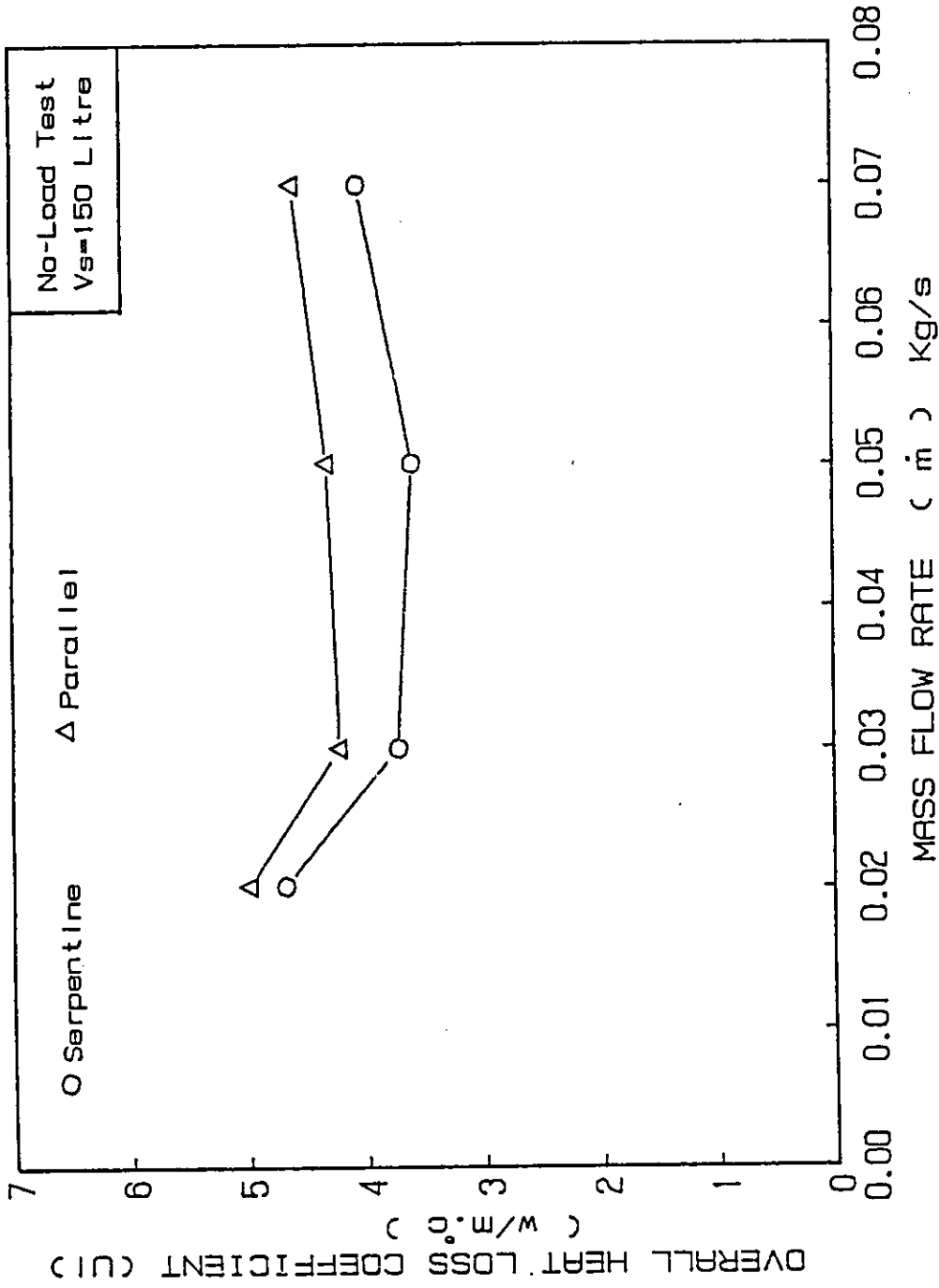


Fig.(4.79) Heat loss coefficient vs. mass flow rate for the serpentine and the parallel tubes flat plate solar collectors.

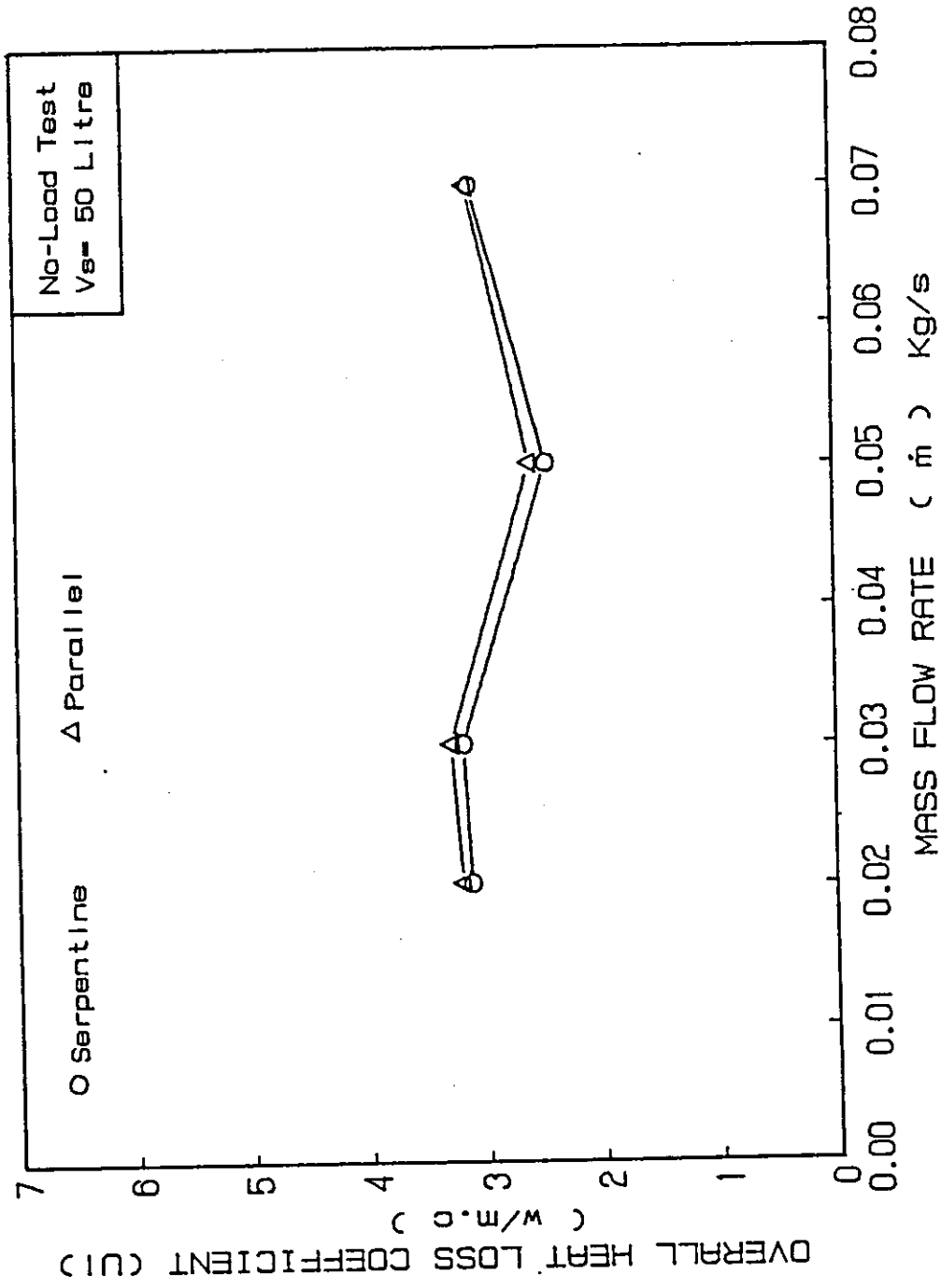


Fig.(4.80) Heat loss coefficient vs. mass flow rate for the serpentine and the parallel tubes flat plate solar collectors.

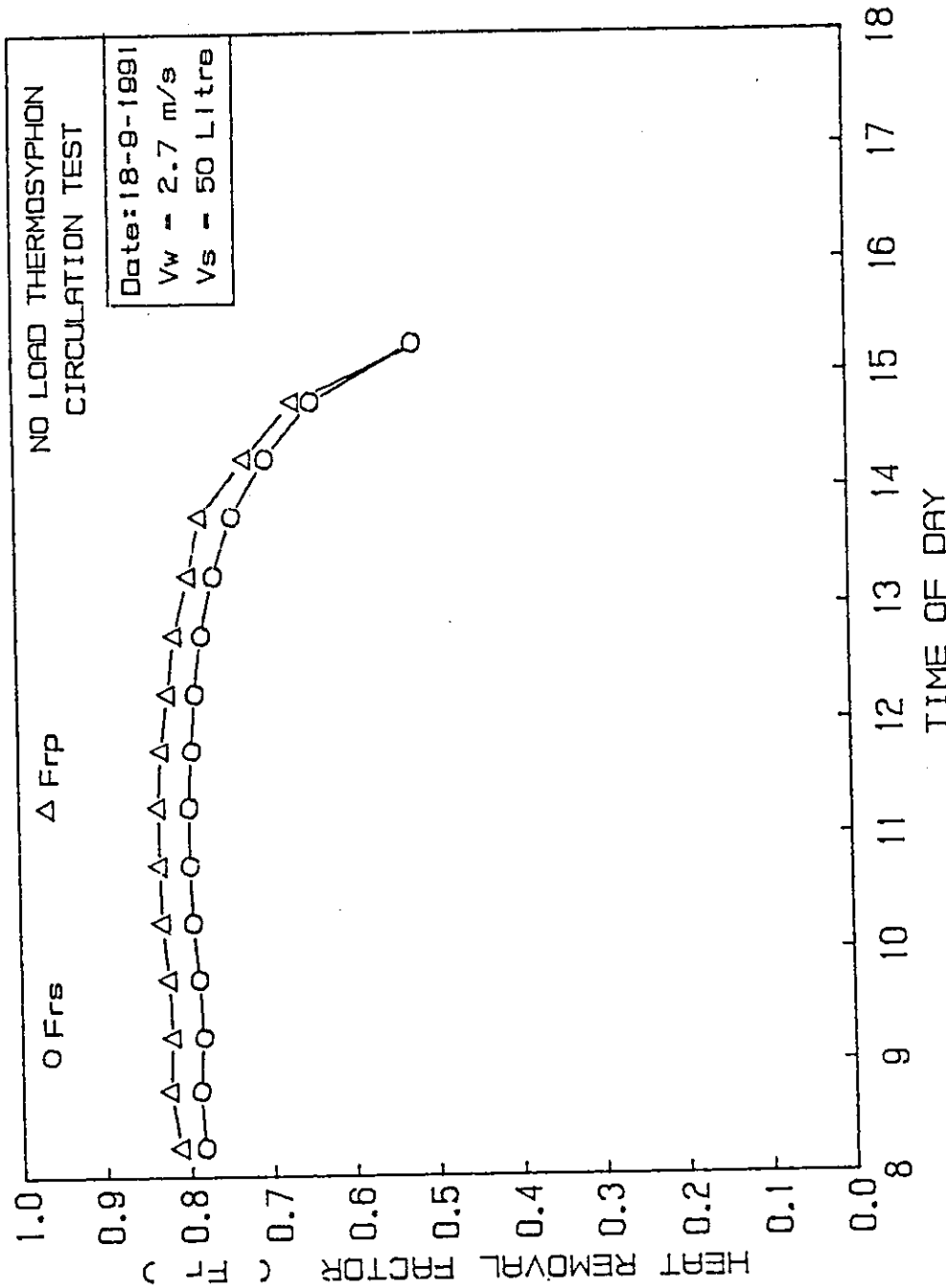


Fig.(4.81) Variation of the heat removal factor with time for the serpentine and the parallel types flat plate solar collectors under no load thermosyphon circulation.

Chapter 5

CONCLUSIONS AND RECOMENDATIONS

5.1 CONCLUSIONS

In this study, two collectors were tested under the same experimental conditions. Seven tests were performed on the proposed collectors. From the results of this study, the following conclusions may be stated:

1. Under forced circulation, the serpentine type has a superior performance when compared to the parallel type, especially, during the time interval 09:30-15:00. (i.e All the performance parameters of the serpentine type are better than that of the parallel type).
2. For both collectors, the heat removal factor is more sensitive to flow rate variations when small storage tanks are used.
3. Under no load conditions, as the storage tank capacity is decreased, the performance parameters of both collectors decreased.
4. The overall heat loss coefficients of both collectors show poor dependence on the flow rate variations.

5. As the solar intensity is increased, the ability of the serpentine type in converting the solar irradiance into useful heat gain becomes more significant than that of the parallel type.
6. After the time interval 14:30-15:00, as the time passes then the performance of both collectors comes nearer to each other. By the end of the test day both collectors have, nearly, the same performance. This behavior becomes more evident under low flow rates.
7. Forced flow tests show that as the flow rate is increased, then the improvements on the performance of the serpentine type is greater than that on the parallel type.
8. The serpentine type shows an inferior performance when compared to the parallel type under a thermosyphon circulation.
9. No load thermosyphon test shows that the heat removal factors of both collectors, approximately, maintain a constant value for most intervals of the test day.
10. Results of the stagnation test show that the overall heat loss coefficients of the serpentine and the parallel types are 4.85 and 5.01 $W/m^2.C^{\circ}$, respectively.
11. The influence of the shading effect on the serpentine type is higher than that on the parallel type. This effect is decreased as the flow is increased.
12. Since most of the solar domestic hot water collectors used in Jordan are thermosyphon systems, then choosing the serpentine type as a solar collector is not

a suitable choice. The parallel type still a convenient selection. On the other hand, the selection of the serpentine type for forced flow systems where pumps are used, is more suitable than the parallel type. The applications of such systems are space heating and building conditioning, where the circulation of water to the collector will usually be kept high.

13. The time constant of the serpentine type is lower than that of the parallel type by about 21%. The time constant of the serpentine and the parallel types are 3.83 and 4.88 minutes, respectively.
14. Time constant test shows that when the flow rate is 0.02 Kg/s , the phase lag between the serpentine and the parallel solar collectors is 9.0 minutes.
15. Although, the pressure drop inside the serpentine collector is higher than that in the parallel type, it is found that the serpentine type was able to circulate water naturally at a maximum flow rate of $5.05 * 10^{-3} \text{ Kg/s}$. While, the parallel type can circulate water by a rate of $5.61 * 10^{-3} \text{ Kg/s}$
16. The connection of an array of collectors of the serpentine type in a parallel arrangement is better than the series arrangement, to maintain a minimum pressure drop across the collectors.

5.2 RECOMENDATIONS

In spite of achieving all the objectives of this study, still there are certain points which are not studied and necessitate a further studies:

1. The effect of using varies sizes of tubes, different tube spacing, different tilt angles, and different types of absorber plate and tube materials, on the performance of both collectors can be investigated and studied.
2. The performance of an array of collectors of both types connected in series and parallel arrangements can be studied and investigated.
3. The performance of the nonmetallic (plastics, concrete,etc) serpentine solar collectors can be studied and investigated.

REFERENCES

1. J.A.Duffie, and W.A.Beckman, *Solar Engineering of Thermal Processes*, Wiley and Sons, New York, 1980.
2. Alsaad,M., Hijazi,M., Habali,S. and Rabadi,N,*An inexpensive and reliable solar water heater for Jordan*, accepted for publication in *Dirasat*, Vol.XII (1985), No.1, University of Jordan.
3. Hottel,H.C., and B.B.Woertz, *Transaction of the American Society of Mechanical Engineers*, 64, 91 (1942). *Performance of flat-plate solar heat collectors*.
4. Moore,S.W., J.D.Balcomb, and J.C.Hedstorm, paper presented at Ft. Collins ISES meeting, August 1974.*Design and testing of a structurally integrated steel solar collector unit based on expanded flat metal plates*.
5. M.Kovarik and P.F.Leese, *Optimal control of flow in low temperature solar heat collectors*, *Solar Energy*, 18(5), 431-435 (1976).
6. R.C.Winn and C.B.Winn, *Optimal control of mass rates in flat plate solar collectors*, *J.Solar Energy Engng*, 103(2), 113-120 (1981).
7. M.F.Young and J.B.Bergquam, *Performance characteristics of a thermosyphon solar domestic hot water systems*, *J. Solar Energy Engng*, 103(3), 193-200

(1981).

8. H.C.Hewitt and E.I.Griggs, *Optimal mass flow rates through flat plate solar collector panels*, ASME Solar Energy Conf., 77-WA/Sol-19. (Aug. 1977).
9. K.O.Lund, *General thermal analysis of parallel-flow flat plate solar collector absorbers*, Solar Energy, 36, 443-450 (1986).
10. S.T.Abdel-Kalik, *Heat removal for a flat plate solar collector with a serpentine tube*, Solar Energy, 18(1), 59-64 (1976).
11. H.Zhang, and Z.Lavan, *Thermal performance of a serpentine absorber plate*, Solar Energy, 34, 175-177, (1985).
12. M.A.Akgün, *Heat removal factor for a serpentine absorber plate*, Solar Energy, 41(1), 109-111, (1988).
13. I.Borde, I.Yaron, and M.Jelinek, *Comparative study of parallel- tubes and serpentine type flat-plate solar collectors*, Proc. Int. Solar Energy Soc. Silver Jubilee, p.277, May(1979).
14. J.P.Chiou and D.G.Perera, *Performance analysis of a serpentine type flat plate solar collector*, Proc. ASME-ASES Solar Energy Conference, Knoxville, March (1985).
15. S.Johnson, *Standardized performance tests of collectors of solar thermal energy - A flat plate collector with a single tube serpentine flow distribution*, NASA Technical Memorandum, NASA TMX-73417, 1-2 Lewis Research Center, Cleveland, Ohio April (1976).

16. J.E.Hill, J.P.Jenkins, and D.E.Jones, *Experimental verification of a standard test procedure for solar collectors*, National Bureau of Standards Building Science Series 117, Washington, D.C., 5-39. Jan (1979).
17. K.O.Lund, *General thermal analysis of serpentine-flow flat plate solar collector absorbers*, *Solar Energy*, 42(2), 133-142 (1989).
18. Lunde, P.J, *Solar Thermal Engineering Space Heating and Hot Water Systems*, Wiley and sons, 1980.
19. ASHRAE STANDARD 93-77. *Methods of testing to determine the thermal performance of solar collectors*, ASHRAE, New York, 1977.
20. F.F Simon, *Flat plate solar collectors as a basis for collector selection and performance prediction*, *Solar Energy*, 18, 451-466 (1976).

APPENDIX (A)
EXPERIMENTAL AVERAGED
MEASURED DATA

Table A.1 : Averaged measured data for the forced circulation test with no load conditions ($\dot{m} = 0.02 \text{ Kg/s}$ and $V_s = 150 \text{ l}$). All temperatures in $^{\circ}\text{C}$.

Time Interval	T_{i_s}	T_1	T_2	T_3	T_{o_s}	T_{ip}	T_{op}	T_a	I Wh/m ²
08:00-08:30	28.2	28.5	28.7	28.9	28.9	28.1	28.65	17.3	198.4
08:30-09:00	28.5	29.1	29.7	30.2	30.35	28.3	29.80	19.3	267.2
09:00-09:30	28.9	29.8	30.6	31.3	31.45	28.6	30.7	20.3	322.8
09:30-10:00	29.4	30.5	31.4	32.2	32.5	28.9	31.55	20.9	376.5
10:00-10:30	30.7	31.9	33.0	33.8	34.2	30.3	33.3	22.3	420.7
10:30-11:00	32.4	33.7	34.9	35.9	36.3	32.1	35.5	23.4	456.4
11:00-11:30	34.0	35.5	36.7	37.8	38.2	33.75	37.50	23.3	487.8
11:30-12:00	35.55	37.1	38.4	39.5	39.90	35.5	39.0	23.6	511.8
12:00-12:30	37.4	38.9	40.2	41.3	41.8	36.8	40.8	24.2	520.7
12:30-13:00	39.4	40.9	42.2	43.3	43.75	38.0	42.0	24.5	523.5
13:00-13:30	41.4	42.9	44.2	45.3	45.6	40.1	43.9	24.7	519.2
13:30-14:00	43.3	44.7	45.9	46.9	47.25	41.4	45.05	25.2	501.2
14:00-14:30	44.9	46.2	47.3	48.2	48.6	43.0	46.35	25.9	475.2
14:30-15:00	46.7	47.9	48.9	49.7	50.05	44.55	47.60	26.0	439.7
15:00-15:30	48.45	49.5	50.3	51.0	51.20	46.4	48.9	26.1	395.3
15:30-16:00	49.9	50.7	51.4	52.0	52.05	47.8	49.75	26.0	348.0
16:00-16:30	51.1	51.6	52.0	52.4	52.6	48.9	50.3	25.3	298.6
16:30-17:00	52.0	52.3	52.6	52.8	52.85	49.6	50.4	25.2	243.7

Table A.2 : Averaged measured data for the forced circulation test with no load conditions ($\dot{m} = 0.03 \text{ Kg/s}$ and $V_s = 150 \text{ l}$). All temperatures in $^{\circ}\text{C}$.

Time Interval	T_{i_s}	T_1	T_2	T_3	T_{o_s}	T_{ip}	T_{op}	T_a	I Wh/m ²
08:00-08:30	29.1	29.5	29.8	30.1	30.2	29.0	30.0	23.5	205.8
08:30-09:00	29.6	30.1	30.5	30.8	30.95	29.4	30.6	24.1	256.2
09:00-09:30	30.6	31.2	31.7	32.2	32.35	30.3	31.9	25.0	315.1
09:30-10:00	32.1	32.8	33.4	33.9	34.2	31.8	33.75	26.1	366.5
10:00-10:30	33.5	34.4	35.2	35.8	35.95	33.1	35.35	26.8	412.3
10:30-11:00	34.9	35.8	36.6	37.3	37.6	34.5	36.95	27.1	449.7
11:00-11:30	36.9	37.9	38.8	39.5	39.75	36.4	39.05	27.2	484.9
11:30-12:00	38.8	39.9	40.8	41.5	41.8	38.35	41.1	27.4	508.8
12:00-12:30	40.7	41.7	42.6	43.4	43.7	40.0	42.8	27.4	519.1
12:30-13:00	42.8	43.9	44.8	45.6	45.75	41.9	44.7	28.0	520.8
13:00-13:30	44.85	45.9	46.8	47.5	47.8	43.95	46.7	28.6	510.9
13:30-14:00	46.65	47.6	48.4	49.1	49.5	45.7	48.3	28.5	493.4
14:00-14:30	48.6	49.5	50.3	50.8	51.1	47.5	49.9	28.4	465.2
14:30-15:00	50.3	51.1	51.8	52.4	52.55	49.1	51.25	28.5	429.1
15:00-15:30	51.75	52.4	53.0	53.5	53.7	50.3	52.1	28.7	385.9
15:30-16:00	53.0	53.5	54.0	54.4	54.55	51.5	52.9	28.5	340.2
16:00-16:30	54.1	54.5	54.8	55.1	55.2	52.5	53.4	28.1	289.9
16:30-17:00	54.9	55.1	55.3	55.5	55.55	53.1	53.65	27.9	245.5

Table A.3 : Averaged measured data for the forced circulation test with no load conditions ($\dot{m} = 0.05 \text{ Kg/s}$ and $V_s = 150 \text{ l}$). All temperatures in $^{\circ}\text{C}$.

Time Interval	T_{i_s}	T_1	T_2	T_3	T_{o_s}	T_{i_p}	T_{o_p}	T_a	1 Wh/m^2
08:00-08:30	28.5	28.7	28.9	29.0	29.05	28.5	29.05	24.0	192.9
08:30-09:00	29.4	29.7	30.0	30.2	30.25	29.5	30.0	25.0	258.1
09:00-09:30	30.85	31.2	31.5	31.8	32.0	30.4	31.45	25.6	312.1
09:30-10:00	32.2	32.7	33.1	33.4	33.5	31.7	32.9	27.0	362.2
10:00-10:30	34.0	34.5	35.0	35.4	35.5	33.2	34.6	27.5	407.7
10:30-11:00	35.8	36.4	36.9	37.3	37.45	35.0	36.55	28.2	447.2
11:00-11:30	37.6	38.2	38.7	39.2	39.4	37.0	38.7	29.8	476.1
11:30-12:00	39.8	40.5	41.1	41.5	41.7	38.95	40.7	30.3	497.3
12:00-12:30	42.1	42.7	43.2	43.7	44.0	40.6	42.4	29.9	510.4
12:30-13:00	44.2	44.8	45.4	45.9	46.05	42.6	44.25	29.8	514.3
13:00-13:30	46.3	46.9	47.5	48.0	48.15	44.8	46.4	30.0	505.8
13:30-14:00	48.3	48.9	49.4	49.8	50.0	46.65	48.2	30.5	488.3
14:00-14:30	50.15	50.7	51.2	51.6	51.7	48.2	49.65	30.9	460.6
14:30-15:00	51.8	52.3	52.8	53.2	53.25	49.6	50.9	31.1	426.5
15:00-15:30	53.35	53.8	54.2	54.5	54.6	50.9	51.9	31.2	387.7
15:30-16:00	54.6	54.9	55.2	55.4	55.45	52.7	53.5	30.5	336.5
16:00-16:30	55.7	55.9	56.1	56.3	56.35	53.0	53.6	29.6	283.5
16:30-17:00	56.2	56.4	56.6	56.7	56.6	53.55	53.9	29.3	227.3

Table A.4 : Averaged measured data for the forced circulation test with no load conditions ($\dot{m} = 0.07 \text{ Kg/s}$ and $V_s = 150 \text{ l}$). All temperatures in $^{\circ}\text{C}$.

Time Interval	T_{i_s}	T_1	T_2	T_3	T_{o_s}	T_{i_p}	T_{o_p}	T_a	1 Wh/m^2
08:00-08:30	30.1	30.2	30.3	30.4	30.35	30.0	30.25	22.3	213.2
08:30-09:00	30.7	30.9	31.1	31.2	31.3	30.6	31.1	22.9	270.4
09:00-09:30	31.8	32.1	32.3	32.5	32.55	31.6	32.3	23.5	325.1
09:30-10:00	33.1	33.4	33.7	33.9	34.0	32.8	33.65	24.5	375.1
10:00-10:30	34.6	35.0	35.3	35.6	35.7	34.3	35.35	25.1	414.9
10:30-11:00	36.5	36.9	37.3	37.6	37.7	36.1	37.2	26.0	455.2
11:00-11:30	38.1	38.6	39.0	39.3	39.4	37.6	38.8	26.9	482.5
11:30-12:00	40.1	40.6	41.0	41.4	41.5	39.5	40.75	27.7	504.1
12:00-12:30	42.7	43.2	43.6	44.0	44.1	41.9	43.2	28.0	515.6
12:30-13:00	44.8	45.3	45.7	46.0	46.15	44.0	45.3	28.7	514.8
13:00-13:30	47.0	47.5	47.9	48.2	48.25	46.1	47.3	29.1	514.4
13:30-14:00	49.0	49.4	49.8	50.1	50.2	48.05	49.2	29.1	496.6
14:00-14:30	50.85	51.3	51.7	52.0	52.0	49.7	50.75	28.9	472.2
14:30-15:00	52.5	52.9	53.2	53.4	53.45	51.3	52.2	29.3	437.4
15:00-15:30	54.0	54.3	54.5	54.7	54.8	52.7	53.45	29.6	393.5
15:30-16:00	55.2	55.4	55.6	55.8	55.8	54.0	54.5	29.4	344.2
16:00-16:30	56.1	56.3	56.4	56.5	56.5	54.95	55.3	29.0	291.7
16:30-17:00	56.5	56.7	56.8	56.9	56.8	55.5	55.75	28.2	235.8

Table A.5 : Averaged measured data for the forced circulation test with no load conditions ($\dot{m} = 0.02 \text{ Kg/s}$ and $V_s = 50 \text{ l}$). All temperatures in $^{\circ}\text{C}$.

Time Interval	$T_{i,s}$	T_1	T_2	T_3	$T_{o,s}$	$T_{i,p}$	$T_{o,p}$	T_a	$I \text{ Wh/m}^2$
08:00-08:30	20.6	20.8	21.0	21.2	21.3	20.6	21.25	16.8	144.4
08:30-09:00	23.9	24.5	25.0	25.5	25.7	23.9	25.6	17.8	232.9
09:00-09:30	29.0	29.8	30.5	31.1	31.3	29.0	31.2	18.8	314.6
09:30-10:00	35.5	36.4	37.2	37.8	38.0	35.5	37.9	19.7	381.5
10:00-10:30	42.6	43.6	44.4	45.1	45.4	42.6	45.3	21.1	428.0
10:30-11:00	50.0	51.0	51.9	52.6	52.85	50.0	52.75	22.2	465.0
11:00-11:30	57.4	58.5	59.4	60.1	60.35	57.4	60.25	22.7	492.6
11:30-12:00	64.5	65.6	66.5	67.3	67.5	64.5	67.4	23.0	513.2
12:00-12:30	70.95	71.9	72.8	73.5	73.8	70.9	73.6	23.6	525.3
12:30-13:00	76.7	77.6	78.4	79.1	79.4	76.7	79.25	24.7	522.8
13:00-13:30	81.2	82.1	82.9	83.6	83.8	81.25	83.7	25.4	513.4
13:30-14:00	84.8	85.6	86.3	86.9	87.1	84.8	86.8	26.1	491.6
14:00-14:30	87.3	87.9	88.5	89.0	89.15	87.3	88.95	26.4	456.7
14:30-15:00	88.5	89.0	89.5	89.9	90.0	88.5	89.8	26.1	420.4
15:00-15:30	88.6	89.0	89.3	89.5	89.6	88.65	89.6	26.6	379.9
15:30-16:00	87.4	87.6	87.8	88.0	88.0	87.4	87.95	26.4	326.9
16:00-16:30	85.1	85.3	85.4	85.4	85.3	85.1	85.3	26.1	268.5
16:30-17:00	81.4	81.6	81.6	81.4	81.0	81.4	81.2	25.7	203.9

Table A.6 : Averaged measured data for the forced circulation test with no load conditions ($\dot{m} = 0.03 \text{ Kg/s}$ and $V_s = 50 \text{ l}$). All temperatures in $^{\circ}\text{C}$.

Time Interval	$T_{i,s}$	T_1	T_2	T_3	$T_{o,s}$	$T_{i,p}$	$T_{o,p}$	T_a	$I \text{ Wh/m}^2$
08:00-08:30	20.45	20.5	20.6	20.6	20.6	20.4	20.5	15.7	86.4
08:30-09:00	23.2	23.4	23.6	23.6	23.65	23.2	23.6	17.0	160.4
09:00-09:30	27.5	27.9	28.3	28.6	28.7	27.5	28.6	19.0	268.8
09:30-10:00	33.0	33.6	34.2	34.7	34.85	33.0	34.7	20.2	369.2
10:00-10:30	39.8	40.5	41.1	41.6	41.9	39.8	41.7	21.0	422.6
10:30-11:00	47.4	48.2	48.9	49.5	49.65	47.4	49.45	21.4	462.3
11:00-11:30	54.9	55.7	56.4	57.0	57.2	54.9	57.0	21.9	495.7
11:30-12:00	62.2	62.7	63.2	63.6	63.8	62.2	64.3	23.0	514.0
12:00-12:30	68.55	69.3	70.0	70.6	70.8	68.5	70.55	23.8	526.2
12:30-13:00	73.8	74.6	75.3	75.8	76.0	73.8	75.8	24.3	526.7
13:00-13:30	78.3	79.0	79.6	80.1	80.25	78.3	80.05	24.8	517.4
13:30-14:00	81.9	82.4	82.9	83.3	83.4	81.9	83.3	25.0	494.6
14:00-14:30	84.0	84.5	84.9	85.2	85.3	84.0	85.2	24.9	460.5
14:30-15:00	84.95	85.3	85.6	85.9	86.1	84.9	85.9	25.2	425.8
15:00-15:30	85.0	85.3	85.6	85.8	85.85	85.05	85.8	25.3	375.7
15:30-16:00	84.0	84.2	84.3	84.4	84.5	84.0	84.4	25.0	321.9
16:00-16:30	81.6	81.7	81.8	81.9	81.8	81.6	81.75	24.8	371.2
16:30-17:00	78.4	78.5	78.6	78.6	78.3	78.4	78.3	24.3	211.8

Table A.7 : Averaged measured data for the forced circulation test with no load conditions ($\dot{m} = 0.05 \text{ Kg/s}$ and $V_s = 50 \text{ l}$). All temperatures in $^{\circ}\text{C}$.

Time Interval	T_{i_s}	T_1	T_2	T_3	T_{o_s}	T_{i_p}	T_{o_p}	T_a	$I \text{ Wh/m}^2$
08:00-08:30	21.3	21.4	21.5	21.6	21.65	21.3	21.6	19.3	180.0
08:30-09:00	25.7	26.0	26.2	26.4	26.5	25.7	26.4	21.0	256.3
09:00-09:30	32.0	32.4	32.7	32.9	33.0	32.0	32.9	23.2	315.9
09:30-10:00	39.0	39.4	39.8	40.1	40.2	39.0	40.05	25.9	363.1
10:00-10:30	46.7	47.1	47.5	47.8	47.95	46.7	47.8	27.0	404.6
10:30-11:00	54.5	54.9	55.3	55.6	55.8	54.5	55.65	27.7	439.8
11:00-11:30	62.0	62.5	62.9	63.2	63.3	62.0	63.15	29.5	463.2
11:30-12:00	69.0	69.5	69.9	70.2	70.3	69.0	70.2	29.4	475.7
12:00-12:30	75.2	75.6	76.0	76.3	76.5	75.2	76.4	29.6	483.1
12:30-13:00	80.5	80.9	81.2	81.5	81.75	80.5	81.6	31.1	499.3
13:00-13:30	85.2	85.7	86.1	86.4	86.5	85.2	86.3	31.5	498.6
13:30-14:00	89.0	89.4	89.8	90.1	90.25	89.0	90.0	32.1	478.9
14:00-14:30	91.9	92.3	92.6	92.9	93.0	91.9	92.75	31.9	451.0
14:30-15:00	92.5	92.8	93.1	93.3	93.4	92.5	93.2	30.3	409.3
15:00-15:30	90.4	90.6	90.8	90.9	91.05	90.4	90.95	30.4	365.8
15:30-16:00	87.7	87.9	88.0	88.1	88.15	87.7	88.05	30.6	315.6
16:00-16:30	85.0	85.1	85.2	85.2	85.25	85.0	85.25	29.7	261.2
16:30-17:00	82.4	82.5	82.5	82.4	82.35	82.4	82.4	29.2	201.8

Table A.8 : Averaged measured data for the forced circulation test with no load conditions ($\dot{m} = 0.07 \text{ Kg/s}$ and $V_s = 50 \text{ l}$). All temperatures in $^{\circ}\text{C}$.

Time Interval	T_{i_s}	T_1	T_2	T_3	T_{o_s}	T_{i_p}	T_{o_p}	T_a	$I \text{ Wh/m}^2$
08:00-08:30	23.8	23.9	24.0	24.0	24.05	23.8	24.0	18.8	202.8
08:30-09:00	28.6	28.8	29.0	29.1	29.2	28.6	29.1	19.8	263.9
09:00-09:30	35.1	35.4	35.6	35.8	35.85	35.1	35.7	20.7	317.5
09:30-10:00	42.15	42.5	42.7	42.9	43.0	42.2	42.9	21.7	376.5
10:00-10:30	49.7	50.0	50.3	50.5	50.6	49.7	50.45	22.4	423.3
10:30-11:00	57.7	58.0	58.3	58.5	58.65	57.7	58.5	23.0	463.3
11:00-11:30	65.3	65.6	65.9	66.1	66.25	65.3	66.1	23.7	490.9
11:30-12:00	71.8	72.1	72.4	72.6	72.7	71.8	72.6	23.9	513.1
12:00-12:30	77.7	78.0	78.3	78.5	78.6	77.7	78.5	24.4	522.6
12:30-13:00	81.75	82.1	82.4	82.6	82.7	81.8	82.6	25.1	521.0
13:00-13:30	84.2	84.5	84.7	84.9	85.05	84.2	84.9	25.6	512.8
13:30-14:00	85.9	86.1	86.3	86.5	86.6	85.9	86.5	26.5	486.8
14:00-14:30	86.6	86.8	87.0	87.1	87.2	86.6	87.1	26.6	460.5
14:30-15:00	86.3	86.5	86.6	86.7	86.8	86.3	86.75	26.3	418.0
15:00-15:30	85.3	85.5	85.6	85.7	85.75	85.3	85.7	26.6	374.2
15:30-16:00	83.7	83.8	83.9	84.0	84.0	83.7	83.95	26.4	322.7
16:00-16:30	81.5	81.6	81.6	81.7	81.65	81.5	81.6	26.0	270.7
16:30-17:00	78.8	79.1	79.0	79.0	78.8	78.8	78.8	25.7	214.0

Table A.9 : Averaged measured data for the forced circulation test with no load conditions and 0.015Kg/s flow rate for the serpentine type and 0.105Kg/s for the parallel type, as performed on 9 - 9 - 1991. All temperatures in $^{\circ}\text{C}$.

Time Interval	T_{i_s}	T_1	T_2	T_3	T_{o_s}	T_{i_p}	T_{o_p}	T_a	$I\text{ Wh/m}^2$
08:00-08:30	21.1	21.4	21.6	21.8	21.95	21.1	21.2	19.7	130.0
08:30-09:00	24.7	25.5	26.1	26.7	26.9	24.7	25.05	21.4	251.4
09:00-09:30	30.8	31.8	32.7	33.4	33.75	30.8	31.25	24.5	308.3
09:30-10:00	37.3	38.5	39.5	40.4	40.8	37.3	37.85	26.8	361.1
10:00-10:30	44.0	45.3	46.4	47.3	47.6	44.0	44.6	28.4	405.4
10:30-11:00	51.1	52.4	53.5	54.4	54.95	51.1	51.75	29.4	435.4
11:00-11:30	58.0	59.3	60.4	61.3	61.75	58.0	58.7	29.5	454.7
11:30-12:00	64.3	65.5	66.5	67.4	67.7	64.3	64.95	30.3	465.3
12:00-12:30	70.0	71.2	72.2	73.1	73.4	70.0	70.6	31.1	484.5
12:30-13:00	74.5	75.8	76.9	77.8	78.15	74.45	75.0	31.2	485.1
13:00-13:30	78.8	79.9	80.9	81.8	82.15	78.8	79.3	31.2	470.3
13:30-14:00	82.1	83.0	83.8	84.5	84.8	82.1	82.6	31.2	452.8
14:00-14:30	84.5	85.2	86.8	87.3	86.55	84.5	84.9	31.3	427.9
14:30-15:00	85.8	86.4	86.9	87.3	87.5	85.8	86.15	31.9	390.8
15:00-15:30	86.25	86.7	87.1	87.4	87.5	86.3	86.6	32.0	344.8
15:30-16:00	85.5	85.8	86.1	86.3	86.4	85.5	85.7	31.5	295.1
16:00-16:30	83.55	83.7	83.7	83.9	84.0	83.6	83.7	31.2	241.2
16:30-17:00	80.4	80.4	80.3	80.3	80.2	80.4	80.45	30.6	184.1

Table A.10 : Averaged measured data for the forced circulation test with load conditions and 0.02Kg/s flow rate, as performed on 12 - 9 - 1991. All temperatures in $^{\circ}\text{C}$.

Time Interval	T_{i_s}	T_1	T_2	T_3	T_{o_s}	T_{i_p}	T_{o_p}	T_a	$I\text{ Wh/m}^2$
08:00-08:30	24.1	24.4	24.6	24.8	24.95	24.1	24.8	21.1	135.4
08:30-09:00	24.2	24.7	25.2	25.6	25.75	24.2	25.5	23.0	244.2
09:00-09:30	24.4	25.1	25.7	26.7	26.4	24.4	26.0	23.8	312.4
09:30-10:00	24.7	25.5	26.2	26.7	27.0	24.7	26.6	23.9	365.7
10:00-10:30	25.0	25.9	26.7	27.4	27.7	25.0	27.25	24.2	412.8
10:30-11:00	25.1	26.1	27.0	27.7	28.05	25.1	27.6	25.2	448.8
11:00-11:30	25.15	26.3	27.2	28.0	28.30	25.15	28.0	26.5	476.0
11:30-12:00	25.3	26.5	27.5	28.3	28.6	25.3	28.25	27.6	495.9
12:00-12:30	25.1	26.3	27.3	28.2	28.55	25.1	28.2	27.7	507.1
12:30-13:00	24.8	26.0	27.0	27.9	28.25	24.8	27.9	27.5	507.1
13:00-13:30	24.6	25.8	26.8	27.6	27.95	24.6	27.95	27.7	496.6
13:30-14:00	24.45	25.6	26.5	27.3	27.6	24.45	27.3	27.4	476.0
14:00-14:30	24.3	25.3	26.2	26.9	27.15	24.3	26.9	27.2	444.9
14:30-15:00	24.1	24.9	25.6	26.3	26.6	24.1	26.4	27.1	404.2
15:00-15:30	24.0	24.8	25.5	26.0	26.25	24.0	26.05	26.9	368.9
15:30-16:00	24.0	24.6	25.1	25.6	25.85	24.0	25.75	26.5	315.0
16:00-16:30	23.9	24.4	24.8	25.2	25.35	23.9	25.3	26.1	262.7
16:30-17:00	23.8	24.2	24.5	24.8	24.95	23.8	24.95	26.0	205.1

Table A.11 : Averaged measured data for the forced circulation test with load conditions and 0.05Kg/s flow rate, as performed on 14 - 9 - 1991. All temperatures in $^{\circ}\text{C}$.

Time Interval	T_{i_s}	T_1	T_2	T_3	T_{o_s}	T_{ip}	T_{op}	T_a	$I\text{Wh/m}^2$
08:00-08:30	25.0	25.1	25.2	25.3	25.3	25.0	25.2	22.1	160.4
08:30-09:00	25.1	25.3	25.5	25.7	25.75	25.1	25.6	23.2	249.6
09:00-09:30	25.3	25.6	25.9	26.1	26.2	25.3	26.0	23.7	304.6
09:30-10:00	25.4	25.8	26.1	26.4	26.5	25.4	26.3	23.8	353.8
10:00-10:30	25.6	26.1	26.5	26.8	26.95	25.6	26.7	24.1	396.5
10:30-11:00	25.8	26.3	26.8	27.2	27.3	25.8	27.1	25.0	435.5
11:00-11:30	26.0	26.6	27.1	27.5	27.6	26.0	27.4	26.3	465.4
11:30-12:00	26.1	26.7	27.2	27.6	27.8	26.1	27.6	27.4	486.2
12:00-12:30	26.2	26.8	27.3	27.8	28.0	26.2	27.8	27.6	498.5
12:30-13:00	26.4	27.1	27.7	28.2	28.4	26.4	28.0	27.7	498.8
13:00-13:30	26.3	26.9	27.4	27.8	28.0	26.3	27.8	27.5	487.2
13:30-14:00	26.1	26.7	27.2	27.627.75	26.1	27.5	27.2	462.8	
14:00-14:30	25.9	26.4	26.9	27.3	27.4	25.9	27.15	27.0	432.6
14:30-15:00	25.65	26.1	26.5	26.8	27.0	25.7	26.85	26.9	397.3
15:00-15:30	25.5	25.9	26.3	26.6	26.7	25.5	26.5	26.8	370.2
15:30-16:00	25.3	25.7	26.0	26.2	26.3	25.3	26.1	26.5	320.3
16:00-16:30	25.1	25.3	25.5	25.7	25.75	25.1	25.6	26.0	265.8
16:30-17:00	24.9	25.0	25.1	25.2	25.3	24.9	25.15	25.8	207.3

Table A.12 : Averaged measured data for the forced circulation test with intermittent load of 5l/h ($\dot{m} = 0.03\text{Kg/s}$ and $V_s = 50\text{l}$) as performed on 19 - 8 - 1991. All temperatures in $^{\circ}\text{C}$.

Time Interval	T_{i_s}	T_{o_s}	T_{ip}	T_{op}	T_a	$I\text{Wh/m}^2$	T_{us}	T_{up}
08:00-08:30	23.0	23.45	22.9	23.35	18.3	186.4	/	/
08:30-09:00	24.8	26.05	24.6	25.65	19.2	256.6	25.4	25.1
09:00-09:30	27.8	29.45	27.4	28.8	20.3	315.6	/	/
09:30-10:00	31.4	33.4	30.9	32.55	21.7	372.2	32.3	31.2
10:00-10:30	35.4	37.65	34.5	36.45	22.7	416.6	/	/
10:30-11:00	39.45	41.9	38.4	40.55	23.0	455.6	40.7	39.1
11:00-11:30	43.2	45.8	41.85	44.2	23.6	486.7	/	/
11:30-12:00	47.1	49.75	45.5	47.85	24.0	508.4	48.6	46.3
12:00-12:30	50.5	53.05	48.55	50.7	24.7	517.2	/	/
12:30-13:00	53.75	56.2	51.7	53.75	25.6	520.2	55.2	52.1
13:00-13:30	56.5	58.95	54.2	56.35	26.1	509.7	/	/
13:30-14:00	59.2	61.5	56.7	58.65	26.7	491.3	60.5	57.5
14:00-14:30	61.6	63.55	58.9	60.55	26.7	463.4	/	/
14:30-15:00	63.2	64.9	60.4	61.85	26.5	431.0	63.9	59.3
15:00-15:30	64.05	65.1	61.2	62.1	26.6	343.0	/	/
15:30-16:00	64.2	64.85	61.05	61.6	26.2	336.2	62.8	58.2
16:00-16:30	63.0	63.55	59.9	60.25	25.3	214.4	/	/
16:30-17:00	61.05	61.2	57.8	57.9	25.0	183.0	61.0	57.8

Table A.13 : Averaged measured data for the forced circulation test with intermittent load of 10l/h ($\dot{m} = 0.03Kg/s$ and $V_s = 50l$) as performed on 20 - 8 - 1991. All temperatures in C° .

Time Interval	T_{i_s}	T_{o_s}	T_{i_p}	T_{o_p}	T_a	I Wh/m ²	T_{u_s}	T_{u_p}
08:00-08:30	23.5	24.0	23.4	23.85	18.2	200.6	/	/
08:30-09:00	25.6	26.8	25.4	26.45	19.5	259.3	26.0	25.7
09:00-09:30	27.8	29.45	27.5	28.95	21.0	315.8	/	/
09:30-10:00	31.0	32.95	30.6	32.35	22.2	363.5	31.9	31.2
10:00-10:30	35.4	37.7	34.75	36.7	22.5	409.9	/	/
10:30-11:00	38.8	41.05	38.1	40.2	23.4	449.9	40.1	39.2
11:00-11:30	42.0	44.35	41.1	43.35	24.2	478.4	/	/
11:30-12:00	45.8	48.25	44.8	47.15	24.6	503.5	47.1	46.0
12:00-12:30	48.8	51.35	47.7	50.2	25.4	511.9	/	/
12:30-13:00	51.35	53.9	50.3	52.8	26.7	513.1	52.6	51.2
13:00-13:30	53.5	56.0	52.25	54.7	27.3	506.5	/	/
13:30-14:00	55.5	57.9	54.1	56.4	27.7	484.5	56.8	55.3
14:00-14:30	56.5	58.75	54.85	56.9	27.5	453.2	/	/
14:30-15:00	57.2	59.15	55.4	57.15	27.0	419.8	58.5	56.1
15:00-15:30	57.25	58.9	55.4	56.7	26.8	373.7	/	/
15:30-16:00	56.9	58.2	54.7	55.65	26.8	325.1	57.4	55.2
16:00-16:30	56.15	57.1	53.8	54.5	27.2	271.1	/	/
16:30-17:00	55.0	55.65	52.4	52.8	27.2	214.0	55.3	52.5

Table A.14 : Averaged measured data for the forced circulation test with intermittent load of 15l/h ($\dot{m} = 0.03Kg/s$ and $V_s = 50l$) as performed on 21 - 8 - 1991. All temperatures in C° .

Time Interval	T_{i_s}	T_{o_s}	T_{i_p}	T_{o_p}	T_a	I Wh/m ²	T_{u_s}	T_{u_p}
08:00-08:30	23.7	24.25	23.7	24.2	21.7	198.1	/	/
08:30-09:00	25.8	27.05	25.7	26.85	22.4	256.2	26.0	25.9
09:00-09:30	28.1	29.75	27.8	29.25	23.1	312.8	/	/
09:30-10:00	31.7	33.7	31.2	32.6	24.3	360.5	32.2	31.8
10:00-10:30	34.4	36.6	33.7	35.7	25.1	403.4	/	/
10:30-11:00	37.3	39.6	36.6	38.7	25.0	444.3	38.0	37.2
11:00-11:30	41.65	44.0	40.9	43.1	25.5	477.8	/	/
11:30-12:00	45.0	47.4	44.05	46.3	26.7	500.2	46.0	44.8
12:00-12:30	47.3	50.05	46.2	48.65	27.5	511.9	/	/
12:30-13:00	48.95	51.7	47.7	50.3	27.7	514.8	49.9	48.3
13:00-13:30	50.6	53.4	49.1	51.7	28.0	506.6	/	/
13:30-14:00	52.4	54.95	50.8	53.2	28.3	488.0	53.3	51.5
14:00-14:30	52.6	54.9	50.85	53.0	28.2	460.4	/	/
14:30-15:00	53.3	55.4	51.4	53.3	27.5	422.5	54.1	52.0
15:00-15:30	53.2	55.0	51.2	52.75	27.5	380.3	/	/
15:30-16:00	52.7	54.1	50.45	51.7	27.8	333.1	53.2	51.0
16:00-16:30	51.85	52.9	49.6	50.5	27.8	280.4	/	/
16:30-17:00	50.5	51.25	48.2	48.8	27.4	220.2	50.9	48.4

Table A.15 : Averaged measured data for the forced circulation test with intermittent load of 5l/h ($\dot{m} = 0.07Kg/s$ and $V_s = 50l$) as performed on 24 - 8 - 1991. All temperatures in C° .

Time Interval	T_{is}	T_{os}	T_{ip}	T_{op}	T_a	I Wh/m ²	T_{us}	T_{up}
08:00-08:30	25.6	25.9	25.6	25.8	23.3	158.2	/	/
08:30-09:00	28.1	28.65	27.9	28.35	24.8	244.4	28.2	28.0
09:00-09:30	31.6	32.3	31.2	31.75	26.1	350.1	/	/
09:30-10:00	35.6	36.4	34.9	35.6	27.1	380.7	35.9	35.4
10:00-10:30	39.95	40.7	38.8	39.6	27.0	396.0	/	/
10:30-11:00	43.9	44.9	42.8	43.7	27.3	432.7	44.5	43.4
11:00-11:30	48.1	49.2	46.8	47.75	28.2	460.1	/	/
11:30-12:00	52.3	53.4	50.5	51.5	29.1	481.7	52.9	51.0
12:00-12:30	56.2	57.25	54.3	55.25	29.6	490.8	/	/
12:30-13:00	59.8	60.8	57.9	58.85	29.9	493.1	60.4	58.5
13:00-13:30	62.6	63.5	60.5	58.9	30.4	486.7	/	/
13:30-14:00	65.0	65.8	62.8	63.5	30.6	470.0	65.5	63.3
14:00-14:30	66.8	67.5	64.5	65.15	30.1	443.7	/	/
14:30-15:00	68.0	68.6	65.6	66.1	29.6	409.7	68.3	65.8
15:00-15:30	68.4	68.85	65.8	66.25	29.8	368.9	/	/
15:30-16:00	68.2	68.55	65.5	65.85	29.9	315.6	68.4	65.7
16:00-16:30	67.4	67.55	64.65	64.8	29.1	262.7	/	/
16:30-17:00	66.2	66.25	63.3	63.35	28.7	204.8	66.2	63.3

Table A.16 : Averaged measured data for the forced circulation test with intermittent load of 10l/h ($\dot{m} = 0.07Kg/s$ and $V_s = 50l$) as performed on 25 - 8 - 1991. All temperatures in C° .

Time Interval	T_{is}	T_{os}	T_{ip}	T_{op}	T_a	I Wh/m ²	T_{us}	T_{up}
08:00-08:30	26.2	26.45	26.1	26.3	21.3	184.4	/	/
08:30-09:00	28.7	29.2	28.4	28.8	22.6	241.7	28.9	28.6
09:00-09:30	31.6	32.2	31.1	31.65	23.9	294.8	/	/
09:30-10:00	35.0	35.8	34.3	34.95	24.9	348.5	35.4	34.7
10:00-10:30	38.3	39.25	37.3	38.15	25.6	395.8	/	/
10:30-11:00	41.6	42.8	40.7	41.6	26.3	430.8	42.1	41.2
11:00-11:30	45.2	46.3	43.6	44.6	26.9	461.0	/	/
11:30-12:00	48.7	49.85	46.9	47.9	28.4	482.5	49.0	47.4
12:00-12:30	51.45	52.6	49.35	50.4	29.2	493.3	/	/
12:30-13:00	54.1	55.25	51.9	52.95	28.8	494.5	54.5	52.5
13:00-13:30	56.2	57.3	53.8	54.75	28.3	489.7	/	/
13:30-14:00	57.9	58.9	55.3	56.2	28.2	470.0	58.4	55.9
14:00-14:30	59.2	60.1	56.4	57.2	28.1	441.2	/	/
14:30-15:00	59.9	60.7	56.9	57.5	28.4	404.2	60.3	57.2
15:00-15:30	60.0	60.7	56.8	57.35	29.1	367.1	/	/
15:30-16:00	59.6	60.1	56.25	56.7	28.8	314.8	59.8	56.5
16:00-16:30	58.5	58.8	55.2	55.5	27.8	260.5	/	/
16:30-17:00	56.6	56.7	53.3	53.4	27.4	202.7	56.6	53.3

Table A.17 : Averaged measured data for the forced circulation test with intermittent load of 15l/h ($\dot{m} = 0.07Kg/s$ and $V_s = 50l$) as performed on 26 - 8 - 1991. All temperatures in C° .

Time Interval	T_{i_s}	T_{o_s}	T_{i_p}	T_{o_p}	T_a	$I Wh/m^2$	T_{u_s}	T_{u_p}
08:00-08:30	26.3	26.55	26.2	26.4	19.9	196.9	/	/
08:30-09:00	28.1	28.65	27.7	28.1	20.4	251.7	28.3	27.9
09:00-09:30	30.6	31.35	30.0	30.6	21.3	296.5	/	/
09:30-10:00	33.9	34.8	33.0	33.75	22.7	365.7	34.3	33.4
10:00-10:30	37.4	38.4	36.2	37.1	23.9	403.7	/	/
10:30-11:00	41.0	42.15	39.6	40.55	24.6	444.3	41.6	40.1
11:00-11:30	44.4	45.6	42.5	43.5	25.0	479.1	/	/
11:30-12:00	47.9	49.1	45.6	46.6	25.8	498.8	48.4	46.2
12:00-12:30	50.1	51.35	47.4	48.45	27.2	509.9	/	/
12:30-13:00	52.0	53.25	48.95	50.0	27.5	514.7	52.6	49.5
13:00-13:30	53.25	54.4	50.0	51.0	27.6	500.6	/	/
13:30-14:00	54.4	55.45	50.8	51.7	28.2	473.5	54.8	51.2
14:00-14:30	55.0	55.9	51.1	51.8	27.7	459.0	/	/
14:30-15:00	55.1	55.85	50.9	51.55	27.4	396.9	55.5	51.3
15:00-15:30	54.4	54.85	50.1	50.5	27.6	302.5	/	/
15:30-16:00	52.9	52.95	48.5	48.55	26.7	240.7	52.9	48.5
16:00-16:30	50.6	50.75	46.15	46.3	27.4	188.7	/	/
16:30-17:00	48.2	48.35	43.9	44.05	26.5	151.4	48.3	44.0

Table A.18 : Averaged measured data for the stagnation test with flow rate of 0.02Kg/s, as performed on 10 - 9 - 1991. All temperatures in C° .

Time Interval	T_{i_s}	T_{o_s}	T_{i_p}	T_{o_p}	T_a	$I Wh/hr$
13:00-13:30	94.2	94.9	92.4	92.9	29.1	460.3
13:30-14:00	94.7	95.1	92.7	93.0	29.0	428.2
14:00-14:30	95.0	95.1	92.9	93.0	28.7	397.0
14:30-15:00	94.8	94.6	92.8	92.7	28.6	370.2
15:00-15:30	94.4	94.3	92.5	92.4	28.5	330.4

Table A.10 : Averaged measured data for the thermosyphon test with no load conditions, as performed on 18 - 9 - 1991. All Temperatures in C°.

Time Interval	T _{1a}	T ₁	T ₂	T ₃	T _{3s}	T _{3a}	T _{3p}	T _{3sp}	T _a	I W/m ²	T _{1p}	T _{1sp}	T _{1sa}	T _{1p}	T _{1sp}	T _{1sa}	T _{1p}	T _{1sp}	T _{1sa}	T _{1p}	T _{1sp}	T _{1sa}	
08:00-08:30	25.4	26.6	27.5	28.4	28.8	21.7	25.5	28.8	21.7	106.6	26.5	27.4	28.3	26.5	27.4	28.3	26.5	27.4	28.3	26.5	27.4	28.3	26.5
08:30-09:00	25.7	28.8	31.4	33.3	34.6	22.8	26.0	34.3	22.8	248.0	28.2	30.5	33.0	28.2	30.5	33.0	28.3	28.3	30.6	33.1	28.3	30.6	33.1
09:00-09:30	26.1	29.8	33.5	36.5	37.9	23.9	28.5	37.5	23.9	306.3	29.2	32.5	35.9	29.2	32.5	35.9	29.8	29.8	33.0	36.0	29.8	33.0	36.0
09:30-10:00	28.2	32.3	36.5	39.5	41.2	24.4	28.8	40.9	24.4	359.9	31.6	35.3	38.9	31.6	35.3	38.9	32.4	32.4	35.8	39.1	32.4	35.8	39.1
10:00-10:30	32.8	36.9	40.9	44.4	46.0	25.2	33.5	45.6	25.2	407.5	36.5	40.0	43.3	36.5	40.0	43.3	37.0	37.0	40.3	43.6	37.0	40.3	43.6
10:30-11:00	37.3	41.5	45.7	49.1	50.8	26.9	38.5	50.9	26.9	443.6	41.1	44.7	48.0	41.1	44.7	48.0	41.9	41.9	45.2	48.4	41.9	45.2	48.4
11:00-11:30	41.7	45.9	50.1	53.7	55.4	27.0	42.5	55.1	27.0	471.8	45.6	49.3	52.7	45.6	49.3	52.7	46.1	46.1	49.5	53.0	46.1	49.5	53.0
11:30-12:00	46.4	50.8	55.2	58.7	60.2	20.8	47.3	60.0	20.8	491.9	50.3	54.1	57.6	50.3	54.1	57.6	51.0	51.0	54.5	58.0	51.0	54.5	58.0
12:00-12:30	50.2	55.1	59.4	62.9	64.7	27.1	51.4	64.6	27.1	502.3	54.7	58.4	61.9	54.7	58.4	61.9	55.2	55.2	58.8	62.3	55.2	58.8	62.3
12:30-13:00	55.3	59.6	63.8	67.5	69.2	27.2	56.2	69.2	27.2	499.5	59.2	63.0	66.5	59.2	63.0	66.5	60.0	60.0	63.6	67.0	60.0	63.6	67.0
13:00-13:30	56.9	63.2	67.5	71.1	72.9	27.1	59.6	72.8	27.1	489.0	62.8	66.6	70.1	62.8	66.6	70.1	63.2	63.2	67.0	70.6	63.2	67.0	70.6
13:30-14:00	62.2	66.5	70.8	74.4	76.0	26.8	62.8	75.0	26.8	465.3	66.1	69.8	73.3	66.1	69.8	73.3	66.7	66.7	70.3	73.9	66.7	70.3	73.9
14:00-14:30	64.5	69.3	73.5	77.0	78.6	27.0	64.8	78.2	27.0	435.0	68.5	72.3	75.8	68.5	72.3	75.8	68.9	68.9	72.7	76.5	68.9	72.7	76.5
14:30-15:00	66.3	70.8	74.8	78.1	79.8	27.3	66.7	79.1	27.3	393.7	70.1	73.7	77.1	70.1	73.7	77.1	70.4	70.4	74.1	77.7	70.4	74.1	77.7
15:00-15:30	66.2	70.8	74.8	78.1	79.6	27.2	67.0	79.2	27.2	346.2	70.0	73.6	77.0	70.0	73.6	77.0	70.9	70.9	74.5	78.0	70.9	74.5	78.0
15:30-16:00	66.1	70.5	74.2	77.3	78.7	26.9	67.0	76.9	26.9	297.5	69.6	73.0	76.2	69.6	73.0	76.2	70.5	70.5	73.8	76.7	70.5	73.8	76.7
16:00-16:30	66.0	68.5	70.7	72.5	73.3	26.6	66.8	71.3	26.6	245.0	68.1	70.1	70.5	68.1	70.1	70.5	68.3	68.3	70.6	71.0	68.3	70.6	71.0
16:30-17:00	65.8	66.9	67.8	68.6	68.7	26.1	66.5	69.3	26.1	185.0	66.6	67.4	68.0	66.6	67.4	68.0	67.3	67.3	68.1	68.9	67.3	68.1	68.9

Table A.20 : Averaged measured data for the thermosyphon test with intermittent load of 5l/h and $V_s = 50l$, as performed on 19 - 9 - 1991. All temperatures in C° .

Time Interval	T_{i_s}	T_{o_s}	T_{i_p}	T_{o_p}	T_a	I Wh/m ²	T_{u_s}	T_{u_p}
08:00-08:30	22.2	26.0	22.3	25.6	18.1	91.0	/	/
08:30-09:00	22.6	35.5	23.7	35.1	19.0	272.0	31.2	31.3
09:00-09:30	23.1	42.9	24.2	41.4	19.3	332.3	/	/
09:30-10:00	24.4	44.8	25.1	44.1	20.7	383.0	42.2	42.4
10:00-10:30	25.9	48.2	26.7	46.8	22.1	426.1	/	/
10:30-11:00	27.1	51.3	28.6	49.7	22.6	464.2	47.9	48.3
11:00-11:30	30.4	54.8	31.1	52.7	23.0	492.2	/	/
11:30-12:00	35.0	57.8	36.8	57.7	23.2	509.0	56.0	56.6
12:00-12:30	38.4	61.0	40.1	60.7	23.9	517.2	/	/
12:30-13:00	43.4	64.3	45.7	65.3	24.1	505.6	63.7	64.3
13:00-13:30	45.5	66.8	47.7	67.1	24.4	479.7	/	/
13:30-14:00	47.6	68.5	48.5	68.6	25.1	450.4	66.0	66.8
14:00-14:30	49.0	69.0	50.0	69.6	24.8	451.3	/	/
14:30-15:00	48.2	68.3	50.7	69.2	24.4	410.4	67.0	67.9
15:00-15:30	47.8	68.1	51.0	68.9	24.2	360.4	/	/
15:30-16:00	47.0	67.4	50.2	67.7	24.2	309.9	66.4	67.3
16:00-16:30	46.5	64.2	50.9	66.9	24.3	253.7	/	/
16:30-17:00	44.5	58.8	47.4	61.5	23.6	181.5	66.0	67.0

Table A.21 : Averaged measured data for the thermosyphon test with intermittent load of 10l/h and $V_s = 50l$, as performed on 21 - 9 - 1991. All temperatures in C° .

Time Interval	T_{i_s}	T_{o_s}	T_{i_p}	T_{o_p}	T_a	I Wh/m ²	T_{u_s}	T_{u_p}
08:00-08:30	21.1	24.8	21.2	24.4	17.5	75.0	/	/
08:30-09:00	21.6	32.3	22.3	31.5	18.0	241.7	25.6	25.7
09:00-09:30	22.2	42.1	22.4	39.8	18.6	310.0	/	/
09:30-10:00	23.0	43.9	23.8	43.2	19.2	373.6	33.2	33.3
10:00-10:30	25.2	47.3	25.8	45.9	20.4	417.4	/	/
10:30-11:00	27.0	50.4	28.5	49.3	21.4	457.7	44.8	45.2
11:00-11:30	29.1	53.1	30.5	51.8	21.9	488.2	/	/
11:30-12:00	31.5	54.8	33.3	54.7	22.7	508.8	52.3	52.8
12:00-12:30	33.4	56.3	35.0	56.5	24.1	518.1	/	/
12:30-13:00	35.5	58.2	37.3	58.7	24.7	517.2	54.8	55.4
13:00-13:30	37.5	60.4	39.2	60.3	24.9	502.6	/	/
13:30-14:00	39.2	60.7	40.5	61.2	24.7	480.8	57.3	57.8
14:00-14:30	40.4	60.9	41.5	61.5	24.6	436.9	/	/
14:30-15:00	40.7	61.6	42.2	61.5	24.3	363.1	57.2	57.7
15:00-15:30	40.3	59.8	42.4	59.5	23.7	322.2	/	/
15:30-16:00	40.0	57.3	42.6	57.8	23.6	286.2	53.1	53.9
16:00-16:30	39.9	56.0	42.3	56.8	23.5	239.9	/	/
16:30-17:00	39.7	51.4	40.7	52.7	22.9	174.6	49.1	49.9

Table A.22 : Averaged measured data for the thermosyphon test with intermittent load of 15l/h and $V_s = 50l$, as performed on 22 - 9 - 1991. All temperatures in C° .

Time Interval	T_{is}	T_{os}	T_{ip}	T_{op}	T_a	IWh/m^2	T_{us}	T_{up}
08:00-08:30	22.5	26.0	22.6	25.5	18.0	62.1	/	/
08:30-09:00	22.9	33.2	23.5	32.8	18.4	238.0	23.2	23.3
09:00-09:30	23.3	43.4	23.8	41.3	19.6	295.0	/	/
09:30-10:00	24.0	44.2	24.9	43.7	20.9	349.4	32.1	32.3
10:00-10:30	26.0	47.9	26.7	47.0	21.5	392.2	/	/
10:30-11:00	27.5	51.1	28.7	49.6	22.5	430.1	42.1	42.4
11:00-11:30	29.2	51.3	30.2	49.9	23.8	456.2	/	/
11:30-12:00	30.7	53.8	32.1	53.3	25.0	472.1	49.7	50.1
12:00-12:30	32.1	56.0	33.4	55.6	25.7	482.6	/	/
12:30-13:00	34.1	57.6	35.2	57.0	26.2	488.3	52.1	52.5
13:00-13:30	35.0	57.8	35.8	57.4	25.6	477.0	/	/
13:30-14:00	35.3	58.0	36.1	57.7	25.7	455.1	52.2	52.6
14:00-14:30	36.5	58.1	36.8	58.0	26.4	424.6	/	/
14:30-15:00	36.8	57.9	37.8	58.1	26.1	383.5	48.3	48.8
15:00-15:30	36.5	57.7	37.9	58.0	26.1	338.2	/	/
15:30-16:00	35.3	55.3	37.6	55.2	26.0	286.4	46.2	46.8
16:00-16:30	35.2	53.3	37.4	53.8	25.6	225.4	/	/
16:30-17:00	35.0	48.4	36.8	49.8	24.8	166.3	42.3	43.0

Table A.23 : Averaged measured data for the time constant test ($T_{is} = T_{ip} = 28.4C^\circ$) as performed on 11 - 9 - 1991.

Time Interval	$T_{os} C^\circ$	$T_{op} C^\circ$
12:59-13:00	32.9	32.5
13:00-13:01	32.0	32.2
13:01-13:02	31.4	31.8
13:02-13:03	30.8	31.4
13:03-13:04	29.9	30.7
13:04-13:05	29.3	29.8
13:05-13:06	29.0	29.2
13:06-13:07	28.8	29.0
13:07-13:08	28.6	28.7
13:08-13:09	28.5	28.5

APPENDIX (B) THE COMPUTER PROGRAM

```

C THIS PROGRAM IS USED TO CALCULATE THE PERFORMANCE
C PARAMETERS OF THE SERPENTINE AND THE PARALLEL TYPES
C SOLAR COLLECTORS, WHERE:
C TIS IS THE INLET WATER TEMPERATURE TO THE
C SERPENTINE TYPE.
C TOS IS THE OUTLET WATER TEMPERATURE FROM THE
C SERPENTINE TYPE
C TIP IS THE INLET WATER TEMPERATURE TO THE
C PARALLEL TYPE.
C TOP IS THE OUTLET WATER TEMPERATURE FROM THE
C PARALLEL TYPE.
C TA IS THE AMBIENT TEMPERATURE.
C SI IS THE SOLAR INTENSITY IN Wh/m^2.
C SI1 IS THE SOLAR INTENSITY IN KJ.
C QUS IS THE USEFUL HEAT GAIN FROM THE SERPENTINE TYPE.
C QUP IS THE USEFUL HEAT GAIN FROM THE PARALLEL TYPE.
C EFS IS THE INSTANTANEOUS EFFICIENCY OF THE
C SERPENTINE TYPE
C EFP IS THE INSTANTANEOUS EFFICIENCY OF THE
C PARALLEL TYPE.
C AS IS THE RATIO OF THE TEMPERATURE DIFFERENCE
C BETWEEN THE SERPENTINE TYPE INLET WATER TEMPERATURE
C AND THE AMBIENT TEMPERATURE TO THE SOLAR INTENSITY.
C AP IS THE RATIO OF THE TEMPERATURE DIFFERENCE
C BETWEEN THE PARALLEL TYPE INLET WATER TEMPERATURE
C AND THE AMBIENT TEMPERATURE TO THE SOLAR INTENSITY.
C CCCCCCCCCCCCCCCCCCCCCCCCCCCCCCCCCCCCCCCCCCCCCCCCCCCCCC
C CCCCCCCCCCCCCCCCCCCCCCCCCCCCCCCCCCCCCCCCCCCCCCCCCCCCCC

REAL*8 TIS(18),TOS(18),TIP(18),TOP(18),TA(18),SI(18)
REAL*8 SI1(18),QUS(18),QUP(18),EFS(18),EFP(18),AS(18),AP(18)
DO 10 I=1,18
10 READ(5,*) TIS(I),TOS(I),TIP(I),TOP(I),TA(I),SI(I)
CONTINUE
DO 20 I=1,18
SI1(I)=SI(I)*1.8*.73*1.59
QUS(I)=A1*4.186*1800*(TOS(I)-TIS(I))
QUP(I)=A1*4.186*1800*(TOP(I)-TIP(I))
EFS(I)=QUS(I)/SI1(I)
EFP(I)=QUP(I)/SI1(I)
AS(I)=(TIS(I)-TA(I))/SI(I)
AP(I)=(TIP(I)-TA(I))/SI(I)
20 CONTINUE
WRITE(6,30)
30 FORMAT(' TIS TOS TIP TOP TA SI ')
WRITE(6,31)
31 FORMAT(50('*'))
DO 32 I=1,18
WRITE(6,*) TIS(I),TOS(I),TIP(I),TOP(I),TA(I),SI(I)
32 CONTINUE
WRITE(6,35)
35 FORMAT(70('*'))
WRITE(6,40)
40 FORMAT('SI1 QUS QUP EFS EFP AS AP')
WRITE(6,50)
50 FORMAT(70('*'))
DO 60 I=1,18
WRITE(6,*) SI1(I),QUS(I),QUP(I),EFS(I),EFP(I),AS(I),AP(I)
60 CONTINUE
END

```


APPENDIX (C)
CALCULATED
PERFORMANCE
PARAMETERS

Table C.1 : Calculated parameters of the performance for the forced circulation with no load conditions ($\dot{m} = 0.02\text{Kg/s}$ and $V_s = 150\text{l}$) as performed on 5 - 8 - 1991.

Time Interval	SI (KJ)	Q_{us} (KJ)	Q_{up} (KJ)	η_s %	η_p %	$\frac{T_{is}-T_a}{I} * 10^2$	$\frac{T_{ip}-T_a}{I} * 10^2$
08:00-08:30	414.5	105.5	82.9	25.0	20.0	5.500	5.444
08:30-09:00	558.3	278.8	226.1	49.9	40.5	3.443	3.368
09:00-09:30	674.4	384.3	316.5	57.0	46.9	2.664	2.571
09:30-10:00	786.6	467.2	399.4	59.4	50.8	2.258	2.125
10:00-10:30	879.0	527.5	452.1	60.0	51.4	1.997	1.902
10:30-11:00	953.6	587.7	512.4	61.6	53.7	1.972	1.906
11:00-11:30	1019.4	632.9	565.1	62.1	55.5	2.194	2.153
11:30-12:00	1069.3	655.8	602.8	61.3	56.4	2.345	2.325
12:00-12:30	1087.9	663.1	602.8	60.9	55.4	2.535	2.420
12:30-13:00	1093.8	655.6	602.8	59.9	55.1	2.846	2.579
13:00-13:30	1084.8	632.9	572.8	58.3	52.8	3.216	2.966
13:30-14:00	1047.2	595.3	550.0	56.8	52.5	3.611	3.232
14:00-14:30	992.8	557.6	504.9	56.2	50.8	3.998	3.598
14:30-15:00	918.7	504.9	459.6	55.0	50.0	4.708	4.230
15:00-15:30	825.9	414.4	376.8	50.2	46.5	5.667	5.135
15:30-16:00	727.1	324.0	293.9	44.6	40.4	6.868	6.264
16:00-16:30	623.9	226.1	211.0	36.2	33.8	8.607	7.500
16:30-17:00	509.2	128.1	120.6	25.2	23.7	11.00	10.00

Table C.2 : Calculated parameters of the performance for the forced circulation with no load conditions ($\dot{m} = 0.03\text{Kg/s}$ and $V_s = 150\text{l}$) as performed on 4 - 8 - 1991.

Time Interval	SI (KJ)	Q_{us} (KJ)	Q_{up} (KJ)	η_s %	η_p %	$\frac{T_{is}-T_a}{I} * 10^2$	$\frac{T_{ip}-T_a}{I} * 10^2$
08:00-08:30	430.0	248.7	226.1	57.8	52.6	2.721	2.672
08:30-09:00	535.2	305.2	271.3	57.0	50.7	2.147	2.069
09:00-09:30	658.4	395.6	361.7	60.1	54.9	1.777	1.682
09:30-10:00	765.7	474.7	440.8	62.0	57.6	1.637	1.555
10:00-10:30	861.4	553.8	508.6	64.3	59.0	1.625	1.528
10:30-11:00	939.5	610.3	553.8	65.0	58.9	1.735	1.646
11:00-11:30	1013.1	644.3	599.0	63.6	59.1	2.000	1.897
11:30-12:00	1063.0	678.2	621.6	63.8	58.5	2.246	2.142
12:00-12:30	1084.6	678.2	632.9	62.5	58.4	2.562	2.427
12:30-13:00	1088.1	666.9	632.9	61.3	58.2	2.842	2.669
13:00-13:30	1067.4	666.9	621.6	62.5	58.2	3.171	2.995
13:30-14:00	1030.9	621.6	587.7	60.3	57.0	3.689	3.486
14:00-14:30	971.9	565.1	542.5	58.1	55.8	4.342	4.106
14:30-15:00	896.5	508.6	486.0	56.7	54.2	5.080	4.801
15:00-15:30	806.3	440.8	406.9	54.7	50.5	5.960	5.597
15:30-16:00	710.8	350.4	316.5	49.3	44.5	7.202	6.761
16:00-16:30	605.7	248.7	203.5	41.1	33.6	8.969	8.417
16:30-17:00	512.9	145.7	125.2	28.4	24.4	11.00	10.70

Table C.3 : Calculated parameters of the performance for the forced circulation with no load conditions ($\dot{m} = 0.05 \text{ Kg/s}$ and $V_s = 150 \text{ l}$) as performed on 3 - 8 - 1991.

Time Interval	SI (KJ)	Q_{us} (KJ)	Q_{up} (KJ)	η_s %	η_p %	$\frac{T_{is}-T_a}{T} * 10^2$	$\frac{T_{ip}-T_a}{T} * 10^2$
08:00-08:30	403.0	207.2	207.2	51.4	51.4	2.333	2.333
08:30-09:00	539.3	320.3	301.4	59.4	55.9	1.705	1.627
09:00-09:30	652.1	433.3	395.6	66.4	60.7	1.666	1.538
09:30-10:00	756.8	489.8	452.3	64.7	59.7	1.436	1.298
10:00-10:30	851.8	565.1	527.5	66.3	61.9	1.594	1.398
10:30-11:00	934.3	621.6	584.0	66.5	62.5	1.699	1.521
11:00-11:30	994.7	678.2	640.5	68.2	64.4	1.638	1.512
11:30-12:00	1039.0	715.8	659.3	68.9	63.5	1.910	1.729
12:00-12:30	1066.4	715.8	659.3	67.1	61.8	2.390	2.096
12:30-13:00	1074.5	697.0	621.6	64.9	57.9	2.800	2.489
13:00-13:30	1055.1	697.0	602.8	66.1	57.1	3.223	2.926
13:30-14:00	1020.2	640.5	584.0	62.8	57.2	3.645	3.297
14:00-14:30	962.3	584.0	546.3	60.7	56.8	4.168	3.756
14:30-15:00	891.1	546.3	471.0	61.3	52.9	4.853	4.338
15:00-15:30	810.0	471.0	376.8	58.1	46.5	5.700	5.081
15:30-16:00	703.1	320.3	301.4	45.6	42.9	7.162	6.597
16:00-16:30	592.3	244.9	226.1	41.3	38.2	9.206	8.254
16:30-17:00	474.9	150.7	131.9	31.8	27.6	11.923	10.647

Table C.4 : Calculated parameters of the performance for the forced circulation with no load conditions ($\dot{m} = 0.07 \text{ Kg/s}$ and $V_s = 150 \text{ l}$) as performed on 25 - 7 - 1991.

Time Interval	SI (KJ)	Q_{us} (KJ)	Q_{up} (KJ)	η_s %	η_p %	$\frac{T_{is}-T_a}{T} * 10^2$	$\frac{T_{ip}-T_a}{T} * 10^2$
08:00-08:30	445.5	131.9	131.9	29.6	29.6	3.659	3.612
08:30-09:00	565.0	316.5	263.7	56.0	46.7	2.885	2.848
09:00-09:30	679.2	395.6	369.2	58.2	54.4	2.553	2.492
09:30-10:00	783.7	474.7	448.3	60.6	57.2	2.293	2.213
10:00-10:30	866.9	580.2	553.8	66.9	63.9	2.290	2.217
10:30-11:00	951.1	632.9	580.2	66.6	61.0	2.307	2.219
11:00-11:30	1008.1	685.7	632.9	68.0	62.8	2.321	2.218
11:30-12:00	1053.2	738.4	659.3	70.1	62.6	2.460	2.341
12:00-12:30	1077.2	738.4	685.7	68.5	63.7	2.851	2.696
12:30-13:00	1075.6	712.1	685.7	66.2	63.8	3.127	2.972
13:00-13:30	1074.7	659.3	632.9	61.3	58.9	3.480	3.305
13:30-14:00	1037.6	632.9	606.6	61.0	58.5	4.007	3.806
14:00-14:30	986.6	606.6	553.8	61.5	56.1	4.638	4.405
14:30-15:00	913.9	501.1	474.7	54.8	51.9	5.304	5.030
15:00-15:30	822.1	422.0	395.6	51.3	48.1	6.201	5.870
15:30-16:00	719.1	316.5	263.7	44.0	36.7	7.496	7.147
16:00-16:30	609.5	211.0	184.6	34.6	30.3	9.290	8.879
16:30-17:00	492.7	158.3	131.9	32.1	26.8	12.00	11.58

Table C.5 : Calculated parameters of the performance for the forced circulation with no load conditions ($\dot{m} = 0.02 \text{ Kg/s}$ and $V_s = 50\text{l}$) as performed on 3-9-1991.

Time Interval	SI (KJ)	Q_{us} (KJ)	Q_{up} (KJ)	η_s %	η_p %	$\frac{T_{is}-T_a}{I} * 10^2$	$\frac{T_{ip}-T_a}{I} * 10^2$
08:00-08:30	301.7	105.5	98.0	35.0	32.5	2.632	2.632
08:30-09:00	486.6	271.3	256.2	55.7	52.6	2.619	2.619
09:00-09:30	657.3	346.6	331.6	52.7	50.4	3.242	3.242
09:30-10:00	797.1	376.8	361.7	47.3	45.4	4.142	4.142
10:00-10:30	894.2	422.0	406.9	47.2	45.5	5.023	5.023
10:30-11:00	971.5	429.5	414.4	44.2	42.7	5.978	5.978
11:00-11:30	1029.2	444.6	429.0	43.2	41.7	7.044	7.044
11:30-12:00	1072.2	452.1	437.0	42.2	40.8	8.087	8.087
12:00-12:30	1097.5	429.5	406.9	39.1	37.1	9.004	9.004
12:30-13:00	1092.3	406.9	384.3	37.3	35.2	9.946	9.946
13:00-13:30	1072.7	391.8	369.2	36.5	34.4	10.87	10.87
13:30-14:00	1027.1	346.6	301.4	33.7	29.3	11.94	11.94
14:00-14:30	954.2	278.8	248.7	29.2	26.1	13.33	13.33
14:30-15:00	878.3	226.1	195.9	25.7	22.3	14.84	14.84
15:00-15:30	793.7	150.7	143.2	19.0	18.0	16.32	16.32
15:30-16:00	682.5	90.4	82.9	13.2	12.1	18.66	18.66
16:00-16:30	561.0	30.2	30.2	5.4	5.4	22.0	22.0
16:30-17:00	426.0	/	/	/	/	27.32	27.32

Table C.6 : Calculated parameters of the performance for the forced circulation with no load conditions ($\dot{m} = 0.03 \text{ Kg/s}$ and $V_s = 50\text{l}$) as performed on 2-9-1991.

Time Interval	SI KJ	Q_{us} KJ	Q_{up} KJ	η_s %	η_p %	$\frac{T_{is}-T_a}{I} * 10^2$	$\frac{T_{ip}-T_a}{I} * 10^2$
08:00-08:30	180.5	33.9	22.6	18.8	12.5	5.440	5.440
08:30-09:00	335.1	101.7	90.4	30.4	27.0	3.865	3.865
09:00-09:30	561.6	271.3	248.7	48.3	44.3	3.162	3.162
09:30-10:00	771.4	418.2	384.3	54.2	49.8	3.467	3.467
10:00-10:30	882.9	474.7	429.5	53.8	48.6	4.449	4.449
10:30-11:00	965.9	508.6	463.4	52.7	48.0	5.624	5.624
11:00-11:30	1035.7	519.9	474.7	50.2	45.8	6.657	6.657
11:30-12:00	1073.9	519.9	474.7	48.4	44.2	7.626	7.626
12:00-12:30	1099.4	508.6	463.4	46.3	42.2	8.495	8.495
12:30-13:00	1100.4	497.3	452.1	45.2	41.1	9.398	9.398
13:00-13:30	1081.0	440.8	395.6	40.8	36.6	10.34	10.34
13:30-14:00	1033.4	339.1	316.5	32.8	30.6	11.50	11.50
14:00-14:30	962.1	293.9	271.3	30.5	28.2	12.83	12.83
14:30-15:00	889.6	260.0	226.1	29.2	25.4	14.02	14.02
15:00-15:30	785.0	192.2	169.6	24.5	21.6	15.89	15.89
15:30-16:00	972.6	113.0	90.4	16.8	13.4	18.33	18.33
16:00-16:30	550.1	45.2	33.9	8.2	6.2	15.30	15.30
16:30-17:00	442.5	/	/	/	/	25.54	25.54

Table C.7 : Calculated parameters of the performance for the forced circulation with no load conditions ($\dot{m} = 0.05 \text{ Kg/s}$ and $V_s = 50\text{l}$) as performed on 4-9-1991.

Time Interval	SI (KJ)	Q_{us} (KJ)	Q_{up} (KJ)	η_s %	η_p %	$\frac{T_{is}-T_a}{I} * 10^2$	$\frac{T_{ip}-T_a}{I} * 10^2$
08:00-08:30	376.1	131.9	113.0	35.1	30.1	1.111	1.111
08:30-09:00	535.5	301.4	263.7	56.3	49.3	1.834	1.834
09:00-09:30	660.0	376.8	339.1	57.1	51.4	2.786	2.786
09:30-10:00	758.6	452.1	395.6	59.6	52.1	3.608	3.608
10:00-10:30	845.3	470.9	414.4	55.7	49.0	4.869	4.869
10:30-11:00	918.9	489.8	433.3	53.3	47.2	6.094	6.094
11:00-11:30	967.8	489.8	433.3	50.6	44.8	7.124	7.124
11:30-12:00	993.9	489.8	452.1	49.3	45.5	8.325	8.325
12:00-12:30	1009.3	489.8	452.1	48.5	44.8	9.439	9.439
12:30-13:00	1043.2	470.9	414.4	45.1	39.7	9.894	9.894
13:00-13:30	1041.7	489.8	414.4	47.0	39.0	10.77	10.77
13:30-14:00	1000.6	470.9	376.8	47.1	37.7	11.88	11.88
14:00-14:30	942.3	414.4	320.3	44.0	34.0	13.30	13.30
14:30-15:00	855.2	339.1	263.7	39.7	30.8	15.20	15.20
15:00-15:30	764.3	244.9	207.2	32.0	27.1	16.40	16.40
15:30-16:00	659.4	169.6	131.9	25.7	20.0	18.09	18.09
16:00-16:30	545.7	94.2	94.2	17.3	17.3	21.20	21.20
16:30-17:00	421.2	/	/	/	/	26.36	26.36

Table C.8 : Calculated parameters of the performance for the forced circulation with no load conditions ($\dot{m} = 0.07 \text{ Kg/s}$ and $V_s = 50\text{l}$) as performed on 27-8-1991.

Time Interval	SI KJ	Q_{us} KJ	Q_{up} KJ	η_s %	η_p %	$\frac{T_{is}-T_a}{I} * 10^2$	$\frac{T_{ip}-T_a}{I} * 10^2$
08:00-08:30	423.7	131.9	105.5	31.1	24.9	2.465	2.465
08:30-09:00	551.4	316.5	275.7	57.4	50.0	3.335	3.335
09:00-09:30	663.4	395.6	338.3	58.6	51.0	4.535	4.535
09:30-10:00	786.6	448.3	369.7	57.0	47.0	5.445	5.445
10:00-10:30	884.4	474.7	395.6	53.7	44.7	6.449	6.449
10:30-11:00	968.0	501.1	422.0	51.8	43.6	7.490	7.490
11:00-11:30	1025.6	501.1	422.0	48.9	41.1	8.474	8.474
11:30-12:00	1072.0	474.7	422.0	44.3	39.4	9.335	9.335
12:00-12:30	1091.9	474.7	422.0	43.5	38.6	10.20	10.20
12:30-13:00	1088.5	501.1	422.0	46.0	38.8	10.88	10.88
13:00-13:30	1071.4	448.3	369.2	41.8	34.5	11.427	11.427
13:30-14:00	1017.1	369.2	316.5	36.3	31.1	12.202	12.202
14:00-14:30	962.1	316.5	263.7	32.9	27.4	13.03	13.03
14:30-15:00	873.3	263.7	237.4	30.2	27.2	14.35	14.35
15:00-15:30	781.8	237.4	211.0	30.3	27.0	15.69	15.69
15:30-16:00	673.6	158.3	131.9	23.5	19.6	17.77	17.77
16:00-16:30	565.6	79.1	52.8	14.0	9.3	20.50	20.50
16:30-17:00	447.1	/	/	/	/	24.81	24.81

Table C.9 : Calculated parameters of the performance for the forced circulation with no load conditions ($\dot{m}_s=0.015\text{Kg/s}$, $\dot{m}_p=0.105\text{Kg/s}$, and $V_s=150\text{l}$) as performed on 9 - 9 - 1991.

Time Interval	SI KJ	Q_{us} KJ	Q_{up} KJ	η_s %	η_p %	$\frac{T_{is}-T_a}{T} * 10^2$	$\frac{T_{ip}-T_a}{T} * 10^2$
08:00-08:30	271.6	96.1	79.1	35.4	29.1	1.077	1.077
08:30-09:00	525.3	248.7	276.9	47.3	52.7	1.313	1.313
09:00-09:30	644.1	333.4	356.0	51.8	55.3	2.043	2.043
09:30-10:00	754.5	359.6	435.2	52.4	57.7	2.908	2.908
10:00-10:30	847.0	406.9	474.7	48.0	56.0	3.848	3.848
10:30-11:00	909.7	435.2	514.3	47.8	56.5	4.984	4.984
11:00-11:30	950.0	423.9	553.8	44.6	58.3	6.268	6.268
11:30-12:00	972.2	384.3	514.3	39.5	52.9	7.307	7.307
12:00-12:30	1012.3	384.3	474.7	38.0	46.9	8.029	8.029
12:30-13:00	1013.5	400.0	450.0	39.5	44.4	8.926	8.926
13:00-13:30	982.6	378.6	435.2	38.5	44.3	10.12	10.12
13:30-14:00	946.0	305.2	395.6	32.3	41.8	11.24	11.24
14:00-14:30	894.0	231.7	316.5	25.9	35.4	12.43	12.43
14:30-15:00	816.5	192.2	276.9	23.5	33.9	13.79	13.79
15:00-15:30	720.4	141.3	237.4	19.6	32.9	15.75	15.75
15:30-16:00	616.6	101.7	158.3	16.5	25.7	18.30	18.30
16:00-16:30	504.0	50.9	79.1	10.1	15.7	21.73	21.73
16:30-17:00	384.7	/	39.6	/	10.3	27.05	27.05

Table C.10 : Calculated parameters of the performance for the forced circulation with load conditions ($\dot{m} = 0.02\text{Kg/s}$) as performed on 12 - 9 - 1991.

Time Interval	SI (KJ)	Q_{us} (KJ)	Q_{up} (KJ)
08:00-08:30	282.9	128.1	105.5
08:30-09:00	510.0	233.6	195.9
09:00-09:30	652.7	301.4	241.1
09:30-10:00	764.1	346.6	286.3
10:00-10:30	862.5	406.9	339.1
10:30-11:00	937.7	444.6	376.8
11:00-11:30	994.5	474.7	422.0
11:30-12:00	1036.1	497.3	444.6
12:00-12:30	1059.5	519.4	467.2
12:30-13:00	1059.5	519.9	467.2
13:00-13:30	1037.6	504.9	444.6
13:30-14:00	994.5	474.7	422.0
14:00-14:30	929.5	429.5	391.8
14:30-15:00	844.5	376.8	346.6
15:00-15:30	770.8	339.1	309.0
15:30-16:00	659.4	278.8	263.7
16:00-16:30	548.9	218.5	211.0
16:30-17:00	428.5	173.3	173.3

Table C.11 : Calculated parameters of the performance for the forced circulation with load conditions ($\dot{m} = 0.05 \text{ Kg/s}$) as performed on 14 - 9 - 1991.

Time Interval	SI (KJ)	Q_{us} (KJ)	Q_{up} (KJ)
08:00-08:30	335.1	113.0	75.4
08:30-09:00	521.5	244.9	188.4
09:00-09:30	636.4	339.1	263.7
09:30-10:00	739.2	414.4	339.1
10:00-10:30	828.4	508.6	414.4
10:30-11:00	909.9	565.1	489.8
11:00-11:30	972.4	602.8	527.5
11:30-12:00	1015.8	640.5	565.1
12:00-12:30	1041.5	678.2	602.8
12:30-13:00	1042.1	678.2	602.8
13:00-13:30	1017.9	640.5	565.1
13:30-14:00	966.9	621.6	527.5
14:00-14:30	903.8	565.1	471.0
14:30-15:00	830.1	508.6	433.3
15:00-15:30	773.5	452.1	376.8
15:30-16:00	669.2	376.8	301.4
16:00-16:30	555.4	244.9	188.4
16:30-17:00	433.1	150.7	94.2

Table C.12 : Calculated parameters of the performance for the forced circulation with intermittent load of 5l/h ($\dot{m} = 0.03 \text{ Kg/s}$, and $V_s = 50 \text{ l}$) as performed on 19 - 8 - 1991.

Time Interval	SI (KJ)	Q_{us} (KJ)	Q_{up} (KJ)
08:00-08:30	389.5	101.7	101.7
08:30-09:00	536.1	282.6	237.4
09:00-09:30	659.4	373.0	316.5
09:30-10:00	777.6	452.1	373.0
10:00-10:30	870.4	508.6	440.8
10:30-11:00	951.9	553.5	486.0
11:00-11:30	1016.9	587.7	531.2
11:30-12:00	1062.2	599.0	531.2
12:00-12:30	1080.6	576.4	486.0
12:30-13:00	1086.9	553.8	463.4
13:00-13:30	1064.9	553.8	486.0
13:30-14:00	1026.5	519.9	440.8
14:00-14:30	968.2	440.8	373.0
14:30-15:00	900.5	384.3	327.8
15:00-15:30	800.0	237.4	203.5
15:30-16:00	702.4	147.0	124.3
16:00-16:30	448.0	113.0	79.1
16:30-17:00	382.4	33.9	22.6

Table C.13 : Calculated parameters of the performance for the forced circulation with intermittent load of 10l/h ($\dot{m} = 0.03\text{Kg/s}$, and $V_s = 50\text{l}$) as performed on 20 - 8 - 1991.

Time Interval	SI (KJ)	Q_{us} (KJ)	Q_{up} (KJ)
08:00-08:30	419.1	113.0	101.7
08:30-09:00	541.8	271.3	237.4
09:00-09:30	659.8	373.0	327.8
09:30-10:00	759.5	440.8	395.6
10:00-10:30	856.4	519.9	440.8
10:30-11:00	940.0	508.6	474.7
11:00-11:30	999.5	531.2	508.6
11:30-12:00	1052.0	553.8	531.2
12:00-12:30	1069.5	576.4	565.1
12:30-13:00	1072.0	576.4	565.1
13:00-13:30	1058.2	565.1	553.8
13:30-14:00	1462.3	542.5	519.9
14:00-14:30	946.9	508.6	463.4
14:30-15:00	977.1	440.8	395.6
15:00-15:30	780.8	373.0	293.9
15:30-16:00	679.2	293.9	214.8
16:00-16:30	566.4	214.8	158.3
16:30-17:00	447.1	147.0	101.7

Table C.14 : Calculated parameters of the performance for the forced circulation with intermittent load of 15l/h ($\dot{m} = 0.03\text{Kg/s}$, and $V_s = 50\text{l}$) as performed on 21 - 9 - 1991.

Time Interval	SI (KJ)	Q_{us} (KJ)	Q_{up} (KJ)
08:00-08:30	413.9	124.3	113.0
08:30-09:00	535.3	282.6	260.0
09:00-09:30	653.5	373.0	327.8
09:30-10:00	753.2	452.1	384.3
10:00-10:30	842.8	497.3	452.1
10:30-11:00	928.3	519.9	474.7
11:00-11:30	998.3	531.2	497.3
11:30-12:00	1045.1	542.5	508.6
12:00-12:30	1069.5	576.4	553.8
12:30-13:00	1075.6	621.6	587.7
13:00-13:30	1058.4	632.9	587.7
13:30-14:00	1019.6	576.4	542.5
14:00-14:30	961.9	519.9	486.0
14:30-15:00	882.7	474.7	429.5
15:00-15:30	794.6	406.9	350.4
15:30-16:00	696.0	316.5	282.6
16:00-16:30	585.9	237.4	203.5
16:30-17:00	460.1	169.6	135.7

Table C.15 : Calculated parameters of the performance for the forced circulation with intermittent load of 5l/h ($\dot{m} = 0.07 \text{ Kg/s}$, and $V_s = 50\text{l}$) as performed on 24 - 8 - 1991.

Time Interval	SI (KJ)	Q_{us} (KJ)	Q_{up} (KJ)
08:00-08:30	330.5	158.3	105.5
08:30-09:00	510.6	290.1	237.4
09:00-09:30	650.1	369.2	290.1
09:30-10:00	750.1	422.0	369.2
10:00-10:30	827.4	475.0	422.0
10:30-11:00	904.0	527.5	474.7
11:00-11:30	961.3	580.2	501.1
11:30-12:00	1006.4	580.2	527.5
12:00-12:30	1025.4	553.8	501.1
12:30-13:00	1030.2	550.1	501.1
13:00-13:30	1016.9	474.7	422.0
13:30-14:00	982.0	422.0	369.2
14:00-14:30	927.0	369.2	342.9
14:30-15:00	856.0	316.5	263.7
15:00-15:30	770.8	237.4	197.5
15:30-16:00	659.4	184.6	145.0
16:00-16:30	548.9	100.0	79.1
16:30-17:00	427.9	35.0	26.4

Table C.16 : Calculated parameters of the performance for the forced circulation with intermittent load of 10l/h ($\dot{m} = 0.07 \text{ Kg/s}$, and $V_s = 50\text{l}$) as performed on 25 - 8 - 1991.

Time Interval	SI (KJ)	Q_{us} (KJ)	Q_{up} (KJ)
08:00-08:30	385.3	131.9	105.5
08:30-09:00	505.0	263.7	211.0
09:00-09:30	615.9	316.5	290.1
09:30-10:00	728.1	422.0	342.9
10:00-10:30	827.0	501.1	448.3
10:30-11:00	900.1	550.0	474.7
11:00-11:30	963.2	580.2	527.5
11:30-12:00	1008.1	606.6	527.5
12:00-12:30	1030.7	606.6	553.8
12:30-13:00	1033.2	606.6	553.8
13:00-13:30	1023.1	580.2	501.1
13:30-14:00	982.0	527.5	474.7
14:00-14:30	921.8	474.7	422.0
14:30-15:00	844.5	422.0	330.0
15:00-15:30	767.0	369.2	290.1
15:30-16:00	657.7	263.7	237.4
16:00-16:30	544.3	158.3	140.0
16:30-17:00	423.5	52.8	40.0

Table C.17 : Calculated parameters of the performance for the forced circulation with intermittent load of 15l/h ($\dot{m} = 0.07\text{Kg/s}$, and $V_s = 50\text{l}$) as performed on 26 - 8 - 1991.

Time Interval	SI (KJ)	Q_{us} (KJ)	Q_{up} (KJ)
08:00-08:30	411.4	131.9	105.5
08:30-09:00	525.9	290.1	211.0
09:00-09:30	619.5	395.6	316.5
09:30-10:00	764.1	474.7	395.6
10:00-10:30	843.5	527.5	474.7
10:30-11:00	928.3	606.6	501.1
11:00-11:30	1000.1	632.9	527.5
11:30-12:00	1042.1	632.9	528.5
12:00-12:30	1065.3	659.3	553.8
12:30-13:00	1074.9	659.3	553.8
13:00-13:30	1045.9	606.6	527.5
13:30-14:00	989.3	553.8	474.7
14:00-14:30	959.0	474.7	369.2
14:30-15:00	829.3	395.6	342.9
15:00-15:30	632.0	237.4	211.0
15:30-16:00	502.9	158.0	139.5
16:00-16:30	394.3	85.0	67.5
16:30-17:00	316.3	45.0	32.5

Table C.13 : Calculated parameters of the performance for the no load thermosyphon test ($V_s = 50L$) as performed on 18 - 9 - 1991.

Time Interval	SI (KJ)	$\dot{m}_s (Kg/s)$	$F_{r,s}$	$\dot{m}_r (Kg/s)$	$F_{r,r}$	$Q_{w,s}$ KJ	$Q_{w,r}$ KJ	η_s %	η_r %	$\frac{F_{r,s} - F_{r,r}}{F_{r,s}} \times 10^3$	$\frac{Q_{w,s} - Q_{w,r}}{Q_{w,s}} \times 10^3$
08:00-08:30	222.7	0.00436	0.7823	0.00469	0.8123	111.7	114.1	50.2	51.2	3.471	3.585
08:30-09:00	518.2	0.00455	0.7872	0.00508	0.8228	307.1	317.7	59.3	61.3	1.170	1.129
09:00-09:30	640.0	0.00436	0.7824	0.00485	0.8181	387.7	402.0	60.6	62.8	0.7183	0.8488
09:30-10:00	751.9	0.00489	0.7873	0.00508	0.8228	449.6	463.1	59.8	61.8	1.0556	1.223
10:00-10:30	861.4	0.00489	0.7834	0.00549	0.8303	486.4	500.5	57.1	58.8	1.885	2.037
10:30-11:00	926.8	0.00505	0.7957	0.00561	0.8324	513.7	524.2	55.4	56.6	2.344	2.615
11:00-11:30	985.7	0.00501	0.7957	0.00557	0.8318	517.2	528.8	52.5	53.8	3.110	3.285
11:30-12:00	1027.7	0.00483	0.7923	0.00535	0.8279	502.2	512.0	48.9	49.8	3.985	4.168
12:00-12:30	1049.5	0.00458	0.7873	0.00491	0.8193	479.7	488.3	45.7	46.5	4.718	4.838
12:30-13:00	1043.6	0.00416	0.7773	0.00448	0.8095	435.7	438.8	41.7	42.0	5.626	5.806
13:00-13:30	1021.7	0.00365	0.7826	0.00368	0.7927	385.0	385.9	37.7	37.8	6.503	6.564
13:30-14:00	972.2	0.00305	0.7396	0.00348	0.7783	317.1	319.9	32.6	32.9	7.608	7.737
14:00-14:30	908.9	0.00235	0.7002	0.00244	0.7233	249.7	246.4	27.5	27.1	8.621	8.690
14:30-15:00	822.6	0.00171	0.6431	0.00181	0.6856	173.9	169.1	21.1	20.6	9.908	10.01
15:00-15:30	727.5	0.00100	0.5208	0.00096	0.5127	101.0	88.3	16.2	12.1	11.200	11.43

ملخص الرسالة

« مقارنة بين أداء المجمع الشمسي ذي الأنابيب المتوازية والمجمع الشمسي ذي الأنابيب الملتوي »
تتعلق هذه الدراسة بمقارنة أداء وفعالية المجمع الشمسي ذي الأنابيب الملتوي بفعالية وأداء المجمع الشمسي ذي الأنابيب المتوازية . ولهذا الغرض تم تعديل وانتاج هذين النوعين من المجمعات الشمسية في مشاغل الهندسة الصناعية في الجامعة الاردنية .

وقد تم اختيار هذين المجمعين الشمسيين وفقاً لمعايير ASHRAE ٩٣ - ٧٧ لعام ١٩٧٧ ، بالإضافة الى الاختبارات التالية : اختبار السريان القسري بإحمال متقطعة ، اختبار السريان الذاتي بدون أحمال واختبار السريان الذاتي بإحمال متقطعة .

وقد اجريت الاختبارات في أشهر تموز وأب وأيلول لعام ١٩٩١ لأربعة معدلات تدفق هي : ٢٠ ، ٣٠ ، ٥٠ ، ٧٠ غرام / ثانية ، وأخذت القراءات اعتباراً من الساعة الثامنة صباحاً وحتى الخامسة مساءً .
ولدى مقارنة أداء هذين المجمعين معاً ، وجد أن المجمع الشمسي ذي الأنابيب الملتوي له أداء أفضل من المجمع الشمسي ذي الأنابيب المتوازية لجميع حالات التدفق القسري ، ووجد أن هذا التفوق في الأداء يكون أكثر وضوحاً خلال الفترة الزمنية التي تمتد ما بين الساعة التاسعة والنصف صباحاً وحتى الساعة الثالثة مساءً .

أما في حالة التدفق الذاتي نتيجة الفرق في الكثافة ما بين الماء الحار والماء البارد ، فقد وجد أن المجمع الشمسي ذي الأنابيب المتوازية يمتاز بكفاءة أعلى من تلك التي يمتلكها المجمع الشمسي ذي الأنابيب الملتوي .

414343

وقد بينت هذه الدراسة أنه وبما أن معظم المجمعات الشمسية المستخدمة في الأردن تعتمد على الدفع الذاتي نتيجة فرق الكثافة فإن اختيار المجمعات الشمسية ذات الأنابيب المتوازية يكون أفضل من اختيار ذات الأنابيب الملتوي . وعلى النقيض من ذلك فإن اختيار المجمعات الشمسية ذات الأنابيب الملتوي للأنظمة التي تستخدم مضخات هو أفضل من اختيار المجمعات ذات الأنابيب المتوازية ، ومن التطبيقات العملية لمثل هذه الأنظمة التدفئة والتبريد والتسخين لمتطلبات الصناعة .